DELFT UNIVERSITY OF TECHNOLOGY

MASTER THESIS

Research into pile toe failure in Amazonehaven

Author:
Reza NEJAD

Committee members:
Prof. dr. ir. S.N. JONKMAN
Dr. ir. J.G. DE GIJT
Dr. ir. J.G. VERLAAN
Ir. H. PACEJKA
Ir. P. MIDDENDORP
Dr. ir. S. H. J. VAN ES

A thesis submitted in fulfillment of the requirements for the degree of Master of Science

in the

Hydraulic Structures & Flood Risk
Construction Management & Engineering

DELFT UNIVERSITY OF TECHNOLOGY

Abstract

Civil Engineering & Geo-sciences
Hydraulic Structures & Flood Risk
Construction Management & Engineering

Master of Science

Research into pile toe failure in Amazonehaven

by Reza NEJAD

Extreme folding damage of open-ended tubular piles could occur during piling in onshore practices. Amazonehaven unique quay wall removal gave the opportunity to study king pile's failure close to toe. King piles are primary piles in a combined wall system, exposed to static and dynamic load. It is argued that the unexpected *pile toe failure* have been caused by dynamic load because of the uniaxial direction of the extreme deformations. However, *research into pile toe failure in Amazonehaven* shows that hammer-induced driving stresses are significantly lower than material's yield stress close to pile toe, given Amazonehaven soil condition. Therefore, the dynamic load has not been solely detrimental to the pile toe integrity. The main reasons for *pile toe failure* are discussed to be (1) pile imperfection, (2) pile inclination and (3) pile inhomogeneous strength. Bear in mind that, *pile toe failure* to such extent when not limited might lead to dysfunction of the asset during its technical lifetime. Therefore, counteractions must be taken to assure quay wall's safety and stability while operating. The remedies when such a *piling risk event* occur could be: replacement, early maintenance, or a reduction in its designed storage capacity. The reactive solutions will bring financial consequences of *pile toe failure* forward. In other words, the client will experience a reduction in its revenues due to asset's malfunction. However, when proactive process-based alternatives are implemented in the current procedure in piling industry, the probability of occurrence of *the failure* is to be reduced. Therefore, financial consequences of *piling risk event* will remain limited.

The main personal objectives creating this master thesis are to present a: ***Compact***, ***comprehensive***, ***consistent***, ***reader friendly***, and ***to the point*** report.

Contents

List of Figures

List of Tables

List of Acronyms

API	American Petroleum Institute
BR	BoomeRang
BS	Bowling Skittles
CC	Closed Curved
CI	Cost Increase
CME	Construction Management and Engineering
COS	Closed One Side
CPT	Cone Penetration Test
CR	Capacity Reduction
CS(1)	Closed Straight (1)
CS(2)	Closed Star (2)
DNPV	Delta Net Present Value
EAU	Empfehlungen des Arbeitsaussschusses Ufereinfassungen
EM	Early Maintenance
EOID	End of Initial Driving
FC	Full Capacity
FEA	Finite Element Analysis
FF	Fatigue Factor
HG	HourGlass
HR	Homogeneity Ratio
HSFR	Hydraulic Structures and Flood Risk
IR	Imperfection Ratio
JIT	Just in Time
LC	Leasing Contract
LEHS	Locally Extremely Hard Spot
LEHT	Locally Extremely High Temperature
LOE	Loss of Earnings
MA	Management Aspect
MC	Moon Cancer
MHSC	Medium to Hard Soil Condition
ML	Moon Leo

MS	Moon Scorpio
MV	MaasVlakte (area)
MVI	MaasVlakte I
ND	No Damage
NPV	Net Present Value
NPVRF	Net Present Value Reduction Factor
OOR	Out of Roundness
OS	Other Section
PD	Port Dues
PDA	Pile Driving Analysis
PDP	Pile Driving Prediction
POR	Port of Rotterdam
PORA	Port of Rotterdam Authority
PPS	Percentage Problematic Section
PS	Problematic Section
PV	Present Value
PVIF	Present Value Increase Factor
R	Replacement
RD	Russian Doll
RIPTFIA	Research into Pile Toe Failure in Amazonehaven
RM	Regular Maintenance
RRF	Revenues Reduction Factor
SB	Shell Bank
SC	Storage Capacity
SO	Municipality of Rotterdam
SNSC	Standard to Normal Soil Condition
SR	Soft Rock
SRD	Soil Resistance to (pile) Driving
TC	Total Cost
TE	Temperature Elevation
ULV	Ultra Large Vessels
WEAP	Wave Equation Analysis Program
YSM	Yield Stress Momentum
ZSF	Zero Shaft Friction

Chapter 1

Introduction

1.1 Aim

Chapter 1 aims to introduce the main *problem* as well as to determine the main research questions. Furthermore, it is briefly touched on the importance of conducting this particular research. In the end, an overview is given of the content of each chapter to guide the reader.

1.2 Background

Amazonehaven, a deep seaport quay wall, was partly demolished through 2012-2013 to widen the harbor's basin. The Amazonehaven, as depicted in Figure 1.1 is located in MaasVlakte I (MVI). After removing the structure which was in itself a unique project, engineers observed *extreme folding damage* to the open-ended tubular piles or king piles [6]. The dispersion of the damage was about one to two times the diameter of the pile [37]. To investigate the *stability* of the entire quay structure as well as the *causes to* the *extreme folding damage*, Municipality of Rotterdam (SO)[1] initiated series of master theses to investigate those above. In a recent study, the stability of the quay wall given the *pile toe failure* was studied.

(A) Aerial photo Amazonehaven (B) Seaport quay wall Amazonehaven

FIGURE 1.1: Amazonehaven basin, retrieved from Google maps

1.3 Research description

The *pile toe failure* described as *extreme folding damage* close to pile toe, has occurred due to forces working in the axial direction. The loads working on the piles are both static load, caused by permanent- and variable- load, and dynamic load. The latter, is the applied force on the piles during installation, to bring the piles up to its designed embedded depth. The dimensioning of the pile is based on the maximum moment due to the static load. Nevertheless, extreme deformation and damage have been discovered close to pile toe.

The terminology, *pile toe failure* refers to the unexpected extreme deformation of the pile which is not desirable without suggesting any succeeding structural failure. *Extreme folding damage* refers to local yielding of the pile. Therefore, it could be argued that:

[1] Stadsontwikkeling

Pile toe failure of open-ended piles, given a not so dense sandy subsoil of Amazonehaven, are caused by pile driving during installation and not by the static load applied during the asset's technical lifetime.

It is then a logical conclusion which is introduced as the *hypothesis*:

Hammer-induced driving stresses are extremely high close to pile toe, exceeding material's yield stress which clarifies the *extreme folding damage*.

The *pile toe failure*, is depicted in Figure 1.2. If the hypothesis is true, a follow up would be to shift from a **static**-based pile dimensioning to a **dynamic**-based pile design, which will be studied in the technical part of the research.

FIGURE 1.2: Extreme deformation close to pile toe, retrieved from [37]

At last, the management aspects of *pile toe failure* plays an important role. Given the *extreme folding damage*, counteractions must be taken to either diminish the consequences of *pile toe failure* or to prevent the occurrence of such a failure. Both types of measurements will lead to the financial burden. The counteractions are ought necessary to sustain the designed performance level of the quay wall throughout its technical lifetime, when *pile toe failure* occurs.

1.3.1 Target group

Target groups are both SO and Allnamics, which is sponsoring this research study. The municipality, together with public and private partners, shapes and maintains the city of Rotterdam. Allnamics is a private company that provides Geotechnical advice, carries out pile measurements and produces measuring equipment.

FIGURE 1.3: Research study is made possible by above institutes

1.4 Worldwide problem

The problem of *extreme folding damage* also appears when open-ended tubular piles are driven into the subsoil, as a foundation or as a structure in itself, elsewhere in the world. In offshore practices, however, Formula 1.1 has been used to calculate the minimum wall-thickness given the diameter [1].

$$t = 6.35 + \frac{D}{100} \qquad [mm] \qquad (1.1)$$

In this formula, D is the diameter of the pile whereas t is its wall-thickness. Figure 1.4, shows deformation at pile head or pile toe due to the dynamic load, during piling, in Bioko island as well as in **Canada**. However, this study does not take into account pile head failure.

In general, to ensure pile toe integrity, it is vital to consider dynamic mold of the load. However, in the past, dimensioning of the piles were solely based on static load; nowadays a (pile) driving prediction prior to installation ensures the driveability of the piles while pile toe integrity during installation is warranted by monitoring pile driving.

FIGURE 1.4: Pile head & toe failure worldwide, retrieved from [36] and [33]

1.5 Scope

The following facts determine the scope of this research: in Amazonehaven, (1) uniaxial direction of the *extreme folding damage* close to pile toe points out installation load to be funest to maintaining *pile toe integrity*, (2) pile dimensioning was based on static load and yet *pile toe failure* have had occurred, (3) the design of the quay wall was **strategically**[2] based on a static load higher than would have happened (intended to be used), yet, *pile toe failure* have had occurred. All in all, the necessity to study the dynamic mold of the load is apparent which makes the focus to be: studying the hammer-pile-soil system of the primary pile during pile driving activity.

1.6 Research Question

Having identified the necessity to study the dynamic mold of load, the up-coming step is to study the entire hammer-pile-soil system to address the leading causes of *pile toe failure* in Amazonehaven. Moreover, the consequences of such a failure need to be discussed along with its remedies. Therefore, the primary research questions are:

1. What are the causes of *pile toe failure* in Amazonehaven?
2. What are the remedies to prevent *pile toe failure*?

[2] See [40]

1.7 Research outline

The Research into Pile Toe Failure in Amazonehaven (RIPTFIA) is divided into four parts: *commence*, *main part*, *conclusion* and *complementary*. The *commence* includes the first three general chapters, chapters 1-3. In chapters 4-8, the general identification of the problem are scaled down into Amazonehaven case study, *the main part*. The *conclusion* includes the last chapter, the results and conclusions of the previous chapters are used to generalize the case-based recommendation and suggestion for its applicability elsewhere. Finally, the *complementary* are the appendices which complements its associated chapter. Figure 1.5 shows an overview of the four main parts. In the next page, the figure is enlarged to assure readability.

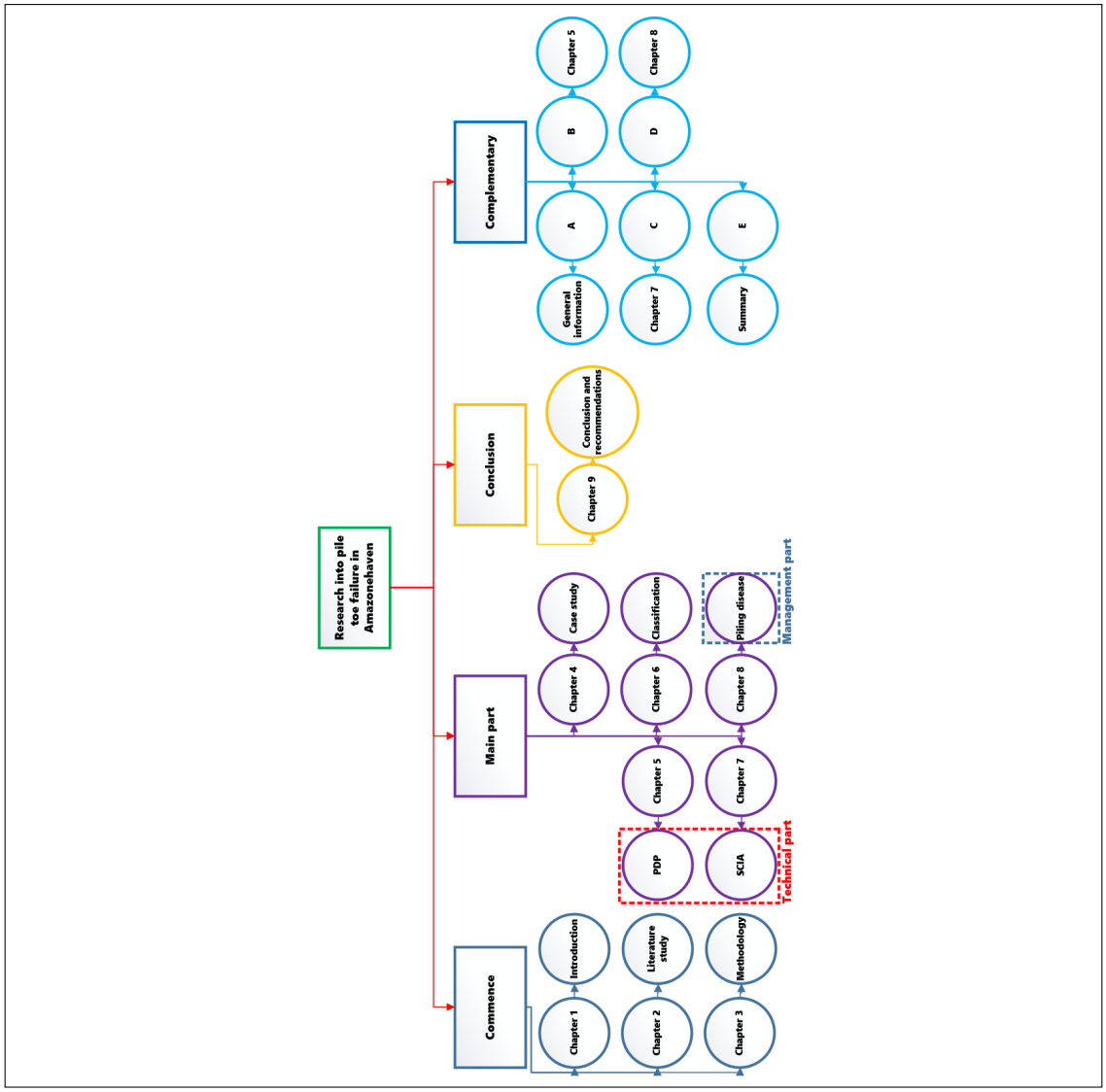

FIGURE 1.5: Overview research outline

Research into pile toe failure in Amazonehaven
Commence
Main part
Conclusion
Complementary
Chapter 1
Introduction
Chapter 2
Literature study
Chapter 3
Methodology
Chapter 4
Case study
Chapter 5
PDP
Chapter 6
Classification
Chapter 7
SCIA
Chapter 8
Piling disease
Management part
Technical part
Chapter 9
Conclusion and recommendations
A
General information
B
Chapter 5
C
Chapter 7
D
Chapter 8
E
Summary

1.7.1 Commence

Chapter 1 sketches a brief problem description of *extreme folding damage* of open-ended piles. The damage occurs during pile driving activity. Furthermore, the chapter follows with introducing a hypothesis for piling and ends up with main questions of this research.

Chapter 2, the literature, gives an overview of the existing knowledge on pile driving activities; its codes, and guidelines, the software to study two-dimensional or three-dimensional effects of the hammer-pile-soil system as well as general information about the structure of quay walls, the conducted research about the specific case study and the comparative research in piling practices.

Chapter 3 handles the methodology used to conduct the research. In this chapter, a validity map is provided which sketches the approach of the author. A validity map, as depicted in Figure 3.1, helps the reader to gain a better insight of the utilized approach in a nutshell. Furthermore, Figure 8.13 and Figure 9.1 are complementary to the validity map in this chapter.

1.7.2 Main part

Chapter 4 presents the case study Amazonehaven. Therefore, general information such as Amazonehaven quay wall design and its geological data as well as the observations and finding, after its removal; are given in this chapter. Moreover, the records and photos are analyzed, and failure modes and popular modes are introduced. It also introduces the stakeholders.

Chapter 5 studies the validity of research hypothesis by modeling the hammer-pile-soil system in a Wave Equation Analysis Program (WEAP). Moreover, it studies how extremely high hammer-induced driving stresses, exceeding the material's yield stress, could be generated.

Chapter 6 treats clusters of three main *failure sources*. In this chapter, a dozen causes of *pile toe failure* are studied and reduced to three leading causes of *the failure* in Amazonehaven.

Chapter 7 uses a Finite Element Analysis (FEA) program to conduct a sensitivity analysis to study the three causes to *pile toe failure*, concluded in chapter 6, to pinpoint the main leading cause to *the failure*.

Chapter 8 studies the Management Aspect (MA) of *piling disease* which mainly includes introducing remedies in (1) pre-piling phase and (2) post-piling phase. It also discusses the financial consequences in a decision-model in both phases. Therefore, a 4^{th} dimension to sources of *pile toe failure* is added, regarding pre-piling phase. It also gives a nutshell of the findings in this study, complementary to the validity map introduced in chapter 3.

1.7.3 Conclusion

Chapter 9, provides answers to questions and recommendations for future research. It also gives a nutshell of the findings in this study, complementary to the validity map introduced in chapter 3.

1.7.4 Complementary

Appendix A includes information about the hammer-pile-soil system as used in Pile Driving Prediction (PDP). It also holds information about the failure mode analysis and other specifications of Port of Rotterdam (POR).

Appendix B, shows a comprehensive result of PDP carried out for various scenarios, which is complementary to chapter 5 and 6.

Appendix C presents different features in SCIA Engineer. It also shows the detailed results of stress development and deformation for the models in chapter 7, given Amazonehaven D/t ratio. Furthermore, it includes a complementary fault tree to the existing fault tree for a relieving platform quay wall structure. Appendix C is complementary to chapter 7.

Appendix D reveals in-depth information about the calculation of the costs and revenues for different scenarios as discussed in chapter 8. Appendix D is complementary to chapter 8.

Appendix E gives an extensive summary of the RIPTFIA including both aspects of technical as well as management.

Chapter 2

Literature study

2.1 Aim

Chapter 2 studies the existing knowledge about quay walls, pile design, piling in offshore practices, hammer-pile-soil system, guidelines for pile design, cost of quay walls, etc. It also reveals information about five papers related to this research, see section 2.10.

2.2 General information of quay wall

2.2.1 Relieving platform quay wall structure

A quay wall is an earth-retaining structure which provides berthing spots to vessels for loading and unloading. The quay wall, separating earth and water, must withstand the lateral loads due to soil pressure and to bear the structural loads; (permanent and variable) vertical loads such as cranes [19]. To be able to carry and transfer these extremely high loads, the entire structure is designed with a firm foundation to guarantee the stability. The optimum design of quay wall is acquired by a study conducted by Municipality of Rotterdam (SO), in the past. In this *quest*, different quay walls were compared, and it is concluded that given a high retaining height, mostly the case for deep seaports, a *deep relieving platform quay wall structure* is the most optimal design [40]. A relieving platform quay wall structure is depicted in Figure 2.1.

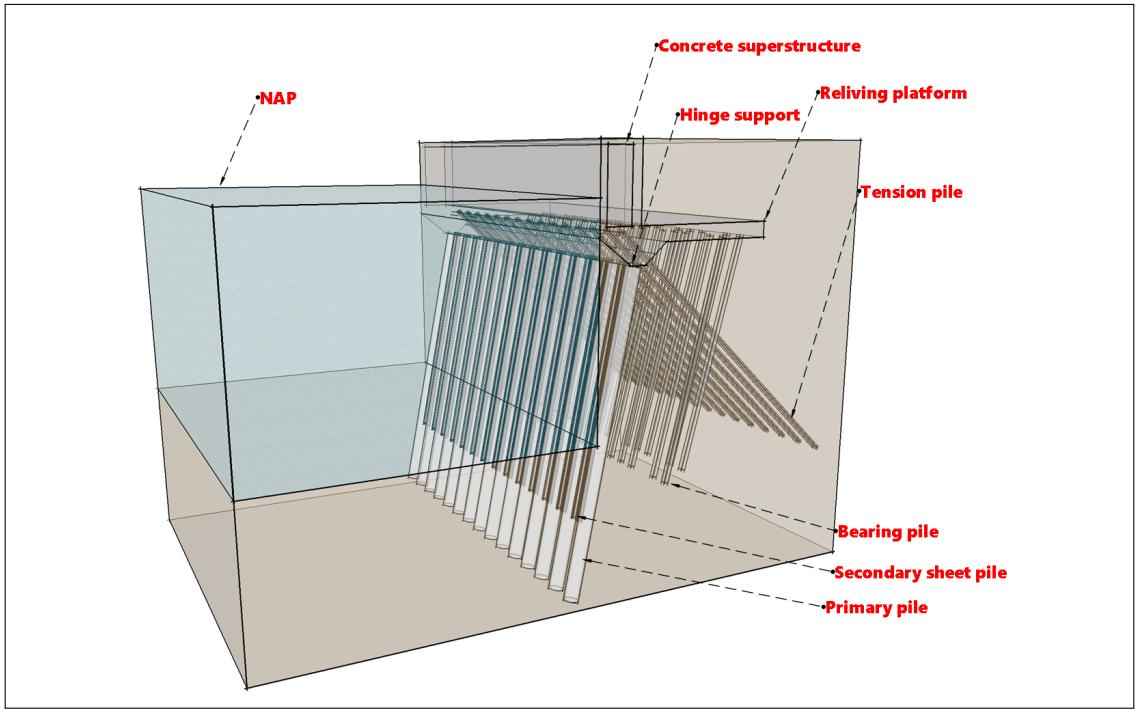

FIGURE 2.1: Cross-section of low relieving platform quay wall structure, used SketchUp

In general, the type of quay wall to be designed is selected based on geological conditions, functional requirements and budget available for the project [19].

2.2.2 Foundation elements

The foundation of a quay wall, guaranteeing the stability, consists of two rows of prefabricated concrete (compression) piles and one row of steel (tension) piles at the land side. At the water side, the relieving platform is resting on a retaining and bearing wall; a combined wall system. The crane track is usually located above the retaining wall to enable transferring the heavy load via the retaining wall to the subsoil. The retaining wall, as well as the concrete bearing piles, are inclined, which means that the structure is leaning on the ground. The inclination of the foundation elements reduces the anchor force which is needed for the stability of the structure. The steel (tension) piles, [**M**üller **V**erfahren] piles, carry the rest of the horizontal anchor- and soil- forces from the superstructure. More advantages of inclined foundation elements are: (1) a reduction in horizontal soil pressure and (2) a reduction in bending moment [40].

Super- & sub- structure

The weight of the relieving platform and the overlying soil is directly carried out by the concrete bearing piles into deep soil layers with enough bearing capacity. Therefore, a reduction of vertical loads on the combined wall system occurs. The **combined wall system** is a combination of open-ended tubular *king* piles, also known as massive primary piles, and the intermediate sheet piles, see Figure 2.2.

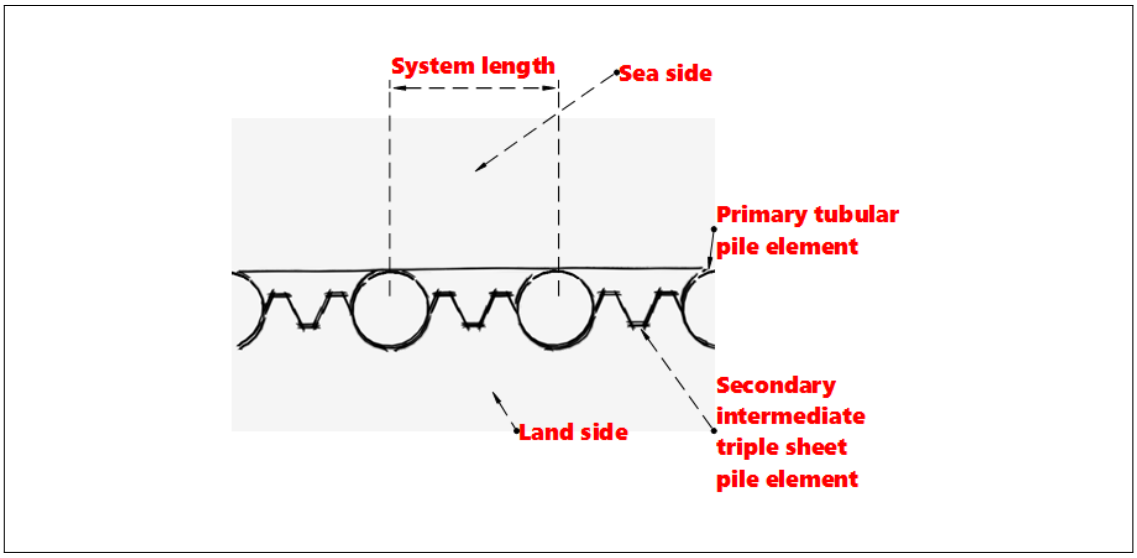

FIGURE 2.2: Top view cross-section of a combined wall system, used SketchUp

The distance between two primary piles is called system length. The primary king piles are partly vibrated and partly driven up to its embedded depth. The secondary light intermediate sheet piles are only vibrated nowadays. The vital role of king piles is to transfer vertical and horizontal loads to soil strata capable of bearing those loads where the intermediate sheet piles function as soil-proof elements and transfer soil pressures to primary piles by arch action. Due to arch action, developed by the fact that rigid parts catch more load, the active earth pressure on the secondary sheet piles reduces significantly [19]. Therefore, intermediate sheet piles are much shorter than the primary piles.

2.2.3 Design requirements and boundary conditions

Functional & technical requirements

A quay wall must fulfill its core functions of (1) retaining, (2) bearing, (3) navigational and (4) safety. Retaining, as mentioned earlier, is the ability of the quay wall to withstand water and to keep the soil. The bearing is transferring the heavy loads exercised on the quay wall to deep soil layers with sufficient bearing capacity. A navigational feature of the design fulfills requirements for vessels to moor; to be loaded and unloaded. Safety function refers to the security of the entire structure against flooding as well as its safety during operation.

The *technical requirements* of the quay wall refer to technical design enabling the quay wall to perform its function during its technical lifetime. The requirements include the structural loads such as terrain loads, berthing- & bollard- loads as well as soil and water pressure, lateral loads [19].

Nautical requirements

Nautical requirements refer to regulations about maneuvering and mooring of the inland- and sea- vessels entering the port area. The regulations are set for both the seaport area and the vessels. Therefore, the requirements influence the design concept from the very beginning [19].

Geo-technical & hydraulic boundary conditions

Geotechnical boundary conditions refer to the very composition of subsoil at the location of the project. A thorough soil investigation is crucial for defining the soil composition, and the bearing capacity which is vital for a proper design and a smooth execution work.

The *hydraulic boundary conditions* refer to the hydraulic environment of the location of the project. The boundary conditions are, e.g., the exceeding frequencies for high and low water levels used to design the height of the quay wall, the groundwater levels, and the waves in the area used to design the irrigation system [19].

2.2.4 Loads on the combined wall

Structural loads

Structural loads on the quay wall are divided into *lateral loads* and *horizontal & vertical loads*. Lateral loads refer to horizontal loads due to earth- and water- pressure on the combined wall system. Horizontal & vertical loads apply to other forces acting on the superstructure as well as on the substructure which should be taken into account when designing the combined wall system. These loads are from crane, berthing, surcharge, terrain, bollard. Also, the weight of the superstructure and the overlying soil layer is considered as structural loads [19]. When dimensioning the king pile, the moment due static load is governing and determines the D/t ratio. Where D is the diameter- and t is the wall thickness- of the pile.

Installation load

The open-ended tubular piles are installed with the aid of an impact hammer and a vibratory driver. The vibratory hammers operate with electric power which functions on a principally different way than the impact hammer. Impact hammers include a diverse range of hammers: a drop hammer, steam or air hammer, diesel hammer and hydraulic hammer [60]. The dynamic load, due to installation, is either a sinusoidal load in the case of vibratory driving or a dynamic load for an impact hammer. When piles are dimensioned due to installation load, the governing force will be the one due to impact hammer.

2.3 Cost of quay wall

2.3.1 Key figures

To have an estimation of the cost of quay walls for a preliminary design; the key figures are usually utilized. In this fashion, different designs could be compared to one another. Table 2.1 shows the costs per running meter per **R**etaining **H**eight (RH) of the quay wall.

TABLE 2.1: Key figures cost of quay wall per retaining height per meter, retrieved from [18]

Retaining Height [m]	Cost per Retaining Height [m^1]
5-10	300-600
10-20	600-900
20-30	900-1200

The retaining height is determined as the difference between the construction depth and the ground level. The overview does not include the costs of scour protection, fencing, and dredging at the front of the quay. Furthermore, for a relieving platform quay wall structure, the following cost division could be made as depicted in Figure 2.3.

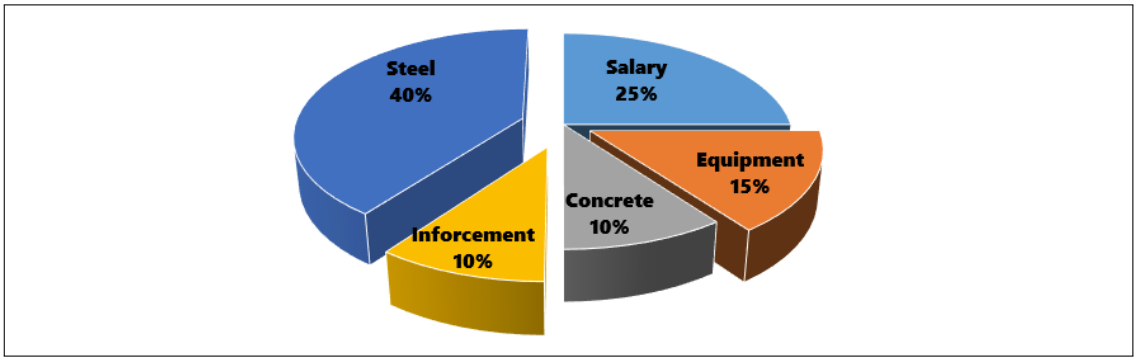

FIGURE 2.3: Division in construction cost of a relieving platform quay wall structure, retrieved from [18]

2.3.2 Quay walls in Rotterdam

The total cost of a quay wall structure in Rotterdam, mainly have a relieving platform, is expressed in following formula [18]:

$$TC = 793.65 \cdot RH^{1.2174} \cdot L \qquad [€] \qquad (2.1)$$

Where, RH is the retaining height of the quay wall, and L is the length of the quay wall. The Total Cost (TC) of the quay wall is presented in Figure 2.4, for increasing retaining height per running meter, in which the two primary formulae are compared, based on equation 2.1, Table 2.1.

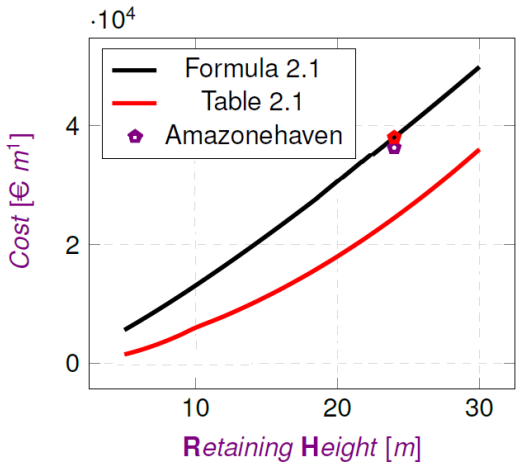

FIGURE 2.4: Cost of quay wall per retaining height per meter, retrieved from [18] and [39]

The Amazonehaven quay wall structure had a retaining height of 24 [m], which brings the red dot if using the Formula 2.1. However, when the cost of Amazonehaven quay wall, as documented, is used the costs are slightly lower as shown with a violet dot.

2.3.3 Net present value

The cost of building a port infrastructure depends on several components [18]. To make a decision, additional to technical considerations, an economic evaluation of different technical designs must be available. Then, a selection is made for the most economical design. To do so, several methods are available. The Net Present Value (NPV) is most widely used method, to evaluate the financial aspects of infrastructural projects. NPV discounts the costs and revenue flow for a project based on the technical lifetime of the asset and the interest rate at the Present Value (PV). Therefore, construction costs, maintenance costs, and demolition costs are calculated based on the initial costs (investment) [18]. When $NPV > 0$, profit is generated meaning the project is worth starting, and financial feasibility is warranted. Therefore, the TC could be expressed as:

$$TC = I_0 + \sum M_i + D \qquad [€] \qquad (2.2)$$

Where the I_0 is the initial costs to build a structure. A sum of **P**lanning **D**esign and **E**ngineering cost and construction cost. The maintenance cost, $\sum M_i$ are those which must be met to ensure that the required functionality is maintained per year. The last term, D, is demolition cost which arises at the end of the technical lifetime of the asset.

2.3.4 Costs

The amount of maintenance cost as well as demolition cost could be expressed in investment cost by following Formula 2.3 [18]:

$$TC = I_0 + 0.01 \cdot I_0 + 0.175 \cdot I_0 \qquad [€] \qquad (2.3)$$

Whereas in terms of PV it becomes, Formula 2.4:

$$PV = I_0 + \left(\frac{0.01 \cdot I_0}{r}\right) \cdot \left(1 - \frac{1}{(1+r)^t}\right) + \frac{0.175 \cdot I_0}{(1+r)^t} \qquad [€] \qquad (2.4)$$

Where r is the interest rate per year, and t is the technical lifetime of the asset.

2.3.5 Revenues

The main revenues of the Port of Rotterdam Authority (PORA) are both leasing of the land to the companies erecting in the vicinity of water and waterborne facilities to guarantee a safe and fast transfer of their goods as well as sea-Port Dues (PD). The latter depends on the (1) number of vessels, (2) their dimensions, (3) number of days staying at the harbor, and (4) the cargo being carried. Figure 2.5 depicts the revenues per Leasing Contract (LC), PD as well as other revenues of the Port of Rotterdam (POR) based on recent years.

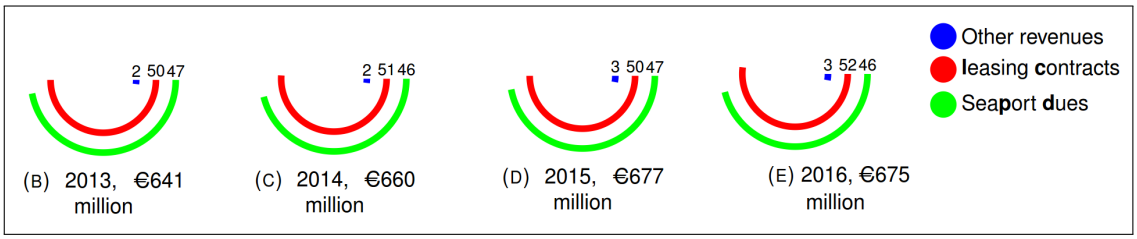

FIGURE 2.5: Revenues POR in recent years, retrieved from [46]

2.4 Stakeholders

The stakeholders in POR, are defined based on the functions assigned to the quay walls. Figure 2.6 shows the storage function per area for the entire port, which are: containers, dry bulk, refinery, wet bulk, distributions spots and other activities. The Amazonehaven quay wall is mainly home to containers, dry bulk, and refinery. Beside Amazonehaven, a total number of 16 locations, are used to store dry bulk goods over the entire harbor [46].

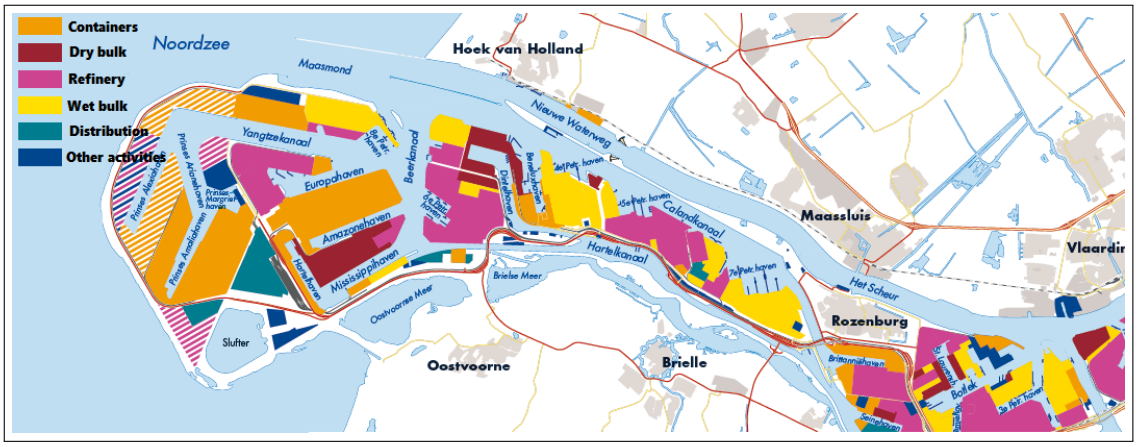

FIGURE 2.6: Functions of quay walls in Rotterdam harbor, retrieved from [46]

2.5 General information design codes and guidelines quay walls

The design of quay wall must be based on requirements and conditions determined in Eurocode. Since the introduction of Eurocode, this guideline is mandatory in the Netherlands. However, other guidelines are also applied, e.g., quay wall manual, Empfehlungen des Arbeitsaussschusses Ufereinfassungen (EAU), CUR166.

2.5.1 Design codes

In *EN 1993-5 (2007) (English)* ***Eurocode 3****: Design of steel structures - Part 5*; Piling, principles and implementation rules for the structural design of bearing piles and intermediate sheet piles are provided. It also includes some examples of detailed foundation and retaining structures in onshore practices.

2.5.2 Guidelines

In **CUR166** various types of *steel sheet piling* structures with anchoring systems are covered. It also examines other alternative structures including a diaphragm wall. Handbooks 1 & 2 of *sheet piling* structures include all information needed for design, implementation and management of those structures [7]. **CUR 211**, new edition of quay walls, outlines essential knowledge for planning, design, execution, and maintenance of quay walls, as well as general information about historical developments and lessons learned from the observations of ports in various countries [8]. In EAU the so-called waterfront structures are handled such as: scour protection, sheet pile walls, anchors, pile foundations, embankments and mooring piles [34]. In this design guideline, load combinations of frequently appeared loads and circumstances of extreme loads are defined. EAU is a *extensively experienced-based* guideline which is still frequently used in The Netherlands.

2.5.3 Other manuals

American Petroleum Institute (API) has introduced design codes for pile dimensioning and associated installation activities for offshore practices, based on many research in America, which is now used as a guideline worldwide [1].

Basics of foundation design presents a background to current foundation analysis and design. It is a compendium of the contents of courses in foundation design given by Fellenius as well as a document to the software UniSoft Ltd. The latter is an application for the analysis of piles and pile groups according to various design methods. It considers bearing capacity, pile group settlement, negative skin friction, and drag load.

Roark's formulas for stress & strain presents a summary of methods, facts, and principles regarding the strength of materials [63].

2.6 General information hammer characteristics

2.6.1 Hammers in general

In general *impact* hammers and *vibratory* drivers are used as a tool to bring foundation elements into its prefixed penetration level. The main differences between these two type of hammers are [27]:

1. a high peak force and a low frequency for the impact hammers, whereas vibratory drivers have a low peak force with a high frequency. Therefore, a respectively short, milliseconds, load duration and a long load duration is to be expected.

2. a constant energy supply for the vibratory hammer, whereas for the impact hammer the energy supply varies depending on the soil reaction and drop height. The intensity of the force is respectively expressed in [kN] and [MPa].

3. a *soil over-stressing* phenomenon occurs due to the transfer of a high-level stress wave into the pile by impact hammer, while *Soil stress relief* phenomenon happens due to the transfer of permanent energy pulses to the soil by vibratory hammers.

4. the weight of the pile plays a minor role for pile driving by an impact hammer, whereas for pile penetration by a vibratory hammer, the weight of the hammer and the pile are the main factors contributing to penetration.

Furthermore, the pile driveability is a function of the cross-section, length, shape and (steel) quality of the pile as well as the applied load on the pile, the duration of the applied load, the implemented installation method and the soil properties [23]. However, there are guidelines available for hammer selection based on the minimum and maximum hammer energy (1) to not damage the pile nor the hammer and (2) to bring the pile to its required depth. **C**anadian **F**oundation **E**ngineering **M**anual (CFEM), API and **CRAPPS** are guidelines commonly used.

2.6.2 Driving hammer

Moreover, a driving cap is used for impact hammers to transmit the blow directly to the pile while protecting the hammer and the pile head. Also, cushions are used which is fitted into the driving cap. It absorbs the blow partially and prevents damage to both the hammer and the cap. Cushions are built with plastic or wooden components, with a combination of steel cables and steel plates that ensure a reasonable life expectancy and also helps to dissipate the generated heat quickly. When hard driving is experienced, the cushion has to be replaced more often than under normal conditions [38].

2.6.3 Soil reaction

During vibration, the soil strength temporarily changes to a lower level, which means a considerably less resistance to penetrating the pile into the ground compared to another sort of hammer or a static load applied on the pile. However, the reduction of soil resistance depends on the: frequency of the vibratory hammer, its operating amplitude, the soil characteristics, the degree of soil saturation, etc. [27]. After which, impact driving, ensures the deeper penetration of the pile into the subsoil to be able to reach the required bearing capacity. Therefore, a combination of vibratory driver and impact hammer is utilized in piling industry.

2.7 General information steel properties

2.7.1 Mechanical properties

The stress-strain diagram shows the mechanical properties of steel, differentiated in four main stages: elastic, plastic, condensation and congestion, as depicted in Figure 2.7.

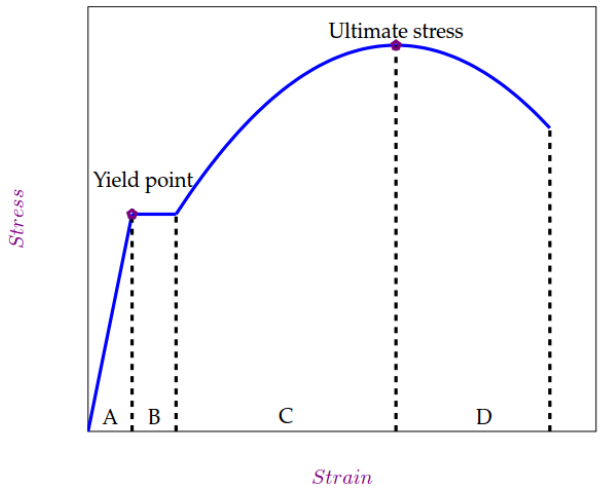

FIGURE 2.7: Stress-strain diagram of steel, retrieved from [59]

In other words, the magnitude of the material's extension given an applied stress is shown. In the first stage (A) the material deforms elastically, whereas in the last three stages it deforms plastically, a continuous deformation. In the last stage (D), the material collapses.

In the first stage (A), the *ut tensio, sic vis* rule of Hooke applies, which means that the strain is proportional to the applied stress. Equation 2.5 shows the linear relationship, where E is the modulus of elasticity [MPa], ε and σ are respectively the strain and the stress. An increase in stress above the elasticity limit will lead to a take-off of material's plastic journey. The specific stress at that point is called material's yield stress, σ_y [N/mm^2] [59].

$$\sigma = E \cdot \varepsilon \tag{2.5}$$

Where $\varepsilon = \Delta L / L_0$.

A description of some mechanical properties of steel is given below:

Elasticity

Elasticity refers to material's ability to jump back to its original state when the applied load is taken away. Therefore, in an elastic trace, the deformation is temporary. When the nature of the deformation is not anymore elastic, it then shows plastic behavior. The material could behave soft or stiff based on their elasticity. The soft material extends very fast where a stiff material does not [59].

Tensile strength

Another mechanical property, tensile strength, is where the maximum load could have been applied into the element. When the tensile strength is reached, soon the two other stages of condensation and congestion will follow. A strong material can bear more load than a weak one [59].

Toughness versus brittleness

Toughness and brittleness refer to the behavior of the material regarding collapsing, while the tensile strength of the material has reached. A brittle material, such as glass, collapses immediately after it has reached its tensile strength. Contrary to a brittle behavior, a robust behavior shows congestion before collapsing [59].

2.8 General information soil characteristics

2.8.1 Soil particle

The soil is classified into various types with distinct mechanical properties [61]. The general subdivision of soil is based on the grain size of the particles. A coarse granular material is called gravel, and finer material is called sand. The grading is shown in Table 2.2.

TABLE 2.2: Grain sizes, retrieved from [61]

Type	Min [mm]	Max [mm]
clay	-	0.002
silt	0.002	0.063
sand	0.063	2
gravel	2	63

The mechanical behavior of various types of soil is somewhat different. Clay is usually much less permeable for water than sand, but it is also much softer. Peat is very light (sometimes hardly heavier than water), and actively non-isotropic because of the presence of fibers of the organic material. Peat is also very compressible. Sand is slightly permeable and stiff, especially

after a certain pre-loading has taken place [61].

2.8.2 Soil analysis

To have a proper soil analysis, accurate identification of soil properties, a soil investigation must be carried out. Therefore, either an in-situ operation, e.g., Cone Penetration Test (CPT) or a laboratory soil investigation is carried out (or both). In-situ soil investigation is executed with a simple method: by pushing a steel rod into the soil, then, measuring the force during the advancement of the rod as a function of depth. The (counter) force is the soil reaction at the toe, also known as cone resistance, as well as the friction along the circumference of the rod [61]. Nowadays an electrical penetration test measures cone resistance and local friction as well as pore pressure.

2.8.3 Soil features

Soil sensitivity & set-up

Soil *sensitivity* and soil *set-up* are essential soil characteristics when determining the penetration rate of the pile. The set-up is predominantly associated with an increase in soil resistance acting in the sides (shaft) of a pile. The majority of set-up is related to (1) dissipation of excess pore water pressure (phase I) and (2) remolding and re-consolidation (aging) of the soil (phase 2) [28]. The duration of set-up in phase I depends on (a) permeability of the soil and (b) volume of the displaced soil by the pile. It is evident that the more impermeable the soil and the larger the pile, the longer the set-up period will become. In Research into Pile Toe Failure in Amazonehaven (RIPTFIA), soil set-up refers to the first reason, dissipation of excess pore water pressure (during driving).

In case set-up is present, cohesive soil like clay, the soil resistance during driving becomes lesser than the long-term capacity of the pile [30]. Therefore, set-up due phase I might appear after several weeks, several months or even years. In case of sand, permeable soil, there is almost no set-up (max. several hours) and therefore immediately after driving, the driving resistance would be more or less the same as the long-term capacity of the pile[1]. In mixed soils[2], however, the set-up due to phase I will appear in several days or several weeks [28].

A set-up factor, determined during driving test piles, is usually used in the calculations [30]. An advantage of taking soil set-up into account is a reduction in the size of driving equipment (both hammers and cranes) leading to cost savings [28].

The soil sensitivity determines the speed at which the soil start to regain its original strength. Thus, soil sensitivity would accelerate the time soil needs to set-up[3]. The importance of soil sensitivity becomes apparent in case of a halt in piling. Usually after a *delay* in piling, about 15 days, the soil resistance becomes higher and reaches the long-term capacity of the pile [30]. Re-driving after a delay could be troublesome regarding a decrease in penetration rate and an increase in blow count. Therefore, it is highly recommended to have a continuous pile driving activity.

Soil quake

A parameter of substantial importance for the drive-ability of the pile is *quake*, which is the movement between pile and soil required to mobilize full plastic resistance [15]. In other words, quake is the displacement at which the initial (elastic) static soil model achieves its ultimate load and goes plastic [31].

[1] phase I: driving-induced excess pore-water pressure dissipates relatively rapidly
[2] a mixture of fine-grained granular and clay soils
[3] reaching its full capacity

The value of quake is usually small, about 2 [mm] to 3 [mm], along with the shaft. The value depends on the soil type and is independent of the pile dimension. In contrast to the shaft, quake is a function of pile diameter at pile toe with a value of about 1% of the diameter. However, the range of values can be as broad as 10% of the pile's diameter [15]. Therefore, the ultimate capacity in which a hammer reaches its refusal driving might be reduced due to quake value (a larger hammer is needed). In this case, a capacity reduction by a factor of three is easily obtained: as the quake increases, the capacity reduction becomes larger.

Thus, given a maximum toe displacement, a pile with a normal quake will have a much larger permanent set (lower blow count) than a pile with a large soil quake. Conversely, to obtain the same blow count, a pile with a large soil quake will require a more substantial displacement. Therefore, more energy is required to mobilize the full resistance for high quake soils [31]. The more significant quake value, the more energy is required to move the pile which means less energy is available to overcome the static soil resistance.

In *plugging research*, the importance of quake values, in piling is discussed. In this paper, the observed *high quake* values are argued to be caused by excess pore water pressure, caused by displacement piles driven into poorly drained soils [31].

Plugging

Plugging is determined as open-ended pile responding nearly the same as a close-ended pile. In a plugged response, the pile has to over-win more soil resistance to sustain its advancement. In this fashion, the toe resistance acts not only on the pile's wall-thickness, but it seizes the entire diameter of the pile. Therefore, assuming a warranted pile toe integrity, plugging could occur in case of a small pile dimension or a cohesive soil or both [23].

During driving, when pile toe integrity is warranted, the open-ended pile toe shovels the same amount of soil inside and outside the pile. However, in case of any (initial) toe damage; more soil is shoveled outside the pile than it is inside. Therefore, a clamped soil just outside; together with an absence of soil inside ensures a lateral soil pressure acting inwards. The pile toe gradually deforms inwards, during piling, which leads to a semi close-ended pile response [32].

The moment plugging is gradually developed during installation, depending on the soil type, is when the shear stresses inside the pile are equal to the resistance of the subsoil. In **plugging research**[4], this static equilibrium is calculate to estimate the moment the plugging commences during installation, and is expressed in *plug length* per different subsoil [13]:

- Clay: $h = 6.25 \cdot D_i$ $[m]$
- Sandy clay or clay-containing sand: $h = 16.67 \cdot D_i$ $[m]$
- Sand: $h = 18.75 \cdot D_i$ $[m]$

where D_i is the inside diameter of the pile. Therefore, the *plug length* is shorter for clay, plugging starts earlier, or piles with a smaller diameter. Moreover, the *plug length* is larger for sand, plugging begins later, or piles with a larger diameter.

2.9 General information software

2.9.1 Wave Equation Program

A Wave Equation Analysis Program (WEAP) enables studying the entire hammer-pile-soil system by considering the whole pile driving system, such as wave propagation characteristics, particle-velocity dependent aspects (damping), soil deformation characteristics, soil resistance, hammer behavior, and hammer cushion & pile cushion parameters [15].

[4] See [13]

Nowadays, the full power of a WEAP is realized by combining the study program with a monitoring system of pile driving. The monitoring system consists of recording and analyzing the hammer-induced strain and acceleration in a pile by attaching sensors close to pile head [15].

GRLWEAP

GRLWEAP is indicated as a one-dimensional WEAP that simulates the pile response to pile driving equipment [41]. GRLWEAP predicts driving stresses, hammer performance as well as the relation between pile bearing capacity and (net) set per blow. It also estimates the total driving time. Therefore, the designer could select a hammer which is most likely sufficient and economical for an absolute pile and soil condition before moving the installation equipment to the site [41].

AllWave programs

AllWave Pile Driving Prediction (PDP) is based on the Method of characteristics for one-dimensional stress waves. PDP enables studying the stresses due to driving load along the pile. Also, other relevant parameters such as Soil Resistance to (pile) Driving (SRD), blow count, driving time, soil fatigue [10]. However, a complementary Pile Driving Analysis (PDA) (Allnamics-PDADLT), monitoring system, is needed to make measurements of force and acceleration close to pile head during driving. PDA enables processing the registered data to determine the soil parameters more accurately to adjust default values in PDP which occurs by signal matching. In this way, the static soil resistance acting on the pile is more accurate. Also, PDA warrants *pile toe integrity* during (pile) installation.

2.9.2 Finite Element Analysis Program

Finite Element Analysis (FEA) program is a computerized method for predicting the reaction of a product to real-world forces, vibration, heat, fluid flow, and other physical effects. FEA shows whether product breaks, wear out, or works the way it was designed for [2]. There is a range of different software that could be employed such as PLAXIS, ABAQUS, ANSYS, DIANA, SICA Engineer. FEA works by breaking down a real object into a large number (thousands to hundreds of thousands) of finite elements, such as little squares. Mathematical equations help the behavior of each element; all the individual responses are added to predict the behavior of the actual object [2].

SCIA Engineer 2D/3D

SCIA Engineer is an integrated, multi-material structural analysis and design software for various types of structures. It is widely used in various construction types: office buildings, industrial plants, bridges, hydraulic structures [49]. In addition to a mesh generator and finite element solver, it features integrated tools to check or optimize the structure to a variety of building codes [49].

DIANA 3D

DIsplacement **ANA**lyzer (DIANA) is a multi-purpose finite element software package that is used to model a wide range of structures in civil engineering [11].

PLAXIS 2D/3D

PLAXIS is another FEA package intended for analysis of deformation and stability in Geotechnical engineering and rock mechanics. Its application ranges from excavations, embankment, and foundations to tunneling, mining and reservoir Geo-mechanics [42].

2.10 State of the art

To study the *extreme folding damage* within a hammer-pile-soil system, information about the hammer-characteristics, pile-properties, and soil-features are of importance. Therefore, five related articles are briefly touched on in this section. In the end, a *statement* is given about the significant findings which are utilized in RIPTFIA.

2.10.1 Stability analysis quay structure at the Amazonehaven port of Rotterdam

In the ***stability research***, the focus is on the stability of the Amazonehaven deep seaport quay wall, given the *pile toe failure*. In this fashion, following questions are answered [37]:

- What is the structural stability of the deep-sea quay structure throughout its functional service lifetime, specifically the combined wall?
- How (un)safe was the quay-structure if it had been exposed to the full surcharge (design load)?

In *stability research*, the *pile toe failure* is modeled as shorter king piles and compared to the calibration model[5]. The model includes one section of 45 [m]. It shows that regardless the reduction of safety factor due to *pile toe failure*, the stability of the section is warranted. In any case, the impact of *pile toe failure* on the stability of the quay wall is apparent due to the large displacement of soil as well as an increase at the moment and a decrease in anchor force [37]. It concludes:

> The total displacements for model 2B are three times larger than the calibration model. This indicates that the opening in the combined wall will influence the displacement of the soil. Besides, the moment will increase by almost 1.8 times moment of the calibration model. Because of the increase at the moment, the anchor force will decrease by 0.4 times the anchor force of the calibration model.

Where model 2B is described as a model most similar to the reality whereas the calibration model is the same as the original design of Amazonehaven quay wall. The *stability research* is conducted using PLAXIS, a FEA program.

A threesome of reasons could have contributed to maintaining of the stability of the *quay wall structure*:(1) the designed capacity of the quay wall has not been reached during its technical lifetime, (2) the soil in front of the combined wall was not excavated up to the designed construction depth, (3) the design of the quay wall was strategically based on storing a heavier material than it was intended to be used for and (4) the design of the quay wall was based on a deterministic approach. Also, the *stability research* has been based on the deterministic[6] design which is a conservative design.

2.10.2 Onshore and offshore pile installation in dense soils

Three cases in piling in dense soil, both onshore and offshore cases, are presented. The main reasons of *extreme folding damage* during piling are: inappropriate hammer, insufficient cushion, misalignment between hammer and pile, heavy driving, the presence of stiff soil layers and concentrated soil resistance (inhomogeneous layer) [25].

In ***installation in dense soil paper***, it is concluded that when piling in a very dense soil comprising cobbles or boulders: (1) the maximum driving stress at the pile head and toe must remain below $0.5 \cdot F_y$ where F_y is the specified material's yield strength, (2) the pile diameter to thickness ratio, D/t, should not exceed 32 providing that the rated hammer energy is less than

[5] The design of quay wall
[6] EAU

3000 [kJ] times the pile cross-sectional area, (3) a thorough soil investigation must be carried out beforehand piling to identify any stiff layers or composition of boulders in the subsoil. It argues that when the recommendation mentioned above is taken into account, the piling disease as *extreme folding damage* is to be reduced, though not eliminated entirely [36].

2.10.3 A study of pile fatigue during driving and in-service and of pile tip integrity

In the second section of ***pile toe integrity report***, mechanisms of pile toe buckling are pinpointed in some formulas, which are taken from classical mechanics and published work on pipeline buckling [32]. It argues that due to lack of methodology in public domain for examining the possibility of pile toe failure, the classic mechanic's formula is used. It argues that during pile installation following pile toe failure might be postulated [32]:

- pile toe local buckling due to high stresses close to toe
- classical ring or shell buckling under lateral pressure
- ovalization of the initially imperfect tubular pile under lateral pressure
- enlargement of the initially dented pile, under the action of lateral soil pressure

2.10.4 Development of a screening tool for impact hammer selection for installation, testing and damage mitigation of steel pile and H-piles

The ***screening tool paper*** brings forward the importance of a sufficient hammer selection regarding pile installation. It compares the recommended hammer energy, momentum and ram weight limits regarding various guidelines. The most used guideline is the API which introduce a maximum limit for ram energy given a specific D/t ratio. In this guideline a minimum wall-thickness t of:

$$\frac{D}{100} + 6.35 \qquad [mm] \qquad (2.6)$$

is suggested for a sustained hard driving given a design set criteria of 250 blows per 300 *milimeters* [1]. However, *screening tool paper* recommends to use API energy threshold and wall-thickness criteria regarding hammer selection; though, to be cautious to use the termination resistance criteria[7] suggested by API [55].

2.10.5 Stability of spiral welded tubes in quay walls

In ***welded tubes paper*** the focus is on the experimental *local buckling* of spiral welded open-ended tubular piles, after partial yielding of the cross-section has occurred. It argues that a strain-based design gives a better insight into strength as well as the deformation capacity of the pile [24]. The conventional stress-based design for king piles, regarding *local buckling*, lead to uneconomical design [24].

Furthermore, it discusses the existence of a regular pattern of imperfections due to cold forming with roller during the production of the tubular piles. It also discusses the existence of residual stresses due to production. However, *welded tubes* paper concludes that the *local buckling* has not been occurred at those imperfection spots in a spiral welded tubular pile [24].

[7] Design set criteria

2.10.6 Statement

A brief description of findings of the research mentioned above was discussed, relevant to this study. The principal matters are: (1) The importance of *pile toe failure* in reducing the capacity of the quay wall and probably endangerment of the asset's stability[8], though not an immediate collapse, as discussed in ***stability research***. (2) The importance of a thorough soil investigation beforehand piling due to the existence of concentrated soil resistance which would endanger maintaining *pile toe integrity* during piling, as discussed in ***installation in dense soil paper***. (3) The importance of considering (a) local buckling due to high stresses, (b) shell buckling and ovalization due to lateral pressure and (c) enlargement of the initially dented pile due to lateral pressure; during piling as discussed in ***pile toe integrity report***. (4) The importance of hammer-selection to drive the piles into the required embedded depth as highlighted in ***screening tool paper***. (5) The importance of any effects of the residual stresses and the manufacturing imperfections in a pile; on the capacity of the pile as discussed in ***welded tubes paper***.

[8] if no actions are taken

Chapter 3

Methodology

3.1 Aim

Chapter 3 presents the methodology used in Research into Pile Toe Failure in Amazonehaven (RIPTFIA). The problematic of *pile toe failure* is studied in an integrated approach including two disciplines of Hydraulic Structures and Flood Risk (HSFR) and Construction Management and Engineering (CME). The first covers the technical part of the *problem* whereas the latter studies the Management Aspect (MA) of the *problem*. Each discipline is divided into steps which lead to the contrived sub-questions, to be answered. When the sub-questions are answered, a sufficient answer could be given to the main research questions. At the end of this chapter, a validity map shows the steps taken and gives the opportunity to the experts to discuss the applied approach for *pile toe failure* investigation.

3.2 First level

In the first level, the problem is outlined as *extreme folding damage*, which seems logical due to extreme deformation as observed close to pile toe. Furthermore, *extreme folding damage* is argued to have been caused due to dynamic load at the pile, during installation. The technical part of the research will provide answers with this regard.

The management part of the *pile toe failure* aims a different problem description. In this part, the *pile toe failure* is described as a *piling risk event* and a *piling disease* to be treated. The risk event could either be prevented or its consequences could be reduced, though it will have financial consequences for the client. Therefore, solutions need to be outlined in pre-piling or post-piling phase. Furthermore, a decision-model based on Net Present Value (NPV) will help the client to select the economical solution. It is believed that process-based alternative as introduced if implemented in pre-piling phase, would diminish the probability of occurrence of *the failure* with minimum financial consequences.

3.3 Second level

In the second level, the study of *pile toe failure* is pursued by looking into (1) observations, (2) static load and (3) dynamic load. In observations, a recent research about the stability of Amazonehaven's quay wall is central. The collected information in the *stability research* is used and analyzed carefully.

Stability analysis quay structure at the Amazonehaven port of Rotterdam, studied the static load applied on the quay wall, given the *pile toe failure*. Therefore, the static load was central. However, RIPTFIA focuses on the dynamic load applied on the king pile during its installation. The stress development due impact hammer is studied, taking into account the hammer-pile-soil interaction.

Sub-questions which arise in this level consider **causes** and observations:

Technical questions

What are the finding & observations of *pile toe failure* in Amazonehaven? - See chapter 4.

What are the causes of *pile toe failure* in general? - See chapter 6.

3.4 Third level

In third level, the dynamic load applied on the pile is analyzed. By using Pile Driving Prediction (PDP), the *hypothesis* in chapter 1 is validated:

> Hammer-induced driving stresses are extremely high close to pile toe, exceeding material's yield stress which clarifies the *extreme folding damage* (in Amazonhaven).

Furthermore, it studies, (1) the stress development due impact hammer in the pile (PDP), (2) the classification of the reasons to *pile toe failure* (3) a sensitivity analysis given the main reasons of *pile toe failure* (SCIA) and (4) the management aspect of *pile toe failure*. In the management part the *piling risk event* is introduced.

3.5 Fourth level

In the fourth level, a detailed bifurcation of the second level is included. The reasons for *pile toe failure* are classified and categorized. Furthermore, remedies are studied to diminish *piling risk event*, in pre-piling phase, or to counteract its consequences during asset's technical lifetime.

Sub-questions which arise in this level consider both **design** and **management aspect**:

Technical questions

How harmful has the *pile toe failure* been for the Amazonehaven asset? - See chapter 2.

Should the dimensioning of primary king piles be based on a dynamic mold of load? - See chapter 5.

What would be suggested for pile's D/t ratio based on the dynamic load? - See chapter 5.

Management aspect (of pile toe failure)

How could the process be improved to reduce or avoid the *pile toe failure*? - See chapter 8.

What are the costs of extra measures, in design- and construction- phase, to improve the process? - See chapter 8.

How much are the Loss of Earnings (LOE) for Amazonehaven, due increasing Percentage Problematic Section (PPS)? - See chapter 8.

Who are the stakeholders of Amazonehaven? - See chapter 4.

Who is the responsible party to bear the cost for the *pile toe failure*? - See chapter 4.

What are the wake-up calls of Amazonehaven *pile toe failure* worth introducing into piling industry? - See chapter 9.

3.6 Validity map

Figure 3.1 shows a validity map depicting the above mentioned levels in a nutshell. Furthermore, Figure 8.13 and Figure 9.1 are complementary to the validity map as presented below. In the next page, the figure is enlarged to assure readability.

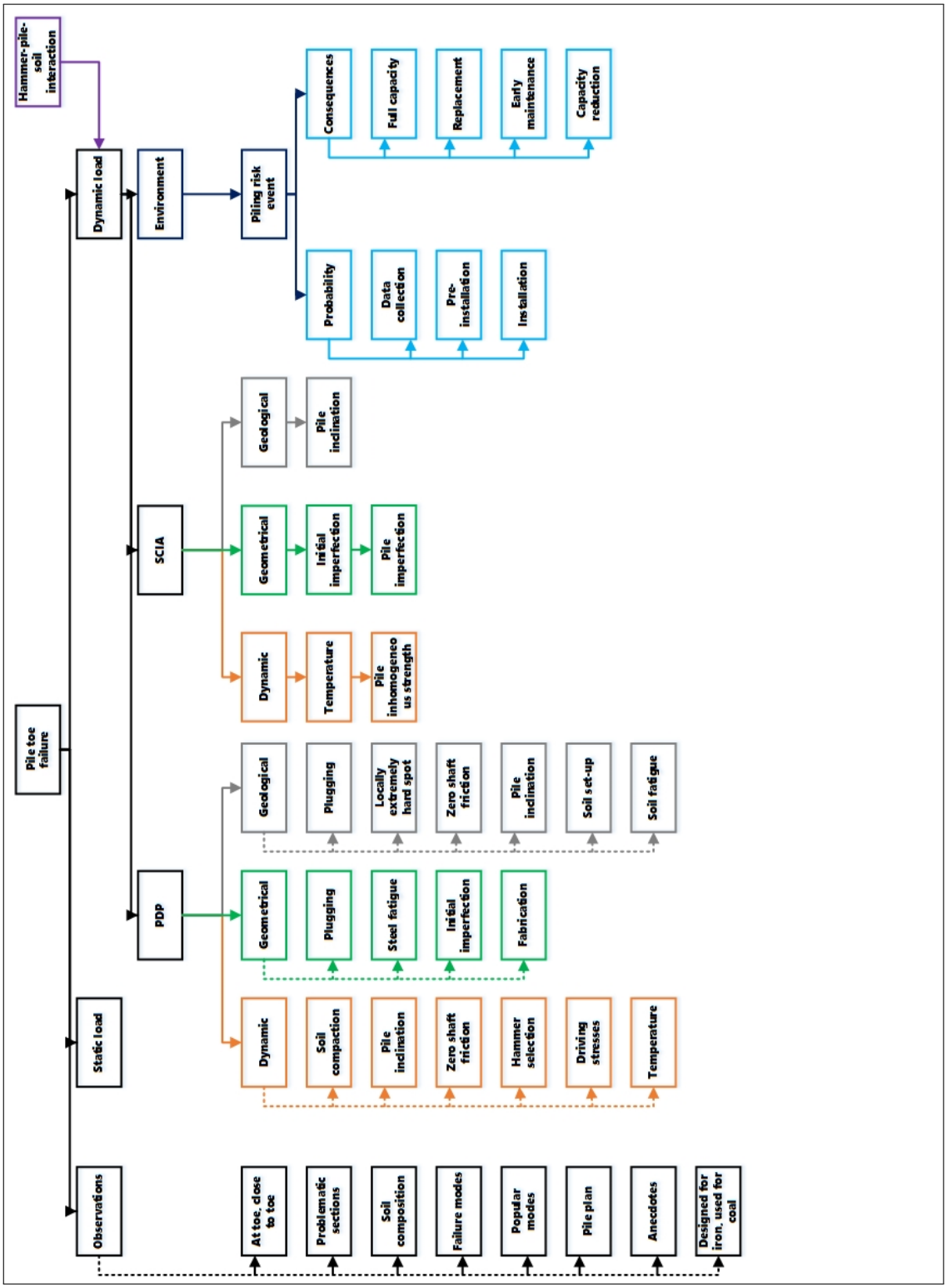

FIGURE 3.1: Validity map, used Visio

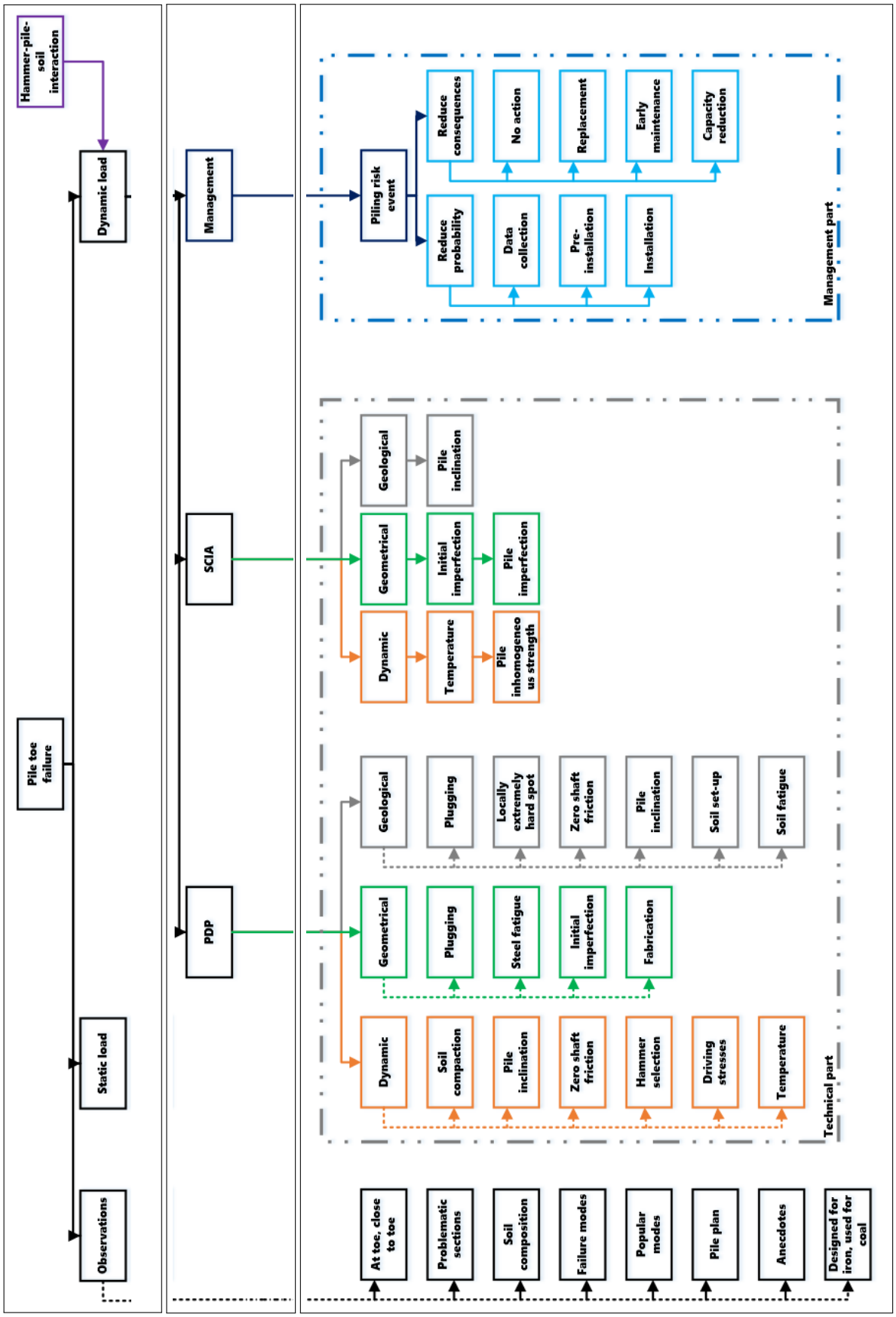
Hammer-pile-soil interaction
Dynamic load
Pile toe failure
Static load
Observations
Management
SCIA
PDP
Piling risk event
Reduce consequences
No action
Replacement
Early maintenance
Capacity reduction
Reduce probability
Data collection
Pre-installation
Installation
Management part
Geological
Pile inclination
Geometrical
Initial imperfection
Pile imperfection
Dynamic
Temperature
Pile inhomogeneous strength
Geological
Plugging
Locally extremely hard spot
Zero shaft friction
Pile inclination
Soil set-up
Soil fatigue
Geometrical
Plugging
Steel fatigue
Initial imperfection
Fabrication
Dynamic
Soil compaction
Pile inclination
Zero shaft friction
Hammer selection
Driving stresses
Temperature
Technical part
At toe, close to toe
Problematic sections
Soil composition
Failure modes
Popular modes
Pile plan
Anecdotes
Designed for iron, used for coal

Chapter 4

Case study

4.1 Aim

Chapter 4 aims to study the Amazonehaven case study narrowly. Therefore, studying its design and technicality as well as its process of the construction phase, in 1990. Furthermore, the collected data of pile toe damage are analyzed in this chapter.

4.2 Design of the Amazonehaven quay wall

The deep seaport quay wall structure in Amazonehaven has a low relieving platform. A low relieving platform is proved to be the optimum design for quay walls with a high retaining height [40]. At the waterside, the relieving platform is constructed on a combined wall system consisting of primary king piles and secondary intermediate sheet piles which function together as bearing and retaining foundation elements. At the land side, the relieving platform is resting on two rows of prefab concrete piles, with slightly different slope and different length. The inclination of the combined wall and other foundation elements is necessary to reduce the anchor forces. Furthermore, a row of M.V. piles warrants the stability of the entire quay wall, encountering the horizontal forces [19]. The king piles in Amazonehaven were segmented into three parts with D/t ratios of 71 to 83 to save material and therefore money. D refers to the diameter of the pile where t is its wall thickness. Figure 4.1 depicts the cross-section of Amazonehaven quay wall.

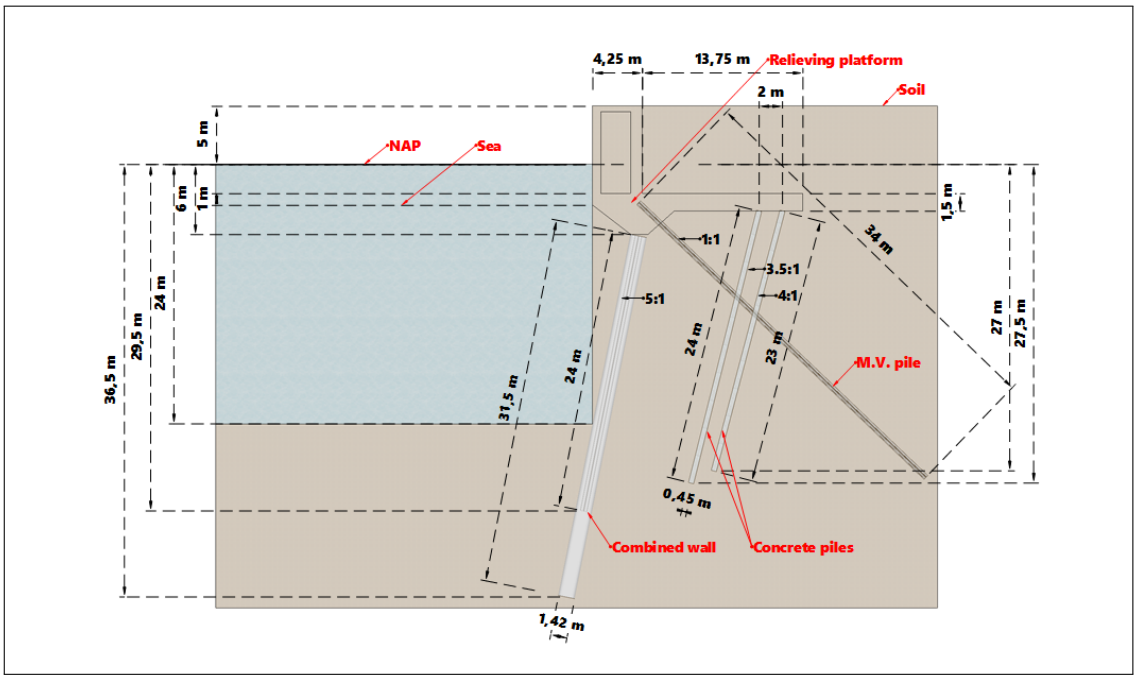

FIGURE 4.1: Cross-section Amazonehaven quay wall, used SketchUp

4.2.1 Geo-technical aspects

Amazonehaven is a human-made land. The soil layer consists of mostly loose sand at the surface, seabed ground composition and in deep layers stiff sand. The Municipality of Rotterdam (SO) had carried out Cone Penetration Test (CPT) in this area to determine the soil structure, in 1998. The digitized version of the CPT, also called **G**eotechnical **E**xchange **F**ormat (GEF)[1], are accessible at the GIS-web of the Municipality. In appendix A, the soil composition as used in this study is depicted.

4.2.2 Hydraulic boundary conditions

Hydraulic boundary conditions are determined by the environment in which Amazonehaven is located. MaasVlakte I (MVI) is an extension of Port of Rotterdam (POR). The normative water levels are determined with the data that SO has received from the operational monitoring system of Port of Rotterdam Authority (PORA). The boundary conditions are important for the design process of the quay wall, for example, to determine its retaining height [19].

4.2.3 Execution aspects

The primary piles were partly vibrated and partly driven with an inclination of 5:1 (11.3°) [48]. It is common to vibrate up to the Pleistocene layer, and afterward to drive the piles up to its required depth. A combination of vibratory drivers and impact hammer driving was used which is more practical, saves time and effort and enables obtaining an adequate soil bearing capacity [20]. The vibration of the piles occurred with an RBH 160 vibrator, 1600 [kN]. The driving, more or less the last 10 [m], occurred with a diesel hammer D62 in commence and later with a more massive diesel hammer, D100 [47]. The hammer change happened after carrying out a (pile) driving analysis, in 1990. Figure 4.2 depicts, the number of blows per 25 [cm] per hammer type. The (pile) driving analysis showed that a D/t ratio[2] of 93, is driveable with a diesel hammer D100 as well as D82, given Amazonehaven soil condition.

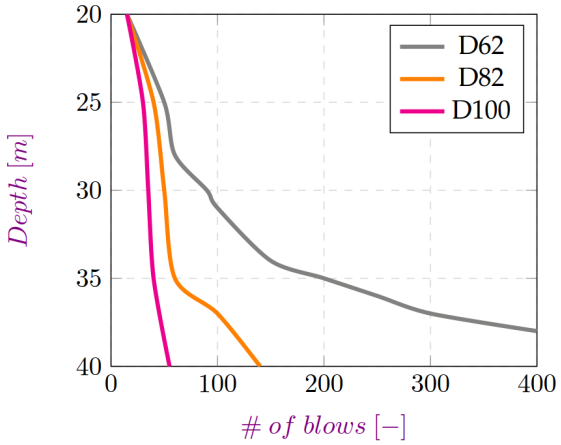

FIGURE 4.2: Driving analysis for Amazonehaven, given a D/t of 93, retrieved from [21]

The inevitable hammer change reduced blows up to 400 per 25 centimeters to below the threshold value of 300 per 25 [cm]. The *refusal* threshold is set to minimize damage to both hammer and pile. The associated driving time when D62 was used, was about 8 hours. After using a D100 diesel hammer, driving time reduced to 1 to 2 hours and blow counts remained between 70 to 120 strikes per 25 [cm] [20]. The drawback of hammer alternation during execution work was a halt in execution work for nearly two weeks which probably had led to the occurrence of soil set-up [40]. Soil set-up refers to soil reaching its full capacity which makes **re**driving troublesome [31].

[1] an easy to transfer soil data
[2] 1420 [mm] x 15 [mm]

Furthermore, a pile is pulled out after an extremely heavy driving[3]. In that specific event, the pile had a complete harmonica shape close to pile toe [J. de Gijt, personal communication]. Also, due to pressure to realize the project as fast as possible, miscommunication did occur [J. de Gijt, personal communication and [40]]. Other than the above mentioned, no driving difficulties were reported during pile installation.

After installation of open-ended tubular piles, the intermediate sheet piles with 24 [m] length were installed. Installation was as follow: first vibrating with an RBH 60 vibrator, then vibrating with water jetting. In the end, driving of the intermediate sheet piles with a diesel hammer D46, if necessary [20]. A drawback of sheet pile driving has been many interlocks openings discovered and repaired by the drivers back then. Therefore, it was concluded that driving is detrimental for intermediate sheet piles, due its low stiffness. Nowadays, intermediate sheet piles are not driven anymore.

Moreover, during installation, a heavy guiding frame was used to secure the positioning and inclination angle of the piles [20]. Therefore, a firmly distributed dynamic load at pile head was ensured next to a manageable transferred energy.

4.2.4 Major events

Two main events have taken place during the short technical lifetime of the Amazonehaven asset. First, immediately after construction interlock openings did occur. Second, due to overloading of one section, a settlement of about 50 [mm] had occurred [37] and [39].

4.3 Widening of Amazonehaven

Amazonehaven in Rotterdam, is partly demolished to widen the port entrance. The decision to widen the harbor was an inevitable decision to (1) continue facilitation for **U**ltra **L**arge **C**ontainer **S**hips according to (2) new safety requirements imposed by PORA [4]. Therefore, to improve sailing conditions the PORA invested € 200 million to widen the basin [5].

4.3.1 Observations

After removal of open-ended tubular piles and the intermediate sheet piles, a mysterious observation was recorded by the staff. Both primary and secondary piles were significantly damaged at a location close to pile toe. The damages are determined as (1) extreme folding of pile toe, (2) completely closed pile toe, (3) ovalisation at pile toe, as depicted in Figure 4.3.

FIGURE 4.3: Pile toe failure in Amazonehaven, retrieved from [37]

[3] an impossible to troublesome driving

It is estimated that about 15% to 20% of a total number of primary piles were damaged in the axial direction. For secondary sheet piles, this number is as high as 50% [4]. Furthermore, scorched sand at pile toe was observed which reveals the occurrence of a Locally Extremely High Temperature (LEHT) of about 400°-500° [4]. The heat is generated by high friction between soil and pile which has happened **during** (pile) driving activity.

4.3.2 Stability of the quay wall

4.4 Old quay wall

In June 1990 the Amazonehaven deep sea quay wall structure was delivered [39]. The entire project cost the SO around *f* 200 million[4] divided into three parts: (1) a docking port, (2) a deep sea quay wall, (3) a processing & transitional quay. The deep seaport is depicted in sub-Figure (a) 4.4 as a red-line.

FIGURE 4.4: (a) Amazonehaven and (b) its functions: **ECT**, **EKOM**, **Gasunie**, retrieved from Google maps

Sub-Figure (b) 4.4 shows the main companies established in Amazonehaven. It was, therefore, necessary to take these companies in any decision making process regarding construction. Two major companies of EKOM and ECT had the desires, regarding the old quay wall, to respectively expand and exploit the docking port in the future. The design of the old quay wall structure was *strategically* based on storage of iron ore, while it was intended to be used for coal storage [39]. The deficit which was approved by municipality council of Rotterdam made the project financially feasible given that the project is economic. After which, the client PORA set the project into an open tender in which the SO acted as the PORA's advisor. The deep seaport and the transitional quay had an apart procurement due to its significance. The deep seaport was tendered to the lowest bid, **H**ollandse **B**eton en **G**roep, for an amount of *f* 42.4 million[5]. The construction of the deep seaport was carried out in 6 month due to pressure to realize the project as fast as possible [40].

4.5 Stakeholders

The primary stakeholders in Amazonehaven area briefly introduced below:

- PORA (**Client**/**Employer**): Port authority's objective is to enhance the port's competitive position as a logistics hub and world-class industrial complex. Therefore, the core tasks of the authority are to develop, manage and exploit the port in a sustainable way and to render speedy and safe services for shipping [45].
- Dutch state: Dutch State might be involved with mega projects in its decision-making process. Nowadays, the Dutch State is a shareholder with no less than 40% in the POR's profits [45].

[4] Gulden, Dutch currency
[5] now: € 72 million

- **E**uropees **M**aasgoed **O**verslagbedrijf (EMO) or **E**rts en **K**olen **O**verslagbedrijf **M**aasvlakte (EKOM): EKOM is the largest bulk terminal in Europe, mainly handling in iron ore and coal, is established in MaasVlakte (area) (MV) since 1973. It has a yearly transshipment of 20 million ton coal and 13 million ton of iron ore.
- **E**urope **C**ontainer **T**erminal (ECT): ECT is located at the north side of the basin. ECT is the Europe's largest container terminal which handles a vast majority of all the containers passing through the port [12].
- SO (Engineering Division of Rotterdam Public Works[6]) (**Advisor/Supervisor**): Municipality is the designer and advisor of the (old) quay wall [48]. Nowadays, the SO is a shareholder with no less than 60% in the POR's profits [45].
- Gasunie: Gasunie is a European gas infrastructure company. It provides the transport of natural gas and green gas in the Netherlands and the Northern part of Germany [17].
- **H**ollandsche **B**eton **G**roep (**Contractor**): HBG has won the tender and has carried out the execution work either on its workforce and knowledge or by outsourcing it to a third party, in 1990 [40].

The parties mentioned above must have been involved in the decision-making process to build the (old) quay wall. A power-interest grid, as depicted in Figure 4.5, helps to create an overview of the roles each party is playing and the importance to be engaged in negotiations, based on two aspects of their power and their interest in the project. However, it should be mentioned that the power and interest of the parties could shift from respectively bottom to top and left to right or vice versa. It is also possible that one party loses its interest and leaves the scene when another might enter the negotiations in decision making.

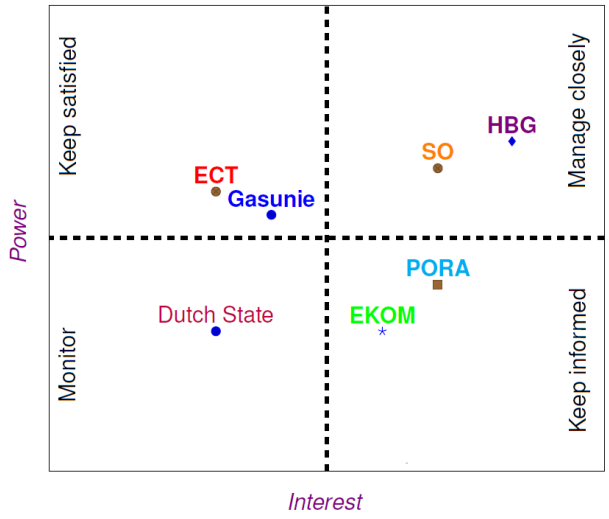

FIGURE 4.5: Amazonehaven's power-interest grid

In this fashion, from the viewpoint of a third party; HBG and SO must be managed carefully. The type of the contract used for Amazonehaven quay wall was based on a bid-build contract which is still the most-used form of procurement [44]. In this agreement, the employer is responsible for the design where the contractor executes the execution works according to the design, under the supervision of the employer or its engineer [44]. SO has designed the quay wall as well as supervised the works during construction whereas the HBG has designed the methods of construction and has executed the work. Therefore, SO and HBG are both ranked high and must be managed closely. PORA is ranked lower than the contractor because the supervision is taking place as well as the strict and detailed clauses in the bid-build contract. One of the main advantages of such a procurement procedure is that the parties know their position, task, authorities, and responsibilities. However, due to an inadequate tuning of design and construction;

[6] the name in 1990

additional works might arise during construction [44]. ECT and EKOM are very interested parties in any construction work which directly benefits them. The (old) quay wall was constructed to facilitate transshipment of coal storage. ECT, on the other hand, might claim more power if its operation becomes troublesome due construction work. Therefore, EKOM is ranked to keep informed and ECT to keep satisfied. Also, Gasunie must keep satisfied, due to any settlements in the area during construction work which might jeopardize the plant. At last Dutch State is ranked to be monitored. However, it does not necessarily mean that it would meddle in any aspects of the decision-making process.

4.6 Costs & revenues

The cost of a quay wall could be calculated by the key figures as to be found in the literature as well as the fact and figures available in the documentation of the Amazonehaven quay wall. The cost of the Amazonehaven seaport quay wall has been about *f* 42 million [39]. The cost of widening of the harbor both demolition and construction, has been € 200 million [5].

One easy way to argue the feasibility of a project is considering the Net Present Value (NPV). Therefore, NPV is a tool to evaluate the financial feasibility of alternative projects [18], given in Formula 4.1:

$$NPV = \sum \frac{R_t - C_t}{(1+r)^t} \qquad [€] \qquad (4.1)$$

Where R and C stands for respectively **R**evenues and **C**osts, r stands for interest and t is the time span considered in years, the technical lifetime of the asset.

The revenues of PORA are two folded: leasing the available land to the companies and sea-Port Dues (PD), payable by vessels docking at the quay [43]. It is, however, not possible due secrecy to acquire exact information about Leasing Contract (LC) as well as PD for Amazonehaven.

4.7 Loads

Loads on the combined-wall system are divided into structural loads and installation loads. The piles are designed to bear and to withstand the structural loads as their vital function. However, in 1990, less attention was paid to installation load, the forces applied to bring the pile into its position. Nowadays, the driveability of the piles are always checked [J. de Gijt, personal communication].

Structural loads

Structural loads on a combined wall are the lateral loads & the vertical loads carried partially by primary piles and transferred to deep Pleistocene layers. Structural loads have a major role in dimensioning and designing primary piles.

Installation loads

Installation load is the load applied on primary piles during pile driving. The dynamic load could be a constant input of cyclic force such as vibratory driving, or an almost dynamic pulse load regarding a clash between a hammer and pile head, impact driving.

4.8 Soil characteristics

Knowledge about the site is essential regarding an accurate assessment of topographical- and geological- conditions of the location. Topography describes the unique environment of the

location concerning working restrictions such as noise and vibration whereas the geological conditions refer to soil characteristics [23].

The soil data in the area were retrievable, and some were accessible in GEF-format, in GIS-web of the municipality. In total, some 6 randomly chosen CPT were compared to DN92 to investigate the variety of soil composition within the area. Appendix A presents the soil composition of DN92 as used in this research. Furthermore, the Problematic Section (PS), blue dashed-box in Figure 4.6, are introduced as sections with the highest number of observed damaged piles. However, only 27% of total king piles were recorded and measured. The numbering of piles made it possible to trace back its exact location, according to an old pile plan.

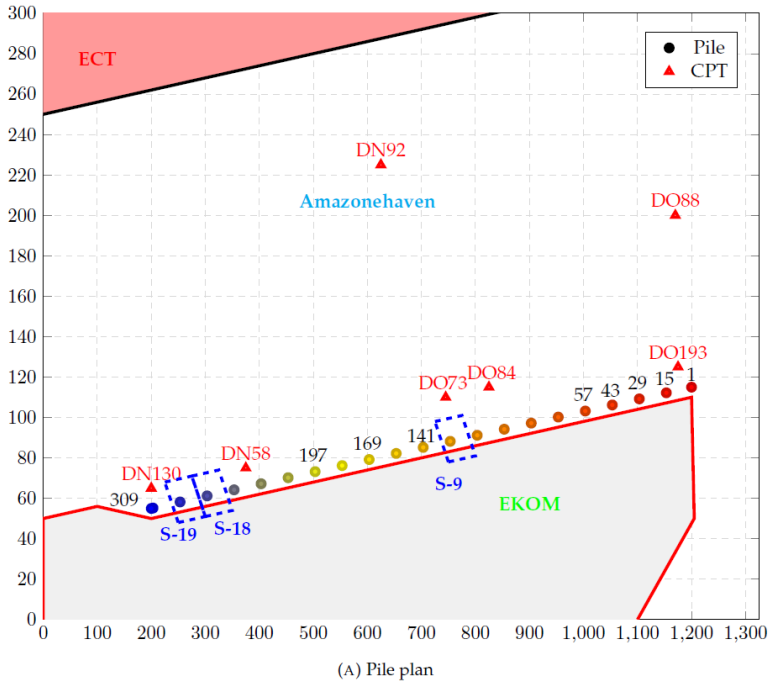

(A) Pile plan

FIGURE 4.6: Pile plan of Amazonehaven, its CPT and its PS

Geological condition

The Netherlands is located in the lower reaches of the rivers Rhine and Meuse. The meandering characteristic of the river, as well as its rise and fall in the past, has manifested itself in significantly diverse soil conditions over short distances [57]. Therefore, the soil mainly consists of sand and clay which originates from coarse stones in mountainous areas transported downstream by gravity and water flow and deposited in the delta area [61]. Therefore, the Pleistocene sand layer slopes downward from east to west of the port [57], from -15 [m] to -22 [m] [NAP]. However, due to human activities, natural soil conditions have been changed, especially in the reclaimed MV area. This change has been due to increasing sand content which has improved the strength and stiffness of Holocene layers [57].

Figure 4.7 shows the soil composition in the Aamzonehaven basin, where q_{conne} is the cone resistance. The CPT characteristics are according to the locations depicted in the pile plan.

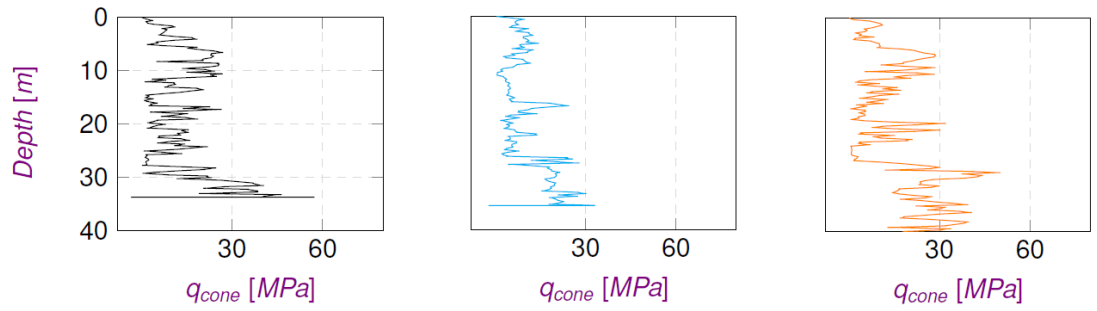

(G) DO88 (H) DO193 (I) DN58

FIGURE 4.7: Random CPT in Amazonehaven

The cone resistance of the subsoil is also expressed in relative density [%], which indicates the strength and stiffness of the sand [14]. The formula is as follow:

$$R_e = \frac{1}{C_2} \cdot ln[\frac{q_c}{C_0 \cdot (\sigma_v') \cdot C_1}] \cdot 100\% \qquad [\%] \qquad (4.2)$$

Where R_e is the relative density in percent, q_c and σ_v' are respectively cone resistance and effective (grain) stress in [MPa]. C_0, C_1 and C_2 are constant values depending on which method is used.

Therefore, the higher the cone resistance, the higher the value of the relative density for the sand. The classification of the sand, non-cohesive soil, based on its relative density and its cone resistance is ([14] and [22]):

- $R_e \leq 15\%$ - (very loose) - $q_c \leq 2.5$ [MPa]
- $35\% \leq R_e \leq 65\%$ - (medium dense) - $7.5 \leq q_c \leq 15$ [MPa]
- $85\% \geq R_e$ - (very dense) - $25 \geq q_c$ [MPa]

4.9 Data analysis Amazonehaven

The king piles, 313 over the entire quay length, were driven into the soil strata with sufficient bearing capacity at a depth of around -40 [m] [NAP]. The 900 [m] long quay wall was divided into 20 sections with a length of 45 [m] giving room to approximately 15 piles per section. Table 4.1 gives the characteristics of the foundation elements.

TABLE 4.1: Dimension, number and type/quality of foundation elements

Elements	Type/Quality	Length [m]	Amount
Open-ended tubular piles	X-70 (483 N/mm^2)	27.5-32	313
Sheet piles	Larssen IIIS	20-24	312
MV piles	Peiner Pst 370/153	30-36	332
Concrete bearing piles	B55	22-28	843

4.9.1 Failure modes

In *stability research*, the (old) quay wall, data was collected regarding photos and measurements of *extreme folding damage* of tubular piles before dumping the king piles and the sheet piles [37].

In Research into Pile Toe Failure in Amazonehaven (RIPTFIA), the collected data are analyzed, and modes of failures are introduced, see Appendix A. Figure 4.8 shows four popular failure modes of *deformed* pile toe as observed in Amazonehaven, among the twelve failure modes as introduced in RIPTFIA.

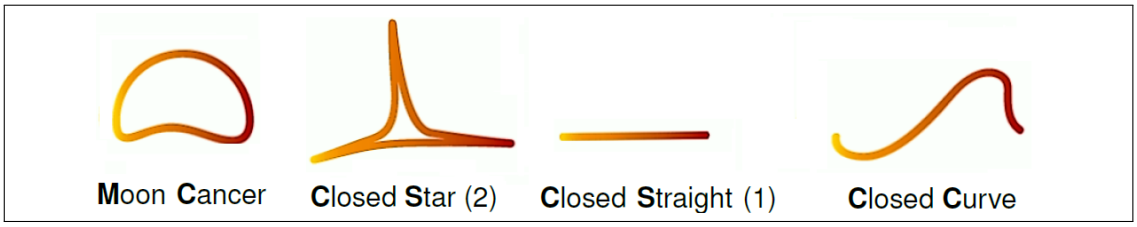

FIGURE 4.8: Cross-section of *deformed* pile toe in Amazonehaven, used Adobe Illustrator

Sub-Figure (A) 4.9 shows the frequency of occurrence of one failure mode over another. 42% of the numbered piles had No Damage (ND) at its toe. Furthermore, 18.1%, 8.4%, 7.2% and 7.2% of the piles had respectively Closed Star (2) (CS(2)), Closed Straight (1) (CS(1)), Moon Cancer (MC) and Closed Curved (CC) at its toe. Sub-Figure (B) 4.9 shows the locations of the most occurred *pile toe failure*. The most *pile toe failure* has occurred in sections 19, 18 and 9 with respectively 15.7%, 13.3% and 8.4% damage. The three locations are introduced as PS whereas the sections with a lower value of 8.4% damage are introduced as Other Section (OS).

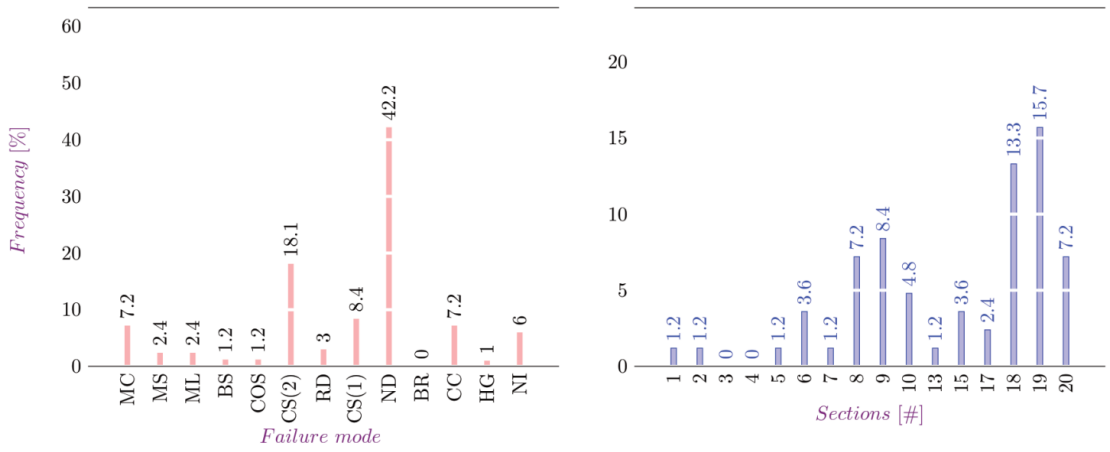

(A) Frequency of failure modes

(B) Frequency of *pile toe failure*

FIGURE 4.9: Frequency- per (A) failure modes, (B) per section

4.9.2 Fault tree

In CUR166, a general fault tree is given for seaport quay wall structures [7]. However, the fault tree does not suggest any failure mechanisms for the installation of the combined wall system. Therefore, RIPTFIA presents a complementary fault tree including more details into the failure of the primary pile. Figure B.10 in appendix B reveals more information about the fault tree. It is believed that taking these possible failures into account, piling disease could be treated.

4.10 Conclusions

Chapter 4 showed that despite strict installation procedure during construction in Amazonehaven, *extreme folding damage* did happen. Therefore, installation of a combined wall, still, requires an experienced and professional performance from the contractor. In other words, the contractor must have equipment and devices to predict as well as to monitor pile driving activities to be able to react to any probable pile damage. Also, the contractor must be aware of the

necessity of a high level of care & skills when it outsources the operations to a third party. A thorough analysis of dynamic load next to static load is a necessity to be encountered in design aspects.

Moreover, a power-interest grid showed an overview of main stakeholders playing a role in Amazonehaven. In any decision-making process, the involved parties must be identified and invited to the negotiation table. Finally, the most occurring failure modes in Amazonehaven are shown to be: Moon Cancer (MC), Closed Star (2) (CS(2)), Closed Straight (1) (CS(1)) and Closed Curved (CC).

Chapter 5

Wave Equation Program

5.1 Aim

Chapter 5 aims to study the hammer-pile-soil system with Pile Driving Prediction (PDP), a Wave Equation Analysis Program (WEAP). In this way, the validity of the hypothesis in chapter 1 is examined. Furthermore, the prediction program is used to conduct a better understanding of wave force travel through the primary pile taking into account the hammer-pile-soil interaction. Also, the magnitude of the hammer-induced driving stress, as well as its location along the pile, is an incentive. Appendix C is complementary to this chapter.

5.2 In-depth AllWave PDP

AllWave PDP is a prediction program to study the driveability of the primary pile within the hammer-pile-soil system. To this end, the program uses the *stress wave theory*, to simulate the pile behavior during driving. Therefore, displacements and forces of the hammer, the driving system, the pile and the soil during pile installation are determined. The inputs are about, hammer characteristics, pile dimensions, and soil characteristics. The outputs are mainly stress development along the pile and the number of blows required to bring the pile into its embedded depth [29]. It, therefore, helps the designer to select a suitable hammer with hammer-induced driving stresses below material's yield stress and the number of blows below refusal threshold.

5.2.1 Method of characteristics in practice

Method of characteristics, introduced by Saint-Venant, presents the phenomenon of stress-wave-travel in a frictionless bar with a constant- velocity & toe resistance [35]. An advanced version of this method is implemented in PDP, in the sense of taking friction into account. This friction is the real interaction between the homogeneous bar and its surrounding, the soil. To do so, the bar is divided into smaller segments where friction-force is applied at interfaces from one segment to another. Therefore, the stress wave travels freely in between the interfaces. When the wave encounters the interface, it partly reflects and partly transits. From the boundary conditions of equilibrium and continuity, information about forces, displacement, velocities are calculated at the interfaces [27].

5.2.2 Wave theory of Smith

In 1960, Smith derived a numerical integration method as a solution for the wave equation in a pile. In this way, the interaction between hammer, pile properties, and soil characteristics during driving activities was investigated [30]. Many programs using wave equation analysis are based on Smith model [56]. In his mathematical model, the dynamic behavior of the hammer-pile-soil system is simulated. Hammer and pile are modeled as series of discrete masses, springs and dash-pots corresponding to respectively weight, stiffness and damping effect. The Soil Resistance to (pile) Driving (SRD) is modeled as a displacement- and a velocity-dependent part. The displacement dependent part is modeled as an elastic-plastic spring where deformation at which the plastic behavior starts is called quake. The velocity dependent part (dynamic soil resistance), also called soil Smith damping, is modeled as a linear dash-pot [54].

5.2.3 Complementary PDA

A significant difference in the number of blows, driving time, the magnitude of stress, etc. between both prediction and measurements, is possible [29]. Therefore, it is highly recommended to do a Pile Driving Analysis (PDA) after carrying out the PDP driving prediction. A PDA is necessary to validate the prediction and to alternate the soil default values, as inserted in the prediction program, accordingly; a back analysis[1] of; fitting the prediction to calendering, the measured stresses and the utilized hammer energy [31]. Carrying out a PDA also reveals information about pile toe integrity, by dynamic and static test piles. The PDA transducer equipment is drilled close to pile head to register strains and accelerations on either two or four side of the pile. The measured data of the test, reveal information about: forces and velocities in the response of impact hammer, number of blows[2], hammer efficiency, tension and compression during driving and SRD.

5.3 Analytic calculation

5.3.1 Extremes

To study and analyze the hammer-pile-soil system, a **hand calculation** is carried out. The king pile is simplified into a one-dimensional bar with Zero Shaft Friction (ZSF) along the bar. Therefore, the stress wave travels the bar freely with a constant velocity. Furthermore, it is assumed that the bar is homogeneous with a fixed D/t ratio and material's properties. When the stress wave reaches the end of the bar, it encounters one of the two extreme circumstances as (constant) toe resistance: (1) poor soil characteristics or (2) stiff soil characteristics. In a poor soil characteristic, the impact wave meets *free end extreme* whereas, in a stiff soil the impact wave meets a *fixed end extreme*.

The reaction forces in both extremes are calculated with basic formulae, as presented in equations 5.1 through 5.4. The formulae are based on the wave equation and the solution of the wave equation given by d'Alembert [51].

$$F = F\downarrow + F\uparrow \qquad [N] \qquad (5.1)$$

$$v = v\downarrow + v\uparrow \qquad [m/s] \qquad (5.2)$$

$$F\uparrow = -Zv\uparrow \qquad [N] \qquad (5.3)$$

$$F\downarrow = Zv\downarrow \qquad [N] \qquad (5.4)$$

In this formula, Z is the pile impedance, important factor for the wave propagation [15]:

$$Z = \frac{EA}{c} \qquad [Ns/m] \qquad (5.5)$$

$$c = \sqrt{\frac{E}{\rho}} \qquad [m/s] \qquad (5.6)$$

where E is the pile modulus, A is the cross-section and c is the wave propagation speed in the pile.

Free end extreme

In *free end extreme*, pile toe experiences no resistance force. Therefore the sum of downward traveling force and the reaction force traveling upward must be zero. In this way, the condition

[1] Signal matching AllWave-DLT
[2] calendering

of equilibrium is fulfilled at toe. The upward wave force is then, equal to downward wave force.

From the basic formula 5.1, it follows that:

$$F = 0 \Rightarrow F\uparrow = -F\downarrow \tag{5.7}$$

Equations 5.3 and 5.4 from the basic formula's presented above, give:

$$F\uparrow = -Z \cdot v\uparrow \Rightarrow v\uparrow = \frac{F\uparrow}{-Z} \tag{5.8}$$

$$F\downarrow = Z \cdot v\downarrow \Rightarrow v\downarrow = \frac{F\downarrow}{Z} \tag{5.9}$$

Substituting into basic equation 5.2 gives:

$$v = v\uparrow + v\downarrow = \frac{F\uparrow}{-Z} + \frac{F\downarrow}{Z} = 2 \cdot \frac{F\downarrow}{Z} = 2 \cdot v\downarrow \tag{5.10}$$

Therefore, the wave-velocity at pile toe is **two times the downward wave-velocity at pile head**. In other words, the stress wave at toe travels back to head twice as fast.

Fixed end extreme

In *fixed end extreme*, pile toe experiences a high resistance force. Also, the pile toe movement becomes zero due to the fixation. Therefore, the boundary condition at toe follows:

$$v = v\downarrow + v\uparrow = 0 \Rightarrow v\downarrow = -v\uparrow \tag{5.11}$$

(5.12)

Equations 5.8 and 5.9 from previous calculations, give:

$$\frac{F\uparrow}{-Z} = -\frac{F\downarrow}{Z} \Rightarrow F\uparrow = F\downarrow \tag{5.13}$$

Substituting into basic equation 5.1 gives:

$$F = F\downarrow + F\uparrow = F\downarrow + F\downarrow = 2F\downarrow \tag{5.14}$$

Therefore, the reaction force at the toe is **twice the downward force at pile head**. In other words, the toe experiences a force two times higher than the impact force experienced by the pile head.

In reality, the circumstances are in between these two extremes due to wave stress reduction in its journey to pile toe. Therefore, the minimum driving stress at pile toe has the same value as the impact hammer at pile head, and maximum driving stress at pile toe has the same values as twice the impact hammer at pile head.

5.4 Numeric calculation

5.4.1 Assumptions to start

To carry out the research, simplifications and assumptions are necessary. In this study, a back-analysis is simply not possible. The scope of the research does not allow any pile tests in the area. Therefore, the model could not be validated and the soil parameters, such as quake

value, are the standard default values of the program. Furthermore, the blow count record of the Amazonehaven quay wall was not retrievable [J.G. de Gijt, personal communication]. Also, it is assumed that the stress-wave travel is one-dimensional meaning that the wavelength is up to three times larger than the pile diameter, to be able to utilize PDP [10]. Moreover, the piles are modeled in the program vertically instead of inclined. When pile inclination is taken into account, the same finding is supposed to be acquired with slightly higher blow counts due to a less energy transfer, in case of eccentric impact at each blow. The soil resistance is based on one soil model, Alm & Hamre, which takes the soil degradation due to driving into account, meaning a reduction in friction [29]. Alm & Hamre is frequently used in practice [P. Middendorp, personal communication]. The plugging response of the piles is not taken into account in the calculations due to the large diameter of the pile as well as non-cohesive soil characteristics of Amazonehaven. At last, the quake value, at toe and shaft, are kept constant and around 2 to 2.5 [mm].

5.4.2 Input parameters in PDP

The model is constructed by selecting the properties of the hammer-pile-soil system. In this system, a hammer needs to be selected. Therefore, the calculations are carried out by a D100-13 diesel hammer for different D/t ratios. In Amazonehaven, this hammer was used after a D62 was not sufficient enough to bring the piles up to its required depth. The specifications of a D100-13 diesel hammer are given in Table A.1, appendix A. The second input is the pile, which is modeled for various D/t ratios, with a fixed diameter value. The D/t ratios vary from low with a thick wall-thickness to high with a thin wall-thickness as follow: 20, 50, 83 (Amazonehaven) and 100. For Amazonehaven, the piles were segmented into three parts with different thicknesses of 17-20-17 [mm]. An overview of pile dimensions, as used in this program, is given in Table A.5, appendix A. The third input, is the soil composition of Amazonehaven, which was retrieved from the GIS-data available at Municipality of Rotterdam (SO). The digitized version of the Cone Penetration Test (CPT) was not available for every location which limited the selection. However, the soil characteristics of the area have more or less the same composition. Figure B.8, see appendix B, compares the soil characteristics of the Amazonehaven basin with the selected one, DN92.

5.4.3 Calculation

The stress-development along the pile in PDP is calculated as follow: First, a *multiple run* is carried out, given an end driving level, which results in a maximum value of *driving stresses per driving level*; over the driving depth. The driving level step is selected to be 0.25 [m], this means 40 unique data points in ten meters of driving. The second step is to choose the highest value among the maximum values of *driving stresses per driving level*. Then, to carry out a *single run* at that specific driving level which reveals information about the stress-development along the pile. In other words, hammer-induced driving stresses are shown along the pile, given its specific driving level. In Research into Pile Toe Failure in Amazonehaven (RIPTFIA), the *multiple run* data is depicted over the **depth** whereas *single run* is depicted over the **length**.

5.4.4 Results

Stresses versus soil fatigue

In PDP, fatigue model Alm & Hamre is assigned to each soil layer. Fatigue of soil benefits the pile driving activity by reducing the soil resistance, as mentioned earlier. In other words, the lower the soil Fatigue Factor (FF), more fatigued soil, the lower the SRD and the lower the blow counts. In theory, a situation which is close to *fixed end extreme* would lead to high driving stresses close to pile toe. In this fashion, the shaft friction along the pile is close to zero, and at toe the soil properties are stiff. Therefore, it is argued that a soil reduction of almost 80%, FF-value of 0.2, supposedly leads to high values of driving stresses close to toe. Figure 5.1 compares the hammer-induced driving stresses along the pile for different soil FF-values per various D/t ratios.

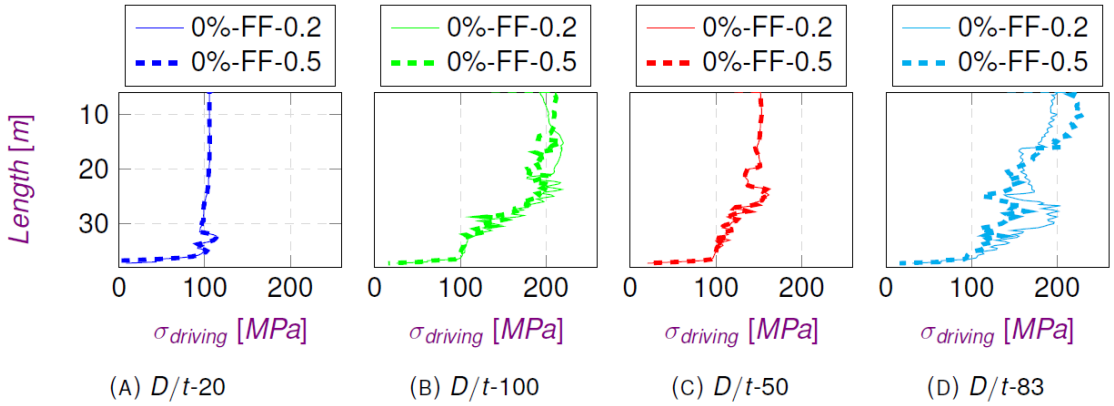

FIGURE 5.1: Driving stresses along the pile, legend: compaction-FF-D/t, retrieved from PDP

In any case, the hammer-induced driving stresses are about four times lower than the material's yield stress for Standard to Normal Soil Condition (SNSC), close to pile toe.

Stresses versus soil compaction

The soil compaction could happen either due to driving activity or pile installation sequence. When installing the king piles, either a small driving step or a large driving step is conducted, as depicted in Figure 5.2. When the small steps are applied, the piles numbered as 3, 5 & 7, will experience a heavier driving compared to the rest of the piles due to soil compaction. When the large steps are applied, the piles numbered as 7 & 5 will encounter heavy driving[3] [38].

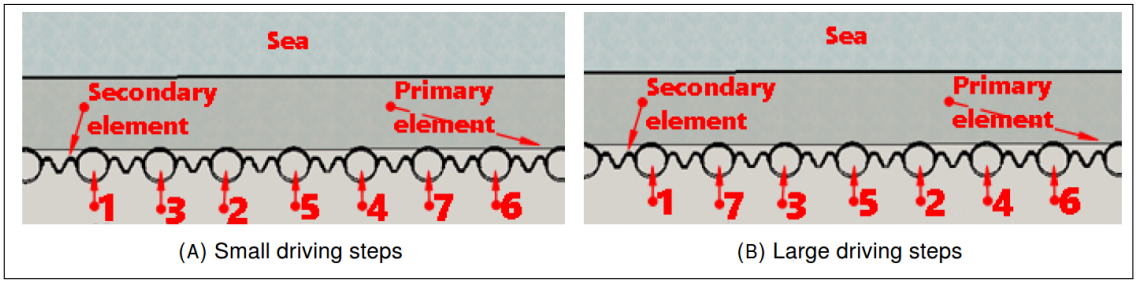

FIGURE 5.2: Driving steps installation of king piles, retrieved from [38]

Therefore, the compaction of the soil would theoretically result in more friction and lesser values of driving stresses close to pile toe. Figure 5.3 compares the driving stresses, for a virgin and compacted soil.

[3] troublesome driving

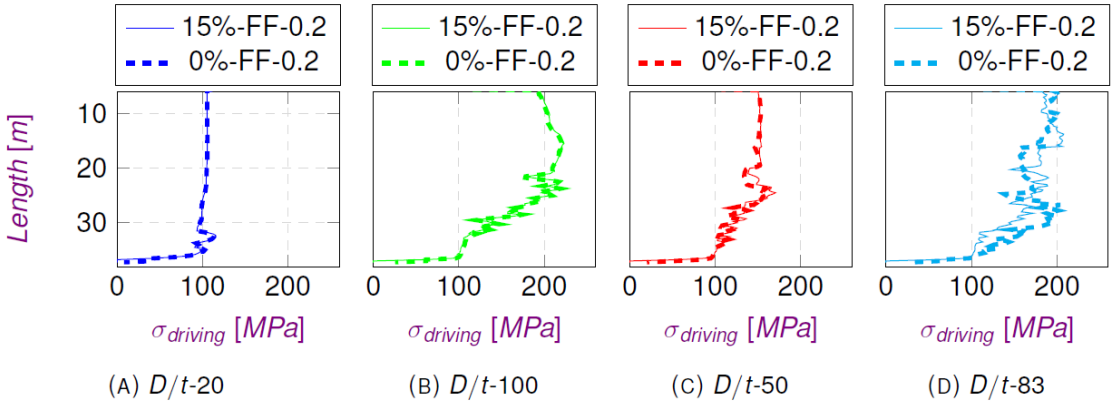

FIGURE 5.3: Driving stresses along the pile, legend: compaction-FF-D/t, retrieved from PDP

In any case, the hammer-induced driving stresses are about four times lower than the material's yield stress for SNSC, close to pile toe. The difference in driving stresses due to soil compaction is not significant.

By taking into account the soil compaction and soil FF-value, it was believed to find a clear-cut conclusion of the magnitude of driving stress as it was discussed in hand calculations. Therefore, a higher hammer-induced driving stress close to pile in case of a less fatigued soil and virgin soil, and vice versa. However, the difference between one another is not significant because the stress wave reduces in its head to toe journey given the SNSC of Amazonehaven. To find the high driving stresses along the pile and close to pile toe, the exact hand-calculation must be simulated in PDP, which means a *fixed-end extreme*. Therefore, a situation of ZSF along the pile accompanied with Locally Extremely Hard Spot (LEHS) at pile toe.

Blow counts

Figure 5.4 compares the number of blows per driving level given D/t ratio versus soil fatigue and soil compaction. It shows a clear distinction in some blows between virgin and compacted subsoil. It also shows that a lower D/t ratio should have been used than an 83. Given a D/t ratio of 20 and 50, the number of blows does not exceed the threshold, depicted as R, which means that the pile reaches its required embedded depth. For a D/t ratio of 83 and 100, the pile does not reach its required embedded depth. Therefore, a lower D/t ratio than used in Amazonehaven is suggested, given both a diesel hammer of D100 and SNSC.

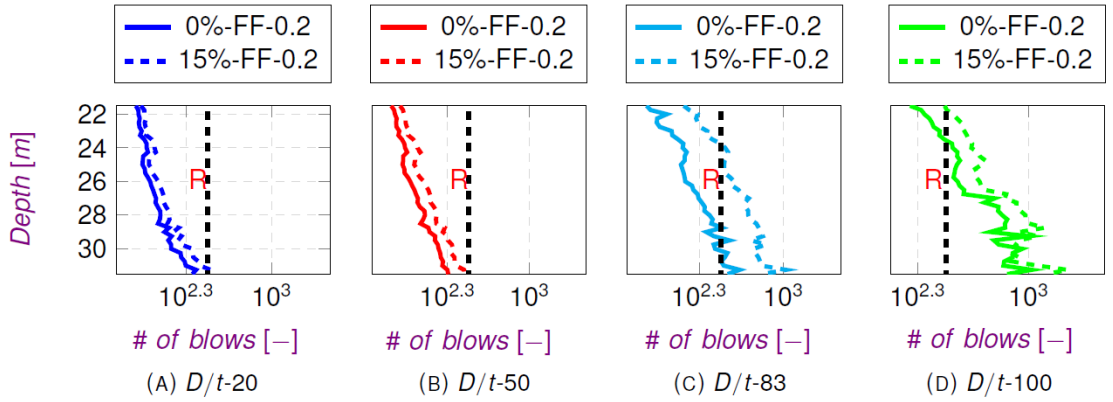

FIGURE 5.4: Number of blows, legend: compaction-FF-D/t, retrieved from PDP

Continuous driving and stiff soil properties

Another scenario, next to compaction and soil fatigue, is the possibility of shaft friction becoming zero in combination with the existence of a LEHS at pile toe. The bizarre situation, then, resembles the *fixed end extreme* which analytically has led to high driving stresses close to pile toe. The ZSF condition could happen in reality when operator carelessly sustains driving without pile advancement, or when soil composition enjoys the so-called Soft Rock (SR) (soil) properties. The SR condition could appear in nature when a rock is located in deep layers whereas the overlying layers have a poor soil characteristic. In both situations, pile toe will be damaged.

Sub-Figure (A) 5.5 shows the stress development along the pile when surrounding soil does not generate any force. The driving stresses are low (almost constant) along the pile and close to pile toe. Sub-Figure (B) 5.5 shows the same in combination with a Shell Bank (SB) or a LEHS as could appear locally in the seabed. The hammer-induced driving stresses are high close to pile toe. A combination of ZSF & SB, sub-Figure (A) & (B) 5.5, lead to high values of hammer-induced driving stresses along the entire pile as well at pile toe as depicted in sub-Figure (C) 5.5. The hand-calculations predicted about the same results.

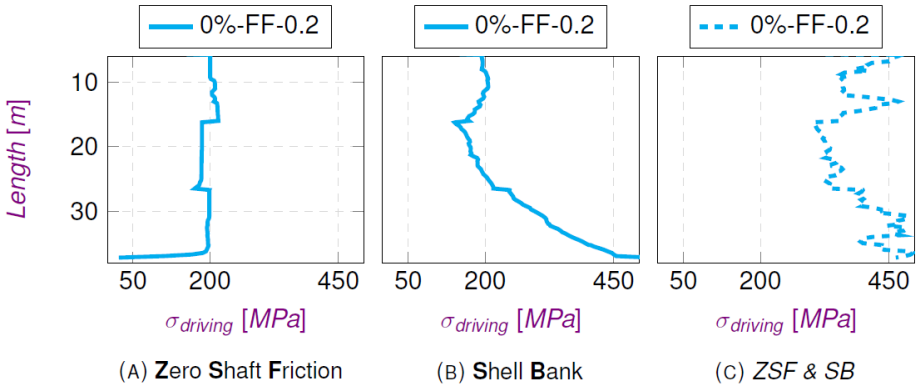

FIGURE 5.5: Driving stresses along the pile, legend: compaction-FF-D/t-83, retrieved from PDP

Stresses versus shell banks

In this scenario, the location of SB properties is studied. Therefore, the SB is located either at pile toe or along the entire depth. Also, the shaft friction along the pile is not excluded. Figure 5.6 depicts, the high driving stresses close to pile toe in both cases.

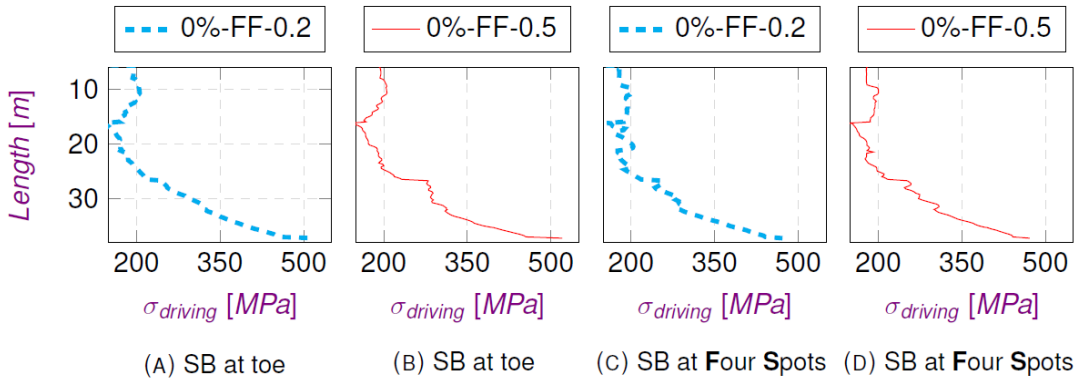

FIGURE 5.6: Driving stresses along the pile, legend: compaction-FF-D/t-83, retrieved from PDP

In case of SB spread over the entire driving level, which is possible in seabed due dumping materials like boulders in the past, the pile toe must over-win a couple of stiff soil properties in

its journey to its required depth. The closer the SB is located to the surface, the lesser shaft friction to be encountered by the stress wave and the more (twice as high) the reaction force at pile toe would be. Therefore, the *pile toe failure*-development starts in early stages of driving. In this case, the pile toe integrity is more prone to suffer from the piling disease. However, when the stiff soil property is located only at the required depth, the severity of damage to pile toe stays limited due to a reduction of the impact wave force by the shaft friction. Therefore, when the stiff layer is close to the pile's required depth, the pile toe integrity is maintained. Quietly said: *the harder you punch something hard, the more you feel, however when punching it with a sponge in between the lesser you might feel*.

Another facilitator of pile toe damage is a combination of the initial dent and the development of an inwards *pile toe deformation* during piling. The development of an inwards *pile toe deformation* will be worsened when piling occurs in stiff layers. In this fashion, when the toe encounters any LEHS, the initial dent will be enlarged at each strike. The inwards enlargement will eventually lead to a close-ended pile where the very high toe resistance stops the pile advancement.

5.5 Overview soil properties

Figure 5.7 depicts an overview of the soil conditions as used in this chapter. This, in order to ease the understanding of different terminologies in RIPTFIA.

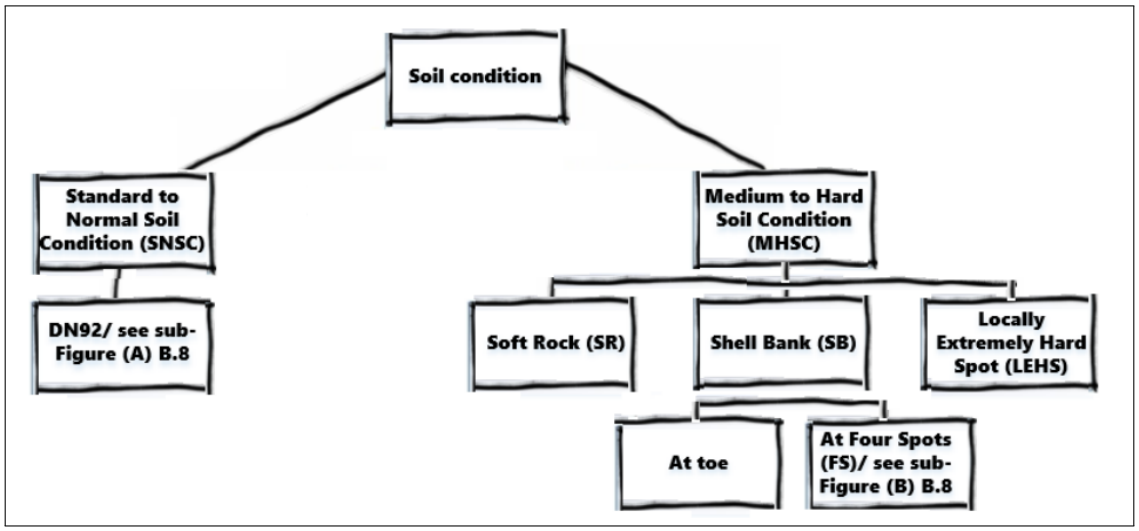

FIGURE 5.7: Overview soil conditions

5.6 Conclusions

In chapter 5, the effects of different pile driving scenarios were examined. The pile was modeled in a hammer-pile-soil environment, where the hammer was fixed whereas pile dimensions and soil properties were exposed to changes.

Soil fatigue is principally a vital factor facilitating pile driving in the first place. The soil fatigue is essential to select the right hammer, a too heavy hammer is economically not attractive, and a light hammer does not mobilize enough soil movement per set[4]. For the selected Fatigue Factor (FF)-values as well as compaction of the soil, the driving stresses were slightly different and up to 50% lower than the value of material's yield stress. In case of compacted soil, the number of blows was higher than a virgin soil. In case of presence of Locally Extremely Hard Spot (LEHS), with a value of 500 [MPa], it was clear that the driving stresses become higher

[4]pile penetration per blow

than material's yield stress. In case of Soft Rock (SR), shaft friction is eliminated, the stresses were high along the entire pile. In case of Shell Bank (SB) or LEHS, the driving stresses show high values only close to pile toe, due to the existence of shaft friction. However, a LEHS- and a SR- conditions are not plausible for Amazonehaven soil characteristics. Therefore, it could be concluded that pile driving is not expected to result in high driving stresses exceeding the material's yield stress close to pile toe, given the Standard to Normal Soil Condition (SNSC) of Amazonehaven.

5.7 Limitations AllWave PDP

The prediction program, logically, has some limitations. Bear in mind the importance of using a Pile Driving Prediction (PDP) with its complementary monitoring program Pile Driving Analysis (PDA) to have a reliable prediction. A PDA consists of software and hardware equipment with sensors and antenna which is attached close to pile head to register measurements, e.g., forces. Only then, the prediction has an added value. However, carrying out a PDA was not possible neither the calendering[5] form 1990 was available. Moreover, PDP does not take any three-dimensional effects into account. Also, the shape of the tubular pile does not play any role, which means that an initial dent at toe could not be modeled. PDP, a one-dimensional program, only takes into account elastic behavior of the material. Furthermore, other aspects of the modeling, e.g., quake value, hammer energy, the thickness of cushioning are not considered in Research into Pile Toe Failure in Amazonehaven (RIPTFIA).

5.8 Recommendations

(1) It is recommended to take into account the quake value as a variable. Quake is the movement between pile and soil required to mobilize full plastic resistance of the soil [15]. It is argued that the quake value is not constant along the shaft and toe and could reach high values [31]. (2) To take into account the driving analysis as presented in Figure 4.2, chapter 4. Therefore, (a) an attempt to carry out a back-analysis is enabled. Then, (b) to compare whether high driving stresses are to be expected even though the LEHS is not taken into account. After which, (c) to adjust the default values within the program to counterfeit the same results. However, the validity of the (pile) driving analysis in 1990 is not detectable. The driving analysis was made after the failure of D62 diesel hammer to bring the piles into its required embedded depth. Finally, (3) it is recommended to manipulate energy transfer from the hammer to pile by simulating the same process as carried out by the operator, in reality. Therefore, a step by step increase of hammer energy as well as adjusting the cushioning thickness when refusal threshold is achieved.

[5] blow count results

Chapter 6

Failure sources Amazonehaven

6.1 Aim

Chapter 6 aims to present and discuss the reasons of *pile toe failure* in an structured way. Therefore, the failure mechanisms are clustered around the three identified main categories of *sources of failure* with a: **dynamic**-, **geometric**- and **geologic**- nature.

6.2 Classification

Different failure mechanisms of *pile toe failure* during driving are divided under three main categories of dynamic, geometry and geology, as depicted in Figure 6.1. A dynamic failure source refers to *the failure* having its origin in dynamic affairs. Mechanisms of probable damage to pile toe due to dynamic nature of piling[1] are named within this category. Failure mechanisms under the geometry, refer to *the failure* having its origin in peculiar properties of the pile. The last category includes failure mechanisms due particular soil characteristics of the site.

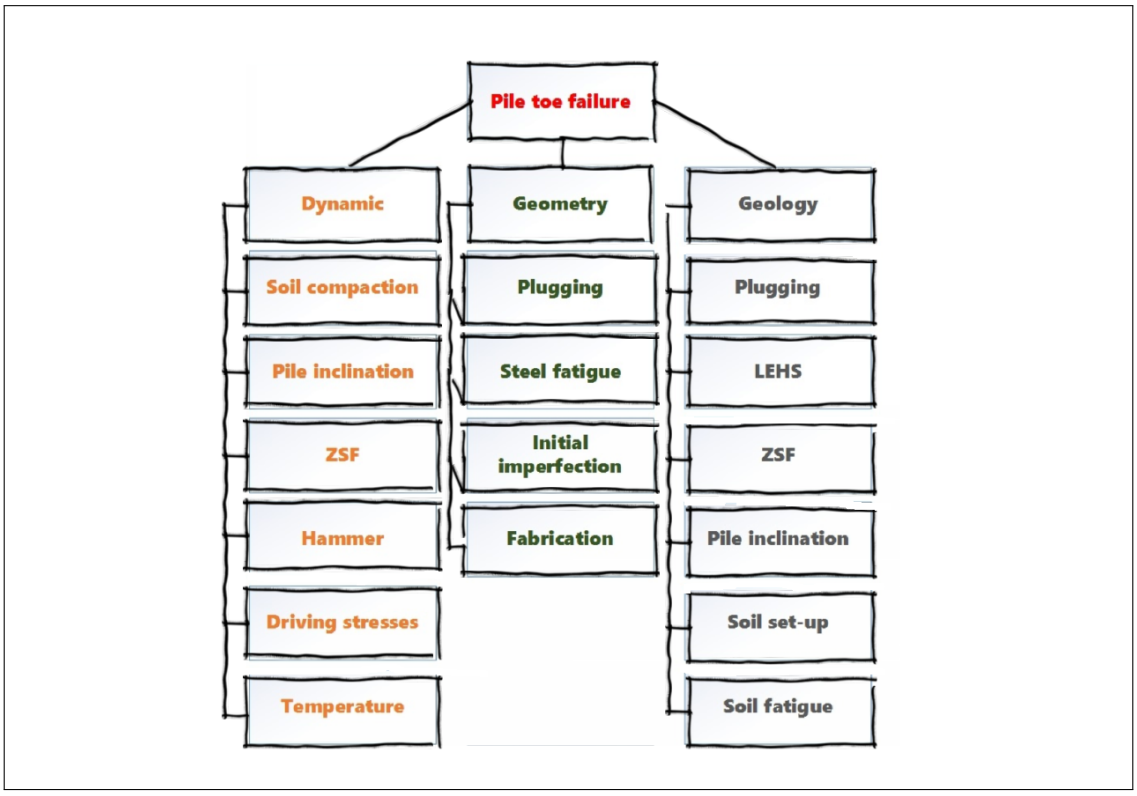

FIGURE 6.1: Overview of possible *sources of failure*

[1] pile driving activity

The Zero Shaft Friction (ZSF) could occur when the soil does not generate any shaft friction, e.g., peat. Locally Extremely Hard Spot (LEHS), refers to the existence of boulders or Shell Bank (SB), locally.

6.2.1 Dynamic failure sources

(a) Soil compaction

The soil is compacted due (1) **vibration** by a vibratory hammer, beforehand driving by impact hammer takes place, (2) conventional installation sequence of a combined wall which results into some piles experiencing denser soil properties [38]. In Pile Driving Prediction (PDP), the shaft friction and toe resistance increased by 15% to resemble the soil compaction, which is decided to be a logical value [J. de Gijt & H. Pacejka & P. Middendorp, personal communication]. Soil compaction leads to more Soil Resistance to (pile) Driving (SRD), and therefore a more troublesome piling, regarding increasing the number of blows needed to bring the pile to its required depth. However, the hammer-induced driving stresses are predicted to be lower close to pile toe than at pile head, as depicted in Figure 6.2.

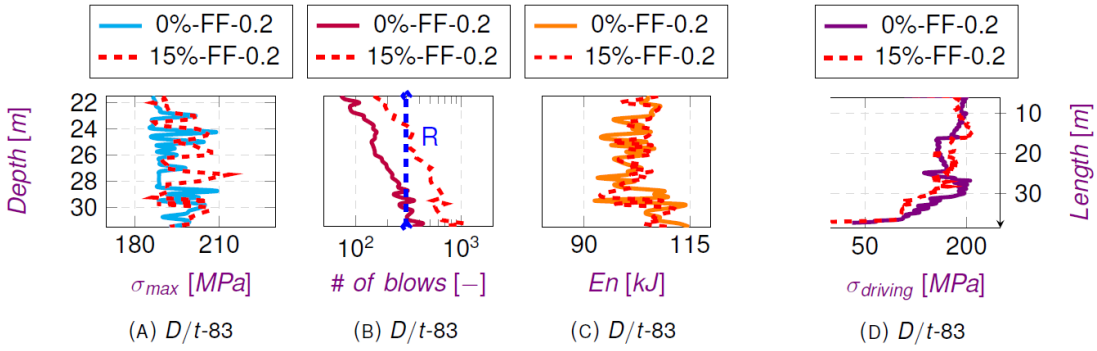

FIGURE 6.2: Specifications of piling, legend: compaction-FF-D/t, retrieved from PDP

Figure 6.2 shows from left to right: the maximum driving stress per driving level, number of blows per driving level, transferred energy per driving level over a **depth** of 10 meters. It also depicts the hammer-induced driving stresses along the pile, for the highest values of the *maximum driving stress per driving level*, over the pile's **length**. The comparison is carried out between a compacted soil, 15%, and a virgin soil, 0%. It shows that, given a Standard to Normal Soil Condition (SNSC), the hammer-induced driving stresses close to pile toe are less than material's yield stress.

(b) Pile inclination

In Amazonehaven, piles were placed with an inclination of 5:1. Therefore, the impact hammer could have hit the pile head concentrically or eccentrically at each strike. If it has not been aligned with pile head, poor energy transfer and possibly damage to pile head due to over-stress at one edge could occur. However, due to development of a concentrated over-stress at one edge, it is most likely that pile head would be damaged and not the pile toe. Also, there was a heavy guiding frame used to secure the positioning and inclination angle of the piles [20]. Therefore, it is highly doubtful that eccentric impact hammering could have caused the *extreme folding damage*. Nevertheless, *pile inclination* is taken into account in chapter 7.

(c) Zero shaft friction

When the surrounding soil does not generate any shaft fiction, along with the pile, ZSF circumstances occur. A ZSF could be due to a state of **pile stagnation & continuous driving**. In PDP, the shaft friction is set to zero. Figure 6.3, compares only the hammer-induced driving stresses along the pile, given ZSF circumstances with the SNSC of Amazonehaven.

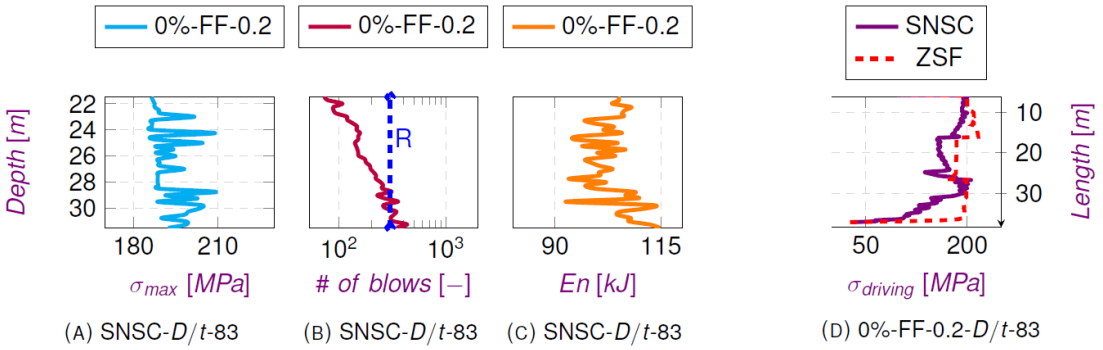

(A) SNSC-D/t-83 (B) SNSC-D/t-83 (C) SNSC-D/t-83 (D) 0%-FF-0.2-D/t-83

FIGURE 6.3: Specifications of piling, legend: compaction-FF-D/t, retrieved from PDP

If a ZSF appears in combination with the LEHS, the driving stresses become extremely high along the pile, as well as close to toe.

(d) Hammer selection

In *screening tool paper*, it is concluded that damage of piles in Amazonehaven could have been anticipated due its high D/t ratio, even though the mainly sandy subsoil was not very dense [55]. In Amazonehaven, first, a D62 diesel hammer was used. When pile advancement stopped, the contractor changed to a heavier one. In fact, a D62 does not even reach the minimum required energy according to the hammer selection guidelines. Sub-Figure (A) 6.4, shows the limitations dependent on the (equivalent) drop height, H_e. Also, given the heavier hammer, the minimum and maximum drop height exceed this minimum and maximum limitation[2]. Sub-Figure (B) 6.4, shows that the minimum and maximum hammer energy, W_r, given a pile dimensioned based on American Petroleum Institute (API) and a D100 diesel hammer; does comply with the minimum and maximum required energy. The drop height is usually between 2.8 and 3.4 [m] in practice ([38] and [55]).

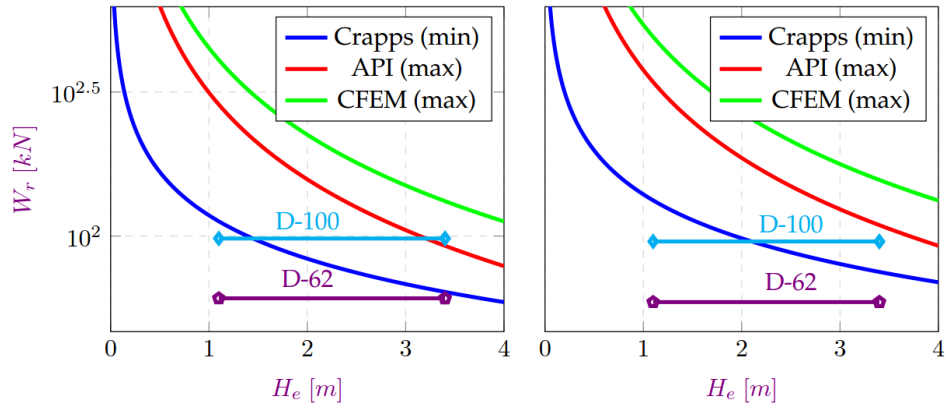

(A) D/t-83-Amazonehaven (B) D/t-69-API

FIGURE 6.4: Minimum and maximum hammer energy per (equivalent) drop height, retrieved from [55]

Figure 6.4 shows *commonly used* guidelines for hammer selection: Crapps, **C**anadian **F**oundation **E**ngineering **M**anual (CFEM) and API. The first one set the minimum (limit) required hammer energy to advance a pile, whereas CFEM and API set the maximum (limit) required hammer energy to advance the pile.

[2]hammer energy or momentum required to advance a pile

(e) Driving stresses

Driving stresses generated by the impact hammer might have resulted in *pile toe failure* if either the phenomenon *pile stagnation & continuous driving* in combination with a Locally Extremely Hard Spot (LEHS) **or** the phenomenon Soft Rock (SR) has happened. Only in those cases, the driving stresses become extremely high close to pile toe. However, it is shown that the *hammer-induced driving stresses* close to pile toe are not necessarily high, as low as $0.5{\cdot}\sigma_y$, given Standard to Normal Soil Condition (SNSC) of Amazonehaven. Sub-Figure (A-D) 6.5 show hammer-induced driving stresses given a SNSC, Zero Shaft Friction (ZSF), Shell Bank (SB) and SR circumstances. Bear in mind, in the latter circumstances, the overlying soil does not generate any shaft friction, and therefore, hammer-induced driving stresses are high along the entire pile.

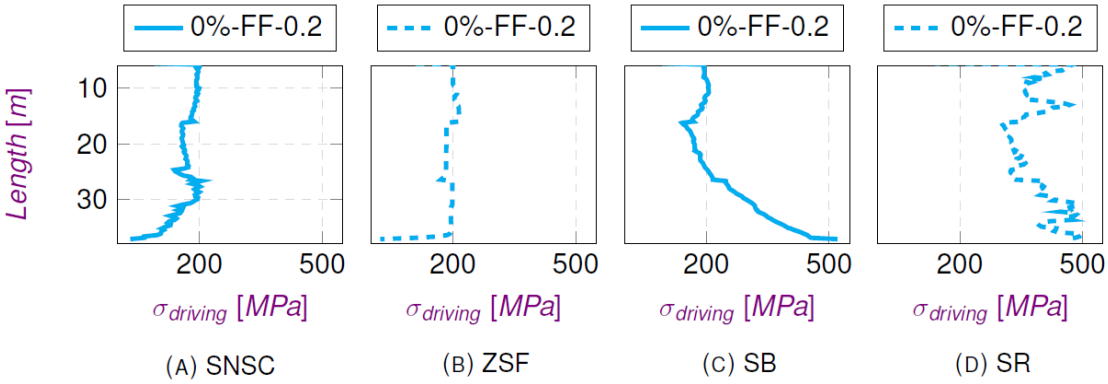

FIGURE 6.5: Driving stresses along the pile, legend:compaction-FF-D/t-83, retrieved from PDP

(f) Temperature

A Locally Extremely High Temperature (LEHT) is likely to be problematic because the pile will locally experience a lower strength and stiffness. The main reason to argue a temperature elevation to have had taken place is the mysterious scorched/glazed sand close to pile toe, as depicted in Figure 6.6 [4].

FIGURE 6.6: Crystallized sand inside the king pile; at toe, released by R. Spruit

This phenomenon is due to extreme friction between the pile and the soil. The friction supposedly arises when sustain piling has facilitated the development of an inward deformation. When king pile, given an initial deformation, encounters a LEHS in its journey to required depth; the pile toe is more prone to an inwards enlargement of the initial imperfection. Where a pile without initial damage, during its journey shovels the same amount of soil in- and out-, an initially damaged pile pushes the soil more out than in. Therefore, just next to the pile toe, the accumulated soil turns into solid *clamped soil* which acts as an inwardly directed force at the pile toe. Furthermore, stress-relief due to lack of soil inside will occur, which eases development of the inwards

deformation. Bear in mind, in Research into Pile Toe Failure in Amazonehaven (RIPTFIA) both terminologies of initial deformation and initial imperfection are used as synonyms. Therefore, the occurrence of Temperature Elevation (TE) fosters this behavior negatively. Chapter 7 studies this phenomenon.

6.2.2 Geometrical failure sources

(g) Plugging

A plugged or an unplugged response is highly correlated with **pile dimensions**. Smaller diameter piles might respond in a plugged one whereas usually larger diameter piles response in an unplugged one [32]. Plugged response refers to a high magnitude of resistance force in which the pile advancement-behavior is similar to a close-ended pile. In a close-ended pile, the toe resistance is distributed over the entire pile diameter which is much higher than the case of the open-ended pile. In case of Amazonehaven, a thin-wall profile (high D/t ratio), the piles could be considered as significant dimensioned piles, where plugging could not appear. However, the smaller the cross-section of pile toe becomes, the more plugged behavior it shows and the higher the resistance becomes. A close-ended behavior might emerge when an initial toe dent is enlarged due to LEHS.

Given a diameter of 1420 [mm], Table 6.1 shows the minimum and maximum *plug length* per D/t ratio:

TABLE 6.1: Plug length per D/t ratio, retrieved from [13]

D/t **ratio**	h_{min} [m]	h_{max} [m]
20	8	24
50	8.5	25.6
83	8.7	26
100	8.7	26.1

The *plugging research* emphasizes that at the *plug length*, as calculated, the plugging is not yet fully activated rather it commences to develop the phenomenon [13]. Therefore, the open-ended piles in the mainly sandy subsoil of Amazonehaven do not tend to show a plug response.

(h) Steel fatigue

Steel failure caused by stress variation, tension, and compression, plays a role as soon as the number of blows becomes exceptionally high. However, for a SNSC the hammer-induced driving stresses, compression, stay low close to toe whereas the hammer-induced driving stresses are high at head. Therefore, fatigue plays probably a role close to pile head due to the exposure of that area to the extreme variation of high stresses. Close to pile toe where stresses are remarkably lower than at pile head, pile's sensitivity to fatigue is believed to be negligible.

(i) Initial imperfection

Initial dent or imperfection in open-ended tubular piles beforehand installation could be a result of, (1) handling operations for transportation, (2) stacking up the piles before installing, (3) uplifting process during installing, etc. The **effects of initial dent or ovalisation** in a pile is that the deformation will gradually grow due to the phenomenon mentioned above, during piling. An extremely stiff layer fosters the enlargement growth extensively, which eventually leads to the pile toe becoming completely flat. Therefore, driving becomes troublesome if not impossible, due to the extensive amount of soil resistance to be mobilized. Piles with a high D/t ratio are more sensitive to undergo an initial dent as well as to experience an enlargement development

during pile advancement, given a Medium to Hard Soil Condition (MHSC), compared to piles with a low D/t ratio [32]. It should be mentioned that RIPTFIA does not discuss pile production imperfections. Chapter 7 discusses the initial imperfection thoroughly.

(j) Fabrication

The **effect of pile's production process** defines how it responds to an unevenly distributed force applied on it [J. Wardenier, personal communication]. To produce piles with a high D/t ratio, spirally welded piles are used [24]. In the production process, initial stresses, dimples, inside the pile exist due to, e.g., cold forming of tubes with rollers during its production. In any case, a recent study using a strain-based method shows that a spirally welded pile does not necessarily indicate *local buckling* at the imperfection spots [24].

In Amazonehaven only two or three piles had a spirally welded profile [N. Mourillon, personal communication]. The majority of the piles had a welded profile. In this way, the pile is welded to one side. Although initial stresses due to welding alongside the pile are present, the damages did not take place at welding locations. Furthermore, Amazonehaven piles were segmented and welded at three parts, with various thicknesses of 17-20-17 [mm]. *The failure* did not take place at an interface of one segment to another, rather it was at a location of either at the toe or 2·D from the toe [37]. In any case, RIPTFIA does not take fabrication into account.

6.2.3 Geological failure sources

(k) Plugging

A plug-response could occur when the inside soil column acts as a rigid body due to its **cohesive soil properties**. Within the pile, a complete toe-resistance over the entire diameter is developed which has the same response as a close-ended pile. The plugged & un-plugged behavior of the pile is mostly conducted by analyzing the output of a static loading test for an open-ended pile regarding its capacity [13]. In Amazonehaven, however, the soil composition is mainly sand due to its human-made character [57]. Therefore, plugging due geological conditions could not be the reason of *the failure*.

(l) Locally extremely hard spots

SB, LEHS, are possible to be found in MaasVlakte I (MVI) area. The first terminology refers to stiffer soil properties like boulders or shell/stiff banks, whereas LEHS particularly refer to extreme values used in RIPTFIA. However, both terminologies are used as synonyms. In this circumstances, an extra effort is needed to overwin the locally high resistance experienced by pile toe regarding a sustained pile advancement. Therefore, high driving stresses close to pile toe are shown to be expected.

(m) Zero shaft friction

In SR, referring to a rocky bed-layer with overlying poor soil characteristic, the shaft friction along the pile is more or less zero. The overlying soil has poor features and does not generate sufficient friction in proportion to the toe resistance. In this circumstance, the *fixed end extreme* is simulated. Therefore, the upward wave force at the toe is becoming twice as high as the downward wave force at the head. In other words, pile toe experiences a force two times higher than the impact force exercised at pile head. However, given the soil characteristics in Amazonehaven; a SR-soil is far from reality and could not be the reason for *pile toe failure*.

(n) Pile inclination

Pile inclination refers to a situation in which the edges of the tubular pile are located in extremely diverse soil characteristics, as depicted in Figure 6.7.

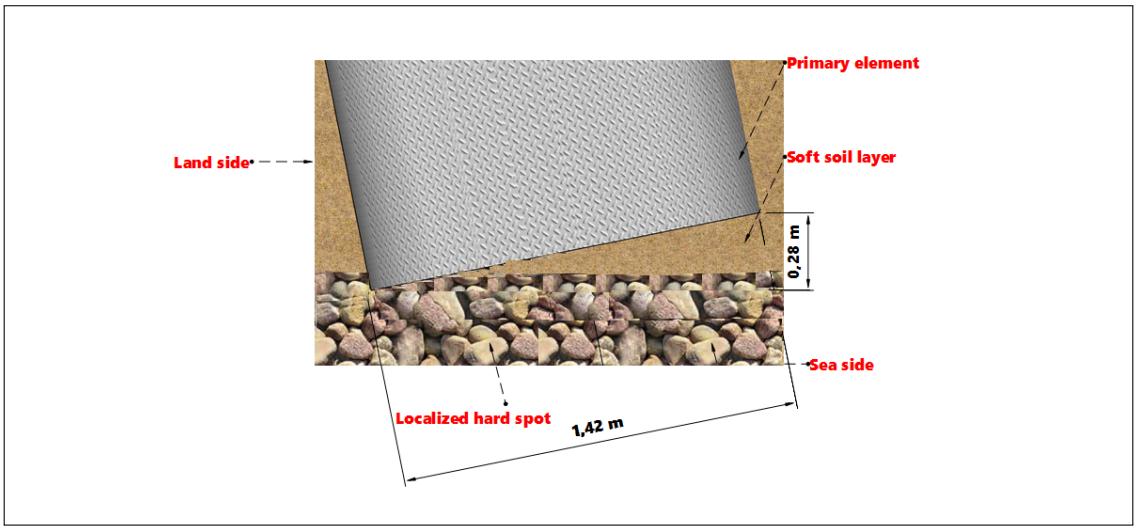

FIGURE 6.7: Cross-section of an inclined king pile, inspired by H. Pacejka, used SketchUp

A **soil inhomogeneous surrounding** or a not uniform soil layer at embedded depth could also trouble vertically installed piles. However, the inclined piles are more prone to suffer from such a circumstances, especially when the diameter is significant. In this case, only one edge receives a soil response of about twice as high the downward impact force, assuming a *fixed end extreme* situation. In Amazonehaven, the edges of the pile are horizontally 1.42 [m] away from each other whereas vertically, it is 0.28 [m]. Chapter 7 discusses this phenomenon.

(o) Soil set-up

Soil set-up refers to a phenomenon in which soil, mainly clay, regains its initial strength after End of Initial Driving (EOID). This factor could be calculated more precisely, but in general, it is around two for clay and one for sand [29]. The effect of *soil set-up* is that re-driving[3] would be more bothersome if not impossible due a greater soil resistance to be mobilized. Therefore, it is very recommended to drive the pile up to its required depth without suspending the driving activities. In Amazonehaven, however, a delay of almost two weeks has occurred due to hammer change. Taking into consideration the soil composition of the area, also clay, it is realistic to take along the soil set-up. It could be argued that the soil set-up, not taken into account in RIPTFIA, has the same effect as the soil compaction.

(p) Soil fatigue

During pile installation, soil fatigue appears. As the name reveals, soil loses its strength and becomes less firm to pile penetration. The piles are vibrated to a maximum depth, before driving. Therefore, the pile installation is divided into two stages. The first stage includes the vibrated length and the second stage includes the length which is yet to be driven. Therefore, in the vibrated stage, the FF-value has an almost constant value. The fatigued soil resistance is kept to 0.5 or 0.2. A decrease of soil resistance by 50% to 80% is used. In the second stage, however, the soil fatigue varies per soil type. The last four meters, the fatigued soil resistance is the same as the *virgin* soil resistance. In other words, the soil is not fatigued, and the full soil resistance is expected, see appendix B.

6.3 Conclusions

An overview of possible origins of *the failure*, divided into three *failure sources*, were discussed in this chapter. It is predicted, using AllWave Pile Driving Prediction (PDP), that hammer-induced driving stresses have low values at pile toe for Standard to Normal Soil Condition

[3] recommencing driving activity

(SNSC), which is assumed to be the case for Amazonehaven soil composition. Therefore, it is concluded that *the failure* has occurred **during** the driving activity, but it is not solely caused **by** *hammer-induced driving stresses* exceeding the material's yield stress close to pile toe. When Medium to Hard Soil Condition (MHSC) exist, a high number of blows and difficulty of pile penetration as well as high values of hammer-induced driving stresses occur due to high soil resistance to be mobilized. Hereafter, a brief conclusion is given per failure source:

Dynamic failure sources

(a) **soil compaction** due vibration; generates more resistance to pile driving, which reduces the downward wave stresses. Therefore, the hammer-induced driving stresses close to pile toe are less than material's yield stress. The study compares the compaction sensitivity of the subsoil for low to high D/t ratios. Soil compaction increases the number of blows needed to bring the pile to its required depth. According PDP, piles with high D/t ratio could not reach their required depth.

(b) **pile inclination** could cause unequal load distribution due to eccentric impact force at pile head. Pile inclination effect is taken into account in chapter 7.

(c) **Zero Shaft Friction (ZSF)** simulates pile driving without any shaft friction, which could happen in reality by pile stagnation & continuous driving in combination with a Locally Extremely Hard Spot (LEHS). The combination will endanger the pile toe integrity.

(d) **hammer selection** is quite important to ensure sustained driving. For Amazonehaven, a D62 hammer did not comply within the ranges of minimum and maximum hammer energy. The hammer-induced driving stresses, given a SNSC, are less than material's yield stress, given a diesel hammer D100.

(e) **driving stresses** are about 60% lower than the material's yield stress close to pile toe, for Amazonehaven SNSC. However, in case of MHSC, the stresses are extremely high close to pile toe.

(f) **temperature** reduces both strength and stiffness of the steel which makes it less resilient to folding. The temperature elevation is caused by a high friction between soil and pile. A local Temperature Elevation (TE) together with, e.g., an initial imperfection will be detrimental to pile toe integrity. Chapter 7 studies the effect of high temperature in a pile.

Geometric failure sources

(g) **plugging** refers to the dimension of the pile which fosters a plugged response of the pile. The dimension of Amazonehavne's piles is argued to be significantly large which does not facilitate plugging. Plugging is, therefore, not taken into account.

(h) **steel fatigue** appears when the number of blows become extremely high. However, the head of the pile is more sensitive to fatigue rather than the toe, because the driving stresses at the toe are shown to be less than at head in SNSC. Therefore, it is argued that the steel fatigue not lead to *pile toe failure* as there is no documentation of extreme deformation at pile head. Fatigue of the material is not taken into account.

(i) **initial imperfection** leads to *pile toe failure*, in terms of *extreme folding damage* when it is accompanied with a LEHS. In case of sustain driving, unequal soil distribution inside & outside occurs, which leads to a gradual (inwards) deformation. Chapter 7 discusses the effect of initial imperfection.

(j) **fabrication** of the piles could affect material's response to unevenly distributed stresses. Research into Pile Toe Failure in Amazonehaven (RIPTFIA) does not take fabrication into account.

Geologic failure sources

(k) **plugging** becomes problematic in cohesive soil properties, where the soil inside the pile acts as a rigid body. Amazonehaven, sandy soil, does not foster the plug phenomenon.

(l) **LEHS** is detrimental to pile toe and could have caused pile toe failure. A combination of LEHS and initial imperfection will magnify any *pile toe failure* development.

(m) **ZSF** plays a role, in case of Soft Rock (SR) phenomenon. In this situation, the overlying layers have poor properties whereas the bed enjoys stiff-rock-ish soil properties. The *fixed end extreme* is simulated in which the stresses at the toe are twice as the impact stresses at the head.

(n) **pile inclination** refers to inhomogeneous soil properties around the toe, which are supposedly exacerbated due to an inclined installation of the pile. Therefore, pile toe experiences at one edge two times higher stresses whereas at the other edge the stresses are limited to impact stresses at the head. Chapter 7 studies the pile imperfection.

(o) **soil set-up** affects the driveability. In this fashion, mainly clay, soil regains its initial strength and re-driving would become troublesome. Therefore, soil set-up has more or less the same effect as soil compaction or a situation without accounting for soil fatigue.

(p) **soil fatigue** affects the drievability. A soil Fatigue Factor (FF)-value of 0.2 reduces the Soil Resistance to (pile) Driving (SRD) considerably, where stress wave travels through the pile *almost* freely.

Therefore, it could be concluded that **initial imperfection**, **pile inclination** and **temperature** are the main reasons to *pile toe failure*, in Amazonehaven.

1. **Initial imperfection**: **Pile imperfection** refers to any initial dent & deformation of pile due *storage*, *transportation*, *uplifting & handling*, and *installation*, which has its origin in operations beforehand any driving activity takes place.
2. **Pile inclination**: **Pile inclination** refers to both eccentric impact hammering and pile toe located in extremely diverse soil layers with weak- and stiff- properties. The eccentric impact hammering leads to another stress redistribution in a pile compared to a centric impact hammering. The weak or stiff soil layers along the pile and close to toe also affects the stress redistribution in a pile.
3. **Temperature**: **pile inhomogeneous strength** refers to appearance of Locally Extremely High Temperature (LEHT). TE close to pile toe could occur, e.g., in case of extremely high friction between pile and soil during driving, due, e.g., pile's behavior altering to a close-ended behavior in which the pile responses similar to a plugged one.

Chapter 7

Finite Element Analysis Program

7.1 Aim

Chapter 7 aims to provide a sensitivity analysis for the three main causes of *pile toe failure*, as depicted in Figure 7.1, to intercept the leading cause to *pile toe failure*.

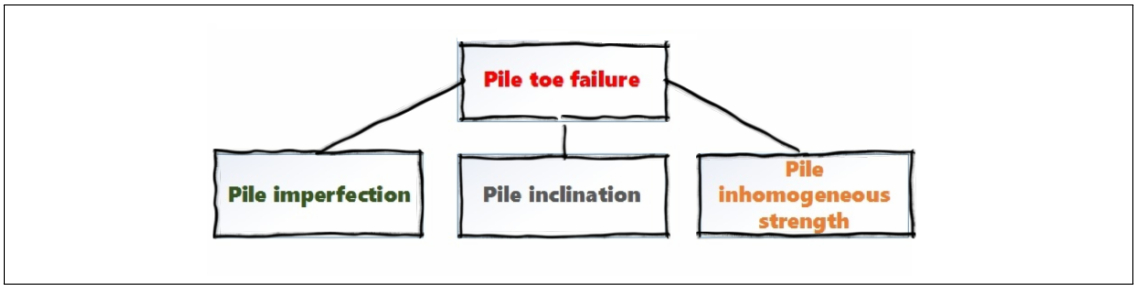

FIGURE 7.1: Main reasons of *pile toe failure* in Amazonehaven

SCIA Engineer enables studying pile's behavior taking into account both properties of geometrically non-linearity and physically non-linearity. In this fashion, the sensitivity of pile to the three failure mechanisms is explored which enables clarifying the leading cause of *pile toe failure* in Amazonehaven. Furthermore, it is looked if the same deformations as the popular modes are to be found. Appendix E is complementary to this chapter.

7.2 Introduction

The non-linearity of the material is defined directly in the material library in SCIA. During a linear analysis, the steel will behave elastically which means that given a load twice high, the stresses and the displacements becomes twice high [52]. The plastic properties of materials, however, are generic for any material. Therefore, plasticity could be enabled by selecting the *isotropic elasto-plastic von Mises* type of plastic behavior. It corresponds to a bilinear stress-strain relationship, identical in tension and compression. In the plastic domain, which occurs when the load becomes very high, the stress remains constant when the strain increases. The other non-linearity feature is referred to as geometrically non-linearity. When a geometrically non-linearity option is enabled in SCIA, the second order effects are taken into account during the calculation [50].

The main difference between a linear and non-linear calculation is that the non-linear calculation gives such results of deflections and internal forces for which equilibrium conditions are satisfied, on a deformed structure [50].

7.3 Numeric calculation

7.3.1 The technique behind finite elements

The structure is divided into a (finite) number of discrete pieces (elements) by mesh-generators. Then, the behavior of each element is simplified through mathematical expressions. Through the inclusion of the elements, a system of comparisons is made which are solved by the computer. After which, the boundary conditions, e.g., the applied load, are set. The finite element program, search for an equilibrium condition given the compatibility[1] of the elements is safeguarded. The solution is the displacements of the nodes. After which, the internal forces and stresses are calculated [52].

7.3.2 Assumptions

In Research into Pile Toe Failure in Amazonehaven (RIPTFIA), the non-linearity properties are taken into account only for the steel, meaning that non-linearity properties are not assigned to the end-support and the surrounding soil. The focus is on a material's yield stress of 483 [MPa] as utilized in Amazonehaven. Furthermore, the material's behavior is identified as elastic-plastic behavior without hardening, bi-linear, based on von Mises. The element size, mesh refinement, is 0.142 [m] for the entire pile while at discontinuities (only) due to imperfection; mesh refinement has an element size of 0.037 [m]. Moreover, the (Timoshenko) calculation is force controlled, based on an iterative method in which the self-weight of the pile is neglected. Last, the initial load with a magnitude of 100 $[\frac{kN}{m^2}]$ is applied on the pile and is increased to find the Yield Stress Momentum (YSM).

RIPTFIA introduces four terminologies essential to a better understanding of the results in the coming sections which are briefly explained below:

- YSM refers to the point where the pile locally reaches its material's yield stress due increasing (static) load; therefore a *YSM* of 100[-] means that the point where yield stress locally appears for the first time is with a load of 10000 $[\frac{kN}{m^2}]$
- Imperfection Ratio (IR) refers to existence of any initial dent, where $IR = 1$ is a perfectly rounded pile toe
- Homogeneity Ratio (HR) refers to existence of any non-uniform soil at pile toe, described as stiff and weak soil, where $HR = 1$ means a homogeneous (stiff) soil properties at pile toe
- Temperature Elevation (TE) refers to a local temperature increase due to generated high friction during piling

7.3.3 Get started

In this section, a general manual is given, to warrant reproducibility of the created model in the SCIA and subsequently the results shown in this study.

Step I

The tubular pile is modeled in SCIA given three different D/t ratios of 50, 83 & 100. The model consists of smaller parts with a length of either $0.2 \cdot D$ or $0.7 \cdot D$, where D is the pile's diameter, as depicted in Figure 7.2. The total length of the model is about ten meters. The smaller parts are segmented into eight pieces, to be able to assign locally different properties to each piece. Also, the size of the discontinuity is manipulated by using either a large part or a smaller part in the model.

[1] connection between the elements

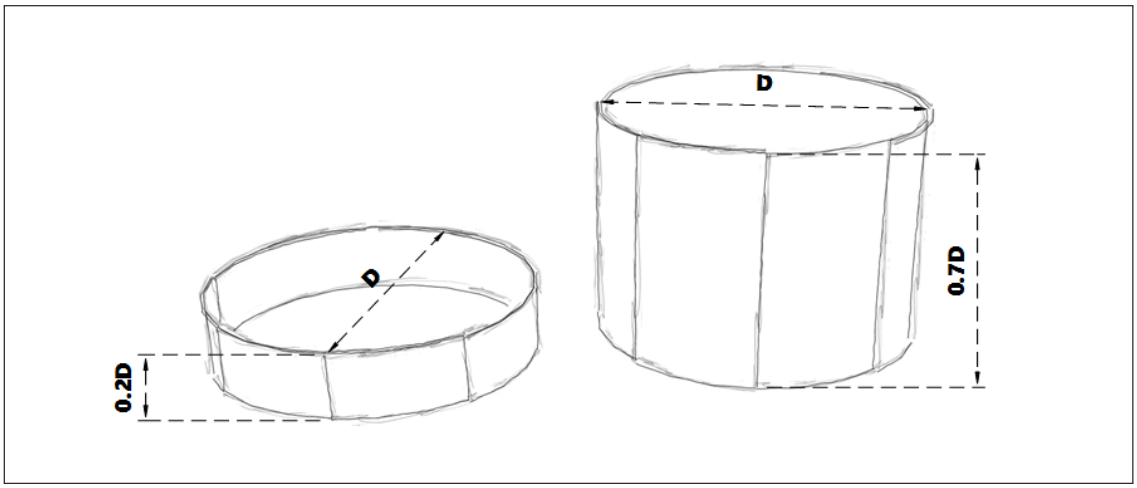

FIGURE 7.2: Small and large parts as modeled in SCIA

Step II

The second step is to choose the non-linear properties and to assign those properties to the selected segments. Other linear features such as surrounding soil and the end support are added to the proper segments. The surrounding soil is chosen either extremely weak or extremely stiff. A weak soil is defined with a stiffness of 15 $[\frac{MN}{m^2}]$ whereas a stiff soil has a stiffness of 120 $[\frac{MN}{m^2}]$. Table 7.1 shows, the bed constant (k_0), for different types of soil.

TABLE 7.1: Stiffness of the subsoil per soil type, retrieved from [3]

Soil type	$k_0[\frac{MN}{m^2}]$
Well graded gravel and sandy gravel	130
Well graded sand and sandy gravel, no fine sand	100
Poorly graded gravel, no fine sand	80
Sandy clay	80
Gravel, sandy gravel, clay-containing sand	50
Poorly graded sand, no fine sand	40
Very fine sand	30
Solid clay	20
Weak clay or peat	10

Step III

Due to pile inclination and likely eccentric impact hammering, both centric and eccentric loads are applied. However, in both situations, the magnitude of the load is the same. In a centric load application, the extent of initial load is 100 $[\frac{kN}{m^2}]$ where for the eccentric load the magnitude of the load in the concentrated part rises to 200 $[\frac{kN}{m^2}]$, as depicted in sub-Figure (A-B) 7.3.

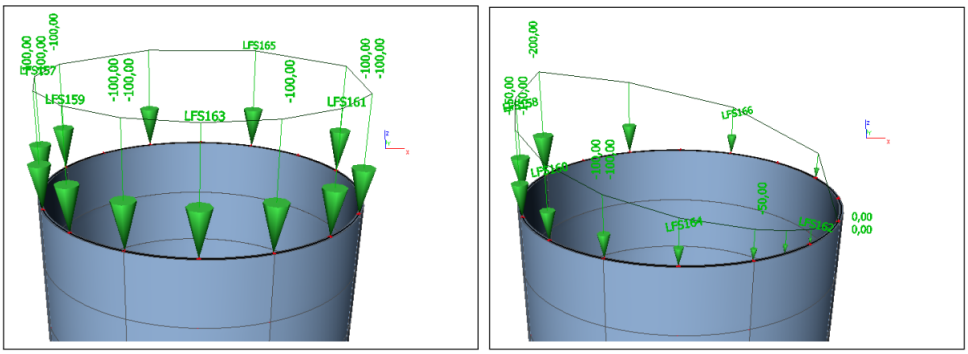

(A) Centric loading (B) Eccentric loading

FIGURE 7.3: Centric and eccentric impact load, retrieved from SCIA

Step IV

Designing different scenarios to investigate **imperfection**, **inclination** and **inhomogeneous strength** . In this fashion, a sensitivity analysis is carried out to study the pile response to the load for either the discontinuity's location or its size.

Step V

The non-linear calculation is carried out, and the load is increased manually up to the point at which the stress reaches the material's yield stress for the first time.

Step VI

Due to bilinear behavior, a manual check is carried out to stay in the logical domain of pile's behavior regarding strain due to load increase. In this check, the strain (ε), must remain below a value of 0.5% [50].

Step VII

The behavior of the pile due to the implemented discontinuities manifest itself in the YSM. In other words, it indicates the speed of reaching that specific point (of material's yield stress) rather than indicating the capacity of the pile, (before collapsing). The YSM is the maximum factored load divided by the initial load, $\frac{q_{yielding}}{q_{initial}}$. By choosing an initial force instead of the collapsing force, which is $(483 \cdot A_c)$, the readability of the graphs is warranted. A_c refers to the cross-section area of the pile.

Step VIII

Figure 7.4 give an indication of schemes as used in SCIA, mandatory for understanding the follow-up schemes. The entire pile is sketched as a square. Centric or eccentric load is shown as an arrow. When the pile toe is located in stiff soil layer, the full end support is represented, which means the pile is fixed in its axial direction. When the pile toe is situated in an incredibly diverse soil layer, weak and stiff, the partial end support is expressed with a rotational spring. The surrounding soil, lateral soil support, is represented by translational spring when the soil is stiff. When the soil properties are weak, the surrounding soil support is not indicated with a transitional spring.

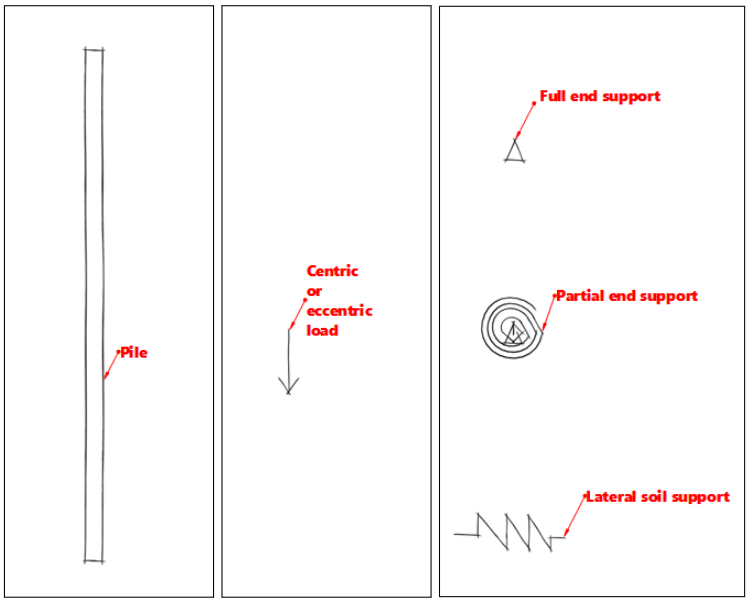

FIGURE 7.4: Sketches of hammer-pile-soil system

Step IX

Bear in mind, that the sensitivity analysis is carried out to compare the three leading causes to *pile toe failure* in Amazonehaven. It does not say anything about the capacity of the pile nor comparing D/t ratios. It is trivial that a pile with a low D/t ratio bears more load and therefore has a higher YSM-value.

Step X

The sensitivity analysis will provide understanding the behavior of the pile, stress development, due to the size and location of the discontinuity.

7.4 Pile imperfection

Pile imperfection, the existence of an initial dent, is studied by analyzing the location of pile imperfection as well as its size. Figure 7.5 shows four scenarios due **I**mperfection's (I) -location and -size. From left to right: discontinuity due imperfection is located at toe and has a size of 0.2·D [I-toe-0.2·D]. Discontinuity due imperfection is located at toe and has a size of 0.7·D [I-toe-0.7·D]. Discontinuity due imperfection is located at 2·D and has a size of 0.4·D [I-0.4·D-0.4·D]. Finally, it is located at 2·D and has a size of 1.4·D [I-2·D-0.4·D].

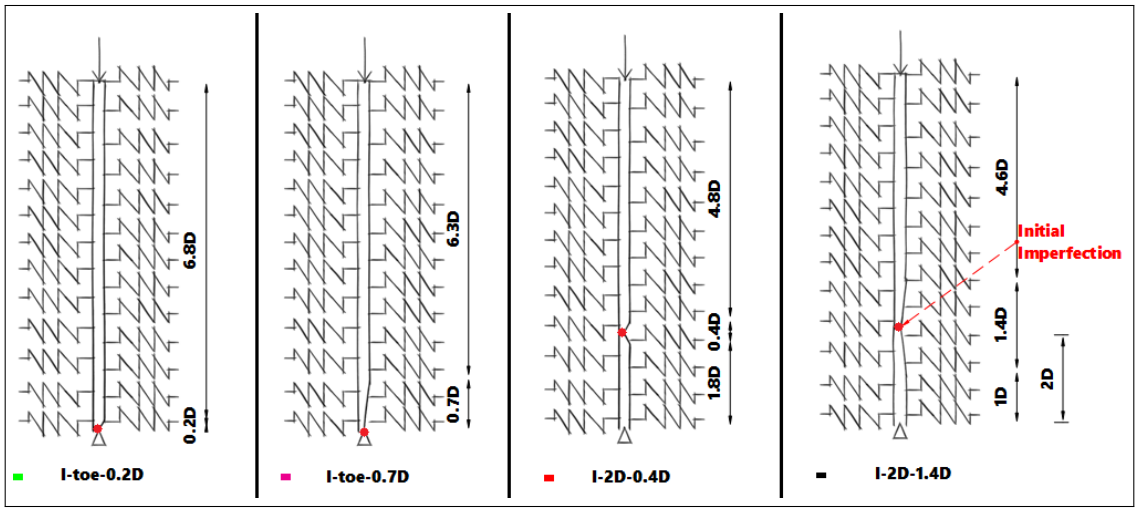

FIGURE 7.5: Sketches of discontinuity due pile imperfection

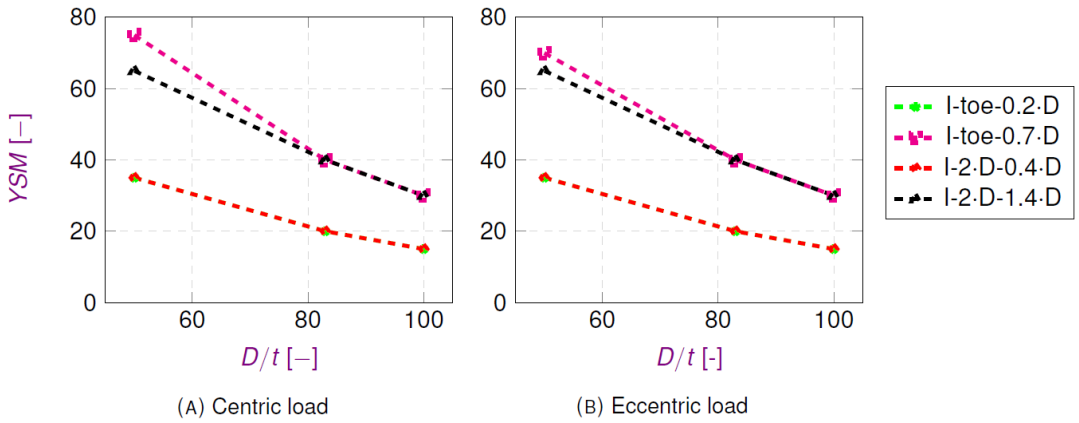

(A) Centric load (B) Eccentric load

FIGURE 7.6: YSM versus D/t ratio per scenario, legend: Source-Location-Size, retrieved from SCIA

Figure 7.6 shows that YSM has a lower value for scenarios in which the size of the discontinuity is 0.2·D-0.4·D. The data is overlapping in Figure 7.6. Therefore, the size of the discontinuity is governing than its location. A reduction of nearly 60% of pile's YSM for both centric and eccentric loading is to be expected.

7.5 Pile inclination

Pile inclination refers to pile being located in non-uniform soil; for both the surrounding soil and soil close to pile toe. Therefore, the pile inclination is studied by analyzing the location of soil homogeneity as depicted in Figure 7.5. From left to right: the **H**omogeneous (H) surrounding soil is weak along the pile, whereas at pile toe the soil support is fully realized [H-100%-Weak]. The homogeneous surrounding soil is stiff along the pile, whereas at pile toe the soil support is fully realized [H-100%-Stiff]. The homogeneous surrounding soil is partially stiff along the pile as well as at toe [H-50%-Partial]. The homogeneous surrounding soil is partially weak and partially stiff along the pile, whereas at pile toe the soil support is fully realized [H-100%-Partial].

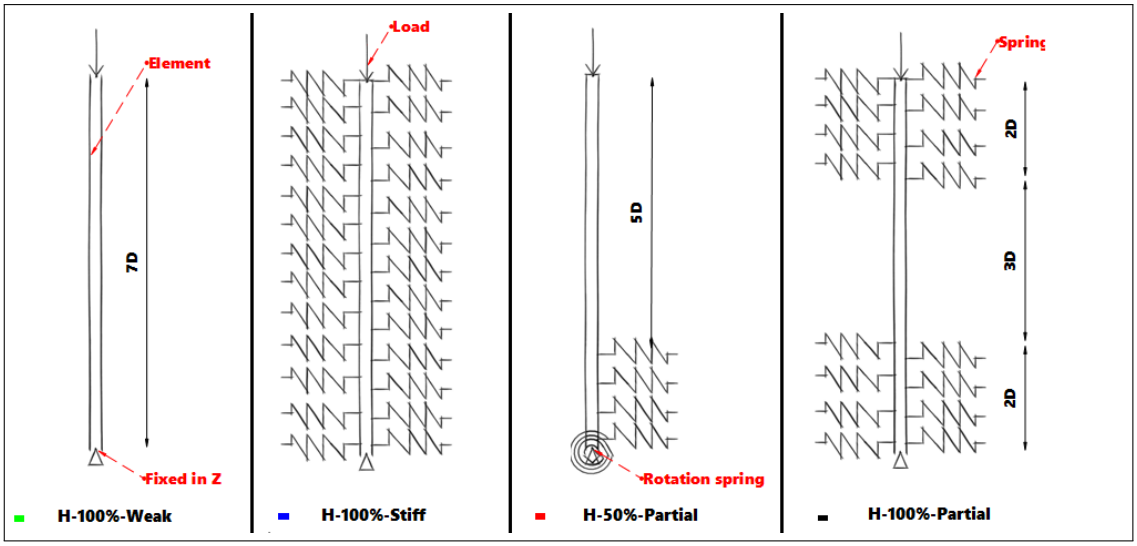

FIGURE 7.7: Sketches of discontinuity due pile inclination

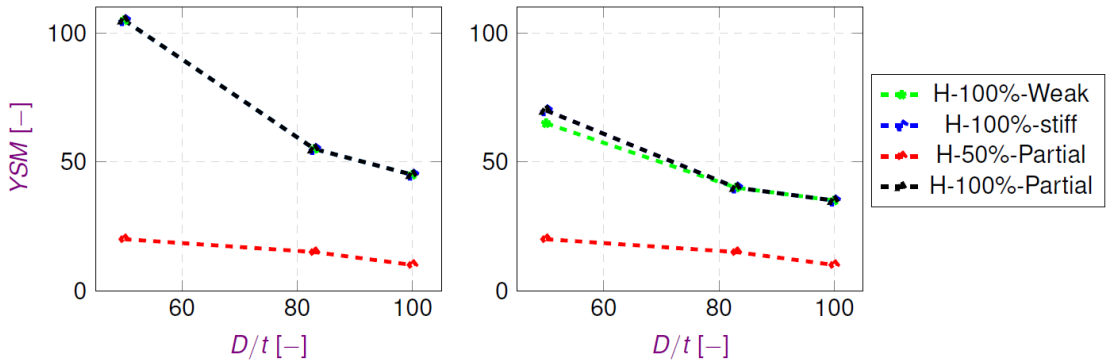

(A) Centric load (B) Eccentric load

FIGURE 7.8: YSM versus D/t ratio, legend: Source-End support-Lateral support, retrieved from SCIA

Figure 7.8 shows that *surrounding soil* does not necessarily plays a role for centric loading, as it was to be expected. However, when the soil inhomogeneity is located at pile toe, a drop in YSM is visible. A reduction of nearly 80% and 75% of pile's YSM for respectively centric and eccentric loading is to be expected.

7.6 Pile inhomogeneous strength

Pile inhomogeneous strength, a local TE, is studied by analyzing the location and size of the discontinuity, by assigning locally different stiffness and strength properties. Pile's stiffness is reduced by 40% whereas its strength undergoes a reduction of 25% assuming a temperature elevation of nearly 500° Celsius. Figure 7.9 shows four scenarios due to *pile inhomogeneous strength*. From left to right: **T**emperature (T) elevation is assigned to toe with a size of 0.7·D [T-toe-0.7·D]. The temperature elevation is assigned to 2·D with a size of 0.4· [T-2·D-0.4·D]. The temperature elevation is assigned to 2·D with a size of 0.7· [T-2·D-0.7·D]. Finally, it is assigned to toe with a size of 0.2· [T-toe-0.2·D].

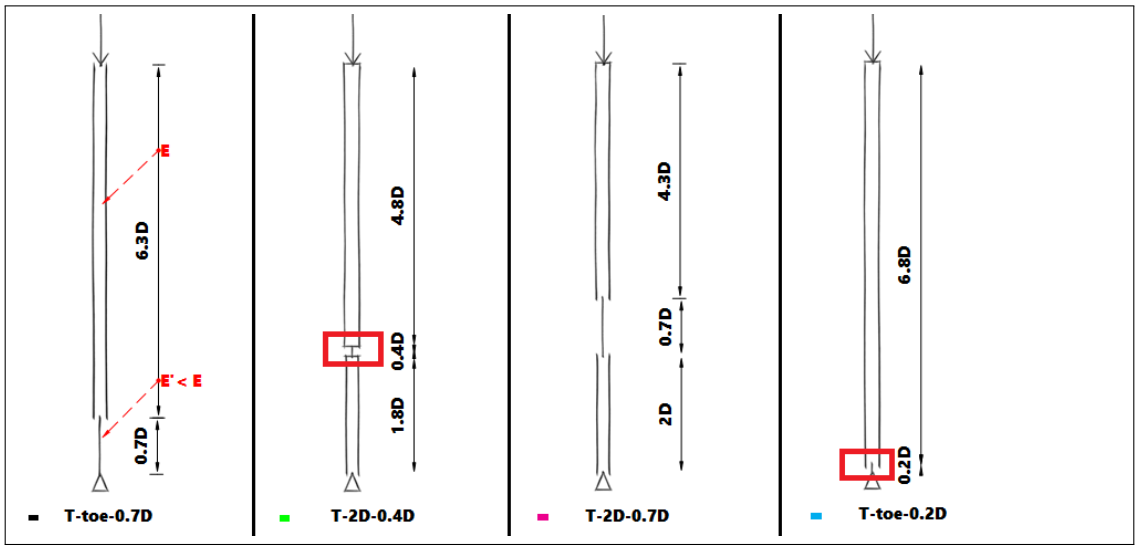

FIGURE 7.9: Sketches of discontinuity due pile inhomogeneous strength

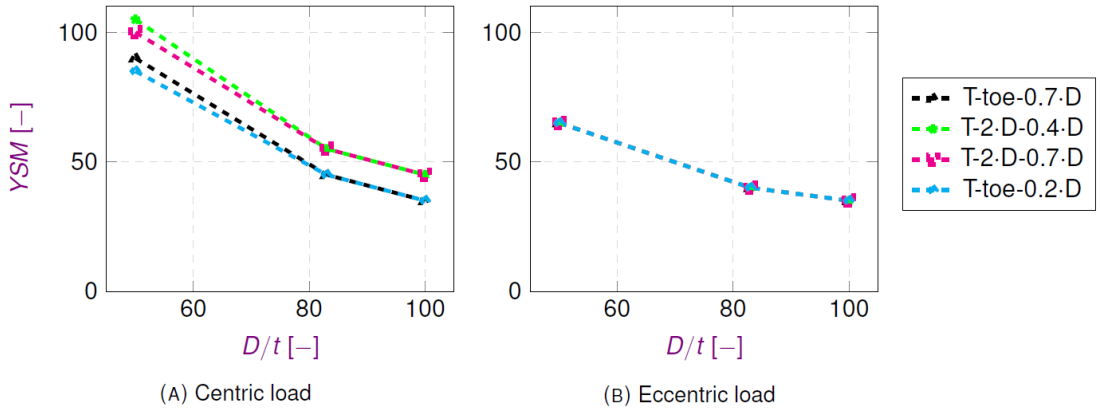

(A) Centric load (B) Eccentric load

FIGURE 7.10: YSM versus D/t ratio, legend: Source-Location-Size, retrieved from SCIA

Figure 7.10 shows that the reaction of the pile to a local temperature elevation is slightly more sensitive to its location than its sensitivity for its size, for centric loading. In case the temperature increase is close to pile toe, a reduction of almost 20% is observed in the YSM. Therefore, a decrease of nearly 20% of pile's YSM for centric loading.

7.7 Inclusion

Figure 7.11 shows the governing scenarios in one overview compared to a situation without any discontinuity. The reduction of pile's Yield Stress Momentum (YSM) is by 20%, 80% and 60%; for respectively: T-toe-0.7·D, H-50%-Partial and I-toe-0.2·D, given a centric loading, given a D/t ratio of 83. For an eccentric loading, these values are respectively 0% (no reduction), 75% and 60%.

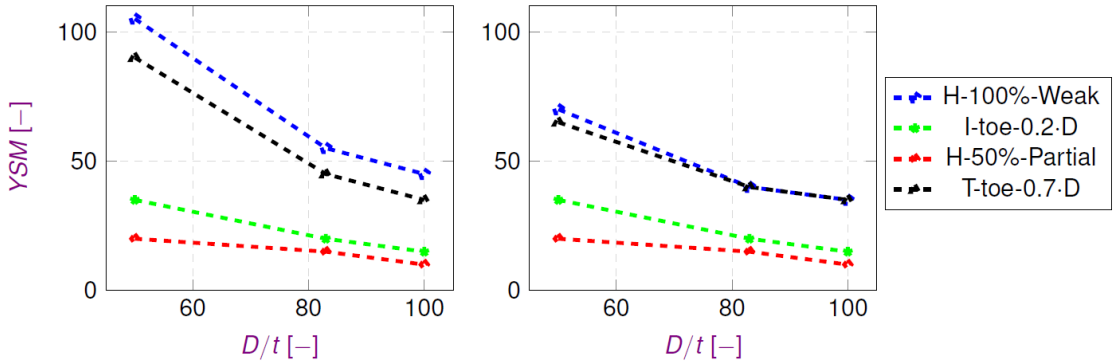

(A) Centric load (B) Eccentric load

FIGURE 7.11: YSM versus D/t ratio, legend: Source-Location-Size, retrieved from SCIA

Bear in mind that even though the YSM drops considerably due to one or other scenario, the YSM reaches for the first time with at least a factor 5 [-] higher than the initial load[2]. Therefore, it is apparent that given the low hammer-induced driving stresses close to pile toe in a Standard to Normal Soil Condition (SNSC); a combination of three leading causes would eventually result in a much lower YSM factor.

In appendix D, a thorough analysis is given for the scenarios mentioned above given the Amazonehaven's D/t ratio. The stress-development and its deflection per scenario are studied in sections C.5-C.6-C.7.

7.8 Triggers

After studying the influence of discontinuity's -location and -size to pile behavior, the ratio of discontinuity is studied. In other words, the pile response to an increasing discontinuity: (1) Imperfection Ratio (IR), (2) (soil) Homogeneity Ratio (HR) at toe and (3) Temperature Elevation (TE). When IR is 1, the pile toe integrity is assured. When HR is 1 the entire toe is located at a stiff uniform layer, whereas decreasing HR means that the bed layer contains weak and stiff soil properties. TE, however, means an elevation in temperature which reduces the pile's stiffness and strength.

Sub-Figure (A-C) 7.12: (A) shows a rapid decline for YSM with a slight change in IR, while in (B) it reduces less drastically with a change in HR. Therefore, a slight imperfection will lead to a decrease in, $\frac{q_{yielding}}{q_{initial}}$. In other words, the force which realizes the yielding point, acting on the pile, will be less compared to a situation without discontinuity. Finally, the effect of TE has been shown to be less influential, up to a temperature of 500° Celsius.

[2] a value of 500 [MPa]

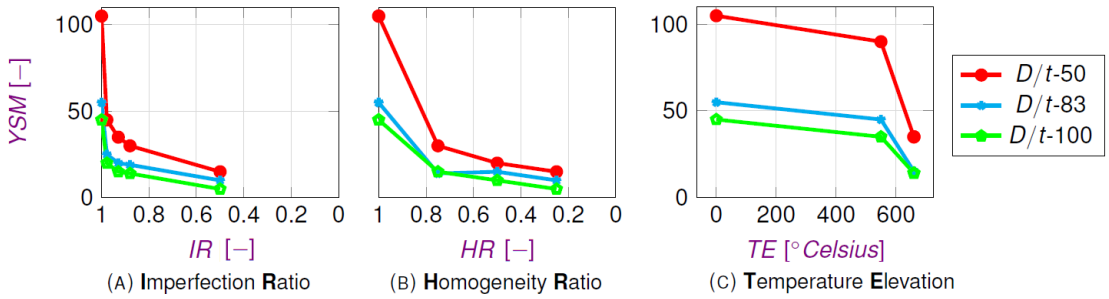

(A) **I**mperfection **R**atio (B) **H**omogeneity **R**atio (C) **T**emperature **E**levation

FIGURE 7.12: YSM for centric loading (A)-(C), retrieved from SCIA

Sub-Figure 7.13 (D-F) shows the same for eccentric hammer impact. An eccentric loading has a lower YSM compared to centric loading circumstances.

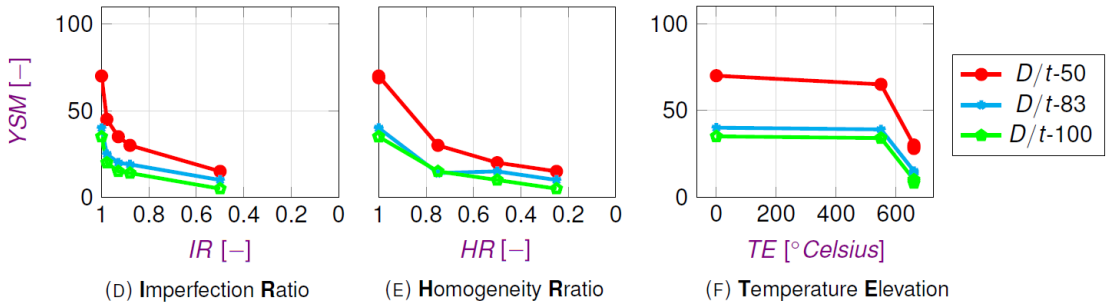

(D) **I**mperfection **R**atio (E) **H**omogeneity **R**ratio (F) **T**emperature **E**levation

FIGURE 7.13: YSM for eccentric loading (D)-(F), retrieved from SCIA

In appendix D, a thorough analysis is given for the scenarios mentioned above given the Amazonehaven's D/t ratio. The stress-development and its deflection per scenario are studied in sections C.8.1-C.8.2-C.8.3.

7.8.1 Failure mode

Figure 7.14 presents a top view of deformations in case of **pile imperfection**. It shows that, given the imperfection at pile toe, the earlier described failure modes of Moon Cancer (MC), BoomeRang (BR), HourGlass (HG) and Russian Doll (RD) are found. Appendix D reveals more information about the stress-development in a pile, and its specific deformations.

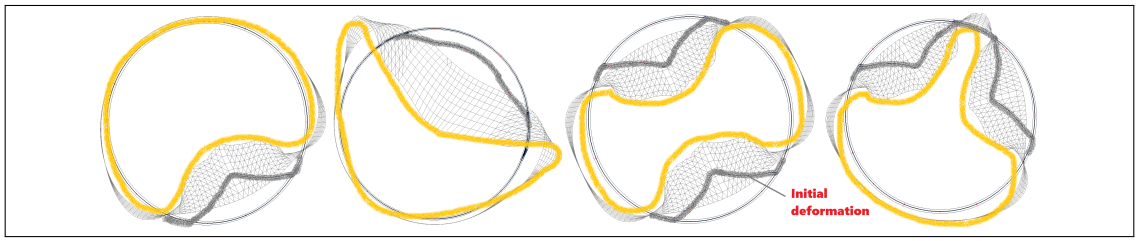

FIGURE 7.14: Top view deformation, left to right: MC, BR, HG and RD, retrieved from SCIA

7.9 Conclusions

The pile sensitivity to its discontinuity due -**imperfection**, -**inclination** and -**inhomogeneous strength** is investigated by looking into different scenarios. In these scenarios, the location and the size of the discontinuity are studied. It is shown that respectively soil inhomogeneity at toe,

initial imperfection with 0.2·D-0.4·D, and temperature increase close to pile toe; have the most influence on the pile response to centric or eccentric loading. In other words, respectively, the point in which the material yield stress is reached occurs with a lower force. Furthermore, the study showed the same deformations as analyzed in chapter 4, the popular modes.

The reduction of pile's Yield Stress Momentum (YSM) is by 20%, 80%, and 60%; for respectively scenario's T-toe-0.7·D, H-50%-Partial and I-toe-0.2·D, given a centric load, given a D/t ratio of 83. For an eccentric load, these values are respectively 0%, 75%, and 60%. Furthermore, triggers studying an increasing ratio of discontinuity showed that YSM versus Imperfection Ratio (IR) declines in a steeper line than the Homogeneity Ratio (HR), which means that pile (initial) imperfection could have a significant role in *pile toe failure* in Amazonehaven compared to both pile inclination and pile inhomogeneous strength.

7.10 Limitations SCIA Engineer

The main limitation of SCIA Engineer is that the non-linear properties could not be assigned to each feature in the model, e.g., soil. In this research, non-linear properties are only assigned to the pile itself. However, programs such as ABAQUS and DIANA are more suitable to carry out a hammer-pile-soil interaction study. Availability of SCIA was the main reason to choose amongst other software. Furthermore, the inclination of the pile could not be modeled due to non-compliance of the load with the direction of the inclination for centric and eccentric loading. This problem was solved initially by adding a plate on top of the pile, in between the load and the *pile head*, but later it was apparent that it does not work appropriately. Furthermore, the geometrically non-linearity property is taken into account for a static load. Therefore, the *extreme folding damage* could not be modeled, in case of a perfect rounded pile, because the damage appears gradually. However, in case of piles with an initial dent, the *extreme folding damage* is approximately modeled as performed in reality. Last, it was not possible to apply a dynamic load; instead, a static load was applied.

In the results presented in Research into Pile Toe Failure in Amazonehaven (RIPTFIA), the limitations did not have a significant influence. The main aim was to develop an understanding in-between three main causes of *pile toe failure* and conducting a sensitivity analysis rather than exact values.

7.11 Recommendations

It is recommended to take into account: (1) non-linearity properties for other features in the model, e.g., surrounding soil along the pile as well as at pile toe. (2) the dynamic mold of load and pile respond both given a perfectly rounded pile and an initially dented pile. (3) the dynamic mold of load and pile respond given both a Standard to Normal Soil Condition (SNSC) and a Medium to Hard Soil Condition (MHSC). (4) the dynamic mold of load and simulation of inwards deformation during piling. (5) capacity reduction of an individual pile, given the *pile toe failure*. (6) capacity reduction of the entire system of foundation elements given the *pile toe failure* of the king piles. (7) capacity reduction of an individual pile, given a combination of three leading causes to *pile toe failure*, as presented in this research.

Chapter 8

Management of *pile toe failure*

8.1 Aim

Chapter 8 aims to study the process and the environment around the problematic of *pile toe failure*. It answers questions like: (1) What are the process-related causes of failure, (2) how could introducing new process-related alternatives help to avoid such damages, (3) what are the Loss of Earnings (LOE) due malfunction of the quay wall. Appendix D is complementary to this chapter.

8.2 Introduction

The Management Aspect (MA) of the *pile toe failure* adds a 4^{th} dimension to the already identified sources of failures in Amazonehaven, as depicted in Figure 8.1. The environment includes the process proceedings the installation, in pre-piling phase, which is divided into three categories of (1) data collection, (2) pre-installation and (3) installation. The reliability of collected soil data, storage of the piles, transportation to the location, handling & uplifting before installation as well as installing operation are the main factors within these categories. The process-based alternatives introduce adjustments to reduce incurring of *extreme folding damage* of open-ended tubular piles.

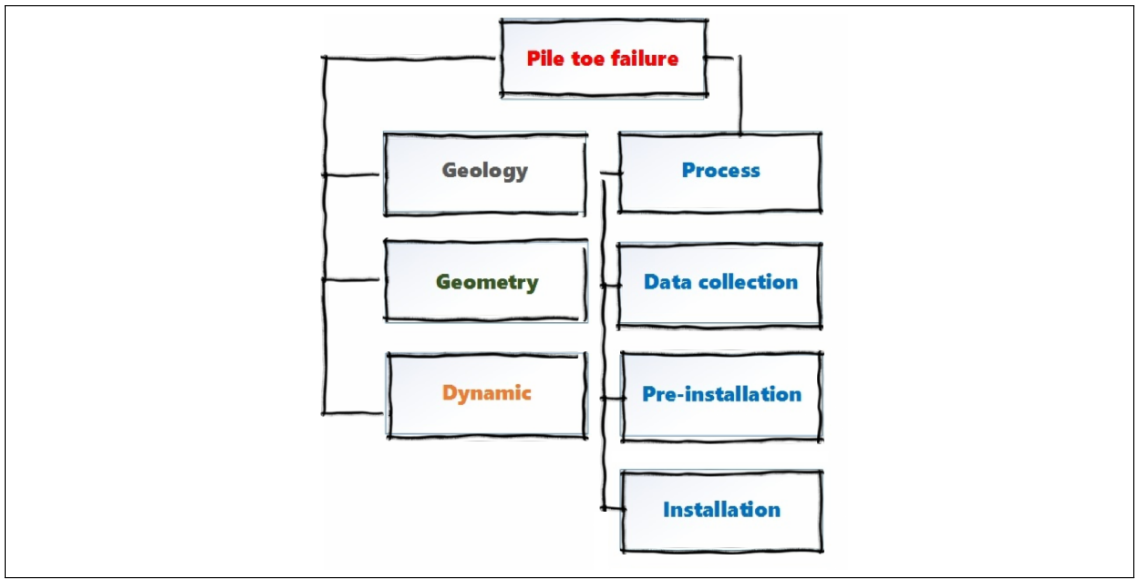

FIGURE 8.1: Overview of origins of *pile toe failure*

8.3 Piling risk event

The *pile toe failure* is a risk for both contractor and client. The *piling risk event* is the *extreme folding damage* close to pile toe which might endanger the stability of the quay wall. Bear in

mind, that the king piles function as bearing and retaining elements. In *stability research*, it is shown that due *pile toe failure* (1) soil displacement increases with a factor three, (2) the moment on the combined wall increases with a factor 1.8 and (3) the anchor force reduces with a factor 0.4 [37]. Therefore, it could be assumed that the *piling risk event*, if occurs, might lead to counteractions to be taken to safeguard the quay wall's functioning (operation) throughout its technical lifetime. Thus, the risk event must be avoided. To prevent this risk[1] from happening, either probability of its occurrence or its consequence when it occurs must be reduced. Therefore, the solution is to be found either in a pre-piling phase which tackles its probability or a post-piling phase which tackles its consequences [44]. It is believed that by adjustments in processes mentioned in above categories, innovative process-based alternatives, the piling disease is to be treated.

8.4 Pre-piling phase

8.4.1 Data collection

The primary variables in a hammer-pile-soil system are (1) type of hammer, (2) D/t ratio of the pile and (3) soil characteristics. Soil characteristics refer to soil properties such as quake value, soil Fatigue Factor (FF), soil type and soil set-up. In a driveability prediction study, the number of blows is prevailing as it depends on the entire system. In conventional pile design, the structural forces are determining the pile's dimensions. Therefore, the D/t ratio is fixed. The soil characteristics are also fixed, which means that only the appropriate hammer to bring the pile to its required depth is unknown and to be selected.

In general three situations could appear: (1) selecting a heavy hammer, (2) choosing the right hammer or (3) selecting a light hammer. These hammer selections, are assumed to be entirely justified and not an engineering selection-error.

- a heavy hammer is purchased than needed. Therefore, more costs than necessary. However, the contractor has taken into account the cost of purchasing a heavy hammer, and no major cost-overruns takes place. Regardless, the full capacity of the hammer is not availed. Also, the number of blows is lesser than anticipated in the prediction.
- perfect situation. A sufficient hammer is selected. The blow counts are approximately the same as expected. There are no extra costs for neither client nor contractor.
- a lighter hammer is selected. The pile does not reach its required depth. A heavier hammer must be purchased which takes time and slacks up the project. After which, re-driving the pile is more troublesome due to soil healing, regaining its initial strength. The cost will increase due to both purchasing a heavier hammer and a halt in the execution work.

Therefore, it is essential to collect data as carefully as possible. Data collection includes both soil investigations in the early design phase as well as the execution of pile tests to assure hammer selection.

8.4.2 Pre-installation

Pre-installation is one of the main categories which requires the most care and attention to prevent *piling risk event*. It includes storage, transportation, uplifting & handling before installing the piles. Storage of piles, stacking up, could lead to pile ovalization. Transportation of the piles requires uplifting which must be executed with care to prevent any pile toe damage. The piles, when arrived at the project's location, will be stored again which could lead to pile ovalization. Also, uplifting & handling before installation could lead to pile toe damage. Piles with high D/t ratio are more prone to such a pre-installation damage.

[1] Risk = Probability · Consequences

Storage

Storage of piles at project's location could cause ovalization of the pile. This ovalization could initiate the damage and lead to *pile toe failure*. However, the height of the pile stock is not that high due to significant pile dimensions [R. Spruit, personal communication]. Nevertheless, to prevent this failure mechanism, a Just in Time (JIT) delivery system could be introduced to the piling industry. A JIT[2] delivery system is commonly used in auto industry, or other mega projects [9]. Assuming that the pile ovalization could only appear in the storage yard of the site and not per se in the fabric, this delivery system helps to maintain pile toe integrity in the storage yard.

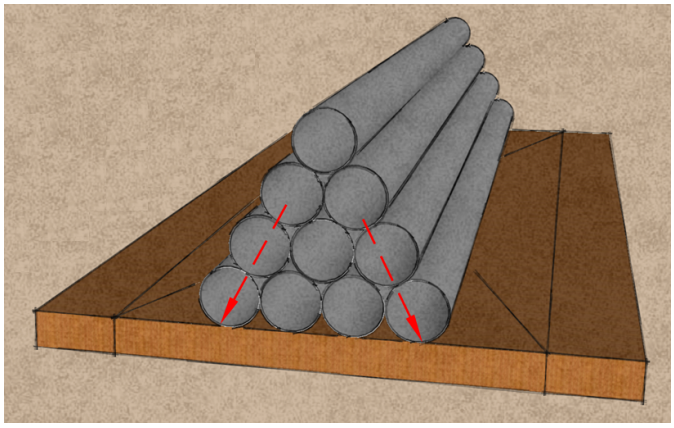

FIGURE 8.2: Impression of king piles stored at site, used SketchUp

In any case, a perfectly rounded pile does not exist. Initial ovalization or Out of Roundness (OOR), are to be expected. Therefore, a value of less than 1% (of the diameter) is implemented and recommendations are to consider a value of 0.05% in the design if no actual values are given [16]. Given the fact that this type of ovalization is acceptable and below the limits, a further ovalization due storage could be prevented. Nevertheless, the values taken into account in chapter 7 are higher than the 1% initial ovalization[3].

Transportation

The transportation of piles is also of importance. By utilizing a simple solution as a wooden cover for both pile toe and pile head, pile toe integrity during uplifting and transporting the piles to its destination beforehand installation will be secured. The wooden *azobé* cover is locked and unlocked easily with a click and could be reused, as depicted in Figure 8.3.

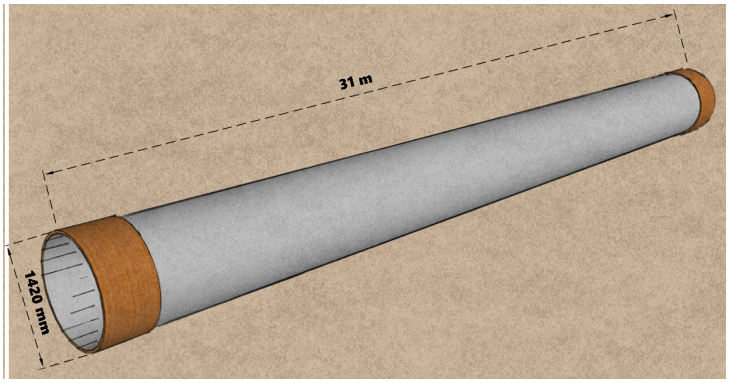

FIGURE 8.3: Wooden cover at pile -toe and -head, inspired by R. Spruit, used Sketchup

[2]materials and components delivered when on site teams need them
[3]See section C.8.1-C.8.2-C.8.3

The *wooden-cover* solution could also be used in other pre-installation processes, such as storage. In any case, the transportation and uplifting of the piles must be executed with care.

Uplifting & handling

Uplifting and handling process before installation is necessary to bring the pile into its position. In the uplifting process, the pile is lifted from the pile head, which means the weight of the entire pile is resting in one corner of the pile toe. Figure 8.4, shows uplifting in practice. When the pile is exactly at its vertical position, the weight is carried over the entire edge equally. A pile with a high D/t & L/D is more prone to handling damages beforehand installation compared to one with a low D/t ratio.

FIGURE 8.4: Left: uplifting in practice MV 06.05.2016; Right: impression concentrated forces during uplifting

The *piling risk event* is always present. To reduce its probability of occurrence both wooden cover as well as in-situ measurements of pile's OOR, are highly recommended. However, the minimum thickness of a wooden-cover i, not studied as well as its actual role to maintain pile toe integrity in pre-piling phase. Nevertheless, it could play a decisive role in the mental effect it has on the operators to handle the tubular piles with care. Bear in mind that in any case, the uplifting operation must be executed with precision and care.

8.4.3 installation

Stiffening ring

To have a safe installation of piles, maintaining pile toe integrity during piling, small adjustments at pile toe could be sufficient. It is believed that these adjustments could also be executed at the site. To prevent a gradually inward growth at pile toe during piling; *strengthening shoe*-remedies to pile toe are recommended. The strengthening shoe covers an area of twice the pile diameter from the toe. The stiffening ring could be either welded inside the pile or outside the pile [58].

Jetting & drilling

Water/air jets could be used to displace granular soils at the pile toe. Therefore, the pile sinks into the created whole without using a hammer [58]. However, the method is only suitable for sandy soil conditions and not where stiff clay is present. The advantage of this method is that pile damage is prohibited over the full or partial penetration depth. Another solution is drilling. In this fashion, the boulders and stiff layers in the soil are removed [58].

8.4.4 Costs

A rough cost-estimation of three process-based alternatives are given in Figure 8.5. These are wooden cover and strengthening shoes. The increase in costs, in percent, per pile shows an investment in-between 3-6% could guarantee the pile toe integrity before installation, given a diameter of 1420 [mm]. The precautions are necessary for a pile with a high D/t ratio whereas a pile with a low D/t ratio does not necessarily suffer from piling disease. Though, the Cost Increase (CI) is high for piles with high D/t ratio while it stays low for low D/t ratios.

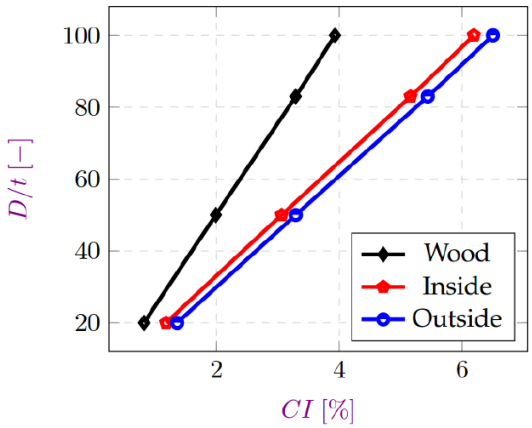

FIGURE 8.5: Cost increase per king pile per D/t ratio for wooden cover and stiffening rings

8.5 Post-piling phase

To recognize symptoms of piling disease an accurate monitoring system, to measure the pile progress, is recommended to be utilized. Therefore, either new devices which simultaneously registers the forces, etc. during driving could be used or *calendering*, recording the number of blows by merely counting the last meters of pile advancement. By then, when the pile toe damage is sensed, in-situ-measurements could be taken to prevent pile toe damage or to reduce its severeness. The most common in-situ treatment is to pull out the pile if it is not advancing. However, when the toe failure is not detected during installation but rather afterward due, e.g., settlements, the Port of Rotterdam Authority (PORA) could decide to take measurements counteracting its consequences. This entity could choose to take actions such as (1) replacement (2) early maintenance, (3) reducing the storage capacity or (4) taking no measures, as introduced in Research into Pile Toe Failure in Amazonehaven (RIPTFIA).

8.5.1 Cost of Amazonehaven

The construction costs of a quay wall, are calculated for a length of 900 meters. The three parts, as depicted in Figure 8.6, could lodge a different amount of dry bulk due to the available surface area in the backyard of the sections.
Bear in mind that the quay wall was divided into twenty sections with a length of 45 [m]. Furthermore, the Present Value (PV) of twenty sections are calculated; however, the available area goes as far as 28 sections. The difference in the number of sections manifests itself in costs and revenues. To study the costs, three scenarios are contrived compared to a Full Capacity (FC) scenario. The calculation of initial expenses has occurred twice, once based on the formula 2.1 introduced in chapter 2, second, the initial costs of Amazonehaven as documented [39]. For each scenario, Problematic Section (PS) are introduced **assuming** that the *extreme folding damage* of king piles will push the PORA to take actions for those sections whereas, for Other Section (OS), no measures are needed to be considered. The decision to select one solution rather than another is decided by a decision-model, based on Net Present Value (NPV)-value.

FIGURE 8.6: Aerial photo Amazonehaven quay wall, retrieved from Google maps

Bear in mind that *pile toe failure* could manifest itself in visible settlements at the associated sections. Based on the *stability research*[4] and a paper about **major events**, see section 4.2.4, it is **assumed** that both **actions need to be taken** in case of *pile toe failure* as well as the **PS are detectable**. Moreover, the calculation of both cost and revenues are for 50 years, from 1989-2038. It is assumed that necessary actions, to keep the harbor operational, had taken place in 2014. Therefore, a timeline is presented per scenario to give an overview of the values used centered at 2014.

Full Capacity

scenario Full Capacity (FC), represents a situation in which the full design capacity of the quay wall is realized, therefore, a full compliance with design. In this scenario, the maximum Net Present Value (NPV), summation of cost and revenues, could be expected. The costs of the quay wall are calculated by Formula 8.1, for the entire quay wall (twenty sections).

$$TC = I_0 + \sum M_i + D \qquad [€] \qquad (8.1)$$

In which, TC stands for Total Cost (TC), I_0 stands for the initial costs, $\sum M_i$ stands for the yearly maintenance, and D represents demolition of the quay wall at the end of its technical lifetime.

Timeline 8.7 shows the backward and forward calculation from 2014. Due to the absence of any Problematic Section (PS), the Regular Maintenance (RM) is carried out through its technical lifetime. However, the first part maintenance cost is based on the initial values of 1989 (I_{-25}), 25 years ago from 2014, whereas maintenance cost for the second period, is calculated by the initial costs based on 2014, (I_{25}). Also, demolition cost in 2038 is a sum of initial expenses based on 1989 and 2014.

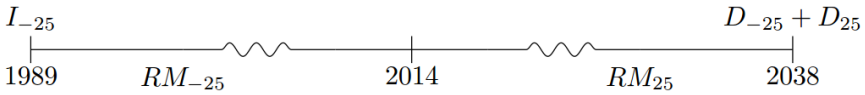

FIGURE 8.7: Time line, FC

In this scenario, the revenues are supposed to be maximum revenues (28 sections). For a detailed calculation on this matter, see Appendix D.

Replacement

In this scenario, the Problematic Section (PS) described as sections with the most number of piles with *pile toe failure*, are demolished and rebuild. The demolition of these sections

[4] Master thesis Mourillon [37]

is necessary to sustain the performance of the quay at its designed storage capacity. The technical lifetime of the new sections is considered to be 24 years, with a construction time of 1 year. The first 25 years, up to 2014, the Early Maintenance (EM) is carried out only for PS whereas for Other Section (OS), Regular Maintenance (RM) is carried out. The second 24 years, after rebuilding, for all sections RM is carried out. It is assumed that RM takes place once a year whereas a EM is as often as ten times a year. Therefore, the operation for PS will come to a stop for six months, in case of EM. In case of RM the disruption is negligible. In this fashion, the Timeline 8.8 is considered. The calculation of maintenance costs, before 2014, is carried out based on the initial costs of 1989 whereas, for the second phase of asset's technical lifetime, the maintenance cost is based on initial costs of 2014. Furthermore, initial costs of new construction in 2014, (D_{-25}), as well as its demolitions at 2038, are taken into account.

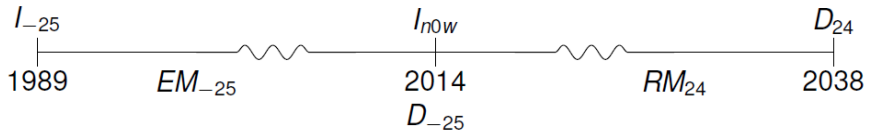

FIGURE 8.8: Time line, R

In this scenario, the quay wall is completely or partially demolished. It is assumed that the demolition and rebuilding takes one year. Therefore, the revenues are set to zero in that year. Furthermore, due to EM for PS before 2014, reduction in revenues occur. It is assumed that leasing price will reduce to compensate the established companies in the area. Number of vessels due to maintenance will also drop which means a reduction in earning.

Early Maintenance

In this scenario, the Problematic Section (PS) described as sections with the most number of piles with *pile toe failure*, are maintained more often than the Other Section (OS). The Early Maintenance (EM) is necessary to increase the storage capacity to the full designed capacity. However, such maintenance is required throughout the entire lifetime of the asset. Also, a halt of 6 months per year is assumed which interrupts a proper operation of the quay wall in those sections. Unavailability of the sections due to Regular Maintenance (RM) is negligible as it occurs just once a year. Timeline 8.9 shows the maintenance costs in both periods, before and after 2014, based on respectively initial values of 1989 and 2014. Also, demolition cost at the end of asset's technical lifetime is based on 1989 and 2014, (D_{-25} + D_{25}).

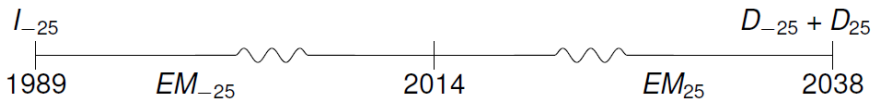

FIGURE 8.9: Time line, EM

In this scenario, the quay wall needs EM through its entire lifetime, for its PS. Both reductions in revenues and increase in costs due to maintenance are expected.

Capacity Reduction

In this scenario, the Problematic Section (PS) described as sections with the most number of piles with *pile toe failure*, undergo a reduction in Storage Capacity (SC) to sustain the functionality of the quay wall till its technical lifetime has reached. Furthermore, it is assumed that Regular Maintenance (RM) is satisfactory due to the reduction in capacity. It is, however, obvious that the Capacity Reduction (CR) in case of iron ore is higher than the CR when coal is stored in the area. Timeline 8.10 shows the maintenance cost of both periods being subsequently calculated by initial costs of 1989 and 2014. Also, the demolition costs, at the end of asset's technical lifetime (D_{-25} + D_{25}) is based on 1989 and 2014.

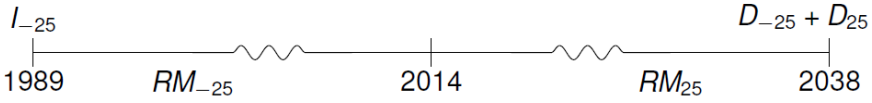

FIGURE 8.10: Time line, CR

In this scenario, a reduction in capacity is implemented for PS of the quay. A decrease of 40% for iron ore and 20% for coal is applied in the calculations.

Facts and figures

Table 8.1 shows the values of investment (I), demolition (D), Regular Maintenance (RM) and Early Maintenance (EM), based on formula 2.1 over a period of 50 years, for the entire quay wall (20 sections). The investment is according literature, formula 2.1, and is calculated for 1989 and 2014 (taking into account the inflation). The demolition is either based on the investment of 1989 or 2014, therefore depending on whether the quay is demolished and replaced in 2014 or 2038 (taking into account the inflation). The cost of maintenance is dependent on the investment and therefore, is divided over two phases (taking into account the inflation). Before 2014, cost of maintenance is based on investment in 1989 whereas, after 2014, it is based on 2014.

TABLE 8.1: I, D, RM and EM values over a period of 1989-2014-2038

$\mathbf{RM}_{1989-2014}$	$\mathbf{RM}_{2014-2038}$	$\mathbf{I}_{1989}$	$\mathbf{I}_{2014}$	$\mathbf{D}_{1989}$	$\mathbf{D}_{2014}$	$\mathbf{EM}_{1989-2014}$	$\mathbf{EM}_{2014-2038}$
€3.1E+06	€5.3E+06	€2E+07	€3.4E+07	€1.3E+06	€2.2E+06	€3.1E+07	€5.3E+07

8.5.2 Decision model

The decision model is a tool, for Port of Rotterdam Authority (PORA), to select the economical solution based on Net Present Value (NPV). NPV is the sum of revenues and the costs per scenario. As mentioned in chapter 4, major revenues of PORA are two folded: revenues due to Port Dues (PD) and revenues due to Leasing Contract (LC). Figure 8.11 shows the factors per increasing Percentage Problematic Section (PPS), for iron ore, given the three scenarios. From left to right: Present Value Increase Factor (PVIF), Revenues Reduction Factor (RRF)-PD, RRF-LC and Net Present Value Reduction Factor (NPVRF) are presented. It shows, sub-Figure (D) 8.11, given the assumptions, Capacity Reduction (CR) is the best choice from the other two scenarios because the NPV-factor reduces less with increasing PPS.

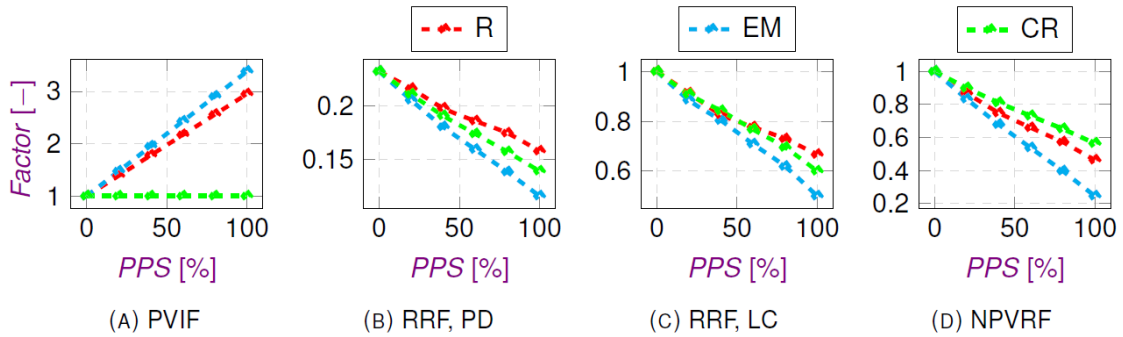

FIGURE 8.11: Factors per increasing PPS, Iron ore, based on formula 2.1

Figure 8.12 shows the factors per increasing PPS, for coal, given the three scenarios. From left to right: PVIF, RRF-PD, RRF-LC and NPVRF are presented. It shows, sub-Figure (D) 8.12, given the assumptions, CR is the best choice from the other two scenarios because the NPV-factor reduces less with increasing PPS. Moreover, comparing sub-Figure (D) 8.12 to

sub-Figure (D) 8.11, the CR is less steep. Therefore, when actions are necessary to take, it is better to change the *storage function* of the quay, (to a lighter material), to reduce the financial consequences.

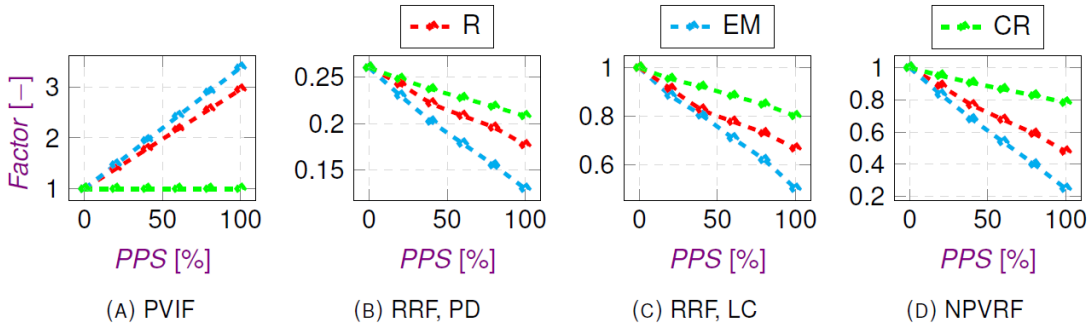

(A) PVIF (B) RRF, PD (C) RRF, LC (D) NPVRF

FIGURE 8.12: Factors per increasing PPS, Coal, based on formula 2.1

Facts and figures

Table D.5 shows Present Value (PV), revenues and Net Present Value (NPV) based on both formula 2.1 and Amazonehaven (documentation) for both iron ore- and coal- storage. These values are in case the quay wall is operating as it was designed. Therefore, the increase in costs and a decrease in revenues, as well as a decrease in NPV could be calculated by simply multiplying these number with factors as presented in Figure 8.11 and 8.12, per increasing Percentage Problematic Section (PPS).

TABLE 8.2: PV, revenues and NPV, given a full capacity, for iron ore and coal

based on [2014]	**PV**		**Revenues**		**NPV**	
-	formula 2.1	Amazonehaven	PD	LC	formula 2.1	Amazonehaven
FC-iron [€]	3.20E+07	3.05E+07	3.26E+08	6.88E+07	3.63E+08	3.64E+08
FC-coal [€]	3.20E+07	3.05E+07	3.26E+08	6.88E+07	3.63E+08	3.65E+08

8.6 Loss of earnings

8.6.1 LOE due PPS

Loss of Earnings (LOE) due increasing Percentage Problematic Section (PPS) of the quay wall presents the losses in monetary terms due piling disease and its counteractions to reduce the consequences of such a condition, as mentioned earlier. Naturally, when no actions are considered, and the entire quay wall is used to its fullest designed capacity either (1) technical lifetime of the asset would be shortened extensively or (2) complete asset collapses which could manifest itself as the loss of lives. However, the *no action* scenario is not taken into account.

Table 8.3 shows the loss of earnings in percent per scenario per increasing PPS, per dry bulk type to be stored. It shows that the reduction in revenues is the same when Replacement (R) & Early Maintenance (EM) are chosen and does not depend on the type of storage good. However, when Capacity Reduction (CR) is considered, LOE is at its minimum if changing the storage function of the quay wall (to a lighter material). In any case, the best option remains the reduction in storage capacity.

TABLE 8.3: LOE per increasing PPS, based on formula 2.1

	Percentage Problematic Section [%]					
formula 2.1	**20**		**40**		**100**	
LOE	**Iron**	**Coal**	**Iron**	**Coal**	**Iron**	**Coal**
R	13%	13%	25%	25%	54%	54%
EM	17%	17%	32%	32%	76%	75%
CR	10%	5%	19%	9%	44%	22%

8.7 Conclusions

Chapter 8 studied remedies in both pre-piling and post-piling phases to respectively avoid- or counteract- (the consequences of) *piling risk event*. It is, however, more convenient to prohibit potential sources leading to *extreme folding damage* beforehand installation. In this fashion, the process-based alternatives will reduce the probability of occurrence of the risk event. Therefore, the remedies in pre-piling phase are:

- Data collection: sufficient soil investigation, pile tests, using prediction program, correct hammer selection
- Pre-installation: Just in Time (JIT) system, Azobé cover, careful execution
- installation: stiffening ring, jetting, drilling, in situ checks of Out of Roundness (OOR), careful execution, using monitoring system, using (pile) driving procedure[5]

Moreover, when the risk event occurs; the consequences could be diminished by selecting one of these remedies: (1) Replacement (R), (2) Early Maintenance (EM) and (3) Capacity Reduction (CR). In this fashion, the Loss of Earnings (LOE) due Percentage Problematic Section (PPS) is calculated per scenario. Table 8.4 shows an overview for LOE due a PPS of 20%, per scenario, per dry bulk type, based on formula 2.1.

TABLE 8.4: Overview LOE, given 20% PPS

LOE	**Percentage Problematic Section [%]**					
-	**20**					
Actions	**R**		**EM**		**CR**	
Dry bulk type	**Iron**	**Coal**	**Iron**	**Coal**	**Iron**	**Coal**
formula 2.1	13%	13%	17%	17%	10%	5%

Therefore, it could be concluded that when consequences of *pile toe failure* are apparent, to limit its financial repercussions, the owner is recommended to reduce the storage capacity or to change the function of the quay. The latter means, to switch from, e.g., a heavy material to a lighter one.

8.8 Limitations

The main limitations to carry out this study was the actual data about the revenues regarding both Port Dues (PD) and Leasing Contract (LC). Furthermore, the EM scenario has become the worse scenario regarding Net Present Value (NPV), due to its reduction factor of 0.5. However, EM does not necessarily lead to such extreme halt in operation.

[5] see section B.2

8.9 Overview results

Figure 8.13 gives an overview of the finding regarding the management aspects of the *pile toe failure*. The overview is complementary to the validity map introduced in chapter 3. In the next page, the figure is enlarged to assure readability.

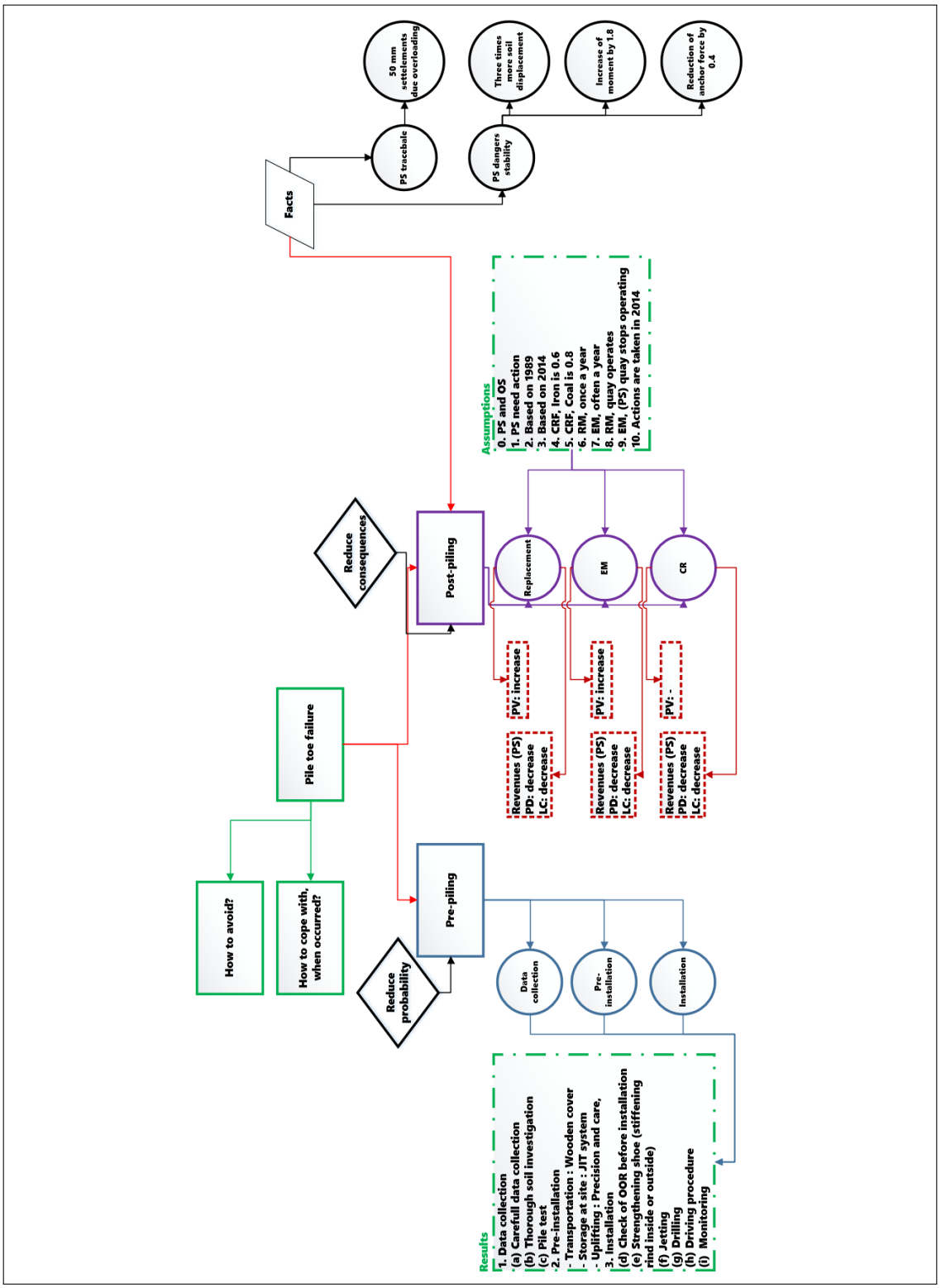

FIGURE 8.13: Overview environment of *pile toe failure*

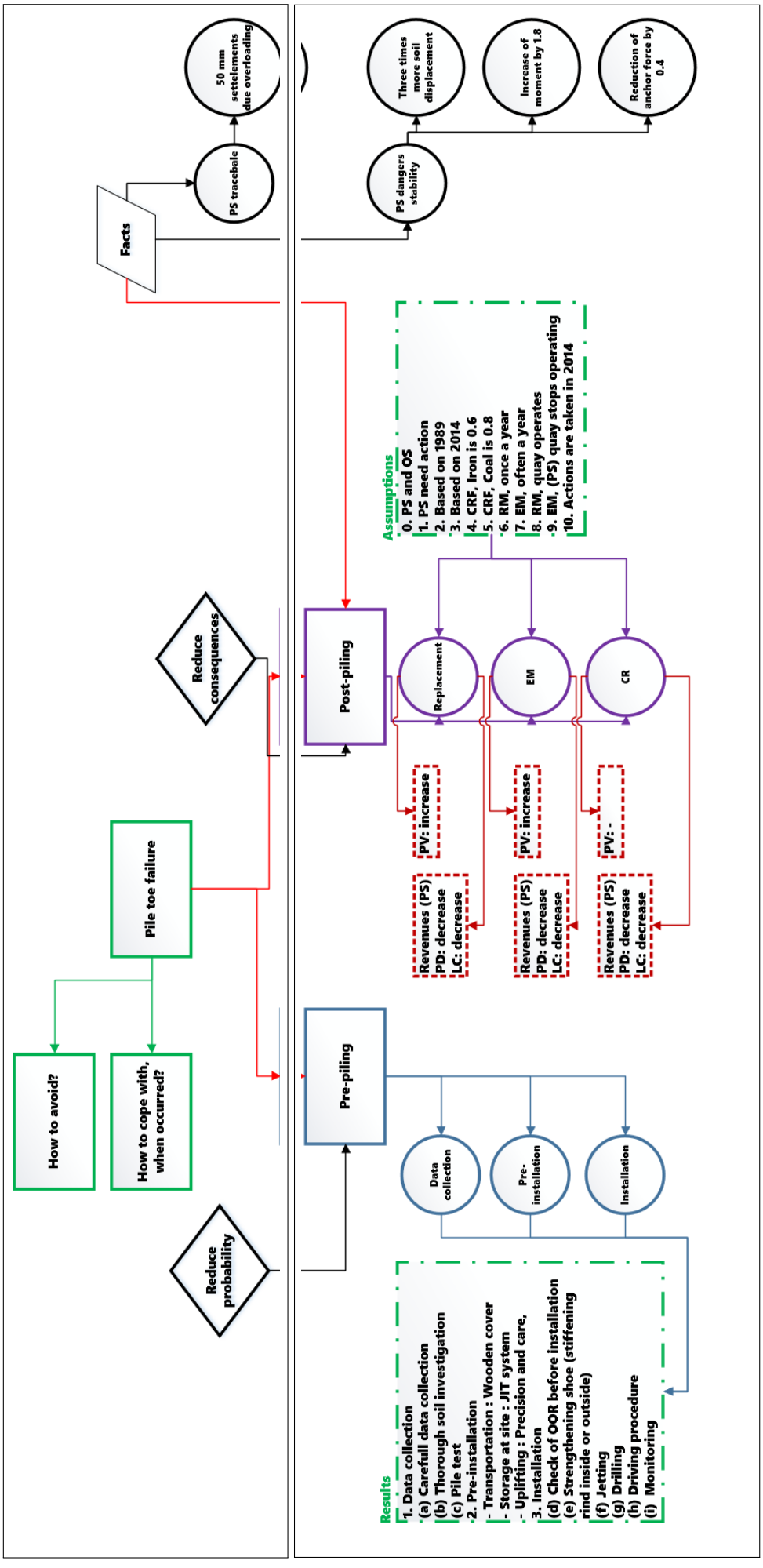
50 mm settelements due overloading
PS tracebale
Facts
Three times more soil displacement
Increase of moment by 1.8
Reduction of anchor force by 0.4
PS dangers stability
Assumptions
0. PS and OS
1. PS need action
2. Based on 1989
3. Based on 2014
4. CRF, Iron is 0.6
5. CRF, Coal is 0.8
6. RM, once a year
7. EM, often a year
8. RM, quay operates
9. EM, (PS) quay stops operating
10. Actions are taken in 2014
Reduce consequences
Post-piling
Replacement
EM
CR
PV: increase
PV: increase
PV: -
Revenues (PS)
PD: decrease
LC: decrease
Revenues (PS)
PD: decrease
LC: decrease
Revenues (PS)
PD: decrease
LC: decrease
Pile toe failure
How to avoid?
How to cope with, when occurred?
Pre-piling
Data collection
Pre-installation
Installation
Reduce probability
Results
1. Data collection
(a) Carefull data collection
(b) Thorough soil investigation
(c) Pile test
2. Pre-installation
- Transportation : Wooden cover
- Storage at site : JIT system
- Uplifting : Precision and care,
3. Installation
(d) Check of OOR before installation
(e) Strengthening shoe (stiffening rind inside or outside)
(f) Jetting
(g) Drilling
(h) Driving procedure
(i) Monitoring

Chapter 9

Conclusions & recommendations

9.1 Aim

Chapter 9 aims to give answers to the research questions and sub-questions as introduced in the chapter 1 and 3. It also presents a recommendation for future research in this field.

9.2 Answering the questions

Sub-questions Hydraulic Structures and Flood Risk (HSFR)-related:

What are the finding & observations of *pile toe failure* in Amazonehaven? - Twenty percent of the king piles had *extreme folding damage* while the quay wall's stability was not endangered according to *stability research* [37].

What are the causes of *pile toe failure* in general? - The causes of *pile toe failure* in a hammer-pile-soil system have a dynamic-, geometric- and geologic- nature.

How harmful has the *pile toe failure* been for the Amazonehaven asset? - The *pile toe failure* has not endangered the stability of the quay wall [37]. Assuming it would have; Research into Pile Toe Failure in Amazonehaven (RIPTFIA) showed that *the failure* lead to counteractions to be taken to safeguard functionality of the quay wall; which are to be translated into financial expenses for Port of Rotterdam Authority (PORA).

Should the dimensioning of primary king piles be based on a dynamic mold of load? - Not per se, but the hammer selection must be based on the guidelines for hammer selection, and it is highly recommended to carry out Pile Driving Prediction (PDP) and Pile Driving Analysis (PDA). With other words, to monitor piling.

What would be suggested for pile's D/t ratio based on the dynamic load? - American Petroleum Institute (API) suggest a D/t ratio of 69 instead of 83.

Sub-questions Construction Management and Engineering (CME)-related:

How could the process be improved to reduce or avoid the *pile toe failure*? - By preferably, adjusting the process beforehand piling to reduce the probability of occurrence of *piling risk event*. Therefore, procedures in current piling industry could be improved by utilizing: Just in Time (JIT) delivery system, wooden cover to maintain pile toe integrity, checks of pile toe integrity beforehand installation, execution with precision and care, using a piling prediction program, using a monitoring system during piling, using a piling procedure.

What are the costs of extra measures, in design- and construction- phase, to improve the process? - The costs of extra measures for wooden cover and stiffening rings are in between 3-7% of one king pile, given the pile dimensions of Amazonehaven.

How much are the Loss of Earnings (LOE) for Amazonehaven, due increasing Percentage Problematic Section (PPS)? - The financial consequences of *pile toe failure* are shown in Table 9.1:

TABLE 9.1: LOE due increasing PPS

	Percentage Problematic Section [%]					
formula 2.1	**20**		**40**		**100**	
LOE	**Iron**	**Coal**	**Iron**	**Coal**	**Iron**	**Coal**
R	13%	13%	25%	25%	54%	54%
EM	17%	17%	32%	32%	76%	75%
CR	10%	5%	19%	9%	44%	22%

Therefore, given a 20% PPS, the most economic (counteraction) solution is to select Capacity Reduction (CR) and to change the storage function of the Problematic Section (PS).

Who are the stakeholders of Amazonehaven? - The main stakeholders playing a role in the harbor are: PORA (employer), Municipality of Rotterdam (SO) (supervisor), HBG (contractor), EKOM (company), Gasunie (company) and ECT (company).

Who is the responsible party to bear the cost for the *pile toe failure*? - The responsible party are both the SO and the contractor, SO could hold responsible if the Cone Penetration Test (CPT) is carried out without care or with vast distances. At the other hand, the contractor could hold responsible for the incorrect hammer selection. Furthermore, the contractor could also be held responsible if proven that *pile toe integrity* was not warranted in pre-piling phase due to careless handling.

What are the wake-up calls of Amazonehaven *pile toe failure* worth introducing to piling industry? - The wake-up calls of Amazonehaven, are the sensitivity of pile toe to any imperfection, initial dent. Therefore, assuming that the hammer selection has been carried out based on guidelines, and PDP, and PDA is carried out to warrant the pile driveability, it is highly recommended to warrant the pile toe integrity in pre-piling phase.

Now the sub-questions are answered, a proper answer could be given to the research questions:

1. What are the causes of *pile toe failure* in Amazonehaven? - The reasons of *pile toe failure* in Amazonehaven are argued to be **pile imperfection**, **pile inclination** and **pile inhomogeneous strength**. Bear in mind; pile imperfection refers to initial dent. The most important reason to *pile toe failure* is shown to be pile imperfection. Nevertheless, either the designer or the contractor must be noted for the pile imperfection. For example, the designer must design a pile taking into consideration an initial dent (more than the already considered ovalisation etc.). The contractor must carry out a *zero-initial-damage*-policy. Both could lead to extra costs.
2. What are the remedies to prevent *pile toe failure*? - The remedies to prevent *pile toe failure* are either based on remedies in pre-piling phase, to reduce the probability of occurrence of the risk event or measurements to be implemented in post-piling phase to counteract the consequences of the *piling disease* as discussed in chapter 8. Furthermore, it is recommended to design the quay wall without any inclination to its combined-wall system, even though the soil composition is Standard to Normal Soil Condition (SNSC).

9.3 Conclusions

The main conclusions shown are:

- hammer-induced driving stresses are lower than material's yield stress, and are not the leading cause of *extreme folding damage*.
- *extreme folding damage* is shown to be caused by **pile imperfection**, **pile inclination** and **pile inhomogeneous strength**. The leading cause is shown to be **pile imperfection** which refers to initial dent at pile toe to be worsened during piling.
- *piling disease* is to be prevented in pre-piling phase, while it has minimum financial consequences.
- the consequences of *piling disease* could be reduced in post-piling phase, while it has maximum financial consequences.

9.4 Looking into future

The recommendations are divided into four parts, recommendations for further research regarding PDP-, Finite Element Analysis (FEA)- part, the *stability research* and Management Aspect (MA)- part.

9.4.1 Technical part

PDP

- match the prediction results to (pile) driving analysis carried out in 1990, which recommends a D100 hammer for piling. However, RIPTFIA showed that pile-advancement would be troublesome at the last meters of driving, exceeding the threshold-value, given a virgin soil.
- carry out, if possible, a pile test (predict by PDP and measured by PDA) and a back-analysis by signal matching AllWave-DLT to validate the actual hammer-pile-soil interaction as well as the pile driving analysis carried out in 1990.

FEA

- study the combination of the three leading causes to *pile toe failure* as presented.
- study the *pile toe failure* with a displacement control approach. In this fashion, the displacement could be entered in the model, and the applied force is an unknown. The displacement-control approach might be a better approach because of the availability of information about the end deformation of the piles.
- study the development of *pile toe failure*, in a dynamic concept, given the scenarios (1) SNSC for virgin and compacted soil if pile has no initial dent, (2) SNSC and Medium to Hard Soil Condition (MHSC) if pile has an initial dent.

Stability

- study the *true*-length of the king pile in a quay wall (shorter piles might be the outcome) as *stability research* has shown [37]:

  > Stability of the entire quay wall, given the *pile toe failure* is not endangered for at least **a certain period of time**.

- study the exact penetration depth of the piles, given that both *pile toe failure* occurs and the stability of the quay wall is safeguarded, costs savings might be achievable.
- study the stability of the quay wall based on design guidelines as used nowadays. The design of Amazonehaven quay wall was based on a deterministic design.

9.4.2 Management Part

Management aspects (of pile toe failure)

- research creative solutions to *piling disease* in pre-piling phase.
- study why the Amazonehaven quay wall has not been fully utilized. Is this also the case for other quay walls in MaasVlakte (area) (MV)?

9.5 Overview results

Figure 9.1 gives an overview of the finding regarding *research into pile toe failure in Amazonehaven*. The overview is complementary to the validity map introduced in chapter 3. In the next page, the figure is enlarged to assure readability.

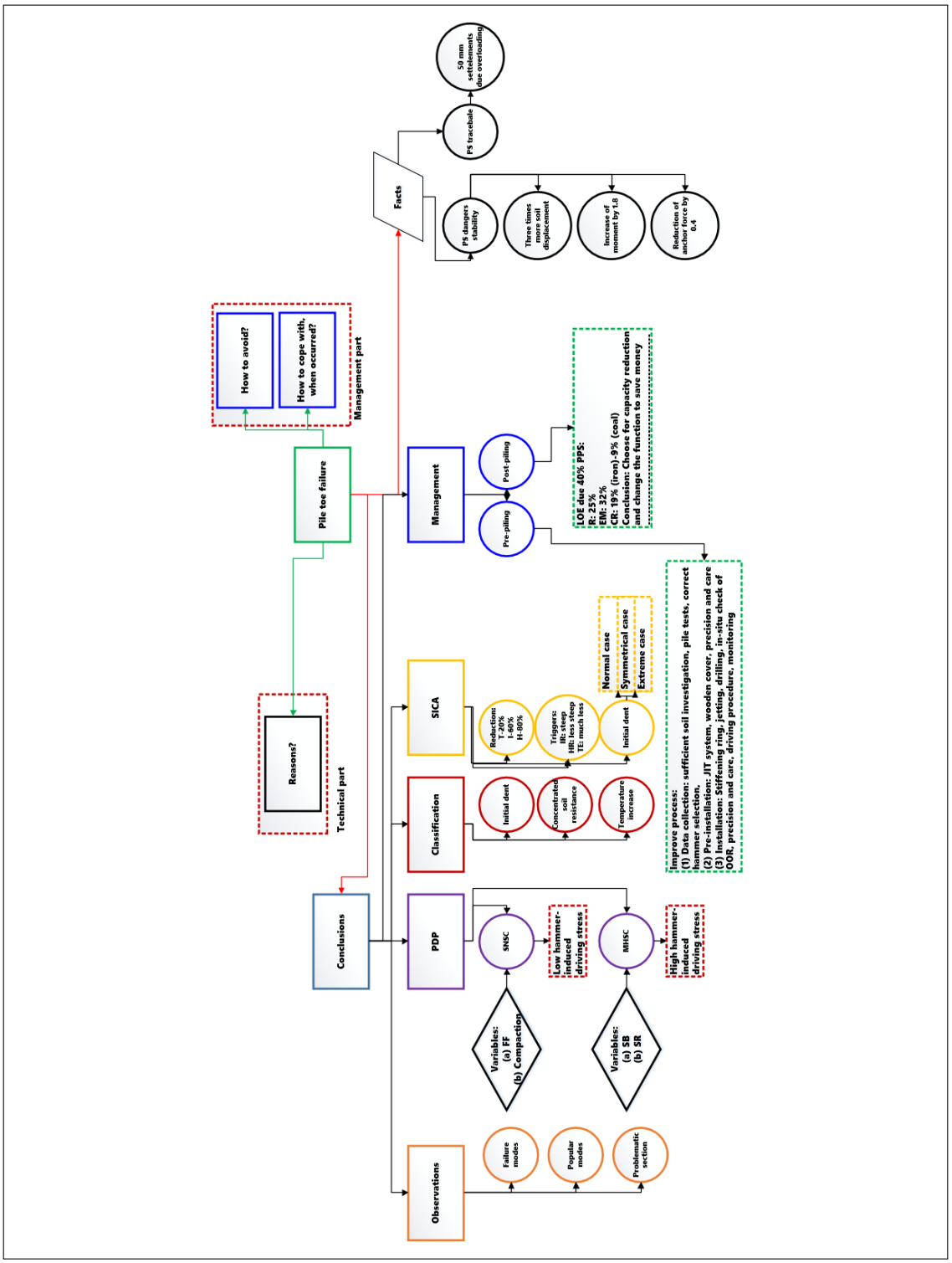

FIGURE 9.1: Overview finding

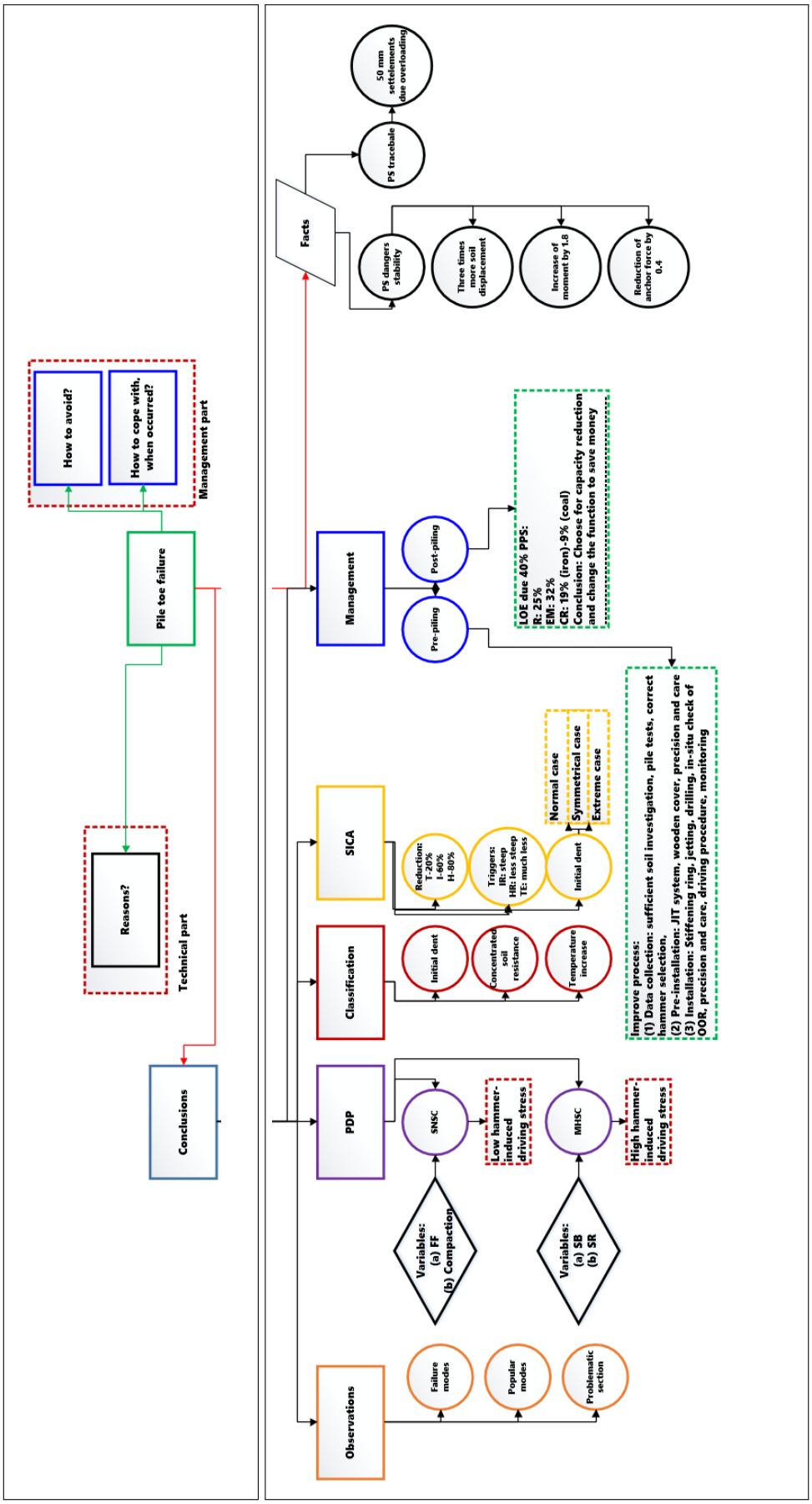
Management part
How to avoid?
How to cope with, when occurred?
Pile toe failure
Technical part
Reasons?
Conclusions
Facts
50 mm settelements due overloading
PS tracebale
PS dangers stability
Three times more soil displacement
Increase of moment by 1.8
Reduction of anchor force by 0.4
Management
Post-piling
Pre-piling
LOE due 40% PPS:
R: 25%
CR: 19% (iron)-9% (coal)
Conclusion: Choose for capacity reduction and change the function to save money
Improve process:
(1) Data collection: sufficient soil investigation, pile tests, correct hammer selection,
(2) Pre-installation: JIT system, wooden cover, precision and care
(3) Installation: Stiffening ring, jetting, drilling, in-situ check of OOR, precision and care, driving procedure, monitoring
SICA
Reduction: T-20% I-60% H-80%
Triggers: JIT: steep HR: less step TE: much less
Normal case
Symmetrical case
Extreme case
Initial dent
Classification
Initial dent
Concentrated soil resistance
Temperature increase
PDP
SNSC
Low hammer-induced driving stress
MHSC
High hammer-induced driving stress
Variables: (a) FF (b) Compaction
Variables: (a) SB (b) SR
Observations
Failure modes
Popular modes
Problematic section

Appendix A

General information

A.1 Hammer data

Table A.1 and A.2 show the main characteristics of the diesel hammer type D100-13. The exclusive hammer library of the Pile Driving Prediction (PDP) program makes it possible to choose from different types of hammers with its specific ram, anvil, and cushion.

TABLE A.1: Specific data diesel hammer D100-13, retrieved from PDP

Hammer data			
Part	Type	Diamater [m]	Length [m]
Ram	Circular	0.63	4.644
Anvil	Circular	0.63	1.07

TABLE A.2: Specific data diesel hammer D100-13, retrieved from PDP

Hammer data			
Part	Thickness [m]	Cross-section [m^2]	Coefficent of restitution [-]
Conbest	0.05	1.5837	0.8

Table A.3 reveals detailed information about the specific hammer as used in the prediction program.

TABLE A.3: Expanded data diesel hammer D100-13, retrieved from PDP

Hammer Type	**D100-13**	**Unit**
Max. Potential Energy	334.1	[kNm]
Actual Potential Energy	213.8	[kNm]
Impact Energy	129.3	[kNm]
Length of Ram	4.644	[m]
Mass of Ram	10000	[kg]
Cross Section of Cylinder	0.3117	[m^2]
Modulus of Elasticity Ram	205800	[MPa]
Distance Exhaust Ports	0.72	[m]
Combustion Chamber Volume	0.0177	[m^3]
Exponent for Compr. Proces	1.35	[-]
Exponent for Expa. Proces	1.3	[-]
Combustion Delay	0.002	[s]
Duration of Combustion	0.003	[s]
Max. Diesel Fuel per Cycle	12000	[mm^3]
Energy per kg Diesel	39.6	[MJ/kg]
Maximum Stroke	3.406	[m]
Impact Stroke	2.18	[m]
Rebound Stroke	2.18	[m]

A.2 Failure registration

Table A.4 presents the registered data from *stability research*[1], which is analyzed per quay wall section. The analysis has led to the introduction of (1) failure modes, (2) its frequency of occurrence, (3) its location and (4) popular modes.

TABLE A.4: Failure register per king pile per section

Section	Pile number	Failure mode
1	13,	Moon Scorpio
2	38,	Moon Cancer
3	45, 50, 51,	No damage
4	54, 55, 56, 57, 64, 65, 66,	No damage
5	70, 71, 72, 73,	No damage
5	81,	Closed both sides straight
6	86, 98,	No damage
6	88,	Moon Cancer
7	101,	Not identifiable
7	104, 105, 106, 107, 108,	No damage
8	118, 119,	No damage
8	120, 122, 125,	Moon Cancer
8	128,	Not identifiable
9	130, 131, 132, 133, 134, 135, 136,	No damage
10	145, 148	No damage
10	146,	Closed both sides
10	147,	Moon Scorpio
10	150,	Moon Leo
10	157,	Bowling skittles
13	190,	Not identifiable
15	219, 223,	Closed both sides
15	227,	Closed one side
16	234,	Closed star
16	247,	No damage
17	250,	Closed both sides straight
17	251,	Hourglass
17	252, 253, 255, 256, 258, 259, 260, 261,	Closed star
17	257,	Russian doll
17	262, 271,	No damage
19	279,	Not identifiable
19	280,	Russian doll
19	281, 287, 292,	Closed both sides
19	282, 285, 286, 290,	Closed both sides straight
19	283, 288, 291,	Closed star
19	293,	Moon Leo
20	294,	Not identifiable
20	298,	Closed both sides straight
20	300,	No damage
20	A, B, C,	Closed star

[1] See [37]

A.3 Pile data

Table A.5 shows low to high D/t ratios which are modeled in the PDP program. The king piles of Aamzonehaven quay wall were segmented in three parts with different D/t ratios.

TABLE A.5: Global pile data per D/t ratio, retrieved from PDP

Pile data						
Part	D	t	D/t	Length	E-modulus	Density
	[m]	[mm]	[-]	[m]	[MPa]	[kg/m^3]
A	1.42	71	20	31.5	210000	7850
B	1.42	28.4	50	31.5	210000	7850
C1	1.42	17	83.5	10.5	210000	7850
C2	1.42	20	71	10.5	210000	7850
C3	1.42	17	83.5	10.5	210000	7850
D	1.42	14.2	100	31.5	210000	7850

Table A.6 reveals information about the moment of inertia, both elastic and plastic and other information as well as the formula used to calculate those values, per D/t ratio.

TABLE A.6: Specific pile data per D/t ratio

D/t	Formula	20	50	83	100
t [mm]	-	71	28.4	17	14.2
A [mm^2]	$\frac{\pi \cdot (D^2 - D_i^2)}{4}$	3.01E+05	1.24E+05	7.49E+04	6.27E+04
I_{zz} [mm^4]	$\frac{\pi \cdot (D^4 - D_i^4)}{64}$	6.86E+10	3.01E+10	1.84E+10	1.55E+10
W_{ely} [mm^3]	$\frac{\pi \cdot (D^4 - D_i^4)}{32 \cdot D}$	9.67E+07	4.23E+07	2.60E+07	2.18E+07
W_{ply} [mm^3]	$\frac{\pi \cdot (D^4 - D_i^4)}{6}$	4.06E+08	1.73E+08	1.05E+08	8.82E+07
M_{ely} [Nm]	$\sigma_{yield} \cdot W_{ely}$	4.67E+07	2.05E+07	1.25E+07	1.05E+07
M_{ply} [Nm]	$\sigma_{yield} \cdot W_{ply}$	1.96E+08	8.35E+07	5.08E+07	4.26E+07
σ_y [MPa]	-	483	483	483	483
S [mm]	$\pi \cdot D_c$	4.24E+03	4.37E+03	4.41E+03	4.42E+03
D_c	$D - t$	1349	1391.6	1403	1405.8
D_i	$D - 2 \cdot t$	1278	1363.2	1386	1391.6
M_{pl}/M_{el}	-	4.20E+00	4.08E+00	4.05E+00	4.04E+00
W_{pl}/W_{el}	-	4.20E+00	4.08E+00	4.05E+00	4.04E+00

A.4 Data strengthening pile toe

Table A.7 reveals information used to eventually calculate the Cost Increase (CI) in percent per king pile for three process-based alternatives: (1) strengthening shoe (inside) (2) strengthening shoe (outside), (3) wooden cover, to prevent the *piling risk event*.

TABLE A.7: Specific pile data per D/t ratio per alternative

	Formula	Inside		Outside	Wood
D/t	-	83	100	all	all
A [mm^2]	$\frac{\pi \cdot (D^2 - D_i^2)}{4}$	8.58E+04	8.62E+04	9.05E+04	2.79E+05
I_{zz} [mm^4]	$\frac{\pi \cdot (D^4 - D_i^4)}{64}$	2.00E+10	2.03E+10	2.35E+10	7.65E+10
W_{ely} [mm^3]	$\frac{\pi \cdot (D^4 - D_i^4)}{32 \cdot D}$	2.89E+07	2.91E+07	3.21E+07	9.94E+07
€/ton	-	1000	1000	1000	-
€/m^3	-	-	-	-	1540
m [kg]	$A \cdot L \cdot \rho_{steel}$	956.67	960.59	1008.5	372.37
D_a [mm]	$1420 - 2 \cdot t$	1386	1391.6	1460	1540
D_i [mm]	$D_a - 2 \cdot t$	1346	1351.6	1420	1420
t [mm]	-	20	20	20	60
L [mm]	-	1420	1420	1420	1420

Table A.8 shows the cost per king pile per D/t ratio, as well as the total cost for a total number of piles.

TABLE A.8: Specific pile data per D/t ratio per alternative

D/t	Formula	20	50	83	100
E [$\frac{N}{mm^4}$]	-	2.10E+05	2.10E+05	2.10E+05	2.10E+05
I [mm^4]	$\pi \cdot \frac{D^4 - D_i^4}{64}$	6.86E+10	3.01E+10	1.86E+10	1.55E+10
A [mm^2]	$\pi \cdot \frac{D^2 - D_i^2}{4}$	3.01E+05	1.24E+05	7.54E+04	6.27E+04
L [m]	-	31.5	31.5	31.5	31.5
m[kg]	L·ρ·A	72526	29927	18174	15116
€/ton	-	1000	1000	1000	1000
€/king pile	-	72526	29927	18174	15116
313 king piles	-	€22.7E+06	€9.3E+06	€5.6E+06	€4.7E+06
t [mm]	-	71	28.4	17.1	14.2
D [mm]	-	1420	1420	1420	1420
D_i [mm]	D-2· t	1278	1363.2	1385.8	1391.6

A.5 Static load Amazonehaven

Figure A.1 depict the static load applied as permanent and variable, on the Amazonehaven quay wall. The king piles were dimensioned based on the static load.

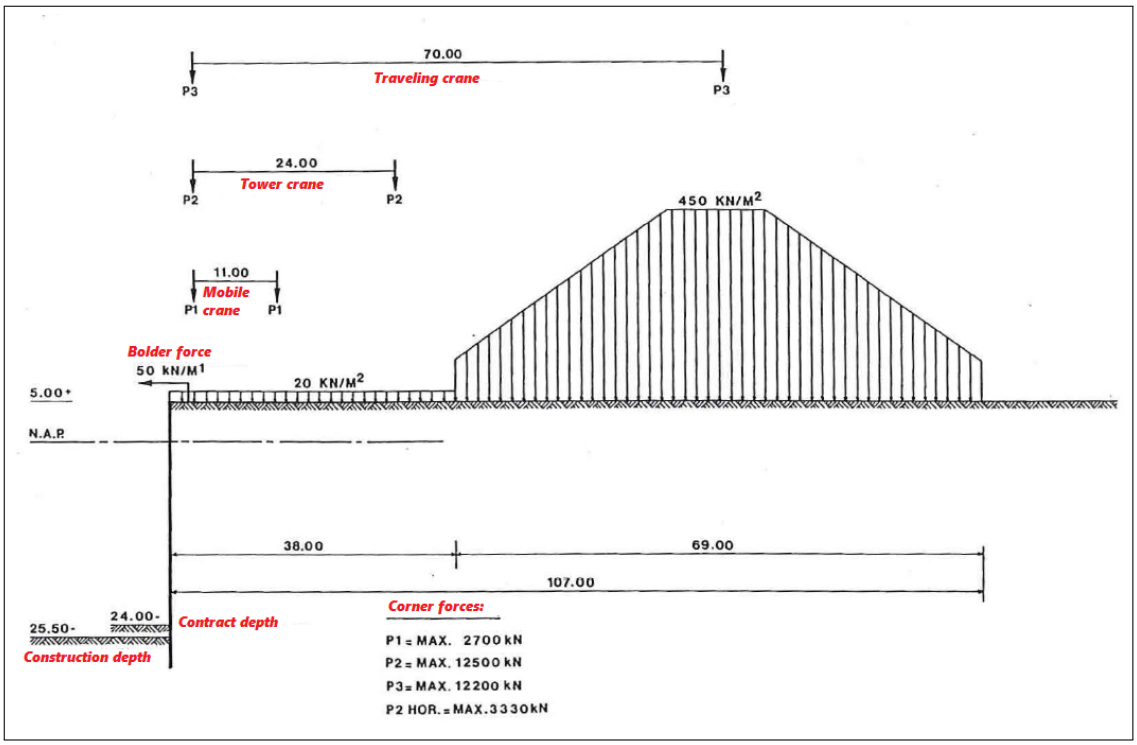

FIGURE A.1: Static load, retrieved from [48]

Figure A.2 depicts the typical moment distribution for the quay wall, given a **M**ean **H**igh **W**ater and **M**ean **L**ow **W**ater level.

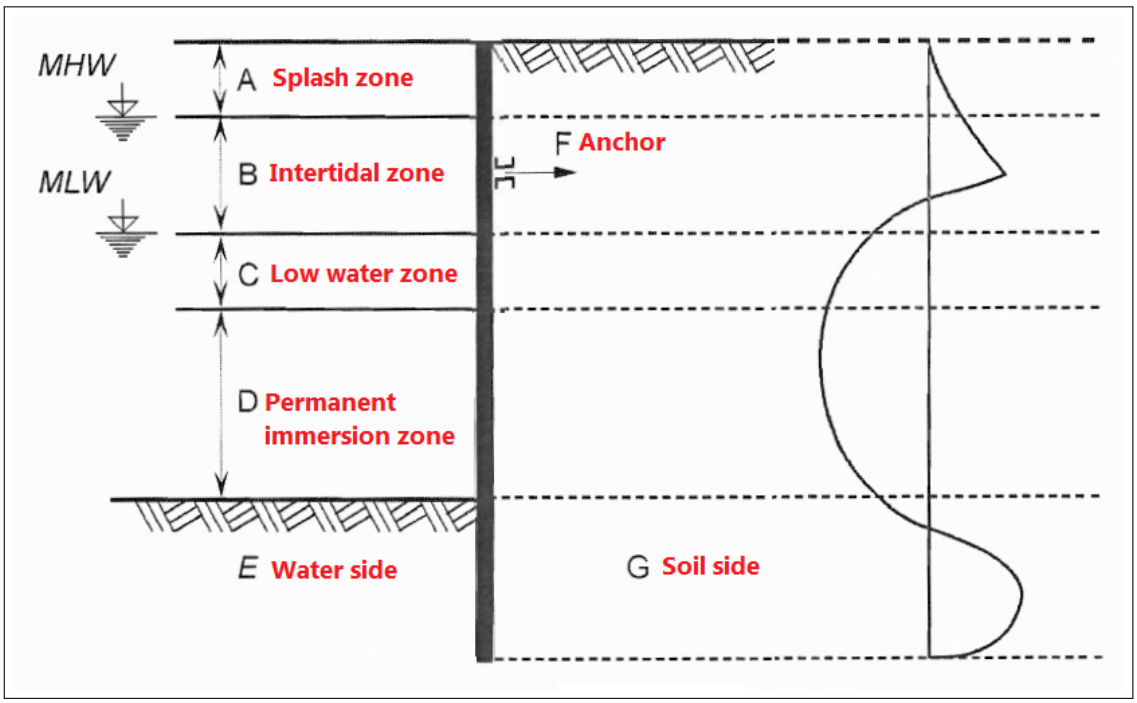

FIGURE A.2: Quay wall,typical bending moment distribution retrieved from EN-1993-5-Eurocode 3-Part 5

A.6 Soil characteristics

Figure A.3 shows Various soil types and its different shading as to be found in Amazonehaven soil condition. The Amazonehaven soil condition is described as Standard to Normal Soil Condition (SNSC).

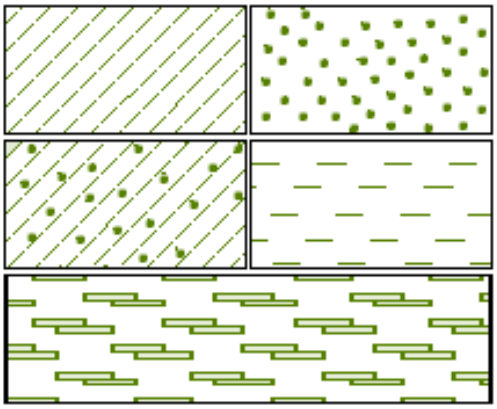

FIGURE A.3: Shading of soil types from left to right, Silt, Sand, Silty sand, Clay, Peat, retrieved from [62]

Figure A.4, a Cone Penetration Test (CPT) of the governing soil composition in Amazonehaven, DN92. The soil composition consists of silt, sand, silty sand, clay, and peat. In general, a combination of cone or toe resistance and shaft friction gives a better insight of the soil type. Nevertheless, a high cone resistance, in a CPT, usually refers to the sandy soil where a low toe resistance means a soil with a low bearing capacity such as peat.

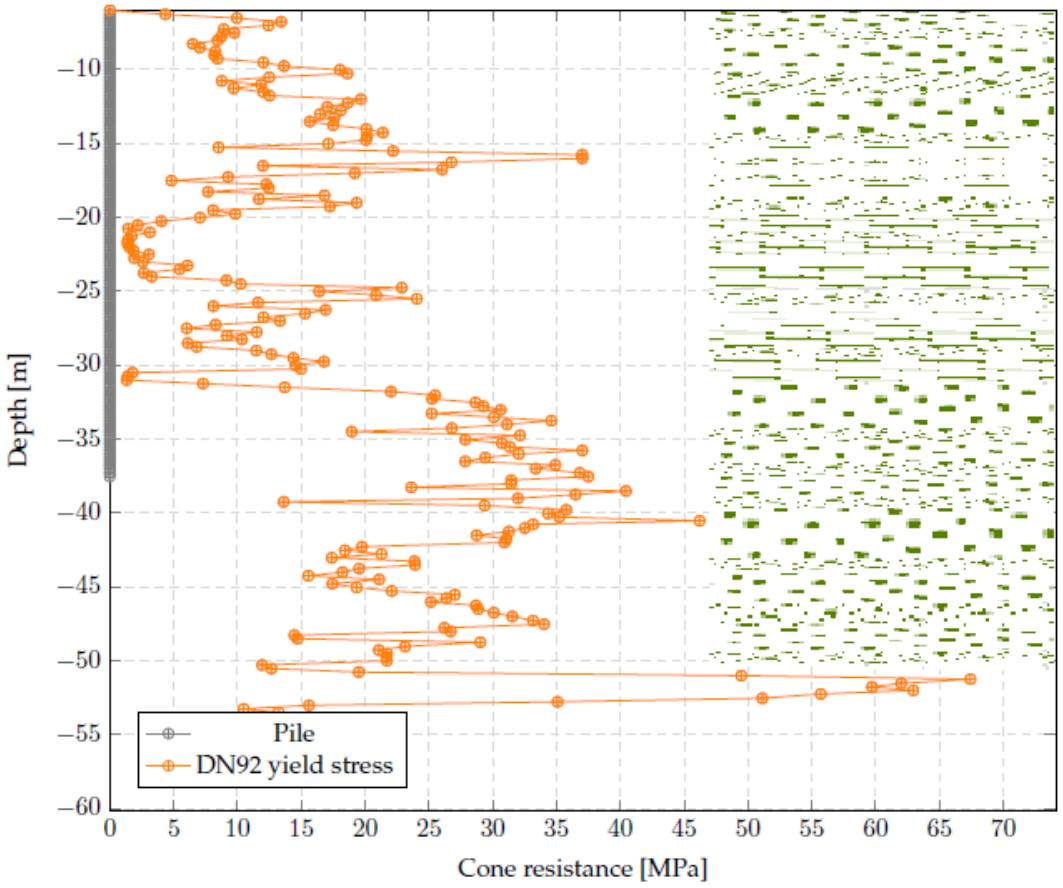

FIGURE A.4: Soil composition Amazonehaven, based on CPT-DN92, retrieved from Gisweb Rotterdam

A.7 Failure modes

Figure A.5 shows the damage per section, regardless its failure mode. It reveals that sections 19, 18 and 9 have the highest frequency of *pile toe failure* occurrence of respectively 15.7%, 13.3%, and 8.4%. Therefore, [$\frac{3}{20}$] 15% of the quay wall had a Problematic Section (PS). The collected data by the previous researcher, in *stability research*, made the analysis possible.

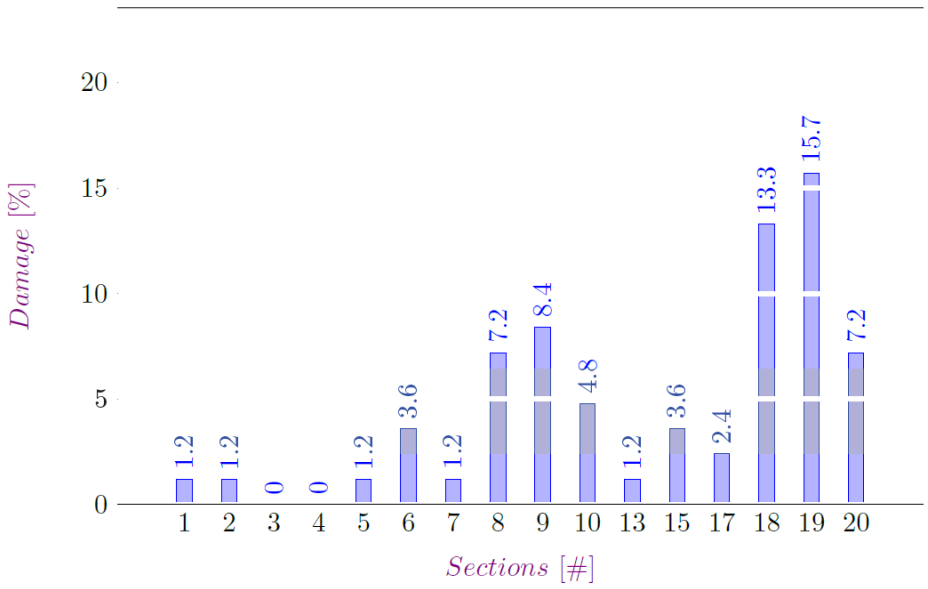

FIGURE A.5: Frequency of *pile toe failure*

Figure A.6 shows failure modes of *deformed pile toe cross-section* as observed in Amazonehaven. The failure modes are developed by analyzing available data and measurements carried out by the previous researcher, in *stability research*. It is obvious that one mode is a further development of another, e.g., Moon Scorpio (MS) is a mode-development of Moon Cancer (MC).

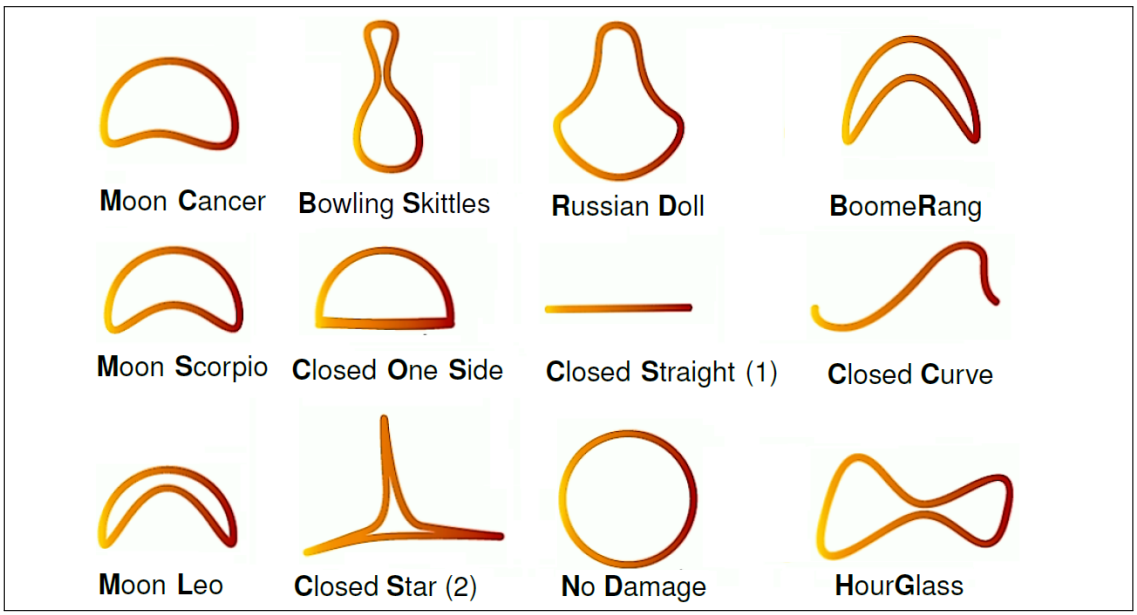

FIGURE A.6: *Failure modes* of *cross-section of deformed pile toe* in Amazonehaven, used Adobe Illustrator

A.8 Cost of quay wall

Table A.9 shows the cost of constructing the quay wall, calculated based on formula 2.1 and the Amazonehaven (documentation) both in Euro and Gulden.

TABLE A.9: Cost of quay wall per running meter given a retaining height of 24 meters, 1989 versus 2014

Based on	1989		2014	
Amazonehaven	€0.95E+06	*f* 2.1E+06	€1.63E+06	*f* 3.59E+06
formula 2.1	€0.99E+06	*f* 2.19E+06	€1.71E+06	*f* 3.76E+06

A.9 Dry bulk vessels

Table A.10 depicts the types of vessels, its DWT[2]-class, its true-DWT-class as used in the calculations. Also, the total number of the vessels in recent years are shown per DWT-class.

TABLE A.10: Specifications of vessels, retrieved from [46]

Type	True-DWT-class	DWT-class	2015	2014
T_1	9000	<10000	164	160
T_2	22500.5	10001-35000	151	178
T_3	45000.5	35001-55000	119	105
T_4	55000.5	55001-60000	86	90
T_5	70000.5	60001-80000	179	158
T_6	110000.5	80001-140000	185	171
T_7	170000.5	140001-200000	239	249
T_8	250000.5	200001-300000	45	47
T_9	310000	300001>	9	13

In the calculations, the storage capacity available at the quay wall is *fitted* into the vessels in such a way that two conditions are satisfied, see Appendix D for the conditions.

Table A.11 shows the specific information of various types of dry bulk vessels. The information is used to calculate the Port Dues (PD) as recommended by Port of Rotterdam Authority (PORA).

TABLE A.11: Specific information of various types of dry bulk vessels, retrieved from PORA

[DWT] $\cdot 10^3$	Type	γ_{bt} [€]	D_{bt} [ton]	λ [%]	μ_{db} [€]	ζ [ton]	μ_{odb} [€]	ρ_{db} [ton]	N_{coal} [#]	N_{iron} [#]
35-55	T_3	0.3	58101	133.7	0.488	10000	0.488	45001	104	118
55-60	T_4	0.3	71012	133.7	0.488	12222	0.488	55001	75	85
60-80	T_5	0.3	90378	133.7	0.488	15556	0.488	70001	161	179
140-200	T_7	0.3	219490	133.7	0.488	37778	0.488	170001	61	68
<10	T_1	0.3	11620	133.7	0.488	2000	0.488	9000	0	0

In this table *DWT*, refers to the type of the vessel. γ_{bt} is the toll per type of vessel (BT-size). D_{bt} is the BT-size. λ is the changeover percentage. μ_{db} and μ_{odb} are the charge rate. γ is the *other wet bulk* tonnage. ρ_{db} is the **true**-DWT class. N_{coal} and N_{iron} are the number of vessels entering the port based on data of 2014.

[2]Dead Weight Tonnage

A.10 Earnings of port

Table A.12 shows the revenues from Leasing Contract (LC) in recent years per square meters. However, in this calculation the total leasing area of Port of Rotterdam (POR) is kept constant, based on information available in 2016.

TABLE A.12: Revenues due LC, leasing area based on 2016, retrieved from [46]

Year	Revenues from contract [million €]	Leasing area [ha]	Leasing [$\frac{€}{m^2}$]
2016	349	5978	5.8
2015	341	5978	5.7
2014	338	5978	5.6
2013	322	5978	5.3
2012	292	5978	4.8

Figure A.7 shows the decrease and increase of respectively PD and LC due inflation.

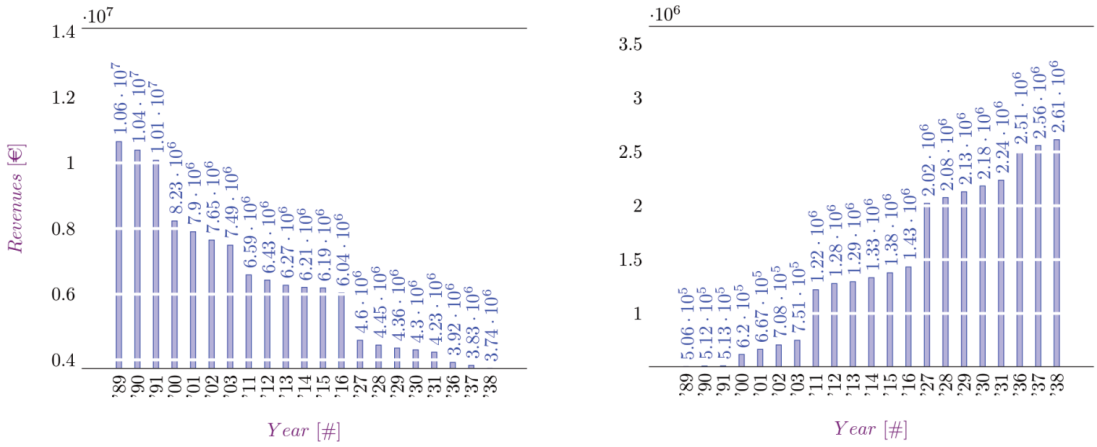

(A) Revenues **P**ort **D**ues, Iron ore

(B) Revenues **L**easing **C**ontract, Iron ore

FIGURE A.7: Revenues of (A) PD and (B) LC, taking into account inflation

To calculate the PD, the number of vessels based on 2014 are used. After which, the revenues due to vessels entering the harbor, are calculated, based on the PORA recommendation. Then, inflation is taken into account and a back- and forward- calculation is done based on the revenues in 2014. Therefore, both numbers of vessels and dues due to utilizing port facilitations are kept constant. As the money loses its value over time, a decrease of PD is to be observed after 2014. An increase in PD is observed in the period prior to 2014, as depicted in sub-Figure (A) A.7.

To calculate the LC, earnings due leasing the area to the companies, the area is kept constant. However, a yearly increase in the leasing price per square meter is taken into account. Also, a yearly inflation is taken into account, as depicted in sub-Figure (B) A.7.

Appendix B

AllWave-PDP results

B.1 Soil characteristics

Sub-Figure (A) B.1, depicts the soil Fatigue Factor (FF) based on Alm & Hamre as used in Pile Driving Prediction (PDP). The pile is vibrated up to -26.5 [m] NAP, after which it is driven further into Pleistocene layer up to the required depth. The driving level has been 10 [m]. In the first part, the FF is kept constant because the soil has experienced a vigorous number of blows. The second stage, when driving takes place, FF is assigned to each soil layer, which varies with soil type. The last 1 [m], the total soil resistance must be overwin, and soil fatigue is not taken into account because the soil has experienced fewer numbers of blows.

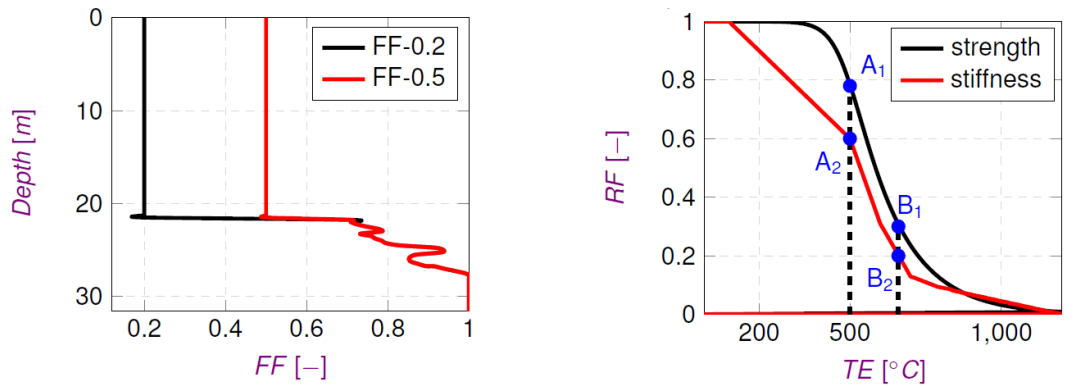

(A) soil **F**atigue **F**actor , based on Alm & Hamre

(B) **R**eduction **F**actor due **T**emperature **E**levation

FIGURE B.1: Left: Soil fatigue model, Right: the sensitivity of steel to TE, retrieved from PDP & [53]

Sub-Figure (B) B.1 shows the steel's sensitivity due TE. The depicted points A_1 & A_2 are used for the **pile inhomogeneous strength**, see section 7.6, where an increase in temperature of about 500° Celsius reduces locally the stiffness and strength of the pile with respectively 40% and 25%. Points B_1 & B_2 are used in section **Triggers** 7.8. In this case, an increase in temperature of about 660° Celsius reduces locally the stiffness and strength of the pile with respectively 80% and 70%.

B.2 Blow count

Figure B.2 depicts the predicted number of blows over a **depth** of 10 meter. The driving with an impact hammer is modeled at a depth of 21.5 [m] up to 31.5 [m], as has happened in reality. The predicted blows are given for: (1) different D/t ratios, different soil FF-values and (3) virgin or compacted soil. The Refusal limit is also depicted as a vertical dotted line. The prediction showed a clear distinction in virgin and compacted soil regarding the number of blows for piles with high D/t ratio. Sub-Figure (G) B.2, however, does not comply with this conclusion. According to sub-Figure (C) B.2, driving would be troublesome at a driving level around 29 meters, in case of a virgin soil for Amazonehaven. If a compacted soil or a higher soil FF-value is considered for Amazonehaven, then the **R**efusal limit exceeds earlier in driving stage. When the number of blows exceeds the R-limit, a driving schedule[1] must be used as a guideline to control the heavy driving [29]. In this fashion, the energy is managed by the operator to achieve optimum efficiency of the hammer. When heavy driving still occurs the thickness of cushioning between the hammer and pile head, to protect both hammer and head, must be reduced by the operator. As a last solution to heavy driving is to change to a heavier hammer. None of these solutions are taken into account in this study.

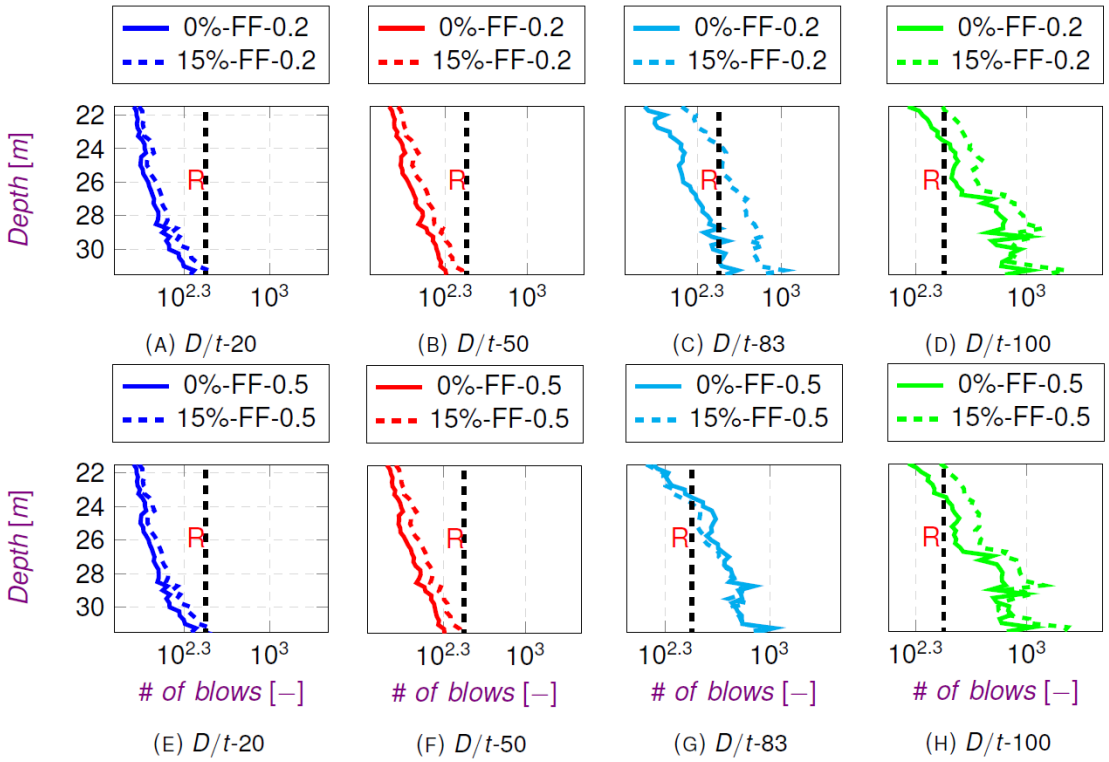

FIGURE B.2: Number of blows, legend: compaction-FF-D/t, retrieved from PDP

[1] (pile) driving procedure

B.3 Maximum driving stresses

Figure B.3 depicts the maximum driving stress per driving level for different (1) D/t ratios, (2) FF-value and (3) virgin or compacted soil. It also depicts that driving stresses are far less than the material's yield stress given the Amazonehaven soil condition, defined as Standard to Normal Soil Condition (SNSC).

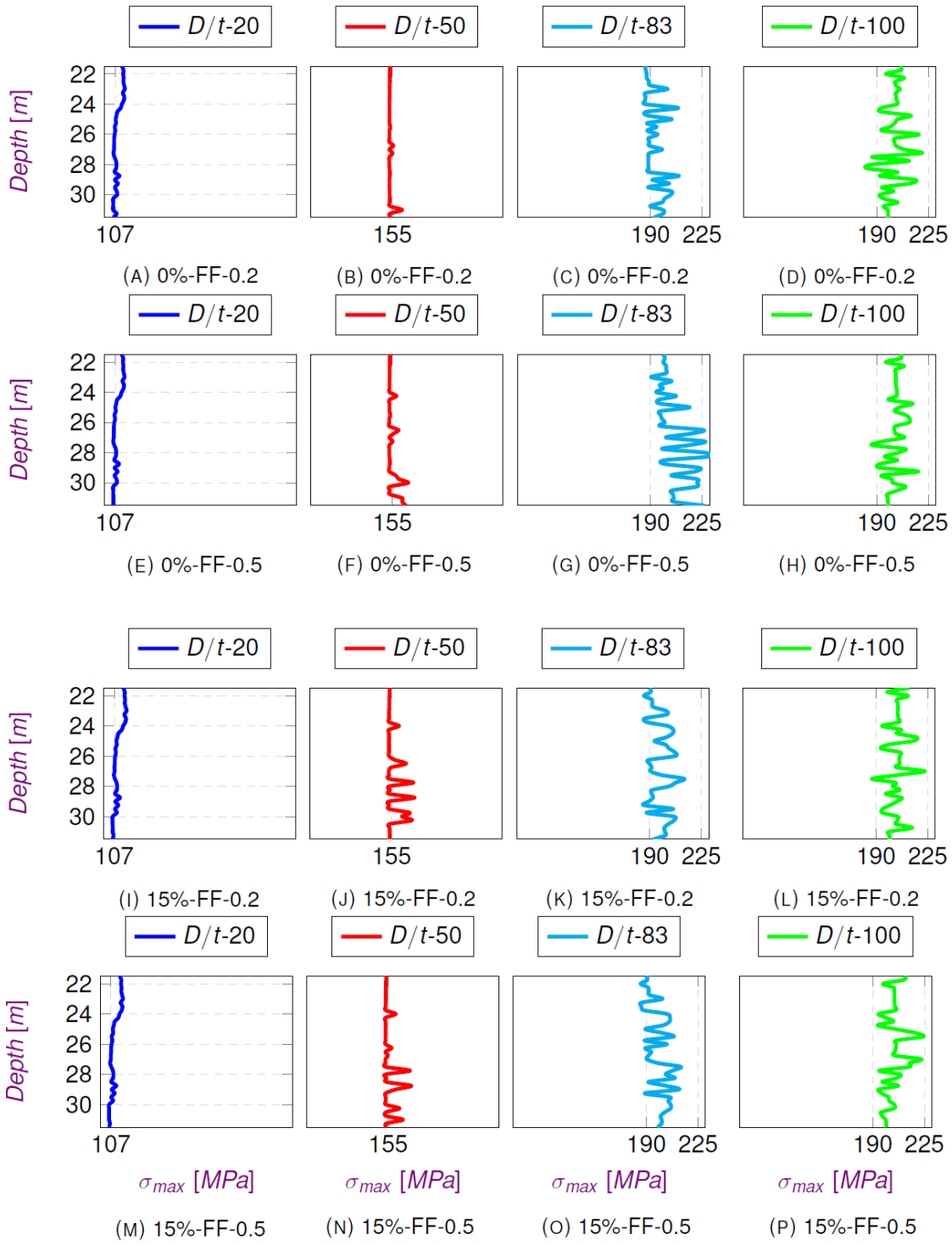

FIGURE B.3: Maximum driving stress per driving level, legend: D/t-Compaction-FF, retrieved from PDP

B.4 Detailed PDP

Figure B.4 shows from left to right: maximum driving stress per driving level, number of blows per driving level, transferred energy per driving level and hammer-induced driving stresses along the pile for the highest value of *maximum driving stress per driving level*. Therefore, sub-Figures (A-C) B.4 are over the **depth** whereas sub-Figure (D) B.4 is over the pile's **length**. It shows that (1) the driving stresses are high at pile head rather than the toe, (2) the driving stresses are far lower than the material's yield stress close to pile toe, given the SNSC. However, the transferred energy is extremely low. A D100-13 have a hammer energy of about 214 [KJ], but the transferred energy is much lower than that due to, e.g., the thickness of cushioning. In reality, however, the cushioning would be replaced to increase the transferred energy which reduces the number of blows, as well as the operator, manages the energy level per driving level. This study did not take into account these variables.

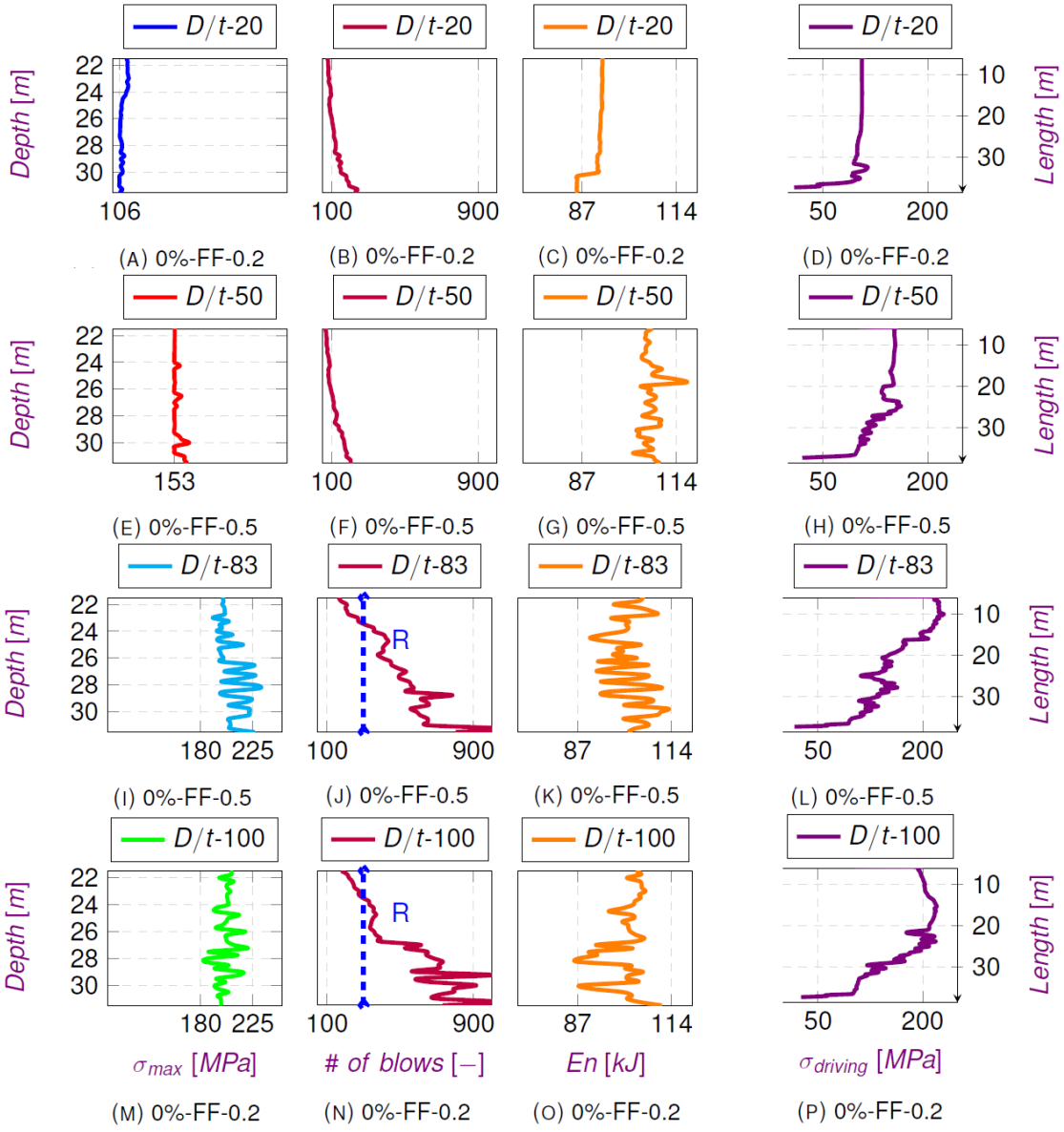

FIGURE B.4: Specifications of piling, legend: compaction-D/t-FF, retrieved from PDP

B.5 Shell bank

Figure B.5 depicts six scenarios of presence of Shell Bank (SB) or a Locally Extremely Hard Spot (LEHS). The stiff soil layer is either located at toe [SB-toe] or located at **F**our **S**pots over the entire depth [SB-FS]. The calculations are carried out for Amazonehaven case, D/t of 83, and a soil FF of 0.2 or 0.5, with or without Zero Shaft Friction (ZSF). The maximum driving stresses per driving level, become very high close to toe, as it was predicted in the *fixed end extreme*.

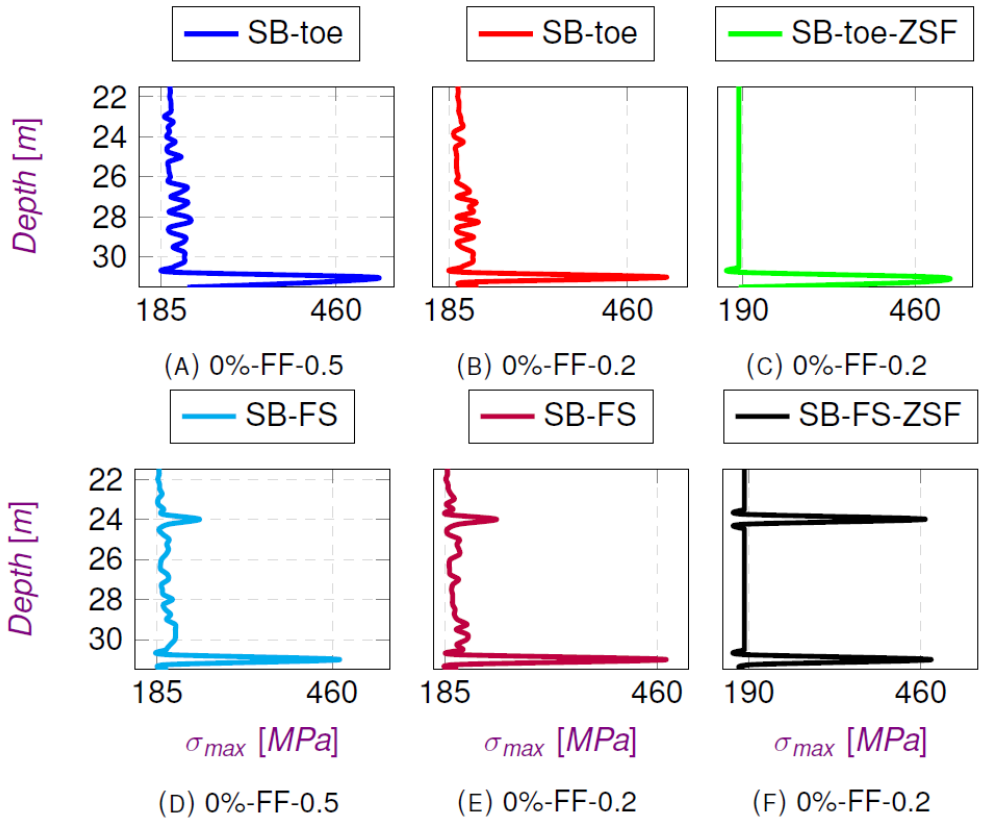

FIGURE B.5: Maximum driving stress per driving level, legend: SB-Location-Compaction-FF, retrieved from PDP

Figure B.6 shows from left to right: maximum driving stress per driving level, number of blows per driving level, transferred energy per driving level and stress development along the pile. It presents both situations of presence of SB in **F**our **S**pots [SB-FS] and SB at toe [SB-toe], where shaft friction is eliminated[2]. The stresses close to pile toe as well as along the pile show extremely high values.

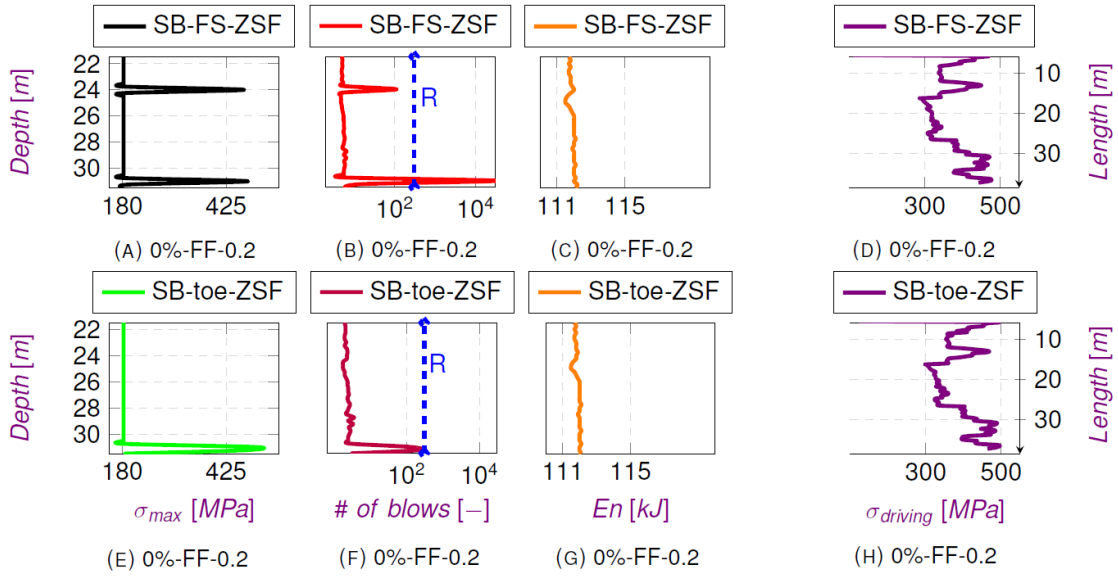

FIGURE B.6: Specifications of piling, legend: compaction-D/t-FF, retrieved from PDP

[2]ZSF

Figure B.7 shows from left to right: maximum driving stress-, the number of blows-, transferred energy- per driving level and development of hammer-induced driving stresses along the pile. When a SB or a LEHS in combination with a ZSF is modeled, the driving stresses close to pile toe as well as along the entire pile become extremely high. However, this circumstance could be defined when a Medium to Hard Soil Condition (MHSC) or Soft Rock (SR) is to be considered whereas Amazonehaven soil composition could be described as SNSC.

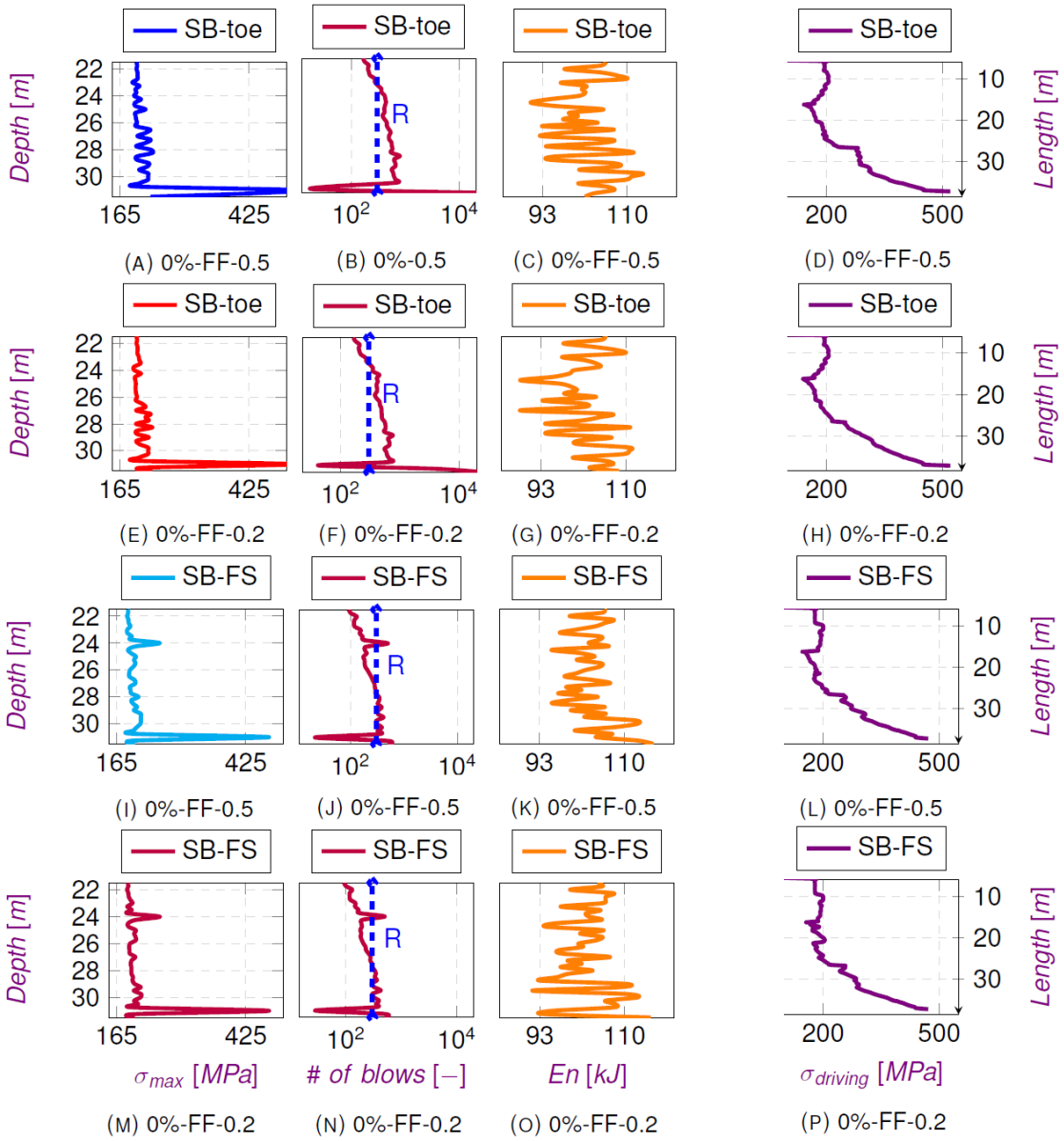

FIGURE B.7: Specifications of piling, legend: compaction-D/t-FF, retrieved from PDP

B.6 CPT

The Cone Penetration Test (CPT) carried out in the area of Amazonehaven are shown in Figure B.8. The selection of the CPT is randomly and according to its availability of GEF-format. The governing soil-profile could be described as the one close to *fixed end extreme*, which means a low shaft friction along the pile and a high toe resistance at the embedded depth. It is apparent that the soil composition of the area is more or less the same when comparing the soil-profiles. However, DN130, DO73 as well as DN58 show a slightly higher cone resistance closer to soil surface level. The CPT is also in the vicinity of the area where Problematic Section (PS) are introduced. However, Research into Pile Toe Failure in Amazonehaven (RIPTFIA) uses values as high as 500 [MPa] to describe SB as depicted in sub-Figure (B) B.8. In this regard, the hammer-induced driving stresses close to pile toe was about the material's yield stress. It is evident that cone resistance deviation of in between 30-60 [MPa] could not result in such values of stresses close to pile toe, given the SNSC.

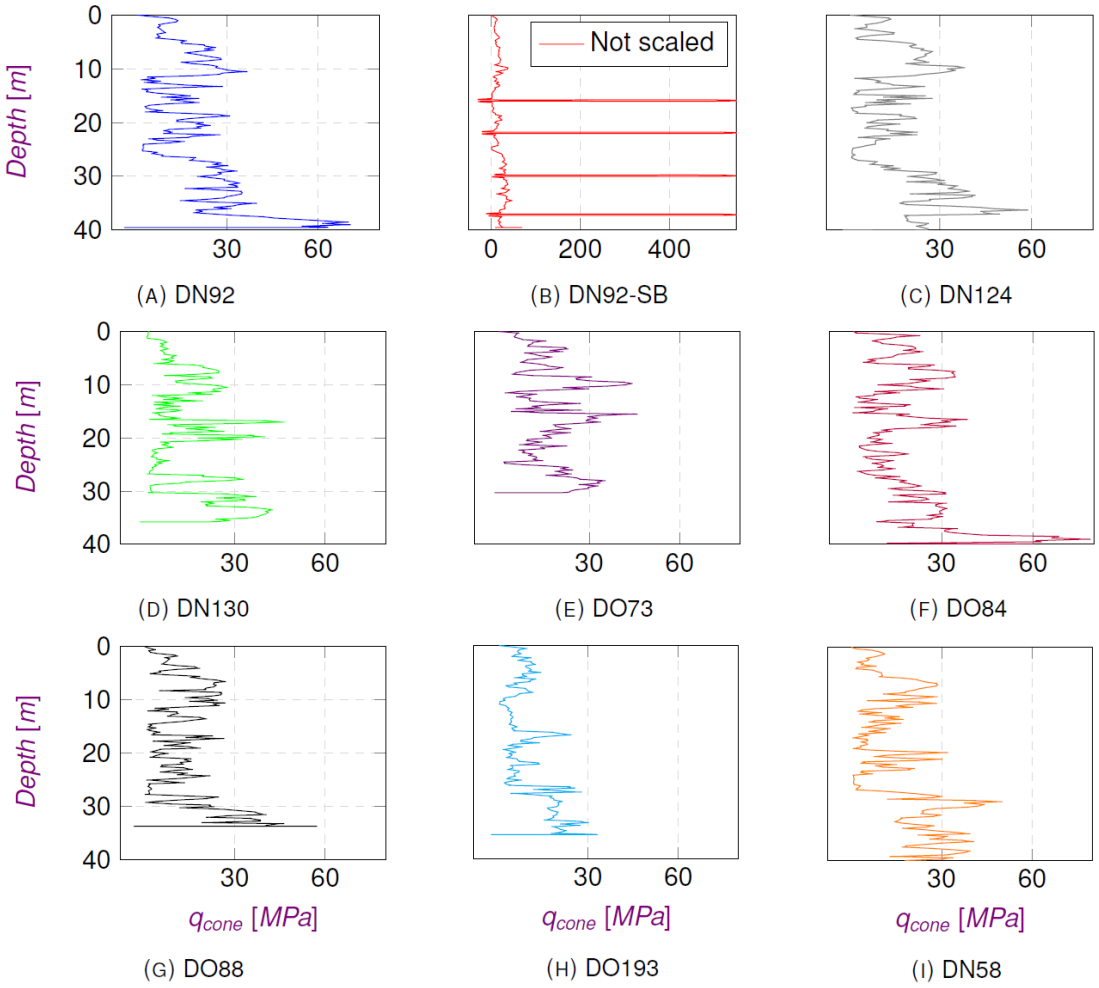

FIGURE B.8: CPT in Amazonehaven, see pile plan-Figure 4.6-Chapter 4, retrieved from Gisweb Rotterdam

B.7 Overview results

Figure B.9 shows an overview of maximum driving stress, its associated driving level and its D/t ratio. The maximum driving stresses per driving level were intended to be used as the initial load on the pile, $F_{initial}$, in the Finite Element Analysis (FEA) program. Afterwards, it was decided to calculate with a constant initial load, to be able to compare the results.

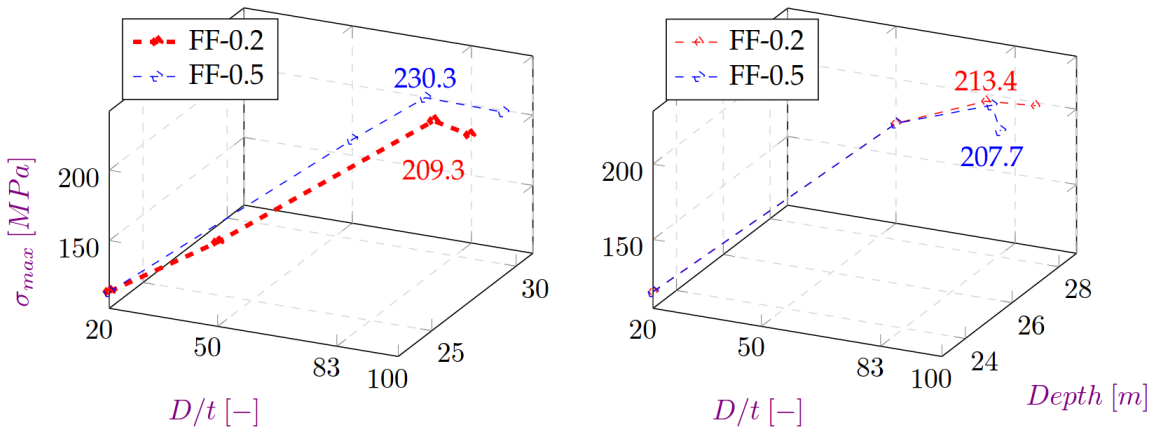

(A) Virgin soil (B) Compacted soil

FIGURE B.9: Maximum driving stress per driving level, legend: FF-Compaction, retrieved from PDP

B.8 Complementary fault tree

The fault tree, Figure B.10, shows an extension of existing one in the literature which does not discuss the *primary pile failure* [7]. The fault tree extension is a description of king pile failure due to failing in maintaining the pile toe integrity. The branches of king pile failure due *pile toe failure* are two-folded: its failure within the hammer-pile-soil system and its failure due to its Management Aspect (MA). The latter focuses on the failure before piling process. In the next page, the figure is enlarged to assure readability.

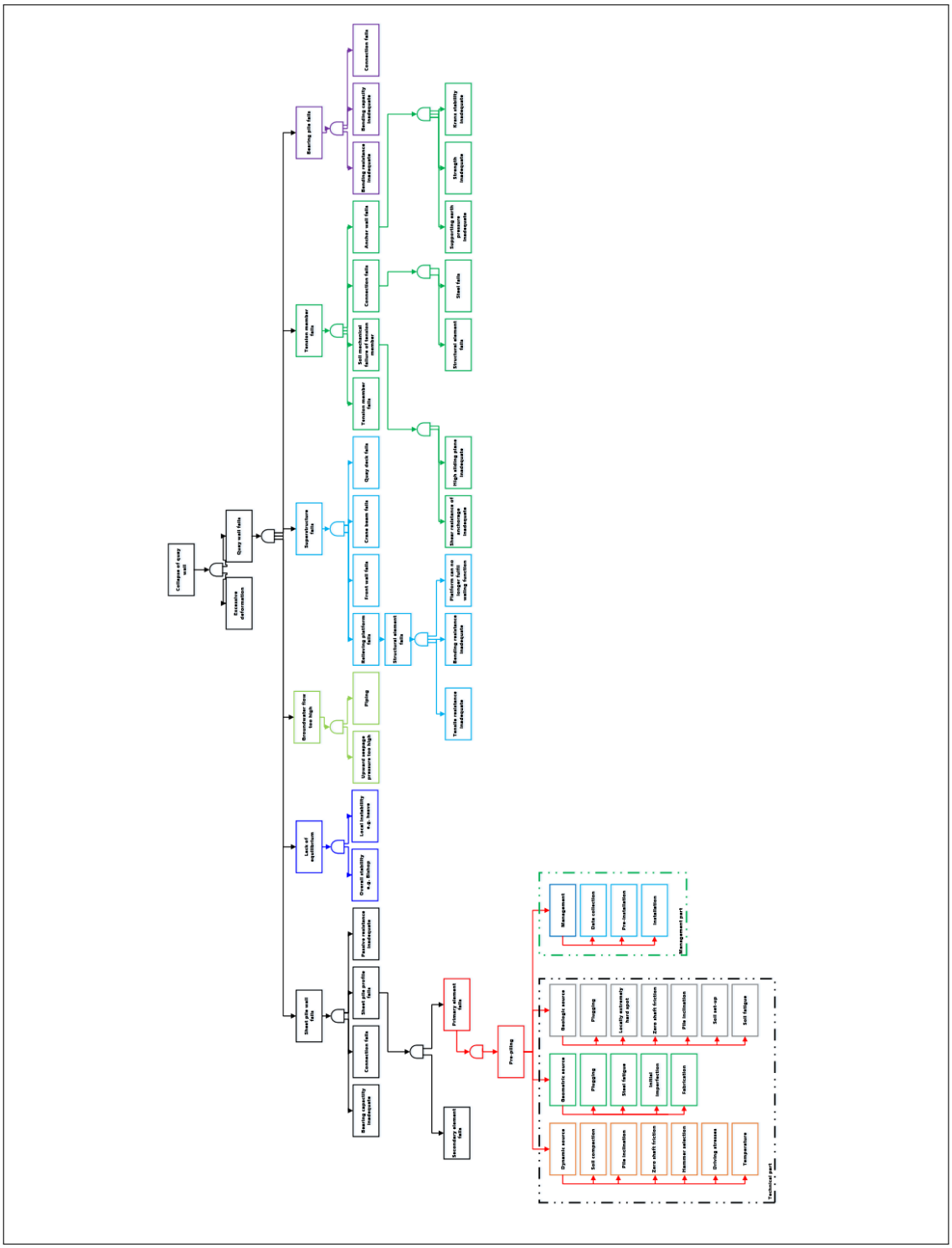

FIGURE B.10: Complementary fault tree of a quay wall, used Visio

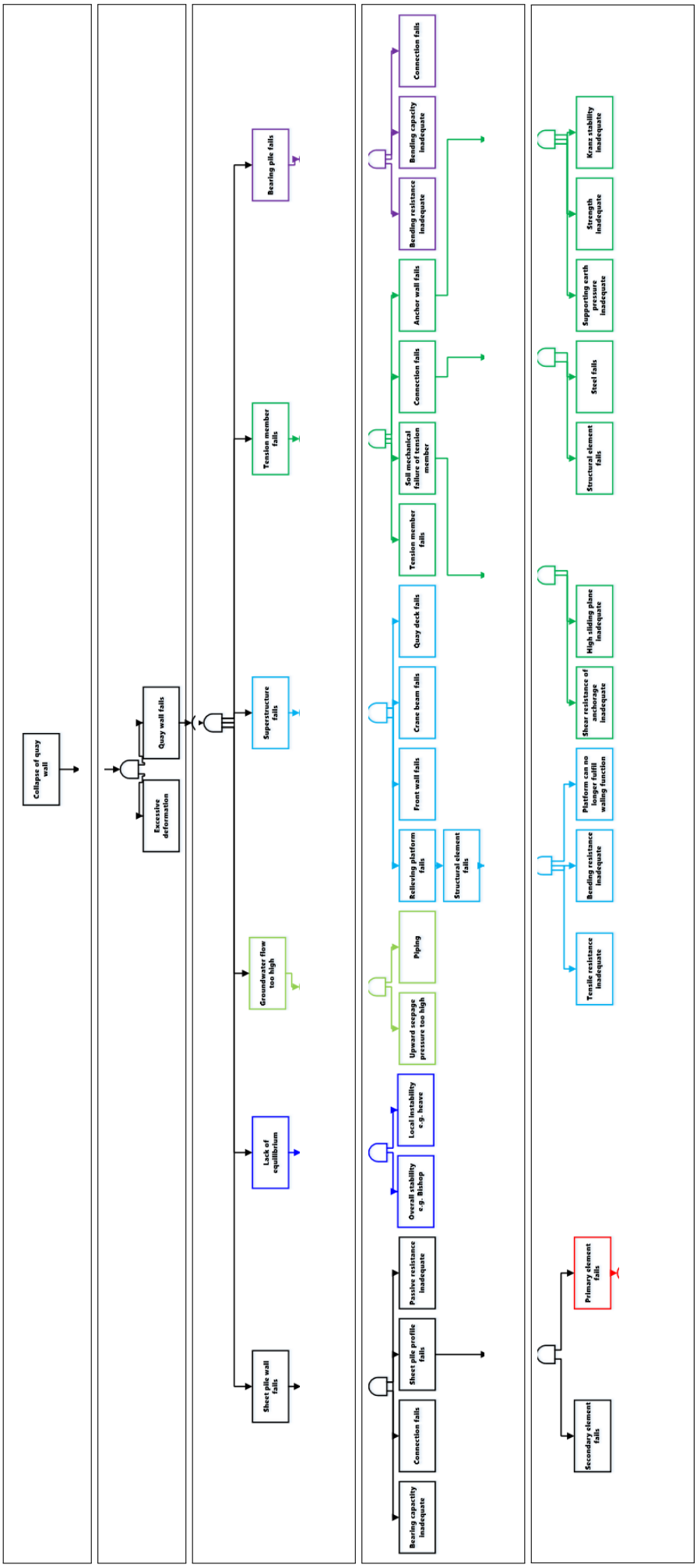
Collapse of quay wall
Excessive deformation
Quay wall falls
Sheet pile wall falls
Lack of equilibrium
Groundwater flow too high
Superstructure falls
Tension member falls
Bearing pile falls
Bearing capacity inadequate
Connection falls
Sheet pile profile falls
Passive resistance inadequate
Overall stability e.g. Bishop
Local instability e.g. buure
Upward seepage pressure too high
Piping
Relieving platform falls
Front wall falls
Crane beam falls
Quay deck falls
Structural element falls
Tension member falls
Soil mechanical failure of tension member
Connection falls
Anchor wall falls
Bending resistance inadequate
Bending capacity inadequate
Connection falls
Secondary element falls
Primary element falls
Tensile resistance inadequate
Bending resistance inadequate
Platform can no longer fulfill waling function
Shear resistance of anchorage inadequate
High sliding plane inadequate
Structural element falls
Steel falls
Supporting earth pressure inadequate
Strength inadequate
Kranz stability inadequate

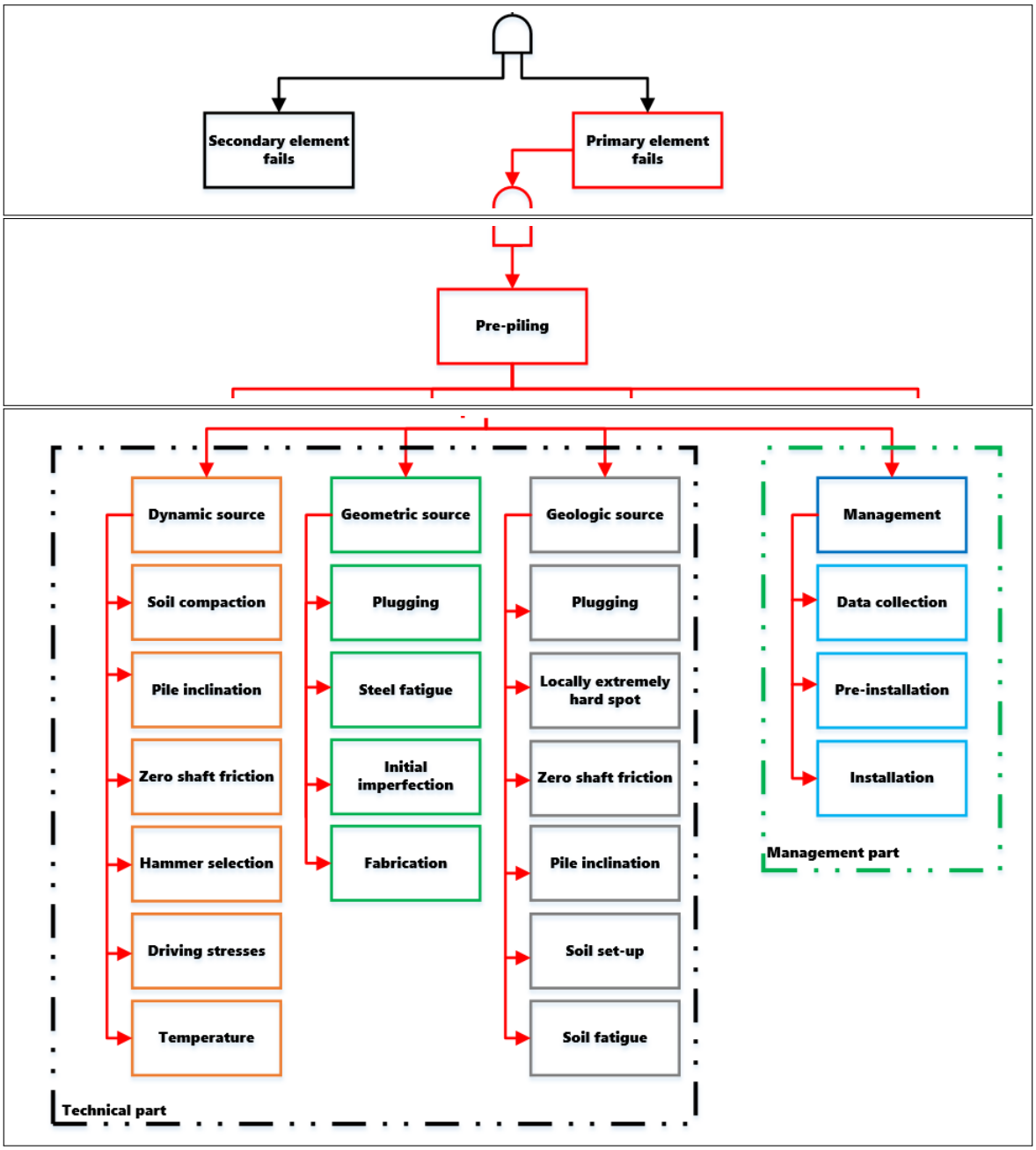

FIGURE B.11: Zoomed in complementary fault tree

Appendix C

SCIA Engineer Results

C.1 Finite element mesh size

The finite element mesh size is often leading for the precision of the acquiring results. In Research into Pile Toe Failure in Amazonehaven (RIPTFIA), it was observed that with increasing mesh size, finer elements, the Yield Stress Momentum (YSM)-value increased and the displacements of the pile vertically as well as horizontally decreased. However, a drawback of finer elements is a more time consuming as well as the more space the solution needs; both during calculation and for storage of the results [2].

Therefore, it was chosen for a mesh size of 0.142 [m] for the entire 10 [m] of modeled pile whereas only for imperfection scenarios, the mesh size was selected to be 0.037 [m] at the discontinuity. In this regard, both a considerable timespan and precision were warranted.

C.2 Non-linear properties

The non-linearity of the material is defined directly in the material library in SCIA. During a linear analysis, the material will behave elastically. The plastic properties of materials, however, are generic for any material. Therefore, plasticity could be enabled by selecting the *isotropic elasto-plastic von Mises* type of plastic behavior. It corresponds to a bilinear stress-strain relationship, identical in tension and compression. In the plastic domain, the stress remains constant when the strain increases, the so-called plastic branch without hardening. Therefore, it should be controlled whether the strain stays below 0.5% [2].

The other non-linearity feature is referred to as geometrically non-linearity. When a geometrically non-linearity option is enabled in SCIA, the second order effects are taken into account during the calculation. Non-linear properties could be assigned to the material and the support, e.g., hinges. However, these properties cannot be assigned to the surrounding soil or so-called bedding along the pile. As a trick, the non-linearity could be enabled for soil properties when the surrounding soil is modeled as support. In this report, only physically and geometrically non-linearity properties for the steel are taken into account.

The main difference between a linear and non-linear calculation is that the non-linear calculation gives such results of deflections and internal forces for which equilibrium conditions are satisfied on a deformed structure [2]. In RIPTFIA conducting a non-linear calculation was crucial due toe *extreme folding damage* due to plastic deformation of the material. In other words, the stresses have exceeded material's yield stress which has led to *extreme folding damage*.

C.3 Calculation

C.3.1 Direct versus iterative solver

The direct solver should be used only for beam structures (without any 2D members) or planar structure composed of 2D members (i.e., a plate or a wall). In other cases, the direct solver should be used as a default solution method. The application of iterative solution depends on

the total number of nodes, bandwidth and memory size of the particular computer. If the direct solution leads to an excessive disk swapping, the process is slowed down significantly, and the iterative solution must be employed [50].

C.3.2 Timoshenko versus Newton-Raphson

The algorithm is based on the exact Timoshenko's solution of a 1D member. The axial force is assumed constant during the deformation. Therefore, the method is applicable for structures where the difference of axial force obtained by 1^{st} order and 2^{nd} order calculation is negligible. This is mainly true for frames, buildings, etc. for which the method is the most effective option. The method is applicable for structures where rotation does not exceed 8 degrees. It assumes small displacements, small rotations, and small strains. Also, it only needs two steps which lead to a significant effect of the method. The first step serves only for the solution of axial force. The second step uses the determined axial forces for Timoshenko's exact solution. The original Timoshenko's solution was generalized in SCIA Engineer, and the shear deformations can be taken into account [2].

The algorithm is based on the Newton-Raphson method for the solution of non-linear problems. The method is robust for most of the problems. It may, however, fail in the vicinity of inflection points of loading diagram. This may occur at compressed 1D members subject to small eccentricity or small transverse load. Except for this, the method can be applied to a wide range of problems. It provides a solution of extremely large deformations. The load acting on the structure can be divided into several steps. The default number of steps is eight. If this number is not sufficient, the program issues a warning. The rotation achieved in one increment should not exceed 5 degrees. The accuracy of the method can be increased through refinement of the finite element mesh or by the increase in a total number of increments [50].

C.4 YSM

The YSM is determined as the point in which the yield stress of the material is reached for the first time. This point is $q_{yielding}$ divided by $q_{initial}$, where $q_{yielding}$ is the factored force applied on the pile where the yield stress of the material appears for the first time. The $q_{initial}$ is the initial load applied on the pile and could be based on the maximum values of driving stresses resulted from the Pile Driving Prediction (PDP) calculations. Sub-Figure (A) C.1 shows the maximum stresses per D/t ratio whereas sub-Figure (B) C.1 depicts the development of the driving stresses along the pile, given the specific driving level where the highest value of driving stress is to be found.

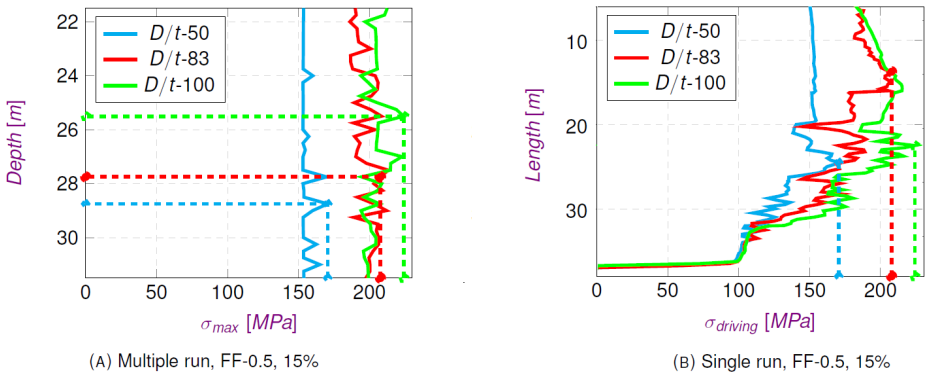

(A) Multiple run, FF-0.5, 15%

(B) Single run, FF-0.5, 15%

FIGURE C.1: Specifications of piling, legend: D/t-FF-compaction, retrieved from PDP

In RIPTFIA, however, the value of $q_{initial}$ is kept constant to enable a proper comparison in the sensitivity analysis.

Table C.1 shows the factored f, $\frac{q_{driving}}{q_{initial}}$. Therefore, the maximum hammer-induced driving stress, $\sigma_{driving}$ given a D/t ratio of 100 is almost the same as the initial (normalized) load as applied in the SCIA model.

TABLE C.1: Calculation of factored f, (predicted) driving load divided by initial load, per D/t ratio

$\frac{D}{t}$ [-]	$\sigma_{driving}$ $[\frac{N}{mm^2}]$	F=$\sigma_{driving} \cdot A$ [kN]	$q_{driving} = \frac{F}{S \cdot L}$ $[\frac{kN}{m^2}]$	f= $\frac{q_{driving}}{q_{initial}}$ [-]
20	115.2	34663.5	259.7	2.60
50	170.6	21181.7	153.8	1.54
83	213.4	16090.8	115.9	1.16
100	224.2	14060.4	101.1	1.01

In Table C.1, S refers to perimeter of the pile, while L is the length of the pile as shown in Table A.6 and A.7.

C.5 Imperfection results

The stress development along the pile due to its discontinuity, regarding imperfection, is presented as a top view in perspective. For the sake of clarity, close to toe, stress development is zoomed in and also presented in top view in perspective.

C.5.1 I-toe-0.2·D

Figure C.2 depicts the stress development due to centric loading in the king pile. From left to right: top view in perspective of stresses in the pile, top view zoom in perspective, top view *extra* zoom in perspective.

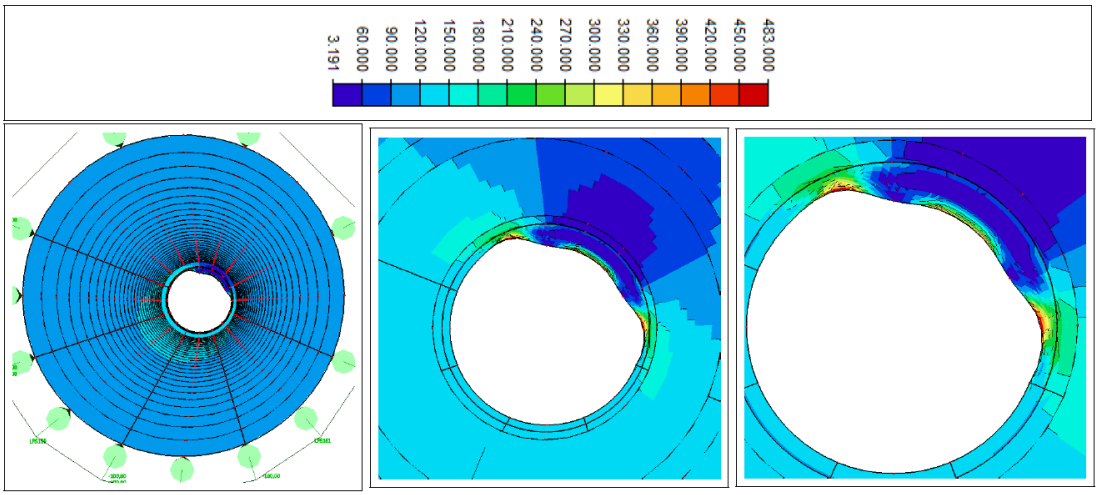

FIGURE C.2: Stress development in the pile, retrieved from SCIA

Figure C.3 depicts the stress development due to eccentric loading in the king pile. From left to right: top view in perspective of stresses in a pile, top view zoom in perspective, top view *extra* zoom in perspective.

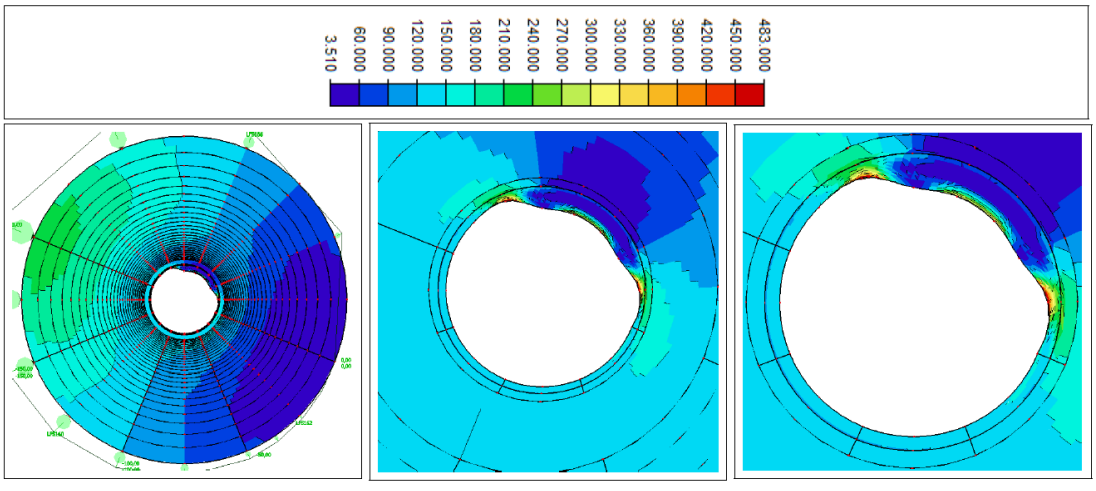

FIGURE C.3: Stress development in the pile, retrieved from SCIA

C.5.2 I-toe-0.7·D

Figure C.4 depicts the stress development due to centric loading in the king pile. From left to right: top view in perspective of stresses in a pile, top view zoom in perspective, top view *extra* zoom in perspective.

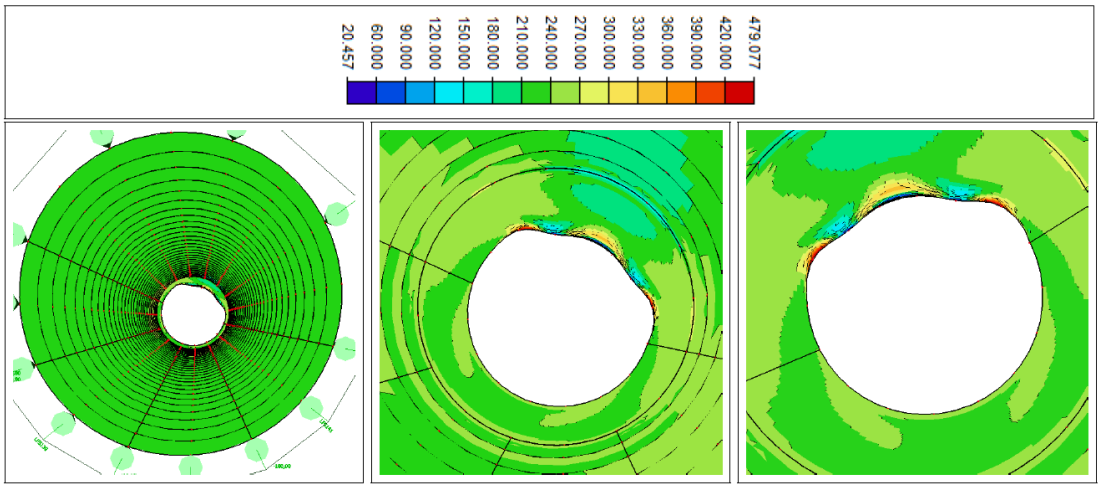

FIGURE C.4: Stress development in the pile, retrieved from SCIA

Figure C.5 depicts the stress development due to eccentric loading in the king pile. From left to right: top view in perspective of stresses in a pile, top view zoom in perspective, top view *extra* zoom in perspective.

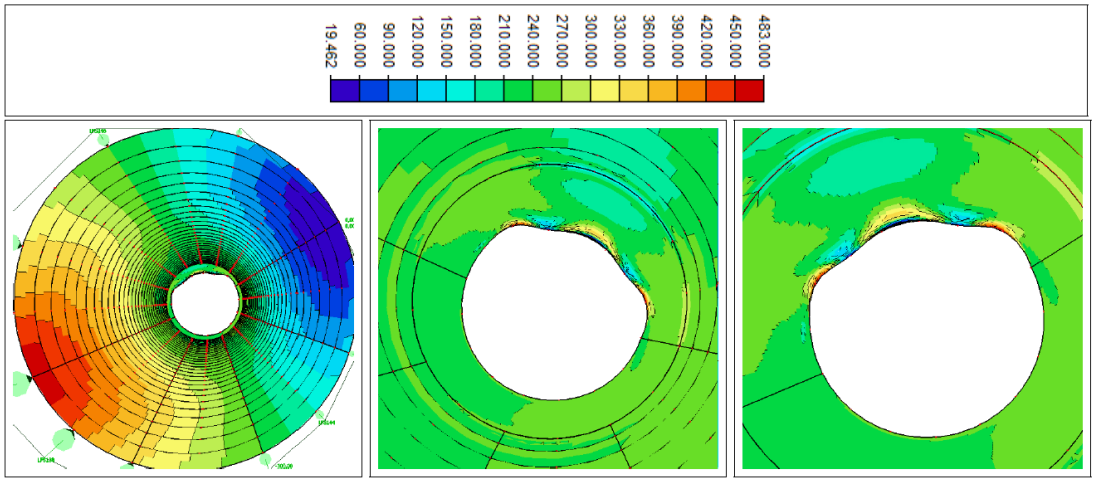

FIGURE C.5: Stress development in the pile, retrieved from SCIA

C.5.3 I-2·D-0.4·D

Figure C.6 depicts the stress development due to centric loading in the king pile. From left to right: top view in perspective of stresses in the pile, top view zoom in perspective, top view *extra* zoom in perspective.

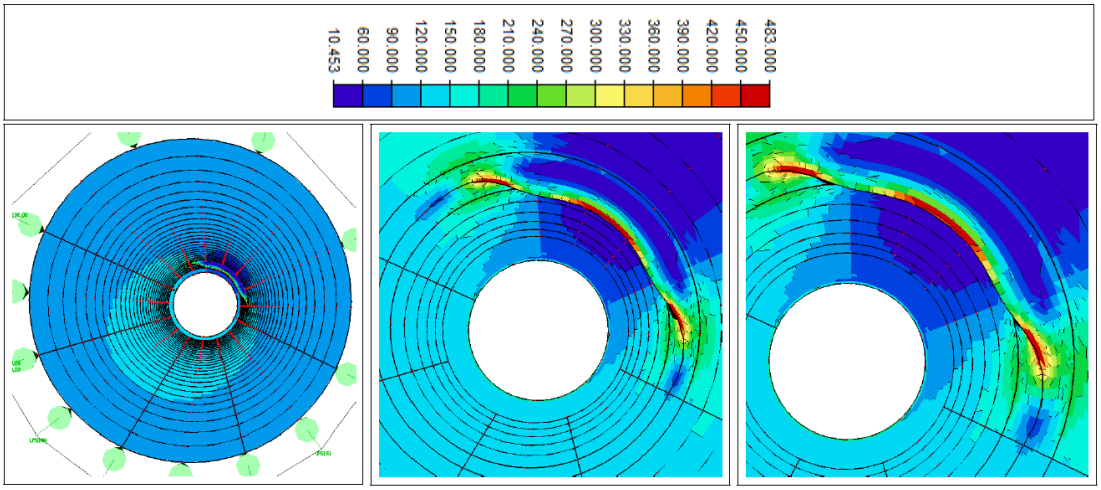

FIGURE C.6: Stress development in the pile, retrieved from SCIA

Figure C.7 depicts the stress development due to eccentric loading in the king pile. From left to right: top view in perspective of stresses in a pile, top view zoom in perspective, top view *extra* zoom in perspective.

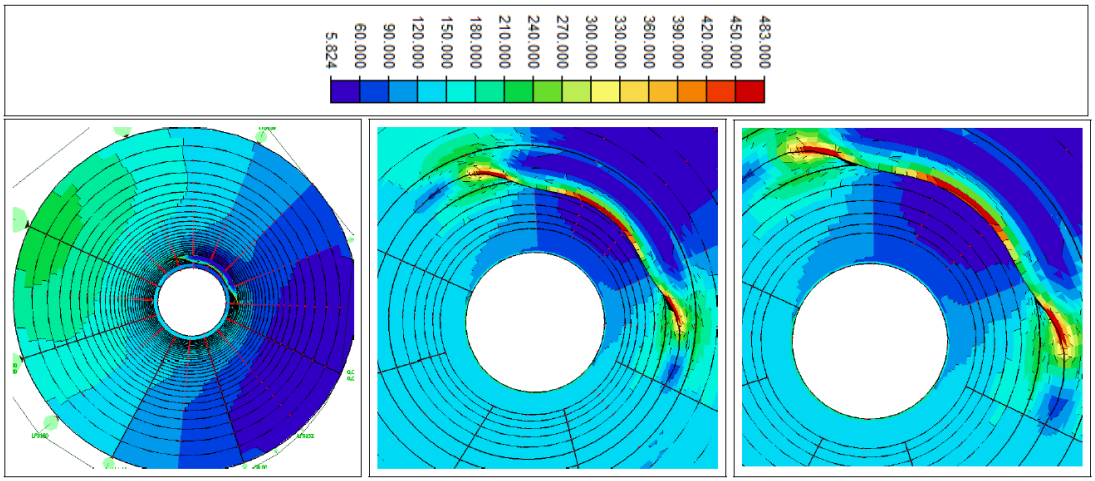

FIGURE C.7: Stress development in the pile, retrieved from SCIA

C.5.4 I-2·D-1.4·D

Figure C.8 depicts the stress development due to centric loading in the king pile. From left to right: top view in perspective of stresses in the pile, top view zoom in perspective, top view *extra* zoom in perspective.

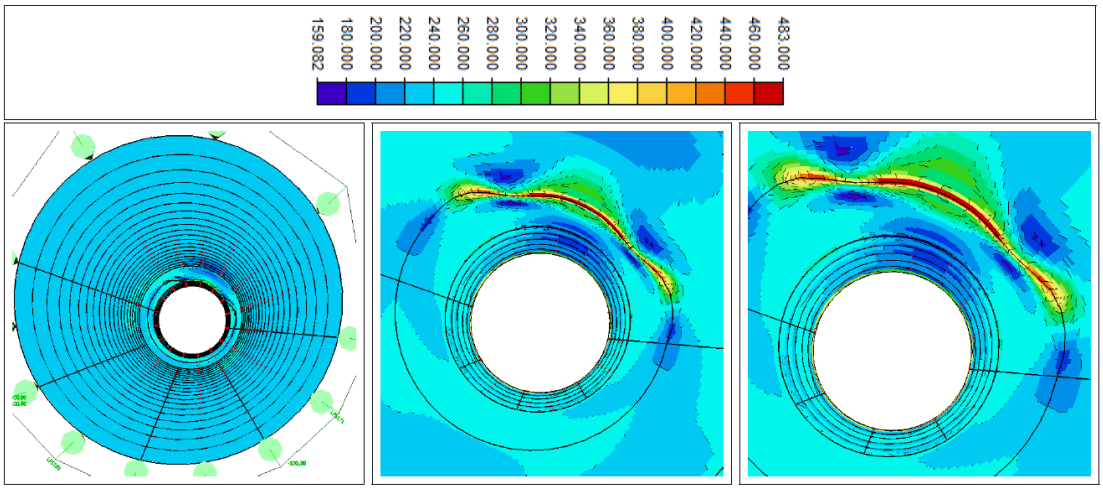

FIGURE C.8: Stress development in the pile, retrieved from SCIA

Figure C.9 depicts the stress development due to eccentric loading in the king pile. From left to right: top view in perspective of stresses in a pile, top view zoom in perspective, top view *extra* zoom in perspective.

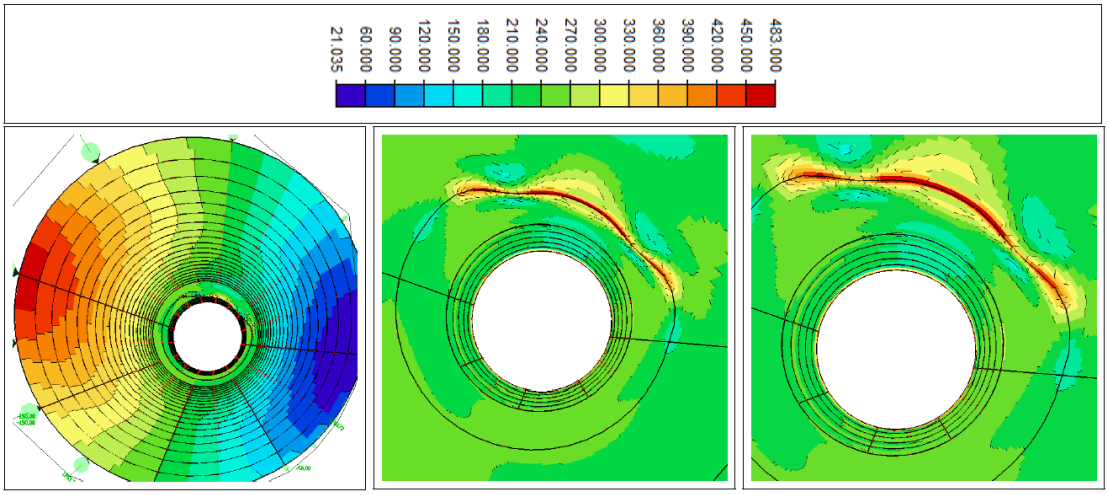

FIGURE C.9: Stress development in the pile, retrieved from SCIA

C.6 Inclination results

The stress development along the pile due to its discontinuity, regarding inclination, is presented as a top view in perspective. For the sake of clarity, close to toe, stress development is zoomed in and also presented in top view in perspective.

C.6.1 H-100%-Weak

Figure C.10 depicts the stress development due to both centric and eccentric loading in the king pile.

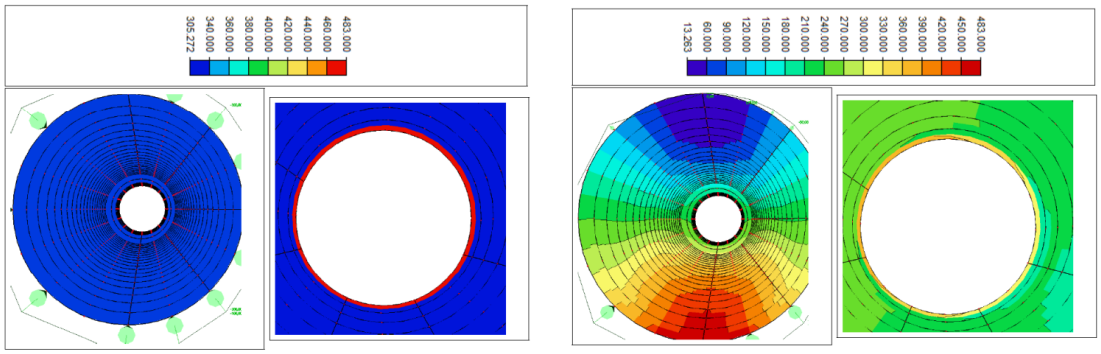

(A) Stress development due centric loading (B) Stress development due eccentric loading

FIGURE C.10: Stress development in the pile, retrieved from SCIA

C.6.2 H-100%-Stiff

Figure C.11 depicts the stress development due both centric and eccentric loading in the king pile.

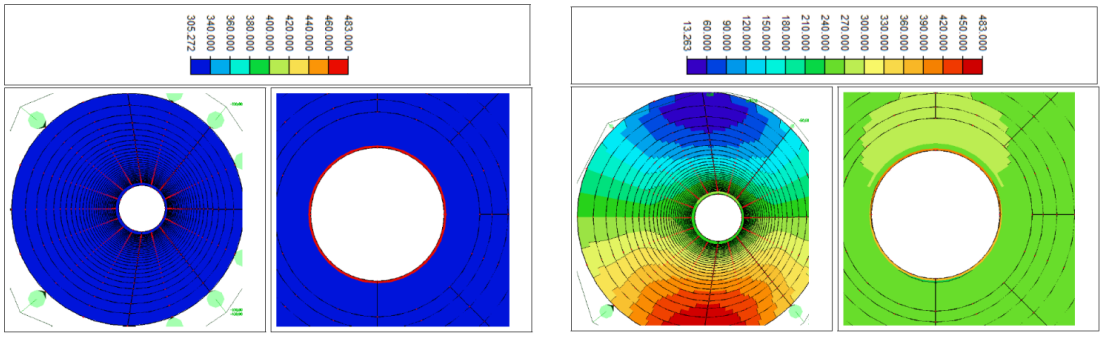

(A) Stress development due centric loading (B) Stress development due eccentric loading

FIGURE C.11: Stress development in the pile, retrieved from SCIA

C.6.3 H-50%-Partial

Figure C.12 depicts the stress development due to both centric and eccentric loading in the king pile.

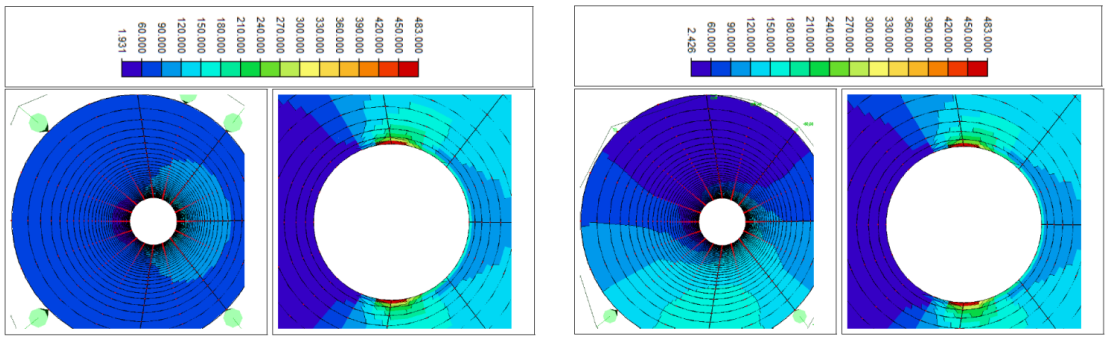

(A) Stress development due centric loading (B) Stress development due eccentric loading

FIGURE C.12: Stress development in the pile, retrieved from SCIA

C.6.4 H-100%-Partial

Figure C.13 depicts the stress development due to both centric and eccentric loading in the king pile.

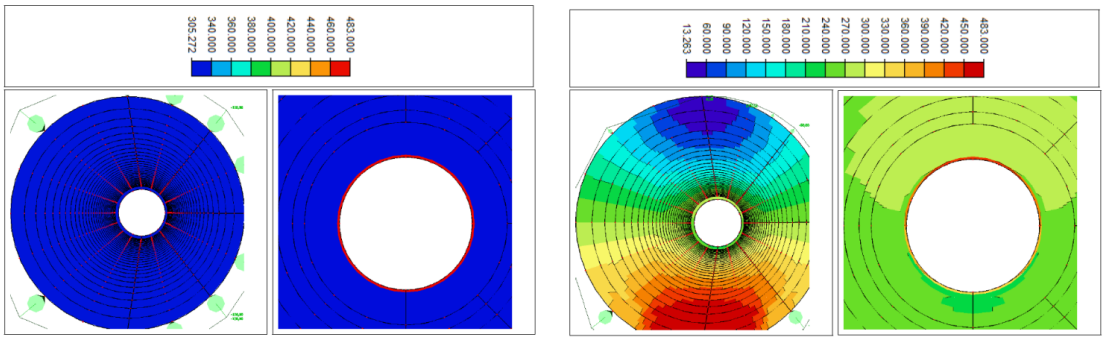

(A) Stress development due centric loading (B) Stress development due eccentric loading

FIGURE C.13: Stress development in the pile, retrieved from SCIA

C.7 Inhomogeneous results

The stress development along the pile due to its discontinuity, in terms of inhomogeneous strength, is presented as top view in perspective. For the sake of clarity, close to toe, stress development is zoomed in and also presented in top view in perspective.

C.7.1 T-toe-0.2·D

Figure C.14 depicts the stress development due to both centric and eccentric loading in the king pile.

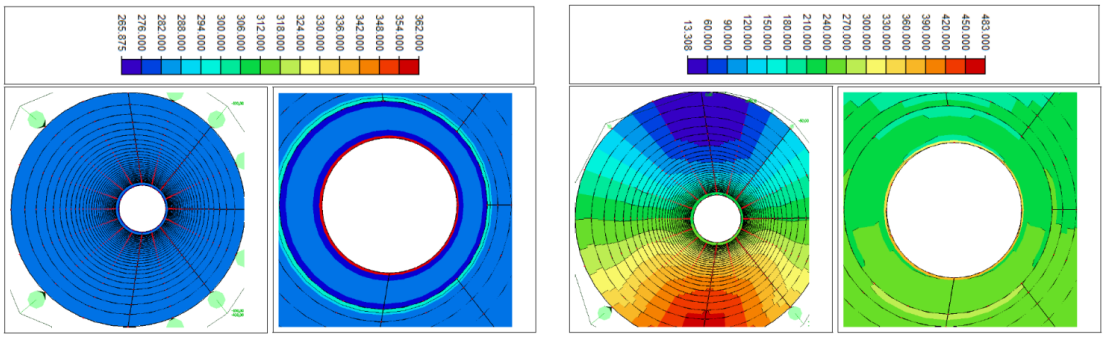

(A) Stress development due centric loading (B) Stress development due eccentric loading

FIGURE C.14: Stress development in the pile, retrieved from SCIA

C.7.2 T-toe-0.2·D

Figure C.15 depicts the stress development due to both centric and eccentric loading in the king pile.

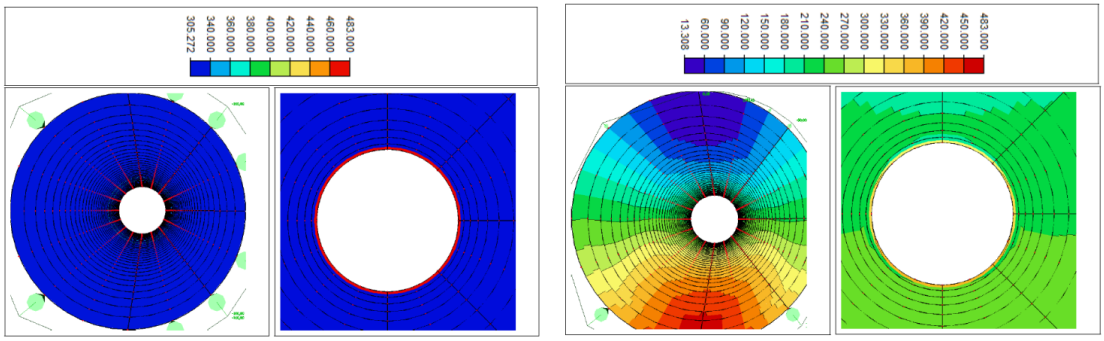

(A) Stress development due centric loading (B) Stress development due eccentric loading

FIGURE C.15: Stress development in the pile, retrieved from SCIA

C.7.3 T-toe-0.2·D

Figure C.16 depicts the stress development due to both centric and eccentric loading in the king pile.

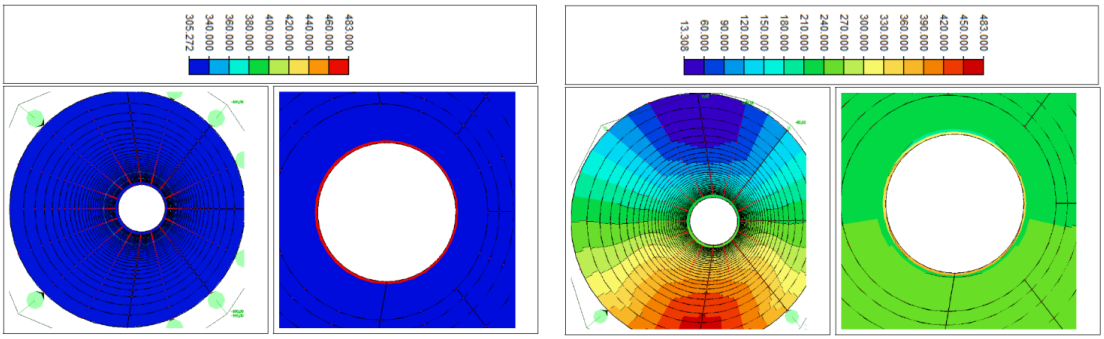

(A) Stress development due centric loading (B) Stress development due eccentric loading

FIGURE C.16: Stress development in the pile, retrieved from SCIA

C.7.4 T-toe-0.2·D

Figure C.17 depicts the stress development due to both centric and eccentric loading in the king pile.

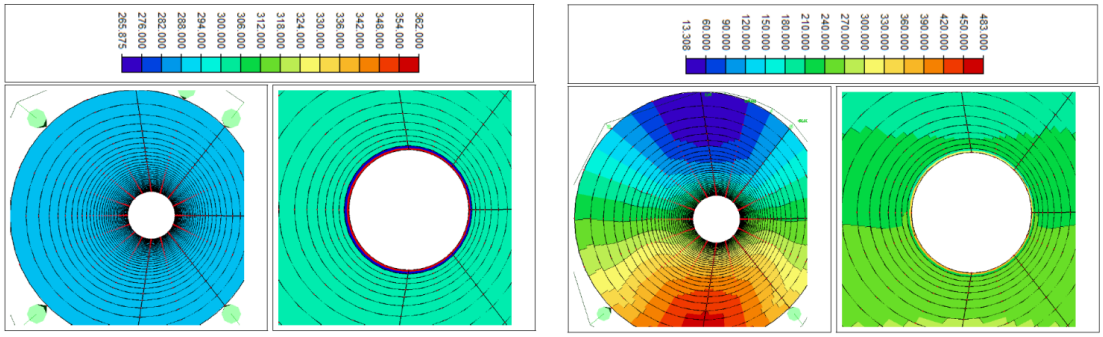

(A) Stress development due centric loading (B) Stress development due eccentric loading

FIGURE C.17: Stress development in the pile, retrieved from SCIA

C.8 Triggers

A threesome of triggers: (1) initial imperfection growth, (2) symmetrical imperfection and (3) extreme imperfection are studied in sections: normal-, symmetrical- and extreme cases.

C.8.1 Normal case

IR-2.23%

Figure C.18 depicts the stress development due to centric loading in the king pile. From left to right: bottom view in perspective of king pile, a top view of stresses in a pile, top view *extra* zoom in perspective.

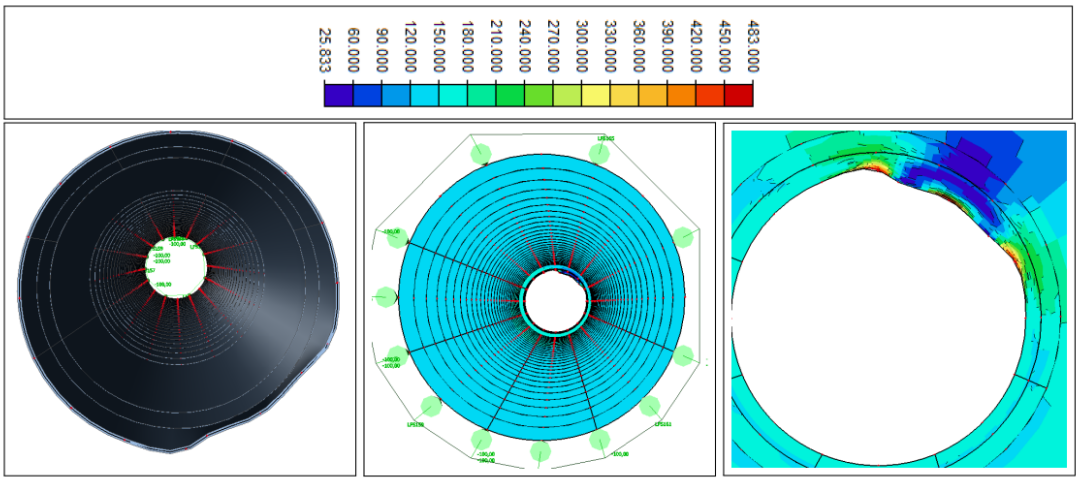

FIGURE C.18: Stress development in the pile, retrieved from SCIA

IR-7.05%

Figure C.19 depicts the stress development due to centric loading in the king pile. From left to right: bottom view in perspective of king pile, a top view of stresses in a pile, top view *extra* zoom in perspective.

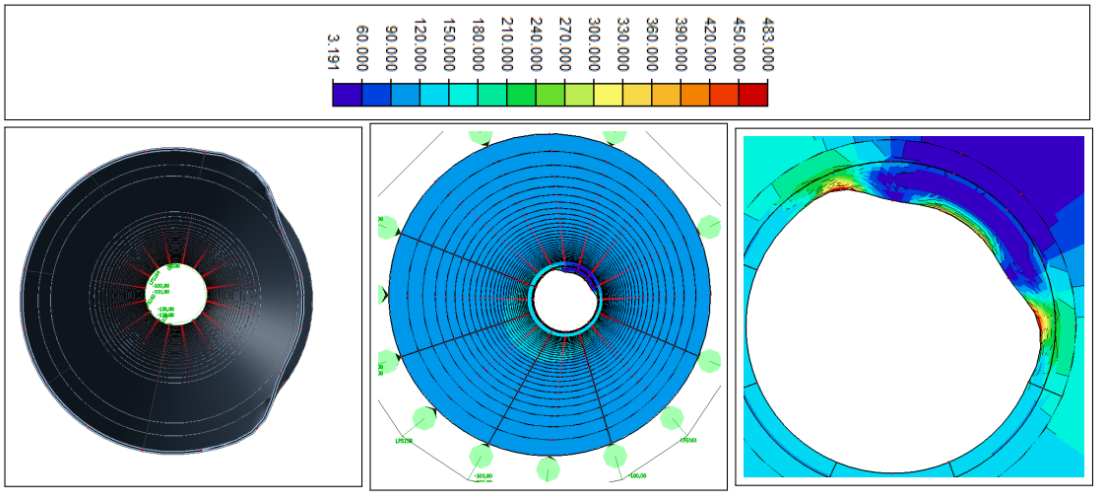

FIGURE C.19: Stress development in the pile, retrieved from SCIA

IR-11.99%

Figure C.20 depicts the stress development due to centric loading in the king pile. From left to right: bottom view in perspective of king pile, a top view of stresses in a pile, top view *extra* zoom in perspective.

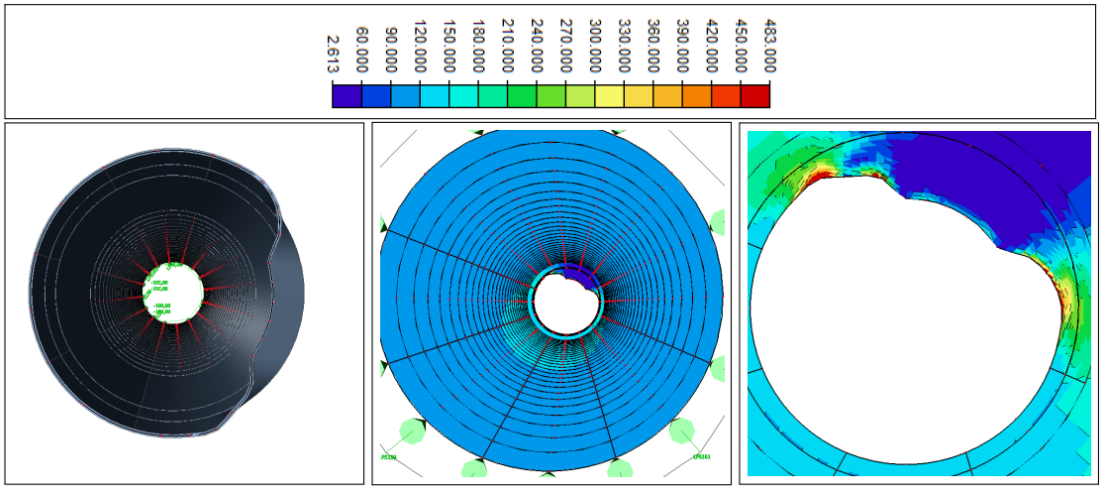

FIGURE C.20: Stress development in the pile, retrieved from SCIA

Deformation

Figure C.21 shows the deformations in the king pile, for aforementioned Imperfection Ratio (IR), for centric loading.

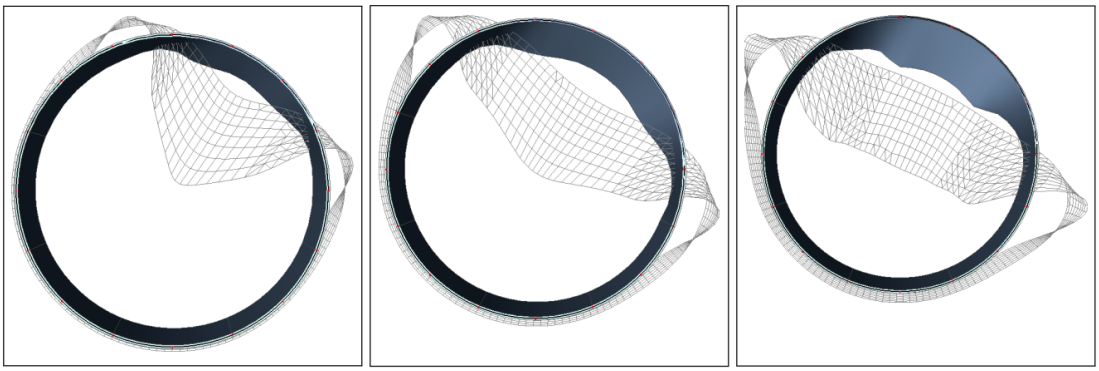

FIGURE C.21: Deformation in perspective, left to right: IR-3%, IR-8%, IR-12%, retrieved from SCIA

C.8.2 Symmetrical case

IR-7.05%

Figure C.22 depicts the stress development due to centric loading in the king pile. From left to right: bottom view in perspective of king pile, a top view of stresses in a pile, top view *extra* zoom in perspective.

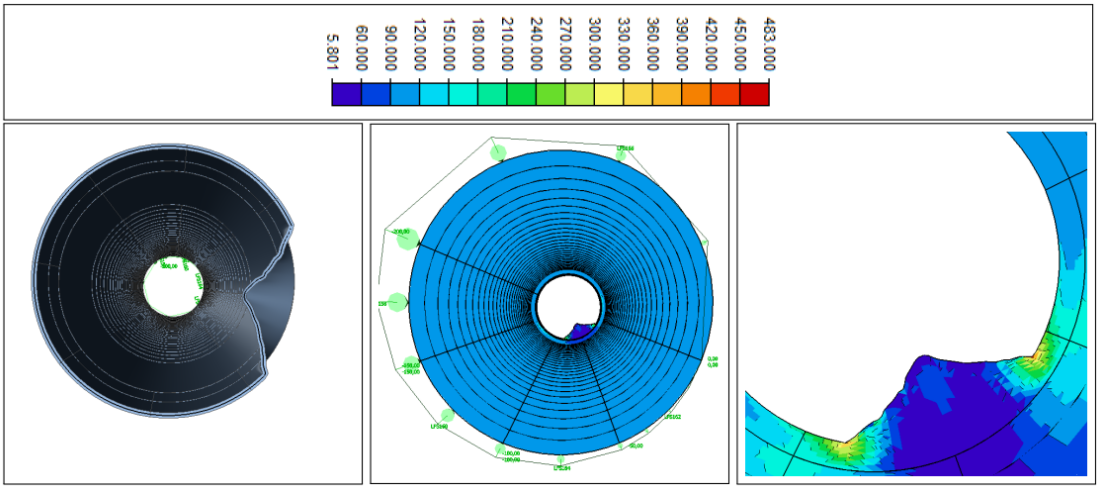

FIGURE C.22: Stress development in the pile, retrieved from SCIA

IR-14.11%

Figure C.23 depicts the stress development due to centric loading in the king pile. From left to right: bottom view in perspective of king pile, a top view of stresses in a pile, top view *extra* zoom in perspective.

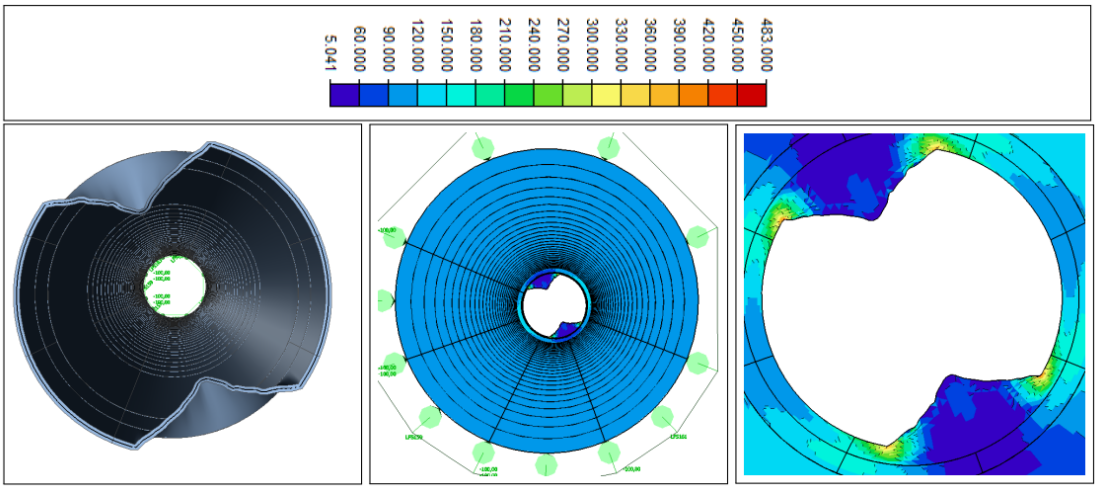

FIGURE C.23: Stress development in the pile, retrieved from SCIA

IR-14.11%

Figure C.24 depicts the stress development due to centric loading in the king pile. From left to right: bottom view in perspective of king pile, a top view of stresses in a pile, top view *extra* zoom in perspective.

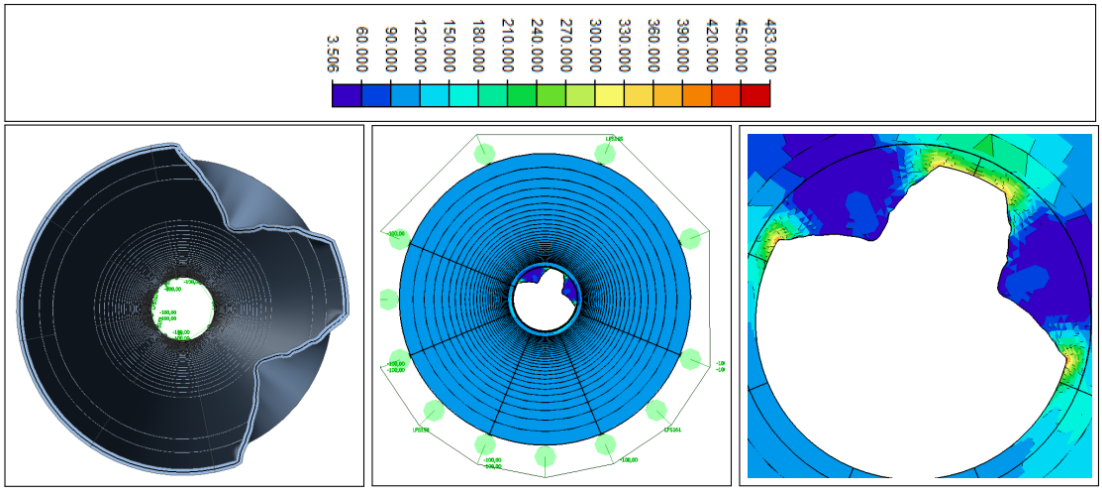

FIGURE C.24: Stress development in the pile, retrieved from SCIA

Deformation

Figure C.25 shows the deformations in the king pile, for aforementioned IRs, for centric loading.

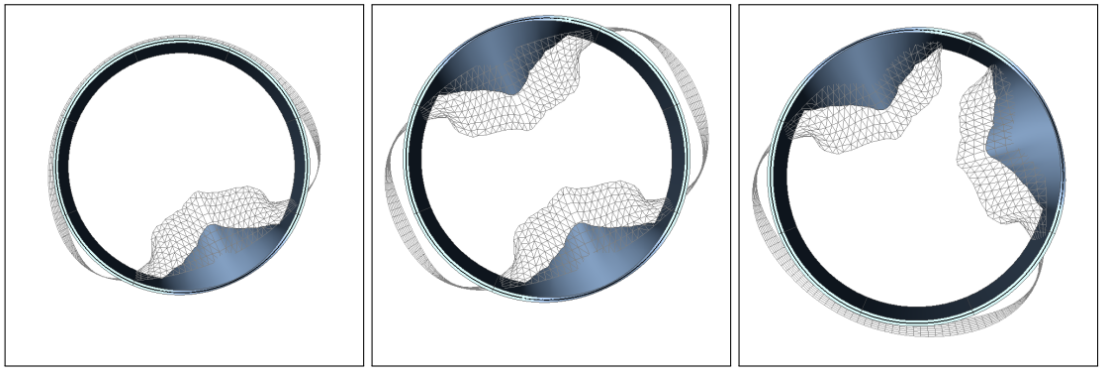

FIGURE C.25: Deformation in perspective, left to right: IR-7.05%, IR-14.11%, IR-14.11%, retrieved from SCIA

C.8.3 Extreme case

IR-21.17%

Figure C.26 depicts the stress development due to centric loading in the king pile. From left to right: bottom view in perspective of king pile, a top view of stresses in a pile, top view *extra* zoom in perspective.

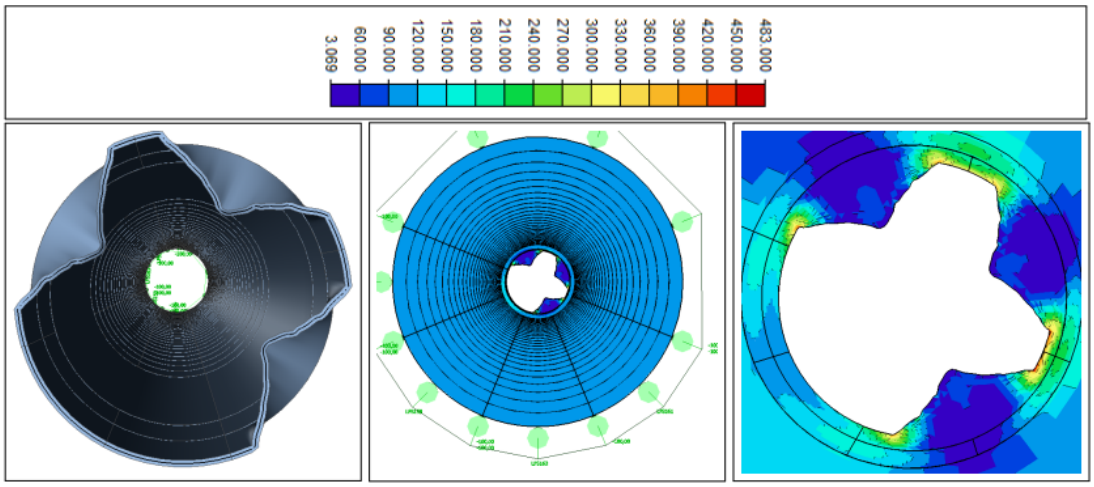

FIGURE C.26: Stress development in the pile, retrieved from SCIA

IR-50%

Figure C.27 depicts the stress development due to centric loading in the king pile. From left to right: bottom view in perspective of king pile, a top view of stresses in a pile, top view *extra* zoom in perspective.

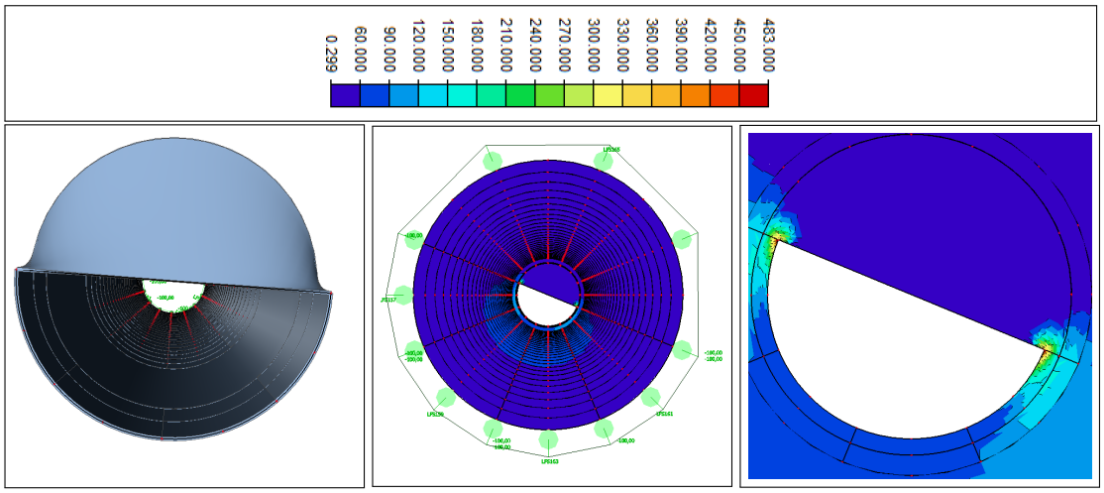

FIGURE C.27: Stress development in the pile, retrieved from SCIA

IR-28.23%

Figure C.28 depicts the stress development due to centric loading in the king pile. From left to right: bottom view in perspective of king pile, a top view of stresses in a pile, top view *extra* zoom in perspective.

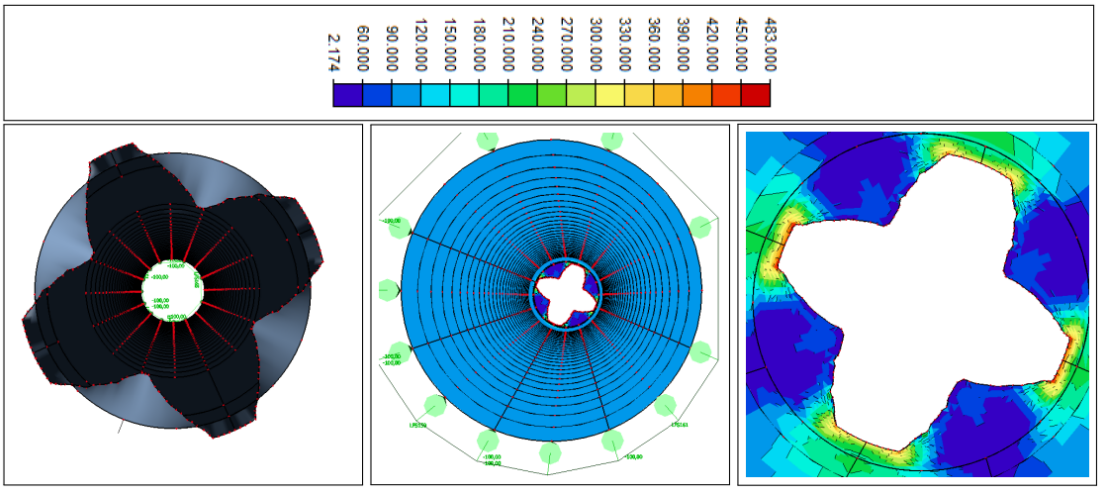

FIGURE C.28: Stress development in the pile, retrieved from SCIA

Deformations

Figure C.29 shows the deformations in the king pile, for aforementioned IRs, for centric loading.

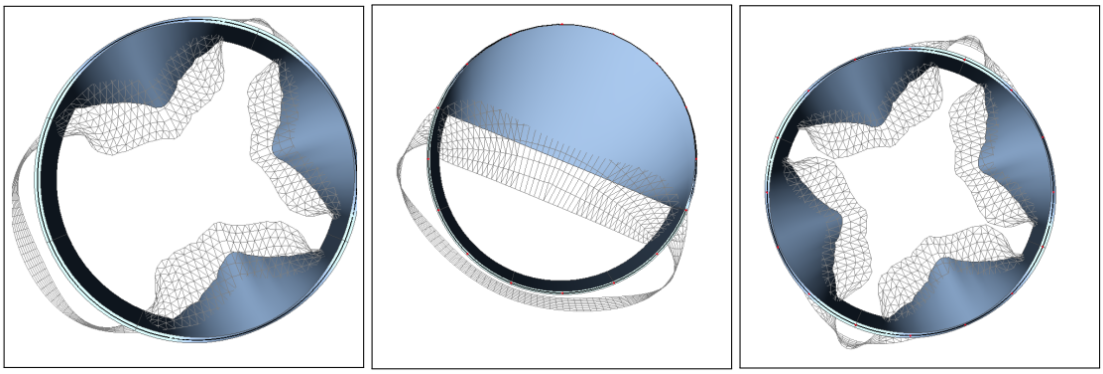

FIGURE C.29: Deformation in perspective, left to right: IR-21.17%, IR-50%, IR-28.23%, retrieved from SCIA

Appendix D

Cost and revenue results

D.1 Introduction

Appendix D explains the calculations carried out for the post-piling phase. The calculation of revenues, for both Port Dues (PD) and Leasing Contract (LC) are explained. In this fashion, a total number of vessels utilizing the harbor in the year 2014 is used. Furthermore, the storage area taken into account as well as its leasing price per square meter are calculated. Finally, per scenario, the increase in cost per Percentage Problematic Section (PPS), the reduction in revenues per PPS, as well as the reduction in Net Present Value (NPV) per PPS are presented. The latter helps to select one solution over the other in the decision model.

D.1.1 Scenario replacement

The quay wall could partially, at its Problematic Section (PS), be replaced. It is assumed that these sections are traceable and could be demolished and rebuild. However, the demolition takes a considerable time, and therefore, the entire quay wall is not operational during the reconstruction phase, even though only some sections undergo such reconstruction. The rebuilding of the sections is necessary to sustain the quay wall's designed performance level.

D.1.2 Scenario early maintenance

Early Maintenance (EM) refers to extra maintenance necessary at PS, given those sections are traceable, to keep the quay wall operational **at its designed capacity**. However, the extra maintenance is assumed to take a longer period in which the PS of the quay wall is not operational. Therefore, the quay wall is divided into two parts defined as PS and Other Section (OS). If PS occurs, EM must be carried out. When OS occurs Regular Maintenance (RM) is required. The disruption in the operation of the quay wall due RM is assumed to be negligible.

D.1.3 Scenario reduction of storage capacity

Another scenario is to implement a reduction in designed capacity at PS. Therefore, when Port of Rotterdam Authority (PORA) implements Capacity Reduction (CR), the consequences of piling disease are reduced. However, it could also be chosen to alternate to store a lighter dry bulk cargo at the PS.

D.2 Amazonehaven quay wall

Amazonehaven is located at MaasVlakte I (MVI), as shown in Figure D.1. The 900 [m] quay wall is divided into three parts with slightly a different storage capacity. The parts are shown in colors, to distinguish its storage capacity and some sections each part concludes. In chapter 4 it was concluded that the PS are sections: 9, 18 and 19. All these sections are in **Part 2**.

FIGURE D.1: Aerial photo Amazonehaven quay wall, retrieved from Google maps

Table D.1 shows an overview of the actions to be taken, to counteract the consequences of the piling disease when *piling risk event* occurs.

TABLE D.1: Actions to be undertaken per scenario

	Part 1		Part 2		Part 3	
Scenario	**PS**	**OS**	**PS**	**OS**	**PS**	**OS**
Full Capacity	-	Regular Maintenance	-	RM	-	RM
Replacement-**b**efore	-	RM	Early Maintennace	RM	-	RM
Replacement-**a**fter	-	RM	Demolition. RM	RM	-	RM
Early Maintenance	-	RM	EM	RM	-	RM
Capacity Reduction	-	RM	Capacity Reduction. RM	RM	-	RM

D.3 Cost of Amazonehaven

Sub-Figure (A) D.2 depicts the storage capacity per section per implemented scenario. In this fashion, Capacity Reduction (CR) is implemented only at Problematic Section (PS) which is section 9, 18 and 19. Therefore, a drop in storage capacity is visible. Furthermore, the three parts as depicted in Figure 8.6, include a different amount of storage which explains the drop and leap between the parts. It also shows that the storage capacity has a smaller value in PS when chosen for Early Maintenance (EM)-scenario.

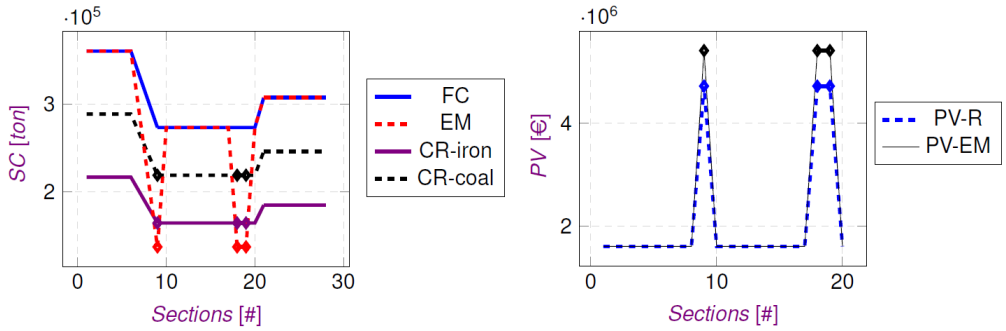

(A) **S**torage **C**apacity dry bulk, three PS

(B) **P**resent **V**alue of quay wall, three PS

FIGURE D.2: (A) SC per section and (B) PV per section, given three PS

Sub-Figure (B) D.2 shows the increase in PV due utilizing one of the scenarios of Replacement (R) or EM. Bear in mind, that the third scenario of CR does not lead to cost increase. Again, it is assumed that only sections 9, 18 and 19 are identified as PS. It also shows that the cost-increase due EM are higher than due R, in the PS.

D.4 Revenues of Amazonehaven

Revenues of Amazonehaven are two folded. First, the earnings due Leasing Contract (LC), leasing land to companies. Second, Port Dues (PD) due vessels entering the harbor, using the facilities, mooring, etc. The sea-PD are calculated as follow, due to lack of information of number of vessels mooring at Amazonehaven,

> the total amount of the dry bulk is fitted to the DWT[1]-class of the vessels entering the Port of Rotterdam (POR).

The PD are among other variables dependent on the DWT-class of the vessels. After which, the sea-PD are calculated based on a five-step calculation used by Port of Rotterdam Authority (PORA). In this calculation, based on 2014, only the inflation is taken into account. However, for LC-calculation, both inflation and a yearly increase in leasing price is taken into account, due to availability of information.

D.4.1 Deep sea vessels

4% of all vessels are bulk carriers. According sub-Figure (A) D.3, the total number of dry bulk carriers is 450 and 401 for respectively iron ore and coal transshipment, based on data from 2014. Sub-Figure (B) D.3 reveals information about the amount of dry bulk cargo.

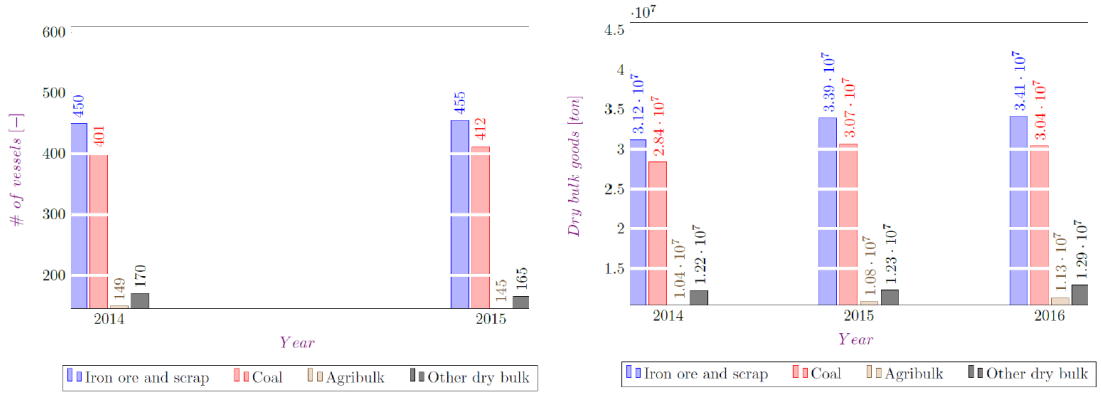

(A) Total number of vessels

(B) Cargo dry bulk vessels

FIGURE D.3: (A) Number of dry bulk vessels and their type, (B) amount of dry bulk, retrieved from [46]

The total number of vessels carrying dry bulk per DWT-class is given in Table A.10, in appendix A, based on 2014 and 2015. However, specific information for dry bulk vessels carrying iron ore or coal is not retrievable. Furthermore, specific information of mooring vessels to Amazonehaven is not retrievable. Therefore, in the first step, the sea-PD are calculated for the entire POR.

In total 9 different types of vessels, are entering the harbor of Rotterdam. The DWT-class as provided has a wide range, whereas the *true-DWT-class* refers to the one as used in the calculations.

[1] Dead Weight Tonnage

Calculation seaport dues

The idea behind calculation of the sea-PD is to consider the entire revenues for the total number of *dry bulk vessels*. After which the number of vessels needed for the amount of dry bulk which could be stored in Amazonehaven (Part 1-Part 2-Part 3) are calculated. In this regard, following conditions must be fulfilled:

$$\sum T_i \cdot \rho_{db-i} \cdot N_i = T_{amount-cargo} \quad [ton] \quad \text{(D.1)}$$

$$\sum N_i \leq T_{\#-vessels} \quad [\#] \quad \text{(D.2)}$$

Formula D.1 must be equal to total amount of cargo, where T_i is the DWT-class of the vessel and ρ_{db-i}, N_i are respectively the tonnage dry bulk the vessel could carry and the number of vessels of that specific DWT-class. Formula D.2 is the condition, in which the N_i per DWT-class should not exceed the numbers as stated in Table A.10. In other words, the vessel must be an existing type, and the number of that specific vessel must be according to the records of PORA.

By using the boundary conditions above, formula D.1-D.2, the exact number of vessel and its type is calculated for Amazonehaven. The PD to be received by PORA is presented, according PORA's calculations, in Table A.11. Finally, the PD per type of vessel is calculated as shown in Table D.2.

TABLE D.2: Specific information of various types of dry bulk vessels, based on calculation of [46]

Steps	Formula	vessel T_3	vessel T_4	vessel T_5	vessel T_7	vessel T_1
Step II	$\gamma_{bt} \cdot D_{bt}$ [€]	17430	21304	27114	65847	3486
Step III	$D_{bt} \cdot \gamma \cdot \mu_{db} \cdot 0.01$ [€]	37908	46332	58968	143207	7582
Step IV-1	$\zeta \cdot \mu_{odb}$ [€]	4880	5964	7591	18436	976
Step IV-2	$\mu_{db} \cdot \rho_{db}$ [€]	21960	21960	21960	21960	4392
Step V	IV-1+ IV-2 [€]	26840	27925	29551	40396	5368
Step VI	II+ min(III V) [€]	44270	49228	56665	106243	8854

It is, however, evident that this method, using the boundary conditions, could have different results as the conditions could be fulfilled in many ways. Bear in mind, that the calculation of revenues due a total number of vessels entering the Amazonehaven is based on information of 2014. Furthermore, the number of vessels is kept constant throughout 1989-2038, and only inflation is taken into, see appendix A.

D.4.2 Leasing land

The second significant revenues for PORA is to lease the land to companies established in the area. Table D.3 reveals information about the characteristics of three parts as identified in Amazonehaven, such as its length, width and surface area. The storage capacity is also shown per part.

TABLE D.3: Specification of storage area in Amazonehaven, retrieved from Google maps

Parts	Surface area [m^2]	Length [m]	Width [m]	Load [$\frac{kN}{m^2}$]	Storage capacity [ton]	sections
Part 1	66000	270	244	328	2.17E+07	1 tot 6
Part 2	100000	540	185	328	3.28E+07	9 tot 20
Part 3	75000	360	208	328	2.46E+07	21 tot 27

Calculation leasing contracts

Table D.4 reveals the calculation of revenues due to leasing land, for Amazonehaven area, based on 2014. In this calculation, the leasing area is kept constant according to information available in 2016. Therefore, the leasing price is about 5.52 [$\frac{€}{m^2}$] and for the entire area of Amazonehaven brings a revenue of about € 1.33 million, when the sections are fully utilized.

TABLE D.4: Specification of maximum revenue per LC in Amazonehaven, FC scenario, retrieved from [46]

Year 2014	Iron ore [ton]	Coal [ton]	Percent [%]	Surface area [m^2]	Leasing [$\frac{€}{m^2}$]	lc [€]
FC	7.92E+06	7.92E+06	100%	241000	5.52	1.33E+06

However, given PS, compensation is taken into account for the companies regarding *not fully* functioning of the quay wall. Therefore, the companies pay a percentage of the full amount per square meter. A not fully functioning quay wall leads to Loss of Earnings (LOE) for PORA.

D.4.3 Calculation of NPV

Net Present Value (NPV) is a summation of costs and revenues. Sub-Figure (A) D.4 shows a yearly growth of Leasing Contract (LC) per square meters, expressed in a linear line. Following this linear line means that in 1989, the revenues due LC are negative. Therefore, it is assumed that the revenues are kept at 2 [$\frac{€}{m^2}$] if the values are smaller than that value. Sub-Figure (B) D.4 shows the fluctuations due inflation from 2000-2038 for both Port Dues (PD) and LC, as used in the calculations.

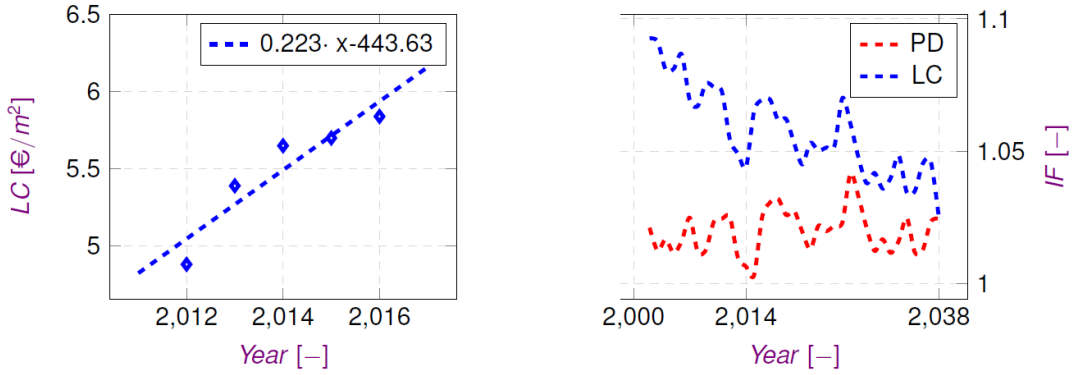

(A) Increase in LC

(B) Inflation Factor PD & LC

FIGURE D.4: Left:LC revenues and Right: inflation, retrieved from [26]

Linear growth is only taken into account for LC due to available information. However, the storage area is kept constant. In case of PD, there is no linear growth. In the calculation of PD, the storage area is kept constant as well as the number of vessels. After which, the revenues due PD are calculated for the years before 2014 and coming years after 2014, based on 2014. A drawback is that, e.g., some DWT-class of vessels as used in the calculations could not be used in 1989 because those vessels did not exist back then.

D.4.4 Facts and figures

Table D.5, shows the amount of Present Value (PV) based on formula 2.1 or Amazonehaven (documentation), for both iron ore and coal. Furthermore, the amount of revenues per PD or LC, for both iron ore and coal are given. Finally, the summation of both PV and revenues leads to NPV, which is based on formula 2.1 or Amazonehaven (documentation), for both iron ore and coal. Therefore, when the full capacity of the Amazonehaven is used, a NPV of € 363 *million* is expected, for both iron ore and coal.

TABLE D.5: Comparison of $NPV = PV + R$ values based on formula 2.1 and Amazonehaven (documentation) [39]

based on [2014]	**PV**		**Revenues**		**NPV**	
-	formula 2.1	Amazonehaven	PD	LC	formula 2.1	Amazonehaven
FC-iron [€]	3.20E+07	3.05E+07	3.26E+08	6.88E+07	3.63E+08	3.64E+08
FC-coal [€]	3.20E+07	3.05E+07	3.26E+08	6.88E+07	3.63E+08	3.65E+08

D.4.5 LOE per scenario

Figure D.5 shows the Net Present Value (NPV) for storage of iron ore and coal as calculated for a period of 50 years, 1989-2038, for different scenarios for increasing Percentage Problematic Section (PPS). It shows that when full capacity of the quay wall is utilized, 0% PPS, the NPV has an amount of € 361 *million*, given the entire period of 1989-2038.

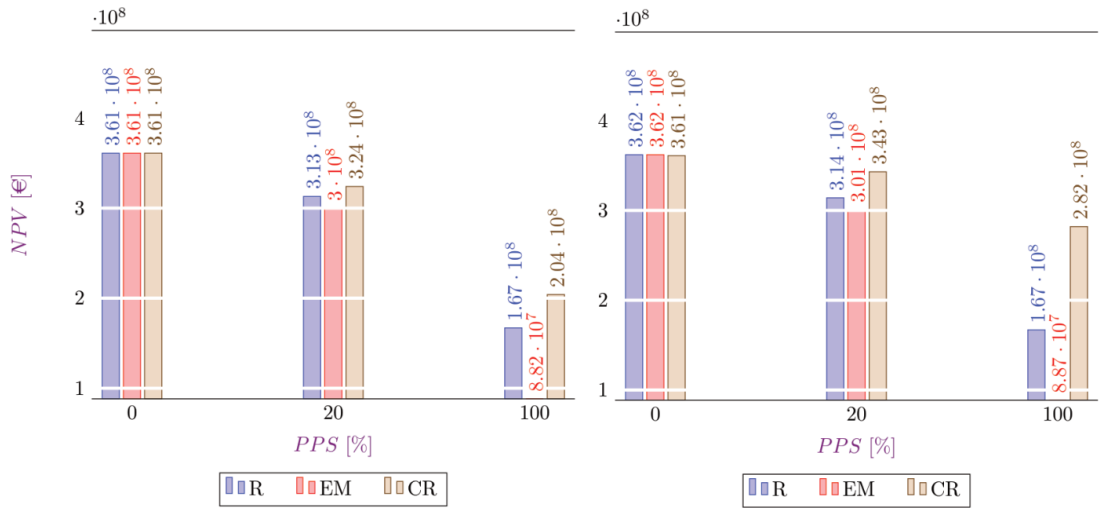

(A) **N**et **P**resent **V**alue, Iron ore

(B) **N**et **P**resent **V**alue, Coal

FIGURE D.5: NPV due increasing PPS of the quay wall, based on formula 2.1

Furthermore, given a PPS of 20%, the best option is to select for the Capacity Reduction (CR) scenario to acquire the highest value for the NPV. It also remains the best solution, given a 100% of PPS. Furthermore, comparing the NPV of iron ore and coal, the revenues increased by 38%, $\frac{2.82}{2.04}$, when altering from a heavy material to a light material, given a 100% PPS.

D.5 Stakeholders

The stakeholders in Port of Rotterdam (POR), are defined based on the functions assigned to quay walls in the area. Figure D.6 shows the storage function per area for the entire port. The functions are: containers, dry bulk, refinery, wet bulk, distributions spots and other activities. The Amazonehaven quay wall is mainly home to containers, dry bulk, and refinery. A total number of 17 locations are used to store dry bulk goods over the entire harbor.

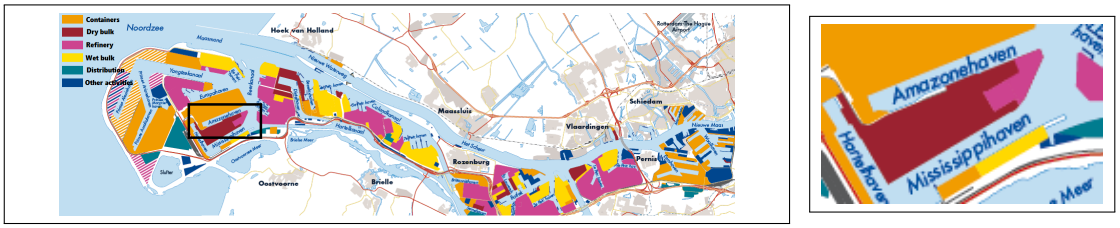

FIGURE D.6: Port of Rotterdam and its functions, retrieved from [46]

In Research into Pile Toe Failure in Amazonehaven (RIPTFIA), instead of fitting the right number of vessels and the correct type of vessels to each area, the revenues due Port Dues (PD) given the entire number of dry bulk vessels were calculated. After which, the revenues were multiplied by a reduction factor, $\frac{PD_{total}}{PD_{Amazonehaven}}$. Where, PD_{total} refers to total revenues for a total number of **dry bulk vessels**, whereas $PD_{Amazonehaven}$ refers to a total number of vessels using the Amazonehaven basin. In this fashion, the $PD_{Amazonehaven} = PD_{total} \cdot \frac{A_{Amazonehaven}}{A_{total}}$, whereas $A_{Amazonehaven}$ is the three storage parts available in Amazonehaven and A_{total} is the total storage area for dry bulk available in the entire POR.

Appendix E

Extended summary

E.1 Introduction

Research into Pile Toe Failure in Amazonehaven (RIPTFIA) focuses on the causes of *pile toe failure* of primary king piles. It also studies the Management Aspect (MA) of the *pile toe failure*. In other words, the environment around *the failure*.

The quay wall consists of a combined wall system and a system of foundation elements. King piles are primary elements within the combined wall system, which function as bearing and retaining elements [19]. The quay wall of Amazonehaven consisted of twenty sections with a length of 45 [m] [48]. After recent removal of the quay wall, due to new safety regulations imposed by Port of Rotterdam Authority (PORA), it was observed that up to 20% of the piles were severely damaged close to pile toe [37]. Figure E.1 depicts significance damage to primary king piles, in one section.

FIGURE E.1: Pile toe failure in Amazonehaven in **one** section, retrieved from [6]

E.2 Problem description

The Amazonehaven quay wall structure was designed based on the static load, EAU[1] regulations [48]. The static load, permanent and variable structural load, is transferred via the quay wall's foundation elements to deep soil layer with enough bearing capacity. The occurrence of *pile toe failure* described as a *piling disease* if not cured will cause troublesome impact driving. In other words, regardless *pile toe failure* consequences during the technical lifetime of the asset, regarding its stability, etc.; it will also negatively affect the driveability, blow count, driving

[1] Empfehlungen des Arbeitsaussschusses Ufereinfassungen (EAU)

time, etc. during installation. Therefore, *pile toe failure* will manifest itself in financial burden to both client and contractor in the short- and long- run.

E.2.1 Hypothesis

The occurrence of *pile toe failure* in Amazonehaven, given static-based design, raises the following hypothesis:

> Hammer-induced driving stresses are extremely high close to pile toe, exceeding material's yield stress which clarifies *extreme folding damage*.

E.3 Scope

The main loads acting on the king piles are; (a) static load to be transferred to the subsoil during the asset's technical lifetime, (b) dynamic load to bring the king pile up to its designed depth. The latter happens partly by vibratory hammers and partly by impact hammers. RIPTFIA focuses on studying the dynamic load on the king pile because of: (1) uniaxial direction of the *extreme folding damage* close to pile toe which points out piling to be funest to maintain *pile toe integrity*, (2) pile dimensioning was based on static load and yet *pile toe failure* have had occurred, (3) the design of the quay wall was **strategically** based on a higher static load than it would have occurred (intended to be used), yet, *pile toe failure* have had occurred.

Furthermore, the research is divided into two parts of technical- and management- part. In the first part, the causes of *pile toe failure* within the hammer-pile-soil system are studied. In the second part, the remedies to either prevent *the pile toe failure* or to cope with its consequences when *pile toe failure* occurs are outlined. The second part also includes a decision model to select the economic solution to counteract the consequences of *piling disease*.

E.4 Results

The results of the research are divided into technical part and management part. The technical part of the research studies the reasons of *pile toe failure* in a hammer-pile-soil system, to undermine the leading causes of *the failure* in Amazonehaven.

The central question is:

- What are the causes of *pile toe failure* in Amazonehaven?

The management part studies the environment around the *pile toe failure*. It introduces *piling risk event* and the occurrence of *the failure* as a *piling disease*. Therefore, conventional as well as creative remedies are recommended to be implemented in the current procedures in the piling industry. The remedies cover both pre-piling and post-piling phase as well as its financial consequences.

The central question is:

- What are the remedies to prevent *pile toe failure*?

E.4.1 Technical part

Analysis of the hypothesis

The stress development along the pile in a hammer-pile-soil system is studied to investigate the earlier mentioned hypothesis. The prediction program[2] enables studying pile driveability. The program uses wave equation theory taking into account the hammer-pile-soil interaction. Therefore, the magnitude of driving stresses, stress development along the pile as well as the number

[2] Pile Driving Prediction (PDP)

of blows to bring the pile to the designed depth, are the outputs necessary for this research. It is shown that given the Standard to Normal Soil Condition (SNSC) of Amazonehaven described as a not too dense sandy subsoil; the driving stresses are as high as about 210 [MPa], which is about 60% lower than the material's yield stress. Therefore, it could be concluded that hammer-induced driving stresses are not exceeding material's yield stress close to pile toe. In other words, given a SNSC, *the failure* has not been caused by the dynamic load. However, in case of a Medium to Hard Soil Condition (MHSC); it is shown that hammer-induced driving stresses are as high as above the value of material's yield stress.

Figure E.2 shows the characteristics for SNSC, given a D/t ratio of 83, where D is the diameter and t is the thickness.

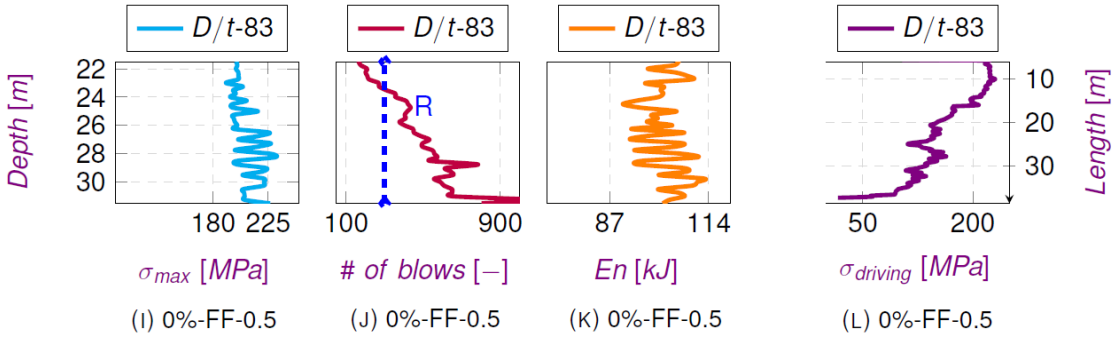

FIGURE E.2: Specifications of piling in SNSC, legend: D/t-83-Compaction-FF, retrieved from PDP

From left to right: Maximum driving stress per driving level, number of blows per driving level, transferred energy per driving level are given. At right, hammer-induced driving stresses along the pile are depicted for the driving level where the highest value of *maximum driving stress* occurs.

Figure E.3 shows the characteristics for MHSC, given a D/t ratio of 83, where D is the diameter and t is the thickness.

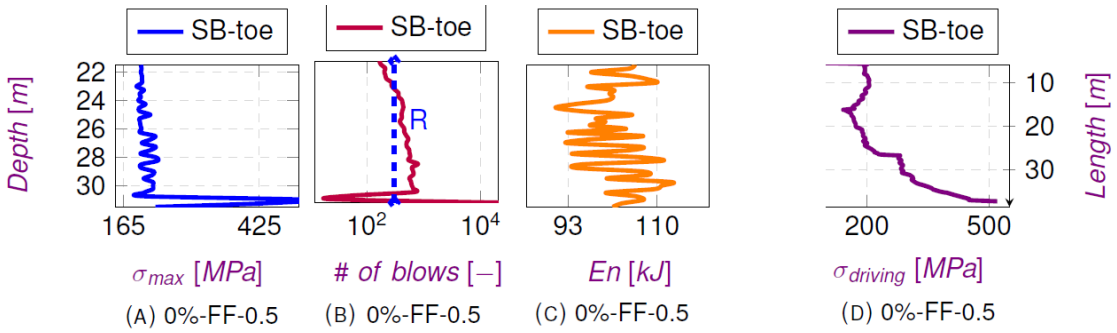

FIGURE E.3: Specifications of piling in MHSC, legend: D/t-83-Compaction-FF, retrieved from PDP

From left to right: Maximum driving stress per driving level, number of blows per driving level, transferred energy per driving level are given whereas at right; hammer-induced driving stresses along the pile are depicted for the driving level where the highest value of *maximum driving stress* occurs.

However, prior construction of the Amazonehaven (old) quay wall, a thorough soil investigation was carried out with both in-situ and drills [40]. The soil investigation did not show any presence of existence of Locally Extremely Hard Spot (LEHS). Therefore, the driving is believed to have occurred in a SNSC described as predominantly sandy subsoil that was not particularly dense. Therefore, the hypothesis is not valid in case of Amazonehaven.

Classifications of failure sources

The quest for causes of *pile toe failure* in Amazonehaven continues. In this regard, the causes to *pile toe failure* are pursued within the **dynamic**- **geometric**- and **geologic**- sources of failure. Figure E.4 shows an overview of the *failure sources* within the mentioned categories.

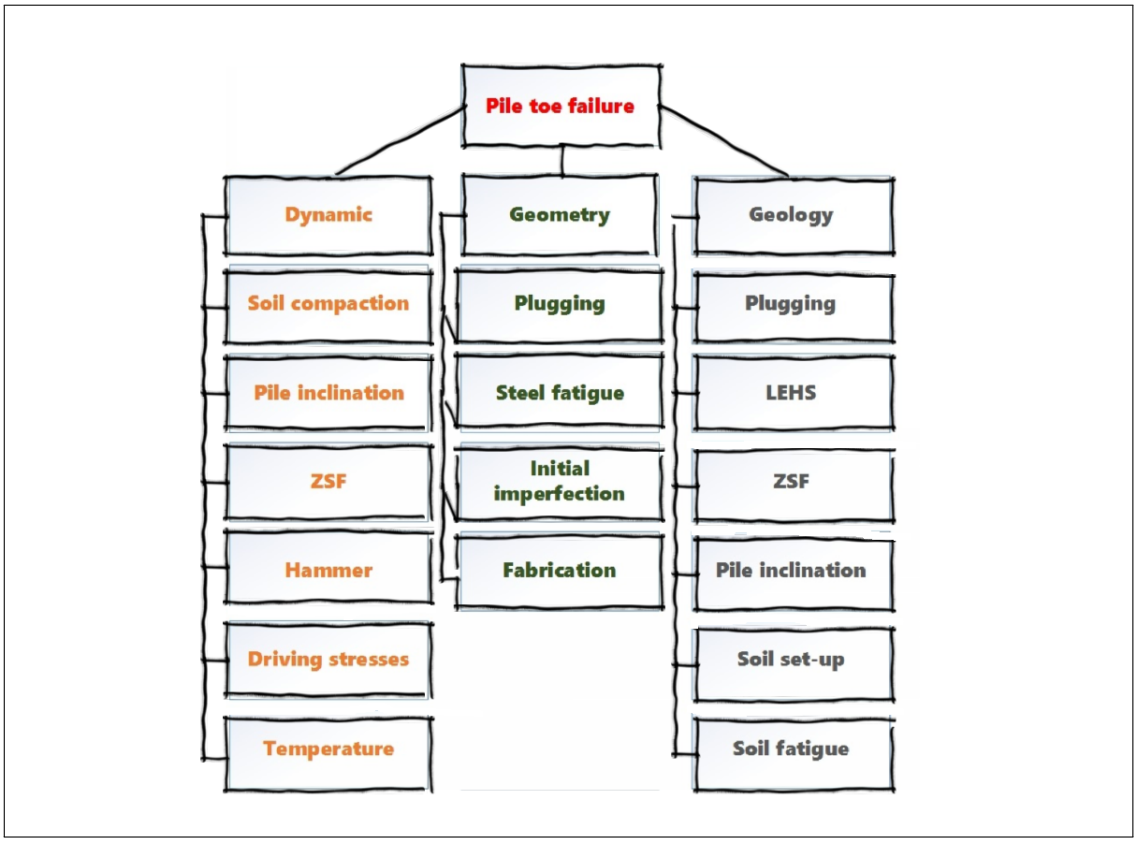

FIGURE E.4: Overview of *sources of failure* of pile toe

Where existence of Zero Shaft Friction (ZSF) and Locally Extremely Hard Spot (LEHS) is also studied. After studying the aforementioned, possible causes to *pile toe failure*, the main reasons to *pile toe failure* in Amazonehaven are discussed to be: **initial imperfection**, **pile inclination** and **temperature**.

Sensitivity analysis

The main objectives to study pile's behavior in SCIA[3], given a (static)load-pile-soil system, is to conduct a sensitivity analysis:

1. for the effect of pile imperfection (initial dent) which covers the **initial imperfection**
2. for the effect of non-uniform soil (stiff and weak) around the pile as well as at the toe, which covers the **pile inclination**
3. for the effect of eccentric impact hammering as well as centric impact hammering due to pile driving with an inclination, which covers the **pile inclination**
4. for the effect of a local Temperature Elevation (TE) in pile, which covers the **temperature**

The study introduces four terminologies essential to understand the results as briefly explained below:

[3]Finite Element Analysis (FEA) program

- Yield Stress Momentum (YSM) refers to the point where the pile locally reaches its material's yield stress due increasing (static) load
- Imperfection Ratio (IR) refers to existence of any initial dent, where $IR = 1$ is a perfectly rounded pile toe
- Homogeneity Ratio (HR) refers to existence of any non-uniform soil at pile toe, described as stiff and weak soil, where $HR = 1$ means a homogeneous (stiff) soil properties at pile toe
- TE refers to a local temperature increase due to generated high friction during piling

Sub-Figure (A-C) E.5 shows the YSM plotted against IR, HR and TE, for centric loading on the pile. Sub-Figure (D-E) E.5 shows the same for eccentric loading on the pile. As mentioned earlier, YSM or $\frac{q_{yielding}}{q_{initial}}$ is the point where the pile locally reaches its material's yield stress due increasing (static) load. The sooner, the segment has reached its material's yield stress, the more prone to *extreme folding damage* it is. In this fashion, the plastic behavior of the steel is taken into account.

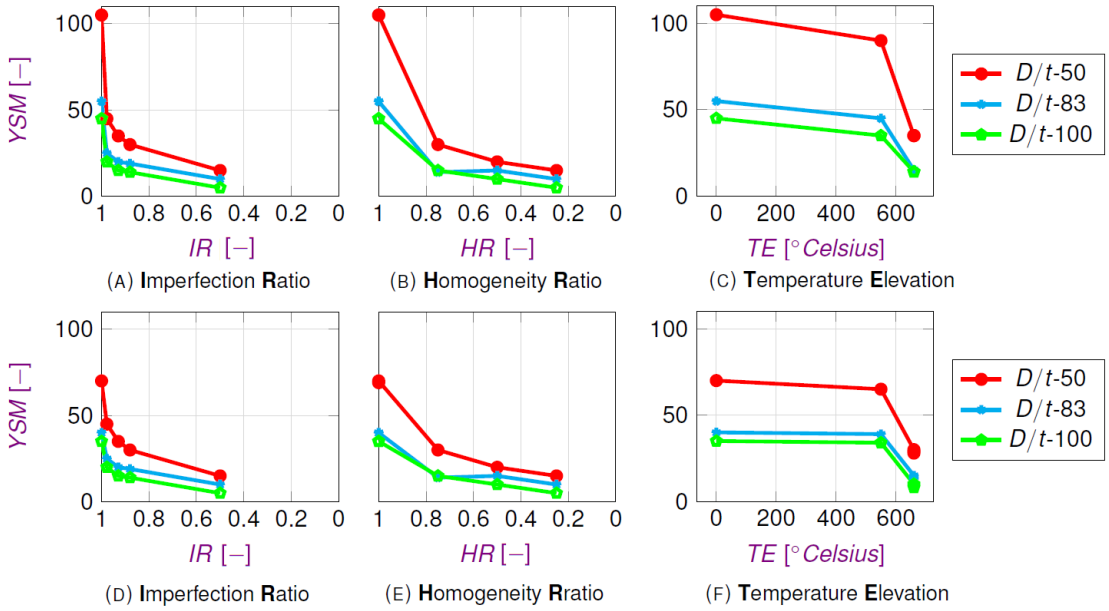

FIGURE E.5: YSM for centric loading (A)-(C) and eccentric loading (D)-(F), retrieved from SCIA

It is concluded that *pile toe failure* of Amazonehaven is most probably caused by (1) **initial imperfection**. The FEA study revealed that YSM is more sensitive to any initial imperfection. In this analysis, it is shown that the YSM regarding IR decreases more drastically compared to YSM regarding HR. YSM regarding TE has the lowest effect on the pile's behavior up to 500°, out of the three.

E.4.2 Management part

Moreover, if *the failure* does not endanger the stability of the entire quay wall; its consequences might force actions to be taken. These consequences could be manifested in, e.g., large settlements of the quay wall. In case of large settlements due *extreme folding damage*, of king piles close to toe; counteractions are required to be undertaken. Therefore, *extreme folding damage* must be introduced as a *piling risk event*. The risk could be avoided by reducing the risk's -probability or -consequences when the risk event occurs. To reduce the probability of the risk event, process-based alternatives are introduced, and extra costs must be considered. To reduce the consequences of the risk event, however, three primary actions could be taken: Replacement (R), Early Maintenance (EM), and Capacity Reduction (CR). Thus, either

the probability of the risk event is diminished before piling, or the consequences of the risk are reduced during the asset's technical lifetime. For the latter, a decision-model is introduced based on the Net Present Value (NPV) per scenario per increasing Percentage Problematic Section (PPS). In this way, the Loss of Earnings (LOE) for Port of Rotterdam (POR) are calculated due *pile toe failure*, given that *the failure* could force the authorities to take actions.

Piling risk event

The occurrence of *extreme folding damage*, given piles with high D/t ratio must be avoided to warrant the functioning of the quay wall during its technical lifetime. Therefore, acknowledging the *piling risk event* gives the opportunity to discuss remedies to this *piling disease*. Bear in mind that when *piling disease* is not treated appropriately, it will lead to *heavy piling* during installation as well as its probable consequences during asset's technical lifetime. Therefore, remedies are to be found within two phases of (1) pre-piling and (2) post-piling. Pre-piling phase refers to procedures before installation as well as installation activity. The latter, post-piling, refers to the entire phase of asset's technical lifetime.

Pre-piling remedies

The management aspects of the *pile toe failure* adds a 4^{th} dimension to dynamic-, geometric- and geologic- *failure sources* of Amazonehaven. The management aspects study the procedures prior piling as well as piling activity. In this fashion, solutions are contrived for king piles from its starting point to its destination. The three categories are (1) data collection, (2) pre-installation and (3) installation. The main process-based alternatives are:

Data collection

- Sufficient soil investigation
- Utilizing a piling prediction program
- Carrying out pile tests
- Carrying out back-analysis to fit prediction to measurements
- Selecting a correct impact hammer

Pre-installation

- Utilizing Just in Time (JIT) (delivery) system for king piles
- Using Azobé cover to protect pile head and pile toe during storage/transport/uplifting
- Executing with care and precision during uplifting/transport

Installation

- Utilizing stiffening rings at pile toe, jetting during piling
- Drilling before piling [58]
- In situ checks of Out of Roundness (OOR) of the pile toe
- Executing with care and precision during installation
- Using a monitoring system to warrant *pile toe integrity* during piling
- Using driving procedure

Post-piling remedies

Post-piling remedies are to reduce the consequences of *pile toe failure*, which might manifest itself in locally large settlements as well as stability issues regarding the entire structure. *Stability research* has shown that due to *pile toe failure*: (1) the soil displacement increases by a factor 3, (2) the moment on the combined wall increases by a factor 1.8 and (3) the anchor force reduces by a factor 0.4 [37]. Furthermore, it is observed, during the technical lifetime of the (old) quay wall, that due overloading one of the twenty sections has settled about 50 [mm] [40]. Therefore, **assuming** that *pile toe failure* both: (a) negatively affects the structure during its technical lifetime, and (b) the Problematic Section (PS) with a high frequency of *pile toe failure* are traceable; a decision model could be presented to Port of Rotterdam Authority (PORA). The decision model, based on NPV, provides a platform to select the most economical remedy between scenarios mentioned above. The NPV is calculated per scenario per increasing PPS as depicted in Figure E.6.

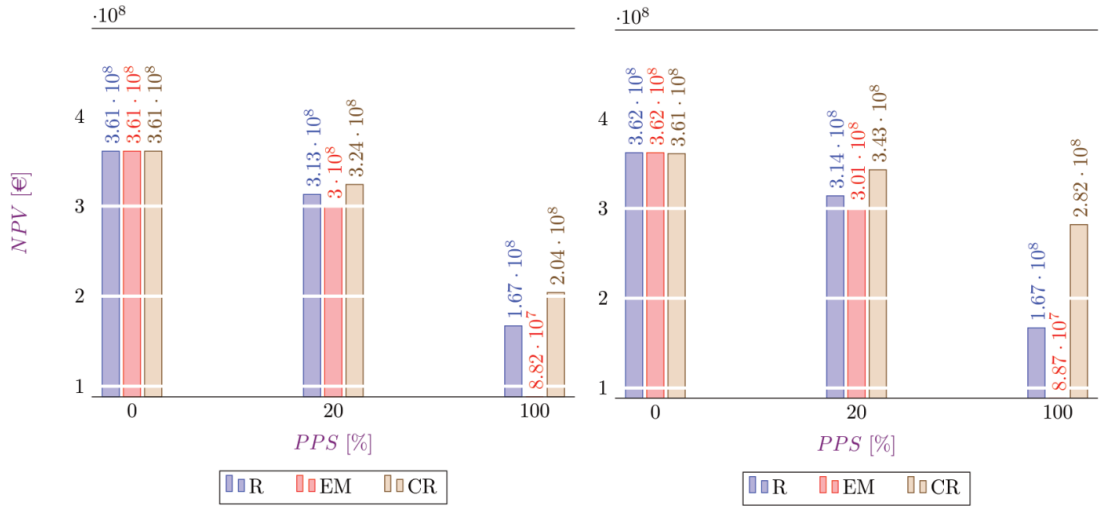

(A) **N**et **P**resent **V**alue, Iron ore

(B) **N**et **P**resent **V**alue, Coal

FIGURE E.6: NPV due increasing PPS per scenario, based on formula 2.1

Therefore, the consequences of *pile toe failure* manifest itself in revenue reduction and cost-increase if chosen for one or another scenario. The most economical option remains implementation of Capacity Reduction (CR), for the Problematic Section (PS). Furthermore, comparing sub-Figure (A) E.6 to sub-Figure (B), it is more economical to change the storage function of the quay wall, heavy storage to light, to reduce the Loss of Earnings (LOE) due *pile toe failure*.

E.5 Conclusions

The main conclusions are:

- hammer-induced driving stresses are lower than material's yield stress, and are not the leading cause of *extreme folding damage*.
- *extreme folding damage* is shown to be caused by **pile imperfection**, **pile inclination** and **pile inhomogeneous strength**, The leading cause is shown to be **pile imperfection** which refers to initial dent at pile toe to be worsened during piling.
- *piling disease* is to be prevented in pre-piling phase, while it has minimum financial consequences.
- the consequences of *piling disease* could be reduced in post-piling phase, while it has maximum financial consequences.

E.6 Recommendations

The main recommendations are:

- match the prediction results to (pile) driving analysis carried out in 1990. Research into Pile Toe Failure in Amazonehaven (RIPTFIA) showed that pile-advancement is to be troublesome at the last meters of driving, exceeding the threshold-value, given a virgin soil.
- study the combination of the three leading causes to *pile toe failure* as presented.
- study the development of *pile toe failure*, in a dynamic concept, given the scenarios (1) Standard to Normal Soil Condition (SNSC) for virgin and compacted soil if pile has no initial dent, (2) SNSC and Medium to Hard Soil Condition (MHSC) if pile has an initial dent.
- research creative solutions to *piling disease* in pre-piling phase.

References

[1] API. *Recommended practice for planning, designing and constructing fixed offshore platforms - working stress design*. Washington, DC 20005: -, 1993.

[2] Autodesk. *Finite Element Analysis*. Nov. 2016. URL: http://www.autodesk.com/solutions/finite-element-analysis.

[3] *Betonverhardingen*. Dutch.

[4] E. Broos and J.G. de Gijt. "The demolishing of the EMO quay wall in the Amazonehaven". In: *Port of Rotterdam* (2014).

[5] E.J. Broos and J.G. de Gijt. "Creating access for ultra large container ship to each berth in Rotterdam, Maasvlakte 2 and widening the Amazonehaven".

[6] E.J. Broos, R. Sibbes, and J.G. de Gijt. "Widening a harbor basin, demolition of a deep sea quay wall in Rotterdam".

[7] CUR166. *Retaining walls*. June 2016. URL: https://www.sbrcurnet.nl/producten/publicaties/damwandconstructies.

[8] CUR211. *Quay walls*. June 2016. URL: http://www.sbrcurnet.nl/producten/publicaties/handbook-quay-walls.

[9] A. Davies, D. Gann, and T. Douglas. "Innovation in megaprojects: systems integration at London Heathrow Terminal 5". In: *California management review* 51.2 (2009), pp. 101–125.

[10] M. van Delft. *Stress wave theory*. Allnamics. 2016.

[11] DIANA. *DIANA FEA*. Nov. 2016. URL: http://dianafea.com/content/DIANA.

[12] ECT. *About the ECT*. Aug. 2017. URL: http://www.ect.nl/en/content/about-ect.

[13] L. Everaert. "Experimenteel onderzoek naar plugvorming bij open buispalen voor de bepaling van het draagvermogen, The response of a plug in an open-toe pipe pile". Dutch. Delft University of Technology, 2010.

[14] A. Feddema. *Ontwerpbasis Geotechniek*. Dutch. 2016.

[15] B.H. Fellenius. *Basics of foundation design*. Sidney, 2016.

[16] R.J. van Foeken and A.M. Gresnigt. *Buckling and collapse of UOE manufactured steel pipes*. 1998.

[17] Gasunie. *About the Gasunie*. Aug. 2017. URL: https://www.gasunie.nl/en/about-gasunie.

[18] J.G. de Gijt. "A history of quay walls: techniques, types, costs and future". Delft University of Technology, 2010.

[19] J.G. de Gijt and M.L. Broeken. *Quay walls, second edition*. Rotterdam, The Netherlands: SBRCURnet Publication C211E, 2013.

[20] J.G. de Gijt, C.N. van Schaik, and R.E. Roelfsema. "Piling and deep foundations". In: *Proceedings of the 4th international conference on piling and deep foundations* 1 (1991).

[21] J.G. de Gijt et al. "Quay-wall design and construction in Port of Rotterdam". In: *Bulletin* (), pp. 62–71.

[22] J. Grabe. "Sheet piling handbook design". In: *Geovancouver* (2008).

[23] J.H. Greenwald. *The impact of steel sheet piling shape and site and soil conditions on driving operations*. 2008, pp. 59–65.

[24] A.M. Gresnigt and S.H.J. van Es. “Stability of spiral welded tubes in quay walls”. English. In: *Proceedings of the 10th Pacific Structural Steel Conference*. 2013, pp. 200–205.

[25] M.H. Hussein and G.G. Goble. “Structural failure of pile foundation during installation”. In: *ASCE construction congress VI*. 2000, pp. 799–807.

[26] IISG. *International institute of social history*. Aug. 2017. URL: http://www.iisg.nl/hpw/calculate-nl.php.

[27] G. Jonker and S. Hartog. “Vibratory pile driving predictions”. In: ().

[28] V.E. Komurka and A.B. Wagner. “Estimating soil/pile set-up”. University of Wisconsin-Madison, 2003.

[29] A. Kooistra, J. Oudhof, and M.W. Kempers. “Heivermoeiing van paalfunderingen bij offshore windpark Egmond aan Zee”. Dutch. In: *Geotechniek* 18 (2008), pp. 36–41.

[30] L. Lee and P.E. Lowery. *Pile driving analysis by the wave equation*.

[31] G.E. Likins. *Pile installation difficulties in soils with large quakes*.

[32] MSL Engineering Limited. *A study of pile fatigue during driving and in-service and of pile tip integrity*. 2001.

[33] L. Maertens. “Ontwerpen en installeren van buispalen voor offshore structuren in moeilijke geotechnische omstandigheden”. Dutch. In: *Geotechniek* (2007), pp. 19–23.

[34] E. Meijer. “Comparative analysis of design recommendations for quay walls”. English. Delft University of Technology, 2006.

[35] P. Middendorp. “Thirty years of experience with the wave equation solution based on the method of characteristics”. English. In: *7th international conference on the application of state wave theory to piles*. 2004.

[36] Y.E. Mostafa. “Onshore and offshore pile installation in dense soil”. In: *Journal of American Science* 7 (2011), pp. 549–563.

[37] N.K.N. Mourillon. “Stability analysis quay structure at the Amazonehaven port of Rotterdam”. English. Technical University of Delft, 2015.

[38] NASSPA. *NASSPA best practices sheet piling installation guide*.

[39] M.G. Parent. “Diepwaterterminal op de Maasvlakte te Rotterdam 1”. Dutch. In: *PT Civiele Techniek* 2 (1990), pp. 10–13.

[40] M.G. Parent. “Moderne kademuren”. Dutch. In: *Cement* 4 (1990), pp. 91–97.

[41] PDI. *Pile dynamics, Inc.* Nov. 2016. URL: http://www.pile.com/pdi/products/grlweap/.

[42] PLAXIS. *PLAXIS*. Nov. 2016. URL: https://www.plaxis.com/product/plaxis-2d/.

[43] PORA. *Facts and figures*. Aug. 2017. URL: https://www.portofrotterdam.com/en/news-and-press-releases/revenue-at-port-of-rotterdam-authority-rises-profits-fall.

[44] H.A.J. de Ridder and J.P. Noppen. *Design and construct in Civil Engineering*. Delft: Delft university of technology, 2009.

[45] Port of Rotterdam. *About the port authority*. Aug. 2017. URL: https://www.portofrotterdam.com/en/port-authority/about-the-port-authority.

[46] Port of Rotterdam. *Key figures*. Aug. 2017. URL: https://www.portofrotterdam.com/nl/de-haven/haven-feiten-en-cijfers/schepen.

[47] C.N. van Schaik. “Diepwaterterminal op de Maasvlakte te Rotterdam 3”. Dutch. In: *PT Civiele Techniek* 2 (1990), pp. 21–26.

[48] C.N. van Schaik. *Ontwerpboek Amazonehaven*. Rotterdam: Gemeente werken Rotterdam, 1989.

[49] SCIA. *SCIA Engineer*. Nov. 2016. URL: https://www.scia.net/en/software/product-selection/scia-engineer.

[50] SCIA. *SCIA, version 5, Advanced calculations*.

[51] M.TH.J.H. Smith. “Een experimenteel onderzoek naar statische en dynamische mantelwrijving op palen in zand”. Dutch. Institute TNO, 1985.

[52] MG technical solutions. *state-of-the-art mechanical engineering*. Oct. 2017. URL: https://www.sbrcurnet.nl/producten/publicaties/damwandconstructies.

[53] Steel. *"Bouwen met staal", building with steel*. Aug. 2016. URL: http://brandveiligmetstaal.nl/.

[54] M.R. Svinkin. “Pile-soil dynamic system with variable damping”. In: (), pp. 240–247.

[55] D. Tara. “Development of a screening tool for impact hammer selection for installation, testing and damage mitigation of steel pipe and H-piles”. In: 2016.

[56] Z.N. Taylan and A. Senol. “Effects of soil dynamic parameters on pile drivability”. In: *OttawaGeo2007* (2007), pp. 1631–1636.

[57] A.F. van Tol and J.G. de Gijt. “Quay walls of the Rotterdam Harbour”. In: *Geotechnical engineering for transportation infrastructure* (1999), pp. 471–487.

[58] M.J. Tomlinson. *Pile design and construction practice, Fourth edition*. London, UK: E & FN Spon, an imprint of Chapman & Hall, 1994.

[59] TOSEC. *About the steel properties*. 2016. URL: https://www.tosec.nl/wiki/spanning-rekdiagram/.

[60] S.H. Tse et al. *Pile design and construction*. 1. Geo Publication, 1996.

[61] A Verruijt. *Soil mechanics*. Delft: Delft university of technology, 2012.

[62] Website. *Soil and rock symbols*. Dec. 2016. URL: http://www.finesoftware.eu/help/geo5/en/soil-and-rock-symbols-01/.

[63] W.C. Young and R.G. Budynas. *Roarks Formulas for Stress and Strain*. New York, U.S.A.: McGraw-Hill, 2002.

Research into pile toe failure in Amazonehaven

Reza Nejad
Department of Civil Engineering and Geo-sciences, Delft University of Technology

Abstract
Extreme folding damage of open-ended tubular piles could occur during piling in onshore practices. Amazonehaven unique quay wall removal gave the opportunity to study king pile's failure close to toe. King piles are primary piles in a combined wall system, exposed to static and dynamic load. It is argued that the unexpected *pile toe failure* have been caused by dynamic load because of the uniaxial direction of the extreme deformations. However, *research into pile toe failure in Amazonehaven* shows that hammer-induced driving stresses are significantly lower than material's yield stress close to pile toe, given Amazonehaven soil conditions. Therefore, the dynamic load has not been solely detrimental to the pile toe integrity. The main reasons for *pile toe failure* are discussed to be (1) initial dent and (2) pile inclination. Bear in mind that, *pile toe failure* to such extent when not limited might lead to dysfunction of the asset during its technical lifetime. Therefore, counteractions must be taken to assure quay wall's safety and stability while operating. The remedies when such a *piling risk event* occur could be: replacement, early maintenance, or a reduction in its designed storage capacity. The reactive solutions will bring financial consequences of *pile toe failure* forward. In other words, the client will experience a reduction in its revenues due to asset's malfunction. However, when proactive process-based alternatives are implemented in the current procedure in piling industry, the probability of occurrence of *the failure* is to be reduced.

Keywords
extreme folding damage — Amazonehaven — piling — driving stresses — open-ended tubular king piles

1. Introduction

After removal of the quay wall in Amazonehaven, it was observed that the king piles, primary elements in a combined wall system, were significantly damaged. The king piles were damaged at the pile toe and close to pile toe as depicted in Figure 1.

Figure 1. Pile toe failure in Amazonehaven

This paper aims to study the reasons of *pile toe failure*, technical part, and its financial consequence of such a failure, in management part.

2. Background

2.1 Relieving platform quay wall structure

A relieving platform quay wall structure is a frequently applied construction type in the Netherlands. This type of structure is applied to reduce the forces on the underlying retaining wall, combined wall, and the tensile forces in the foundation. The relieving platform quay wall structure consists of primary (king) piles which transfer the forces to the subsoil and anchors the system with the tension piles; the secondary intermediate sheet piles are placed between the primary king piles [2]. The concrete bearing piles are transferring the forces from the relieving platform into the strata capable of taking those forces. Figure 2 gives an impression of the Amazonehaven quay wall.

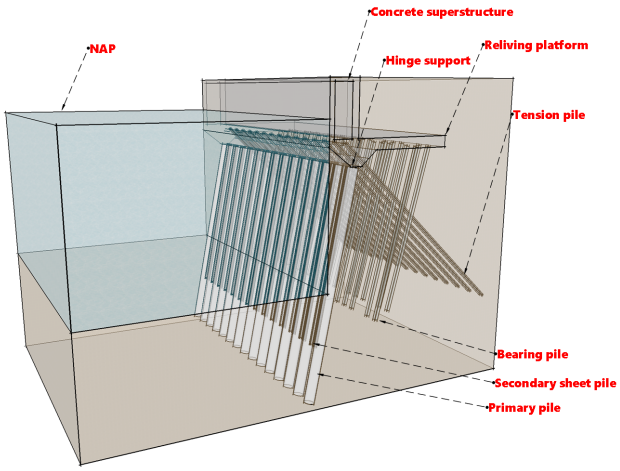

Figure 2. Amazonehaven relieving platform quay wall

2.2 Removal

Amazonehaven in Port of Rotterdam (POR), a deep seaport, has partly been demolished to widen the port entrance. The widening of the harbor was an inevitable decision to enable a continuous facilitation for ultra large vessels, due to new safety regulations imposed by the Port of Rotterdam Authority (PORA) [1].

2.3 Observations

After removal of open-ended tubular piles and the intermediate sheet piles, throughout 2011-2013, a mysterious observation was recorded by the staff. Both primary and secondary piles were significantly damaged at a location close to pile toe. The damages could be identified as (1) extreme folding of pile toe, (2) completely closed pile toe, (3) ovalisation at pile toe. It is estimated that about 15% to 20% of a total number of primary piles were damaged in the axial direction. For secondary sheet piles, this percentage is as high as 50% [7].

Furthermore, scorched sand at pile toe was observed which reveals the occurrence of a Locally Extremely High Temperature (LEHT) of about 400°-500° [7]. The heat is generated by high friction between soil and pile which could only happen **during** (pile) driving activity.

2.4 Execution work

The primary piles were partly vibrated and partly driven with an inclination of 5:1 (11.3°). It is common to vibrate up to the Pleistocene layer, and afterward to drive the piles up to its required depth. A combination of vibratory drivers and impact hammer driving is more practical, saves time and effort and enables obtaining an adequate soil bearing capacity [13]. The vibration of the piles occurred with an RBH 160 vibrator, 1600 [kN]. The driving, more or less the last 10 [m], occurred with a diesel hammer D62 in commence and later with a heavier D100 diesel hammer [8]. The change of hammer happened after carrying out a (pile) driving analysis, in 1990. The analysis showed that a D/t[1] ratio of 93, is driveable with a diesel hammer D100 as well as D82, given Amazonehaven soil condition described as Standard to Normal Soil Condition (SNSC).

The inevitable hammer change reduced blows up to 400 per 25 centimeters to below the threshold value of 300 per 25 [cm]. This threshold is set to minimize damage to both hammer and pile. The associated driving time was about 8 hours, however, using a diesel hammer D100, driving time reduced to 1 to 2 hours and blow counts remained between 70 to 120 strikes per 25 [cm] [13]. The drawback of hammer alternation during execution work was apparently both a halt in execution work for nearly two weeks and a probable soil set-up occurrence. Soil set-up refers to soil reaching its full capacity which makes **re**driving troublesome.

[1] 1420 [mm] x 15 [mm]

Furthermore, it was mentioned that in 1990 when pile advancement stopped with a diesel hammer D62; the contractor was forced to pull out the pile. In that specific event, the pile had a complete harmonica shape close to pile toe [J. de Gijt, personal communication]. Also, due to pressure to realize the project as fast as possible, the old quay wall, many miscommunications did occur [J. de Gijt, personal communication and [15]]. Other than this, no driving difficulties were reported during pile installation.

2.5 Major events

Two main events have taken place in the short (25 years) technical lifetime of the asset. First, immediately after construction interlocks openings did occur (between the sheet piles and tubular piles), second; due to overloading of one section (out of 20), settlement of 50 [mm] has occurred [3].

2.6 Stability of the quay wall

A Recent study has shown that the stability of the quay wall has not been endangered given a significant damage of the king piles close to toe [3]. In this study, the open-ended piles were designed into PLAXIS. It shows that the moment (lateral soil load) on the combined wall increases by 1.4 and the anchor force reduces by 0.8 due *extreme folding damage*. Also, the soil displacement increases by a factor 3. Nevertheless, the entire structure would have remained stable, if it was not demolished, **for a certain period** [3]. The main reasons as mentioned in the *stability* study are: (1) the quay wall's design is based on a deterministic (conservative) approach, (2) in front of the quay wall the contract depth is reached and not the designed (deeper) depth, (3) the quay wall has not been fully utilized during its technical lifetime and (4) the quay wall was strategically designed for a higher static load than it was intended to be used for [5].

2.7 Failure modes

The available data about the *extreme folding damage* of tubular king piles, photos and measurements, are analyzed, and modes of failure are introduced. Figure 3 depicts a cross-section of *deformed* pile toe, as observed in Amazonehaven. The four *popular* failure modes have the highest frequency of occurrence among the twelve failure modes, identified in this study.

Figure 3. Cross-section of *deformed* pile toe

2.8 Loads

The main loads on a quay wall are: structural- and installation-loads. The first refers to the loads which are present during the technical lifetime of the asset. The latter refers to the loads

being applied on the pile during piling [2]. This paper focuses on the dynamic mold of load, during piling, because of the uniaxial direction of the *extreme folding damage* close to pile toe.

3. Research methodology

3.1 Introduction

The research methodology of *pile toe failure* includes both technical part as well as the management aspects of *the failure*.

3.2 Technical part

The technical part includes both Pile Driving Prediction (PDP) and SCIA Engineer. PDP is a one-dimensional program where the hammer-pile-soil interaction could be studied. After which, general reasons of *pile toe failure*, within the hammer-pile-soil system, are clustered and categorized. Then, the main probable causes of *pile toe failure* in Amazonehaven, are studied by SCIA which is a Finite Element Analysis (FEA) program. SCIA enables carrying out a sensitivity analysis given the (static)load-pile-soil interaction.

3.2.1 PDP

AllWave PDP is a prediction program to study the driveability of the primary pile within the hammer-pile-soil system. To this end, the program uses the *stress wave theory*, to simulate the pile behavior during driving [14]. Therefore, displacements and forces of the hammer, the pile, and the soil during pile installation are determined. The inputs are about, hammer characteristics, pile dimensions, and soil characteristics [6]. The outputs are: Soil Resistance to Driving (SRD), driving time, soil fatigue, stress development along the pile and the number of blows required to bring the pile into its embedded depth. It, therefore, helps the designer to select a suitable hammer with hammer-induced driving stresses below material's yield stress and the number of blows below refusal threshold. In this fashion, the pile toe integrity during piling is maintained, as well as both the hammer and pile head are not damaged.

3.2.2 SCIA Engineer

SCIA Engineer is an integrated, multi-material structural analysis and design software for various types of structures. In SCIA, it is possible to carry out a calculation which takes into account the (non-linear) plastic behavior of the steel. It is assumed that *extreme folding damage* has occurred due to development of high stresses, exceeding the material's yield stress. Moreover, SCIA enables studying pile's behavior taking into account geometrically non-linearity.

3.3 Management part

The management aspects of the *pile toe failure* needs a literature study, introduction of a *piling risk event*, and a search for remedies in pre-piling and post-piling phase. Furthermore, a decision model helps the client to select the optimum, economic, solution when the risk event occurs. To make a decision, an economic evaluation of different technical designs must be available. To do so, several methods are available. The Net Present Value (NPV) is a simple and widely used method which discounts the costs and revenue flow for a project based on the technical lifetime of the asset and the interest rate at the Present Value (PV) [10]. In this method, financial aspects of the infrastructural projects are evaluated, including its construction, maintenance, and demolition cost. When $NPV > 0$, profit is generated meaning the project is worth starting, and its financial feasibility is warranted. Therefore, the Total Cost (TC) could be expressed as [10]:

$$TC = I_0 + \sum M_i + D \tag{1}$$

Where the I_0 is the initial costs of construction. The maintenance cost, $\sum M_i$ are those which must be met to ensure that the required functionality is maintained per year. The last term, D, is demolition cost which arises at the end of the technical lifetime of the asset.

4. Analysis

4.1 Introduction

The analysis of *pile toe failure* includes both technical parts as well as the management aspects of the *piling disease*.

4.2 Technical part

The technical part, includes both PDP and SCIA. The failure sources are studied within a **hammer**-**pile**-**soil** system. Therefore, the failure has a **dynamic**-, **geometric**- or **geologic**- nature.

4.2.1 PDP

(a) **soil compaction** due vibration; more soil resistance to pile driving is generated, which reduces the downward wave stresses. Therefore, the hammer-induced driving stresses close to pile toe are less than material's yield stress. Figure 4 shows (B) the number of blows over the entire driving **depth**, given the threshold (R), for both virgin or compacted (15%) soil. The Fatigue Factor (FF) due piling, degradation of the soil resistance, is 0.2. Due to compaction, the piling becomes troublesome[3], if not impossible.
Figure 4 shows (D) the hammer-induced driving stresses over the entire **length** of the pile. The compaction does not affect stress-development along the pile, significantly.

(b) **pile inclination** could cause unequal load distribution due to eccentric impact force at pile head. Therefore, another stress-development is to be expected along the pile.

(c) **Zero Shaft Friction (ZSF)** simulates piling while shaft friction is completely eliminated. A ZSF circumstance

[2] pile driving activity

[3] heavy piling

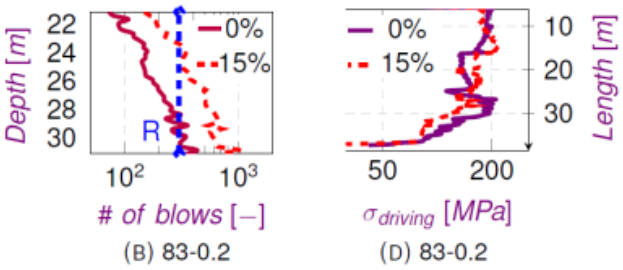

Figure 4. Piling prediction for a D/t-83, FF-0.2

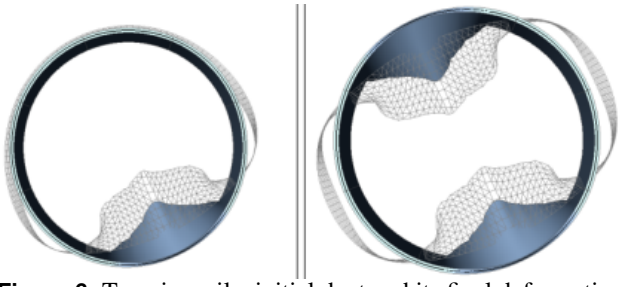

Figure 6. Top view pile, initial dent and its final deformation

could happen in case of (pile) stagnation & continuous driving.

(d) **hammer selection** is quite important to ensure sustained driving. For Amazonehaven, a D62 hammer did not comply within the ranges of minimum and maximum hammer energy [4].

(e) **driving stresses** are about 60% lower than the material's yield stress (483 [MPa]) close to pile toe, for Amazonehaven SNSC. However, in case of Medium to Hard Soil Condition (MHSC), the stresses are extremely high close to pile toe as depicted in Figure 5.

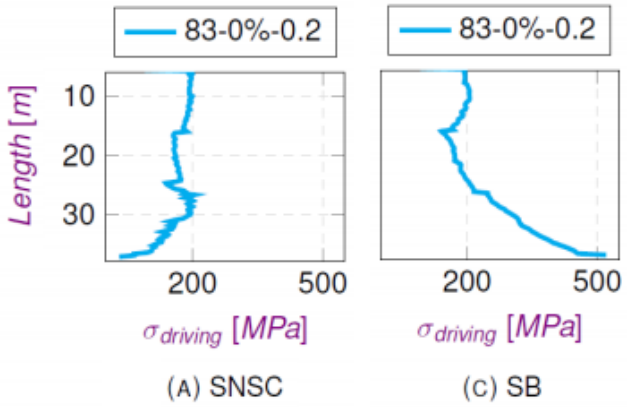

Figure 5. Piling prediction for a D/t-83, virgin, FF-0.2

(f) **temperature** reduces both strength and stiffness of the steel which makes it less resilient to folding. The temperature elevation is argued to be caused by a high friction between soil and pile. A local Temperature Elevation (TE) together with, e.g., an initial imperfection will be detrimental to maintain pile toe integrity during piling.

(g) **initial imperfection** leads to *pile toe failure*, in terms of *extreme folding damage* when it is accompanied with a Locally Extremely Hard Spot (LEHS). In case of sustained driving, unequal soil distribution inside & outside occurs, which leads to a gradual inwards deformation due to clamped solid soil next to pile toe. Figure 6 shows, the imperfection as modeled in SCIA and its final deformation.

(h) **plugging** refers to the dimension of the pile which fosters a plugged response of the pile. The dimension of Amazonehavne's piles is argued to be significantly large which does not facilitate plugging. Plugging is, therefore, not taken into account.

(i) **steel fatigue** appears when the number of blows become extremely high. However, the head of the pile is more sensitive to fatigue rather than the toe, because the driving stresses at the toe are shown to be less than at head in SNSC. Therefore, it is argued that the steel fatigue not lead to *pile toe failure* as there is no documentation of extreme deformation at pile head. Fatigue of the material is not taken into account.

(j) **fabrication** of the piles could affect material's response to unevenly distributed stresses. This study does not take fabrication into account.

(k) **plugging** becomes problematic in cohesive soil properties, where the soil inside the pile acts as a rigid body. Amazonehaven, sandy soil, does not foster the plug phenomenon.

(l) **LEHS** is detrimental to pile toe and could have caused pile toe failure. A combination of LEHS and initial (dent) imperfection will worsen the extent in which *pile toe failure* occurs.

(m) **pile inclination** refers to a non-uniform soil property (stiff and weak) at the toe as depicted in Figure 7. Pile inclination is assumed to exacerbate the occurrence of such non-uniform soil properties. Therefore, pile toe experiences at one edge higher stresses whereas at the other edge the stresses are limited to impact stresses at the head.

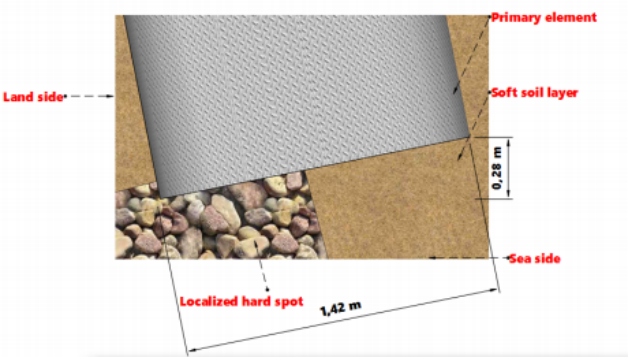

Figure 7. Pile inclination, non-uniform bed

(n) **ZSF** plays a role, in case of Soft Rock (SR) phenomenon. In this situation, the overlying layers have poor properties whereas the bed enjoys stiff-rock-ish soil properties. Therefore, the stresses at the toe are much higher than the impact stresses at the head.

(o) **soil fatigue** affects the drievability. Due to piling, soil degradation occurs, which means that due to vicious blows the soil loses its strength. Therefore, impact driving becomes easier. A soil FF-value of 0.2 reduces the SRD considerably, where theoretically stress wave travels through the pile *almost* freely.

(p) **soil set-up** affects the driveability. In this fashion, mainly clay-ish soil regains its initial strength for re-driving after a delay. Therefore, soil set-up has more or less the same effect as soil compaction or a situation without accounting for soil fatigue.

4.2.2 SCIA Engineer

The main reasons to *pile toe failure* in Amazonehaven are shown to be: **initial imperfection** and **pile inclination**. The pile is modeled in the SCIA to carry a sensitivity analysis regarding the above mentioned causes to *pile toe failure*.

Figure 8 and 9 show the Yield Stress Momentum (YSM) with (A) increasing initial dent and (B) a decreasing soil homogeneity at pile toe, given various D/t ratios, for respectively centric and eccentric loading. The YSM is the point in which the material's yield stress reaches for the first time. Therefore, it could be argued that a pile with a lower YSM-value be locally more prone to *extreme folding damage*.

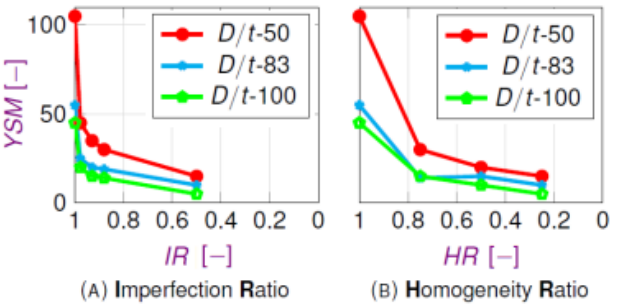

(A) Imperfection Ratio (B) Homogeneity Ratio

Figure 8. YSM for centric loading

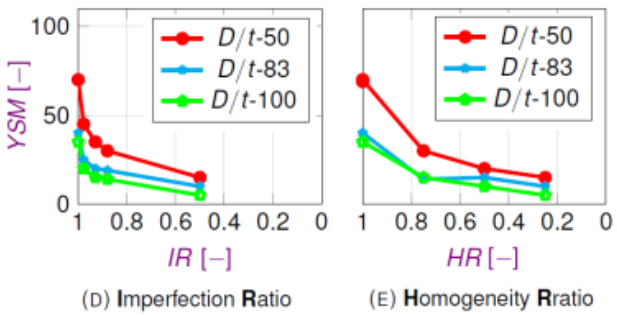

(D) Imperfection Ratio (E) Homogeneity Rratio

Figure 9. YSM for eccentric loading

The YSM decreases drastically in case of decreasing Imperfection Ratio (IR), where $IR = 1$ means a perfectly rounded pile. However, it decreases less drastically for Homogeneity Ratio (HR) at pile toe, where a $HR = 1$ means a uniform (stiff) soil-bed. A decreasing HR means a non-uniform (stiff and weak) soil-bed.

Also, due to eccentric loading, YSM-value is lower which pinpoints inclined piling could be detrimental for maintaining *pile toe integrity* during piling.

4.3 Management part

The remedies for both pre-piling and post-piling phases to respectively avoid- or counteract- (the consequences of) *piling risk event*. The *pile toe failure* is introduced as a risk[4] event. It is, however, more convenient to prohibit potential sources leading to *extreme folding damage* beforehand installation. In this fashion, the process-based alternatives will reduce the probability of occurrence of the risk event. Remedies in pre-piling phase are:

- Data collection: sufficient soil investigation, utilizing a prediction program, carrying out pile tests, carrying out back-analysis to fit prediction to measurements, select a correct impact hammer,
- Pre-installation: utilizing Just In Time (JIT) (delivery) system[5] for king piles [9], Azobé cover to protect pile head and pile toe during transport/uplifting, careful execution during uplifting/transport
- Installation: utilizing stiffening rings at pile toe, jetting during piling, drilling before piling [12], in situ checks of Out of Roundness (OOR) of the pile toe, careful execution of installation, using a monitoring system to warrant *pile toe integrity* during piling,

Moreover, when the risk event occurs; the consequences could be diminished by selecting one of the following remedies (post-piling phase): (1) Replacement (R), (2) Early Maintenance (EM) and (3) Capacity Reduction (CR). R refers to removing of the Problematic Section (PS), which will bring forward extra costs and a reduction in revenues. EM refers to maintaining the PS more often than the Other Section (OS) which needs a Regular Maintenance (RM). Therefore, both increases in costs and decrease in revenues due to more maintenance are to be expected. CR refers to a reduction in storage capacity in PS which manifests itself in (only) a reduction in revenues.

Figure 10 shows the NPV per increasing percentage of PS for above mentioned scenarios, for both iron ore and coal. Iron ore is ten times heavier than coal. Therefore, the NPV due CR of coal is higher than iron ore.

[4] Risk=Probability · Consequences[11]
[5] used in auto-industry, mega projects

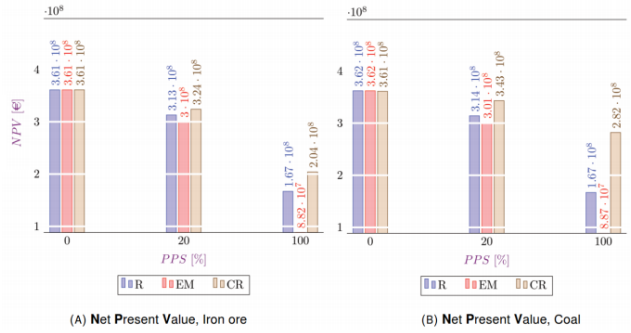

Figure 10. NPV per increasing PPS

It is recommended to select CR, the highest value of NPV with increasing PPS, as a counteraction to *piling disease* in post-piling phase. Furthermore, the PORA is recommended to change the storage function of the quay wall, to a lighter goods, when facing consequences of *pile toe failure* regarding settlements or endangerment of the quay wall's stability. as

5. Conclusions

A variety of causes to *pile toe failure* are discussed, and in case of Amazonehaven, the main reasons for such a failure are shown to be (1) initial (dent) imperfection and (2) pile inclination. The research showed that given a Standard to Normal Soil Condition (SNSC), the hammer-induced driving stresses are incredibly lower than material's yield stress close to pile toe. However, given a Medium to Hard Soil Condition (MHSC) the stresses become extremely high close to pile toe. The latter is very doubtful to be the case given Amazonehaven soil conditions. The finding is valid given a diesel hammer D100-13 and a range of D/t ratios of 20 to 100. Furthermore, it was shown in a sensitivity analysis that the initial dent fosters development of *extreme folding damage* during piling more than a non-uniform soil layer at pile toe.

The research also discussed the need for remedies to *piling disease*. To avoid such a risk event, either pre-piling remedies must be implemented or post-piling remedies. It is apparent that post-piling remedies have a higher value of financial burden for the client. It is, therefore, very recommended to introduce creative and process-based remedies in the pre-piling phase, next to conventional solutions.

References

[1] Broos, E.J. and de Gijt, J.G. (2013): "the demolishing of the EMO quay wall in the Amazonehaven, port of Rotterdam".

[2] Municipality Rotterdam Port of Rotterdam (2013): "Quay walls, second edition".

[3] Mourillon, N.K.N. (2015): "stability analysis quay structure at the Amazonehaven port of Rotterdam".

[4] Tara, D. (2016): "development of a screening tool for impact hammer selection for installation, testing and damage mitigation of steel pipe and H-piles", Geovancouver.

[5] Gemeente werken Rotterdam (1989): "Ontwerpboek Amazonehaven", "Design book Amazonehaven".

[6] Kooistra, A. AND Oudhof, J. AND Kempers, M.W. (2008): "Heivermoeiing van paalfunderingen bij offshore windpark Egmond aan Zee", Geotechniek.

[7] Broos, E. AND de Gijt, J.G. (2014): "The demolishing of the EMO quay wall in the Amazonehaven", Port of Rotterdam.

[8] van Schaik, C.N. (1990): "Diepwaterterminal op de Maasvlakte te Rotterdam 3 ", PT Civiele Techniek.

[9] Davies, A. AND Gann, D. AND Douglas, T. (2009): "Innovation in megaprojects: systems integration at London Heathrow Terminal 5", California management review.

[10] de Gijt, J.G. (2010): "A history of quay walls: techniques, types, costs and future", Delft University of Technology.

[11] Oxenham, D. (2010): "The next great challenges in systems thinking: A defense perspective", Civil Engineering and Environmental Systems.

[12] Tomlinson, M.J. (1994): "Pile design and construction practice, Fourth edition",

[13] de Gijt, J.G. AND van Schaik, C.N. AND Roelfsema, R.E. (1991): "Piling and deep foundations", Proceedings of the 4th international conference on piling and deep foundations.

[14] Middendorp, P. (2004): "Thirty years of experience with the wave equation solution based on the method of characteristics", 7th international conference on the application of state wave theory to piles.

[15] Parent, M.G. (1990): "Moderne kademuren", Cement.

Acronyms

R	Replacement
RM	Regular Maintenance
EM	Early Maintenance
CR	Capacity Reduction
PV	Present Value
NPV	Net Present Value
TC	Total Cost
PPS	Percentage Problematic Section
PS	Problematic Section
OS	Other Section
OOR	Out of Roundness

JIT	Just In Time
POR	Port of Rotterdam
PORA	Port of Rotterdam Authority
PDP	Pile Driving Prediction
WEAP	Wave Equation Analysis Program
FEA	Finite Element Analysis
FF	Fatigue Factor
LEHS	Locally Extremely Hard Spot
LEHT	Locally Extremely High Temperature
SR	Soft Rock
ZSF	Zero Shaft Friction
SNSC	Standard to Normal Soil Condition
MHSC	Medium to Hard Soil Condition
SRD	Soil Resistance to Driving
YSM	Yield Stress Momentum
IR	Imperfection Ratio
HR	Homogeneity Ratio
TE	Temperature Elevation